Philipps Universität Marburg

Impact of Physiological Rhythms on Energy Homeostasis in Rodents

---

Dissertation

for the degree of
Doctor of Natural Sciences
(Dr. rer. nat.)

submitted to the
Faculty of Biology at the
Philipps-Universität Marburg by

Alisa Boucsein

born in Frankenberg/Eder

Marburg, 2018

Accepted as dissertation by the Faculty of Biology at the
Philipps-Universität Marburg: 19.11.2018

First referee: Dr. Alexander Tups

Second referee: Prof. Dr. Uwe Homberg

Date of the oral examination: 20.12.2018

University reference number: 1180

Table of contents

Statement on the contribution to publications in this dissertation

I declare that this thesis has been composed by myself and without external assistance and that the work presented has not been submitted for any other degree or professional qualification. I furthermore declare that I have not made any prior doctoral attempt. I confirm that no sources other than those indicated have been used and that appropriate credit has been given within this thesis where reference has been made to the work of others. I confirm that the work submitted is my own, except where work that has formed part of jointly-authored publications has been included. My contribution to this work has been explicitly stated below.

_____

(Alisa Boucsein)

Dunedin, September 2018

Chapter 4.1.:

Central adiponectin acutely improves glucose tolerance in male mice

- Performance of *in situ* hybridization experiments in figure 1 and 2 in collaboration with Chrishanthi Lowe and Karen Legler
- Analysis and statistical analysis of data in figure 1 in collaboration with Chrishanthi Lowe

This manuscript was published in *Endocrinology* in May 2014. PMID: 24564394

Authors on this publication: Christiane E. Koch, Chrishanthi Lowe, Karen Legler, Jonas Benzler, **Alisa Boucsein**, Gregor Böttiger, David R. Grattan, Lynda M. Williams, Alexander Tups.

Chapter 4.2.:

Photoperiodic and diurnal regulation of WNT signaling in the arcuate nucleus of the female Djungarian hamster, *Phodopus sungorus*

- Performance of all experiments
- Analysis of all data in figures 2 and 3
- Analysis of data in figure 4 with assistance from Dr. Cindy Hempp
- Statistical analysis of data in figures 2 and 3 with assistance from Dr. Gisela Helfer
- Statistical analysis of data in figure 4
- Preparation of figures in collaboration with Sigrid Stöhr
- Authoring of the manuscript in collaboration with Dr. Alexander Tups

This manuscript was published in *Endocrinology* in February 2016. PMID: 26646203

Authors on this publication: **Alisa Boucsein**, Jonas Benzler, Cindy Hempp, Sigrid Stöhr, Gisela Helfer, Alexander Tups.

Chapter 4.3.:

Hypothalamic Leptin Sensitivity and Benefits of Time-Restricted Feeding are Dependent on the Time of Day

- Performance of all experiments with assistance from Dr. Mohammed Rizwan
- Analysis and statistical analysis of all data
- Preparation of all figures
- Authoring of the manuscript in collaboration with Dr. Alexander Tups

This manuscript is in submission to *Cell Metabolism*.

Authors on this manuscript: **Alisa Boucsein**, Mohammed Z. Rizwan, Alexander Tups.

Chapter 4.4.:

All in the Timing: Regulation of Body Weight, Glucose Homeostasis and Memory Coordination by the Circadian Clock

- Authoring of the review article in collaboration with Aline Löhfelm and Dominik Pretz (joint first authorship)

This review article was accepted for publication in *Trends in Endocrinology and Metabolism* in August 2018.

Authors on this manuscript: **Alisa Boucsein**, Aline Löhfelm, Dominik Pretz, Alexander Tups.

Abbreviations

AANAT	Arylalkylamine N-acetyltransferase
ACSF	Artificial cerebrospinal fluid
α-MSH	α-melanocyte-stimulating hormone
AgRP	Agouti-related peptide
AMPK	Adenosine monophosphate-activated protein kinase
AKT	Protein kinase B
APC	Adenomatous polyposis coli
APPL	Adapter protein phosphotyrosine interacting with PH domain and leucine zipper
ARC	Arcuate nucleus
BMAL-1	Brain and muscle ARNT-like protein 1
BMI	Body mass index
Ca^{2+}	Calcium
CART	Cocaine- and amphetamine-regulated transcript
C/EBPα	CCAAT-enhancer binding protein α
cDNA	Complementary deoxyribonucleic acid
CK	Casein kinase
CLOCK	Circadian locomotor output cycles kaput
CNS	Central nervous system
CRY	Cryptochrome
CSF	Cerebrospinal fluid

DIO	Diet-induced obesity
DKK	Dickkopf-related protein
DMH	Dorsomedial hypothalamus
Dsh	Dishevelled
ELISA	Enzyme-linked immunosorbent assays
ERK	Extracellular-regulated kinase
Fz	Frizzled
GSK-3β	Glycogen synthase kinase-3β
GTT	Glucose tolerance test
HFD	High-fat diet
HRP	Horseradish peroxidase
Icv	Intracerebroventricular
IKKβ	Inhibitor of nuclear factor-κB kinase β
IL-6	Interleukin-6
Ip	Intraperitoneal
IR	Insulin receptor
IRS	Insulin receptor substrate
JAK2	Janus kinase 2
JNK	c-Jun N-terminal kinase
LAN	Leptin antagonist
LD	Long day
LEF	Lymphoid enhancer factor
LepRa	Short isoform of the leptin receptor

LepRb	Long isoform of the leptin receptor
$Lep^{ob/ob}$	Leptin-deficient C57BL/6J mouse line
LFD	Low-fat diet
LHA	Lateral hypothalamic area
LRP	Low-density lipoprotein receptor-related protein
M	Molar
mHFD	moderate HFD
mRNA	Messenger ribonucleic acid
NF-κB	Nuclear factor-κ-light-chain-enhancer of B-cells
NPY	Neuropeptide Y
P	Phosphorylated
PA	Perifornical area
PCP	Planar cell polarity
PCR	Polymerase chain reaction
PER	Period
PFA	Paraformaldehyde
PI3K	Phosphatidylinositol 3-kinase
POMC	Pro-opiomelanocortin
PPARγ	Peroxisome proliferator-activated receptor γ
PTT	Pyruvate tolerance test
PVN	Paraventricular nucleus
REV-ERBα	Reverse erythoblastoma α
RHT	Retinohypothalamic tract

RORα/β	Retinoid orphan receptor α/β
SCN	Suprachiasmatic nucleus
SD	Short day
SFRP2	Secreted Frizzled-related protein 2
SHP2	Src homology 2-containing tyrosine phosphatase
SOCS3	Suppressor of cytokine signalling 3
STAT3	Signal transducer and activator of transcription 3
TBS	Tris-buffered saline
TCF	T-cell factor
TMB	Tetramethylbenzidine
TNFα	Tumour necrosis factor α
TRF	Time-restricted feeding
VMH	Ventromedial hypothalamus
ZT	Zeitgeber time

1. General introduction

1.1. Central regulation of energy metabolism

In healthy humans, the amount of energy consumed matches the amount of energy expended over a long-term period, even though short-term mismatches in energy balance can occur (1). This phenomenon is called energy homeostasis and works to a surprisingly precise extend, considering that adult mammals, including humans, maintain a relatively stable body weight over long periods of time even when presented with unlimited access to food sources. A study conducted in rats demonstrated that an extended period of fasting accompanied by body weight loss results in an increase of energy intake once animals regain *ad libitum* access to food. This increase only lasted for a limited time though, until rats recovered baseline body weight (2). These data demonstrate a highly accurate regulatory system controlling energy homeostasis. Already in 1953 a mechanism was proposed that aimed to explain this phenomenon, postulating inhibitory signals that are secreted in proportion to fat depots, acting in the hypothalamus to reduce energy intake (3). Decades later, this hypothesis turned out to be very precise, when the adiposity signal leptin was discovered (4).

1.1.1. Leptin and its role in the development of obesity

In 1994, a novel adipocyte-derived hormone was discovered by Jeffrey Friedman and colleagues (4). It was named leptin (from Greek *leptos*, meaning ‘thin’) for its anorexigenic and catabolic effects observed in mice (5). The absence of leptin results in hyperphagia, decreased energy expenditure and severe obesity, as observed in the $Lep^{ob/ob}$ mouse, which is leptin deficient due to a mutation in the *obese* gene (4). After this discovery, leptin was believed to have great potential as an ‘obesity drug’ for the growing obesity problem of our modern society. However, this initial euphoria soon abated, after leptin was shown to be secreted by white adipose tissue and to circulate in proportion to body fat mass (6). In fact, most obese individuals have elevated leptin levels, whereas monogenetic defects as described for $Lep^{ob/ob}$ mice are extremely rare

in humans, although they result in extreme cases of obesity if present (7). In both leptin-deficient humans as well as mice, leptin administration leads to rapid decrease in food intake, increase in energy expenditure and weight loss, demonstrating that these subjects are highly leptin sensitive (7-10), whereas this does not apply to obese patients with elevated serum leptin concentrations (11). This diet-induced obesity (DIO) is characterized by hyperleptinemia and leptin resistance, the failure of leptin to mediate its catabolic effects. In mice, DIO can be induced by feeding mice a high-fat diet (HFD) enriched in saturated fatty acids. These mice become obese and develop hypothalamic leptin resistance (12). The molecular cause for hypothalamic leptin resistance is still not fully understood.

The main target tissue for leptin resides in the brain, specifically the mediobasal hypothalamus, which forms the regulatory centre of hunger and satiety and plays a key role in energy balance regulation (13, 14). Intracerebroventricular (icv) leptin injections were shown to decrease food intake and body weight, in both wild-type and leptin-deficient $Lep^{ob/ob}$ mice (15). Leptin crosses the blood-brain-barrier via the short isoform of the leptin receptor (LepRa) and enters the brain in proportion to its serum concentration (16-18). In the mediobasal hypothalamus, the long form of the leptin receptor (LepRb) is expressed particularly in the arcuate nucleus (ARC), ventromedial hypothalamus (VMH), dorsomedial hypothalamus (DMH) and lateral hypothalamic area (LHA) (19, 20). Of particular interest is the ARC, due to its crucial role in the regulation of energy metabolism and other homeostatic systems (21-24).

Leptin conveys its weight-reducing effects by binding to LepRb, causing a conformational change and activating the associated Janus kinase 2 (JAK2), a tyrosine kinase. This results in phosphorylation of three intracellular receptor tyrosine residues; these are tyrosine 985, tyrosine 1077 and tyrosine 1138 (25, 26). Tyrosine 985 and tyrosine 1077 are involved in signal transduction via extracellular-regulated kinase (ERK) and Src homology 2-containing tyrosine phosphatase (SHP2) and will not be further discussed in this thesis. Phosphorylation of tyrosine 1138, on the other hand, leads to recruitment of signal transducer and activator of transcription 3 (STAT3), which then gets phosphorylated at its phosphorylation site tyrosine 705 by JAK2. Phosphorylated STAT3 (pSTAT3) homodimerises and translocates into the nucleus, where it acts as a transcription factor and activates target gene expression (26, 27). Among those are effector molecules that cause satiety and increased energy

expenditure as well as the suppressor of cytokine signalling 3 (SOCS3). Through negative feedback regulation, SOCS3 binds to LepRb and inhibits JAK2 activity, making SOCS3 an effective inhibitor of leptin signal transduction via JAK2/STAT3 signalling (28, 29) (Figure 1).

Two distinct populations of neurons in the ARC co-express LepRb. These are neuropeptide Y/agouti-related peptide (NPY/AgRP)-expressing neurons, which are inhibited by leptin (30, 31), as well as pro-opiomelanocortin/cocaine- and amphetamine-regulated transcript (POMC/CART)-expressing neurons, which are activated by leptin (32-34). Icv injections of NPY as well as AgRP cause hyperphagia, decreased energy expenditure and obesity (35-39), identifying both neuropeptides as anabolic signals. In contrast, catabolic effects were demonstrated for both α-melanocyte-stimulating hormone (α-MSH), which is cleaved from the POMC precursor molecule, and CART (40-42). These ARC-located neurons are first-order neurons in the hypothalamic response to circulating hormones and send projections to other nuclei, such as the LHA, paraventricular nucleus (PVN) and perifornical area (PA), which are locations of second-order neurons involved in energy metabolism (43, 44). Stimulation of LHA and the adjacent PA provokes feeding, whereas PVN stimulation inhibits food intake (23, 45).

In wildtype mice, leptin injections increase pSTAT3 levels, which serve as a marker for activated intracellular leptin signal transduction. In mice that are obese due to HFD feeding, this response to exogenous leptin is deteriorated, particularly in the ARC (12). Impaired leptin transport via the blood-brain-barrier into the brain potentially plays a role in the manifestation of leptin resistance. In healthy mice with normal circulating leptin levels the transport mechanism via LepRa processes linearly. However, during obesity accompanied by hyperleptinemia this system is saturated, suggesting that the hypothalamus receives misinformation about the peripheral energy state and integrates these signals into an inapt neural response (46, 47). Furthermore, expression of *Socs3* has been shown to be upregulated and lead to impairment of leptin signalling in obese mice as well as other rodent models of leptin resistance (28, 48). Notably, *Socs3* is a target gene of different pro-inflammatory pathways (49). Our laboratory provided evidence that chronic low-grade hypothalamic inflammation, which has been associated with the development of metabolic disorders (50), plays a crucial role in the disruption of normal energy and glucose metabolism and the development of obesity

(51, 52). To date, the molecular mechanisms underlying the manifestation of hypothalamic leptin resistance and the development of obesity are still not entirely understood and have to be further determined.

1.1.2. Insulin and its central control of energy metabolism

Insulin is a peptide hormone produced by β-cells of the pancreatic islets of Langerhans and was the first hormone to be implicated in the control of glucose homeostasis. Circulating insulin concentrations are proportional to body fat mass (53). Since its discovery in the early 1920s insulin injections in type 1 diabetic patients proved to normalise their blood glucose concentrations and eliminate glycosuria. The blood glucose-lowering actions of insulin had long been regarded as solely peripheral, even though as early as in 1854, the French physiologist Claude Bernard discovered that lesions in the base of the fourth ventricle led to glycosuria in rabbits, demonstrating a crucial role of the central nervous system (CNS) in glucose homeostasis (54). Since then, icv injections of insulin have been shown to lead to body weight loss and reduced food intake in both monkeys and rats (55, 56). Additionally, neuron-specific insulin receptor knockout mice exhibit increased food intake, body fat, plasma leptin and insulin levels as well as mild insulin resistance (57), demonstrating that the brain is a key target tissue for insulin to mediate its catabolic and anorexigenic effects on energy metabolism.

Circulating insulin from the periphery passes the blood-brain-barrier and binds to insulin receptors (IR) that are expressed throughout the brain and in particular abundance in the hypothalamic ARC (58, 59). As described for leptin, insulin acts on NPY/AgRP- and POMC/CART-expressing neurons in the ARC (23). Upon insulin binding to IR, the intrinsic tyrosine kinase domain of the receptor activates insulin receptor substrate (IRS) through phosphorylation at tyrosine residues, which in turn activates phosphatidylinositol 3-kinase (PI3K). This leads to downstream phosphorylation of AKT (protein kinase B) at its positive phosphorylation sites serine 473 and threonine 308. AKT is a serine/threonine-specific protein kinase and in turn activates multiple insulin-sensitive metabolic pathways and gene expression, thereby controlling energy and glucose metabolism (23, 60). The enzyme glycogen synthase kinase-3β (GSK-3β) plays a crucial role in this signal transduction. Upon stimulation of

the insulin pathway GSK-3β gets phosphorylated at its negative phosphorylation site serine 9, thereby being inhibited (61-63). Furthermore, inhibition of GSK-3β has been demonstrated to improve glucose homeostasis in glucose-intolerant rodent models (64-66), presenting GSK-3β as a potential modulator of insulin sensitivity (Figure 1).

1.1.3. The connection of obesity and type 2 diabetes

During obesity, circulating insulin concentrations are elevated, but insulin is unable to mediate its catabolic effects, as already described for leptin. Obesity is regarded as one of the major risk factors for the development of type 2 diabetes (67). During early stages of type 2 diabetes insulin sensitivity is attenuated. This leads to elevated insulin secretion from the pancreas in order to counteract this condition (68). During the further manifestation of type 2 diabetes this mechanism loses its ability to compensate for the disrupted insulin sensitivity and leads to deteriorated glucose tolerance, eventually resulting in the destruction of insulin-producing β-cells in the pancreas and insulin deficiency. At this stage, glucose homeostasis is fully disrupted and other physiological disorders can develop in the long-term, including nephropathy, retinopathy and cardiovascular disorders (69).

In obese rats icv insulin injections fail to decrease food intake and body weight (56), thereby demonstrating a close relationship between obesity and insulin insensitivity and providing evidence for the importance of central insulin signalling for normal energy homeostasis. Both leptin-deficient $Lep^{ob/ob}$ mice as well as leptin resistant subjects develop obesity accompanied by glucose intolerance and reduced hypothalamic insulin sensitivity (4, 70). Our laboratory and others showed that intact leptin signalling is necessary to sensitise insulin signal transduction, through modulation of IRS and subsequent activation of PI3K by leptin (71, 72) (Figure 1). These results reveal the potential connection between obesity and the related metabolic disorder type 2 diabetes.

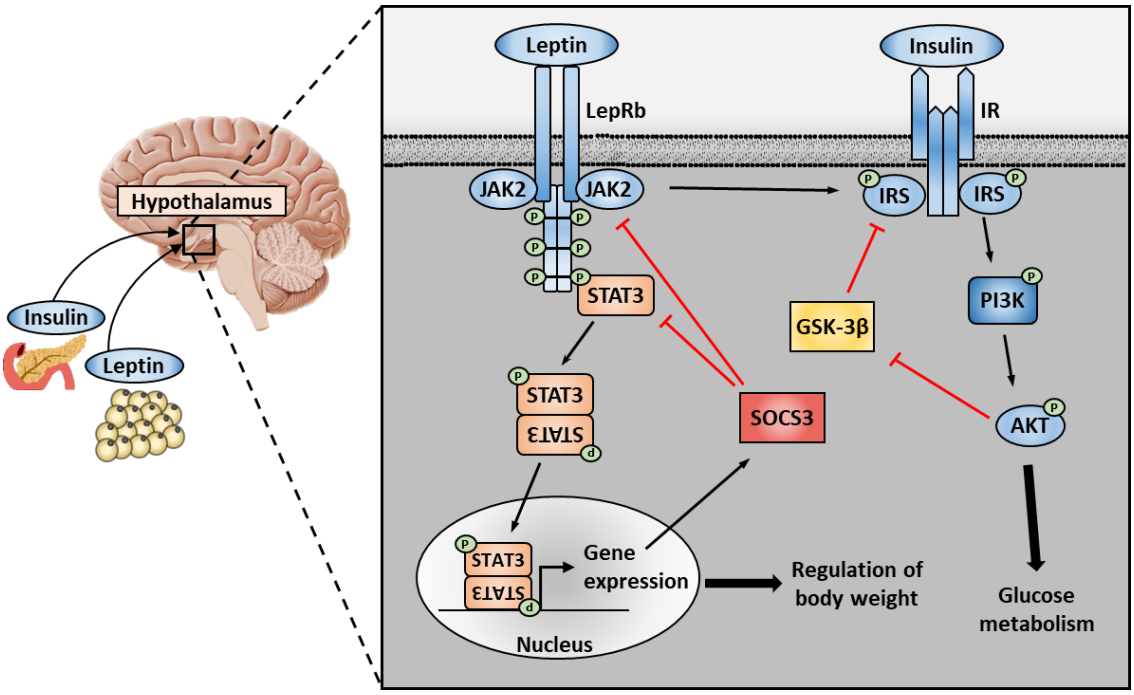

Figure 1: Central regulation of energy metabolism via leptin and insulin. Pancreatic insulin and adipose tissue-derived leptin cross the blood-brain-barrier and bind to their respective receptors in the hypothalamus. Upon binding, leptin leads to activation of the intracellular JAK2/STAT3 signalling cascade and the translocation of pSTAT3 homodimers into the nucleus. There, they activate the expression of target genes such as SOCS3, which in turn initiates a negative feedback loop and thereby decreases leptin action. Binding of insulin to IR leads to activation of the intracellular IRS-PI3K-AKT pathway and inhibition of GSK-3β, thereby regulating glucose homeostasis. Furthermore, leptin results in the sensitisation of insulin signalling by modulation of IRS. Glycogen synthase kinase-3β (GSK-3β), Insulin receptor (IR), Insulin receptor substrate (IRS), Janus kinase 2 (JAK2), Leptin receptor (LepRb), Phosphatidylinositol 3-kinase (PI3K), Protein kinase B (AKT), Signal transducer and activator of transcription 3 (STAT3), Suppressor of cytokine signalling 3 (SOCS3).

1.1.4. Adiponectin and its effects on energy metabolism

The cytokine adiponectin is secreted by adipocytes and has been described to possess anti-inflammatory and insulin-sensitizing effects (73, 74). Due to the inversely correlated levels of circulating adiponectin and the amount of adipose tissue, a causative link between obesity and type 2 diabetes based on adiponectin has been proposed (75-77). Qi and colleagues observed rising adiponectin levels in the cerebrospinal fluid of mice after intravenous injections (78). Despite these findings, whether adiponectin is in fact able to cross the blood-brain-barrier or whether it is also expressed in the brain has long been a matter of debate, with some evidence indicating central expression of the hormone (79-81).

Adiponectin has been shown to have very contradictory effects on metabolism, depending on its route of application. While peripherally administered adiponectin had orexigenic and anabolic effects, central administration revealed anorexigenic and catabolic effects on energy metabolism (78, 82, 83). Adiponectin mediates its effects by binding to one of the two adiponectin receptors, AdipoR1 and AdipoR2, both of which are seven-transmembrane domain receptors. Studies conducted in peripheral tissues demonstrated that adiponectin leads to an increase in adenosine monophosphate-activated protein kinase (AMPK) activity, mainly mediated through the interaction with AdiopR1 (83, 84). After adiponectin binds to AdipoR1, the adapter protein phosphotyrosine interacting with PH domain and leucine zipper 1 (APPL1) is activated, leading to phosphorylation of AMPK at the positive phosphorylation site threonine 172. AMPK monitors the energy status of the cell and phosphorylation at threonine 172 results in an increase in food intake (85).

Notably, both AdipoR1 and AdipoR2 were found to be expressed in the hypothalamus and are located on NPY/AgRP as well as POMC/CART neurons in the ARC (84, 86, 87). Furthermore, APPL1 was shown to phosphorylate and activate JAK2 and IRS1-4, thereby suggesting a crosstalk between adiponectin and insulin as well as leptin signal transduction (73). Most of our knowledge about the effects and the mechanisms underlying adiponectin signal transduction derives from peripheral studies. However, whether central adiponectin signalling is mediated similarly and how it affects glucose and energy metabolism remains to be further determined.

1.1.5. WNT/β-catenin signalling pathway

The WNT pathway is a highly conserved signal transduction pathway that is present in species throughout all of animal kingdom, from sponges and worms to insects and mammals. It regulates numerous cellular processes, such as stem cell differentiation and proliferation and has been well characterized in tumorigenesis and embryogenesis (88-90). Much of our early knowledge about the WNT pathway derived from developmental studies conducted in the fruit fly *Drosophila melanogaster*. The term WNT is composed of the gene names *wg* (*wingless*), characterized in *D. melanogaster*, and *int-1* (*integration-1*), characterized in mice (91, 92). Both described the same highly conserved ligand, therefore later named WNT-1.

As of today, three different WNT pathways have been identified, which are classified as either non-canonical or canonical. The non-canonical pathways are β-catenin-independent. Of those, the WNT/planar cell polarity (PCP) pathway regulates cytoskeletal rearrangements as well as cell migration and tissue polarity during development (93, 94). The WNT/Ca^{2+} pathway, on the other hand, regulates intracellular Ca^{2+} concentrations and activates various kinases, such as the protein kinase-C (94-96). The canonical, β-catenin-dependent WNT pathway is most prominently involved in proliferation, differentiation and cell survival during development, whereas aberrant pathway activation is linked to carcinogenesis and the pathogenesis of other diseases, such as Alzheimer's disease (97, 98). In the last decade, intriguing evidence was provided, linking the WNT/β-catenin pathway to the pathogenesis of type 2 diabetes and other metabolic risk factors. Polymorphisms in the genes encoding for T-cell factor-7 (TCF-7) and low-density lipoprotein receptor-related protein-6 (LRP-6) were shown to be associated with a higher risk of developing type 2 diabetes in humans (99-102).

While both canonical and non-canonical WNT pathways include the G protein-coupled, seven-transmembrane domain receptor Frizzled (Fz) (103-105), the co-receptor family LRP-5/6 is specific for the canonical, β-catenin-dependent WNT pathway (106-108). In mammals, the WNT protein family consists of 19 different WNT ligands (WNTs). The WNT pathway involves several regulatory steps for its activation. While in steady-state, receptors are intracellularly phosphorylated and thereby inhibited. Additionally, there are several classes of extracellular antagonists, such as Dickkopf-related protein-1

(DKK-1) and secreted Frizzled-related proteins (SFRP). While DKK-1 exclusively targets the canonical WNT/β-catenin pathway by binding and blocking LRP-5/6 receptors (109), members of the SFRP family act on WNT signalling in general by binding to WNTs, due to their close sequence homology to the WNT-binding domain of Fz receptors (110, 111).

In the absence of WNT stimulation, which represents the steady-state of the canonical WNT/β-catenin pathway, a β-catenin destruction complex lingers in the cytoplasm, which contains the pathway's key regulatory enzyme GSK-3β, casein kinase-1α (CK-1α), adenomatous polyposis coli (APC), dishevelled (Dsh), as well as the scaffolding protein Axin (112-114). Cytoplasmic β-catenin is bound by this destruction complex and phosphorylated by GSK-3β, thereby targeting β-catenin for ubiquitination and proteasomal degradation (115, 116).

The WNT/β-catenin pathway is activated when extracellular WNTs bind to Fz receptors, leading to heterodimerisation between those and the co-receptor LRP-5/6 and resulting in the recruitment of Dsh to the receptor complex. In the next stage, the destruction complex is recruited and CK-1α phosphorylates and thereby activates LRP-5/6 at its phosphorylation site serine 1490 (106). Phosphorylated LRP-5/6 inhibits the destruction complex and GSK-3β is targeted for negative phosphorylation at serine 9 and is thereby inhibited (117). As a consequence of this inhibition, hypophosphorylated β-catenin is stabilized and accumulates in the cytoplasm, before it translocates into the nucleus. Here, it acts as a co-transcriptional factor by activating the transcription factors TCF-7 and lymphoid enhancer factor (LEF). This leads to the transcription of WNT target genes, such as *Cyclin-D1* and *Axin-2* (118) (Figure 2).

Recently, we provided strong evidence suggesting that hypothalamic WNT signalling is involved in the neuroendocrine control of energy metabolism in genetically obese and diabetic $Lep^{ob/ob}$ mice (119, 120). Other studies further supported the role of the WNT pathway in energy homeostasis as well as an implication of WNT and leptin signalling in peripheral tissues (121-123). Furthermore, hypothalamic WNT signalling was shown to play a crucial role in adult neurogenesis as well as the cellular and structural remodelling of the hypothalamus (124, 125). Interestingly, alterations in the central WNT signal transduction seem to be at least partially regulated by photoperiod in photoperiod-responsive rats, suggesting an important role of the WNT pathway in the

control of seasonal biology in rats (125-127). However, whether this also applies to other seasonal species and whether hypothalamic WNT signalling is regulated by temporal rhythms remains to be determined.

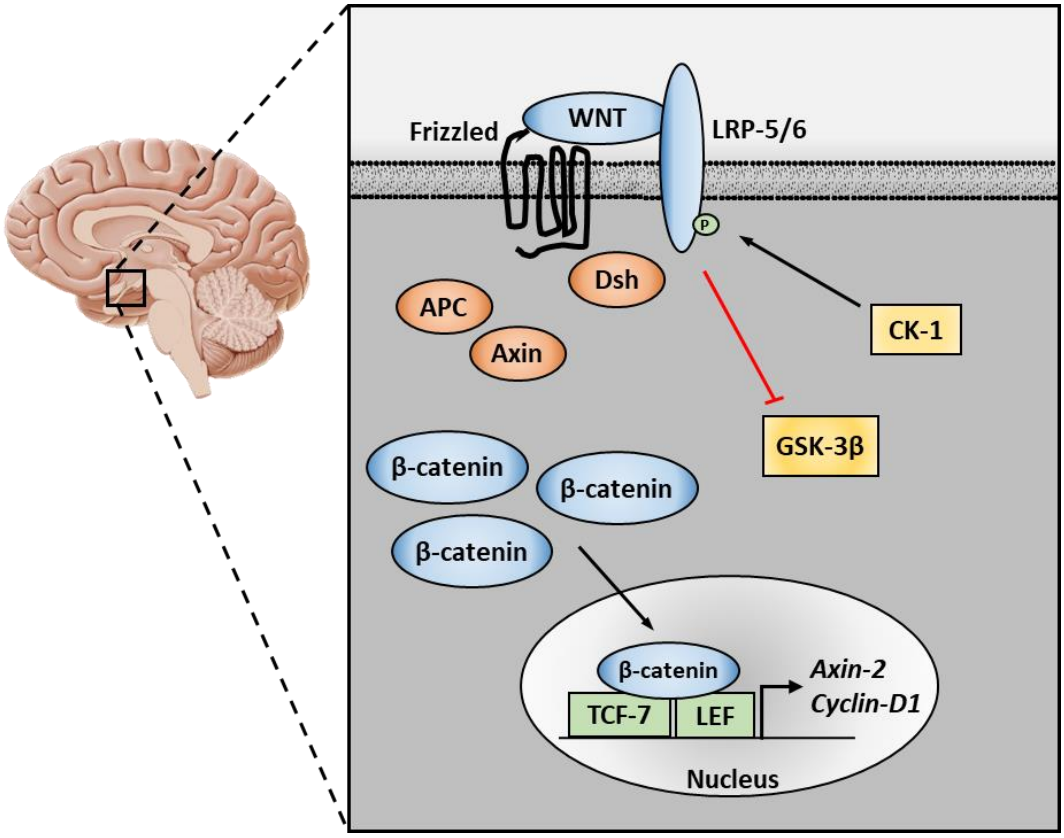

Figure 2: WNT/β-catenin signalling pathway in the presence of WNT ligands. Upon binding of WNT ligands to their receptors Frizzled and LRP-5/6, CK-1 phosphorylates LRP-5/6, which in turn results in the inhibition of GSK-3β. As a result, β-catenin is stabilized and translocates into the nucleus, where it activates the transcription factors TCF-7 and LEF, leading to the expression of WNT target genes such as *Axin-2* and *Cyclin-D1*. Adenomatous polyposis coli (APC), Casein kinase 1 (CK-1), Dishevelled (Dsh), Glycogen synthase kinase-3β (GSK-3β), Lymphoid enhancer factor (LEF), Low-density lipoprotein receptor-related protein 5/6 (LRP-5/6), T-cell factor 7 (TCF-7).

1.2. Biological rhythms in life on Earth

All living organisms are exposed to ever-changing environmental conditions. Daily rotations of the earth around its axis generate distinct differences in the amount of light, temperature, humidity and various other environmental factors between day and night. The annual orbit of the earth around the sun results in the origin of seasons, due to Earth's axial tilt relative to its ecliptic plane. This leads to seasonal periodicity of day length (photoperiod), the intensity of light, weather conditions, temperature and food availability. In temperate and polar climate zones, these changes are specifically pronounced. Warm summers accompanied by a long photoperiod and plenty of food alternate with cold winters accompanied by a short photoperiod and limited food supplies. To survive in these varying conditions, organisms must be able to anticipate these changes and optimize their metabolism and behaviour accordingly. Animals have evolved to be either diurnal or nocturnal, depending on factors such as their source of food and the presence of predators. Seasonal adaptations involve numerous behavioural, morphological and physiological modifications, including, amongst other things, reproduction, energy metabolism, body weight and pelage. To ensure these adaptations are accomplished in time, animals need a reliable environmental cue that notifies them of upcoming seasonal changes. While temperature and weather conditions can be rather variable, the photoperiod is always precise and is therefore used by a large variety of organisms to predict environmental changes. However, these daily and seasonal phenotypic oscillations are not merely passive responses to environmental changes. Instead, they are generated endogenously. The mechanisms that underlie both adaptive systems are closely interlinked and will be discussed in the next chapters.

1.2.1. Circadian rhythmicity

The notion of an internal timekeeping system that runs independent from external cues was first documented in the early 18th century, when French astronomer Jean-Jacques d'Ortous de Mairan observed the daily rhythm of leave movement of a *Mimosa* plant. De Mairan reported that the rhythmic opening and closing of the plant's leaves persisted even in constant darkness (128). About a century later, the French-Swiss botanist Alphonse de Candolle repeated de Mairan's experiment and recorded that

while in constant darkness, the rhythmic opening of leaves occurred not every 24 hours, but one hour earlier each day (129). This observation sparked further research in the field of chronobiology and eventually led to the introduction of the term circadian (derived from the Latin *circa diem*, meaning 'about a day'), referring to endogenously generated rhythms of approximately 24-hour cycles (130). Today we know that all organisms depict circadian rhythms in physiology and behaviour, from simple cyanobacteria to mammals (131). Without external entrainment, the free-running period of circadian rhythms deviates slightly from 24 hours. Generally, in nocturnal animals it is slightly shorter than 24 hours, whereas diurnal animals show a slightly longer free-running period.

1.2.1.1. The suprachiasmatic nuclei as the master circadian clock

In 1972, two independent research groups found evidence that the master pacemaker of circadian rhythms in mammals is located in the anterior hypothalamus, directly above the optic tract. Lesions in this brain region, later named the suprachiasmatic nucleus (SCN), resulted in the complete loss of circadian rhythms (132, 133). The SCN was fully verified as the central master pacemaker by an elegant study performed in 1990 in hamsters. Wildtype hamsters were SCN-lesioned and received SCN transplants from hamsters with a clock gene mutation, which displayed circadian rhythms with a shorter free-running period than wildtypes. Intriguingly, wildtype hamsters with mutant SCN transplants now displayed the same shortened free-running period, confirming that the SCN dictates peripheral circadian rhythms (134).

As the central circadian clock, the SCN controls various local clocks, both in other brain areas and the periphery (135-137). To distinguish between those two different clock systems, the term 'peripheral clocks' was introduced for the latter, in opposition to the central clock. Interestingly, local outputs from peripheral clocks remain rhythmic even without a functional input from the SCN. However, all these peripheral circadian rhythms then desynchronize from each other (138-143), suggesting that the main role of the SCN is to align peripheral clocks and ensure a smooth coordination between an organism's physiology and behaviour.

Circadian clocks feature three basic components: 1) they are endogenously generating circadian rhythms that have a free-running period of approximately 24 hours, meaning that they persist under constant conditions; 2) they receive input signals and are entrainable by these external cues, called *Zeitgebers*, of which light is the primary entrainment signal (144, 145); and 3) they generate output signals that mediate physiological and behavioural rhythms, which display a 24-hour oscillation (146).

1.2.1.2. Molecular clockwork of biological clocks

On a molecular level, the mechanism of the circadian clock is driven by a cell-autonomous rhythmic transcriptional-translational feedback loop that is present in virtually all cells. The first clock gene was discovered in 1971 in *Drosophila* and named *Period* (147). Since then, the clock gene machinery has been largely unravelled. Joseph Takahashi and colleagues identified the first mammalian clock gene responsible for circadian rhythms in behaviour in 1994 and named it *circadian locomotor output cycles kaput* (*Clock*) (148). The positive arm of the mammalian feedback loop consists of the proteins CLOCK and brain and muscle ARNT-like protein 1 (BMAL-1) (135), which heterodimerise and bind to E-box regions in promotors of the clock genes *Period* (*Per1 – 3*) and *Cryptochrome* (*Cry1/2*), thereby inducing their transcription (149, 150). The protein products PER and CRY represent the negative arm of the feedback loop. PER/CRY heterodimers translocate into the nucleus and inhibit the activity of CLOCK/BMAL-1 heterodimers, thereby inhibiting their own transcription (151). PER and CRY are post-translationally targeted for degradation by casein kinases (CK-1ε/δ) and GSK-3β (151-153). The degradation of PER and CRY subsequently leads to the initiation of a new cycle. This feedback loop takes roughly 24 hours to completion, thereby defining the near-24-hour period of circadian rhythms. Additionally, CLOCK/BMAL-1 initiates transcription of *Rev-erbα* (*reverse erythoblastoma*) and *Rorα/β* (*retinoid orphan receptor*) nuclear receptors. Their protein products in turn either inhibit (REV-ERBα) or activate (RORα/β) *Bmal-1* transcription (Figure 3).

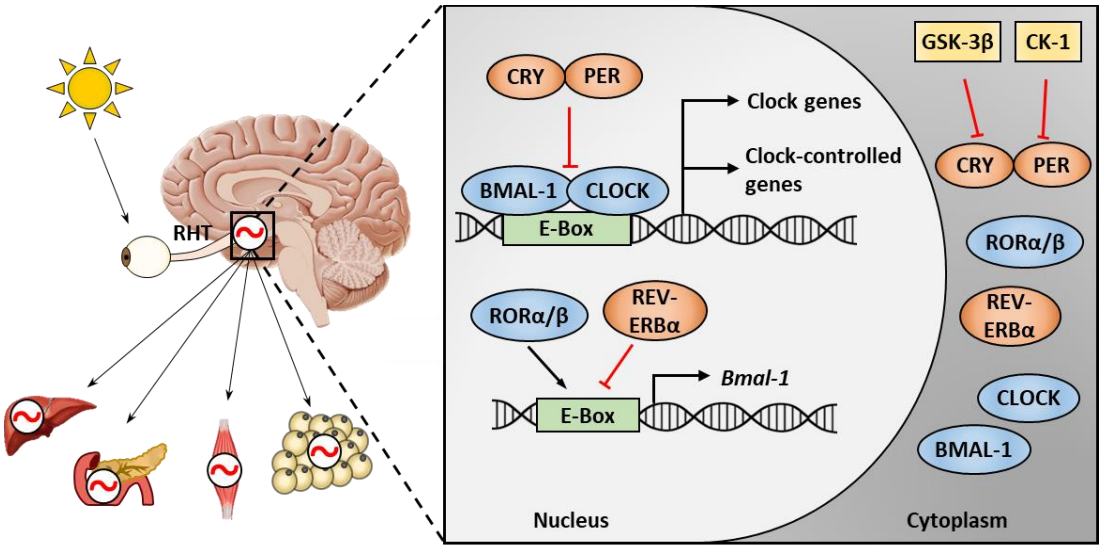

Figure 3: Cell-autonomous regulation of the circadian clock in mammals. The central circadian clock, which resides in the SCN of the hypothalamus, receives light input via the RHT and synchronises peripheral circadian clocks that are present in virtually all tissues. On the molecular level, the transcription factors CLOCK and BMAL-1 activate gene expression of *Per*, *Cry, Rev-erbα and Rorα/β* as well as a variety of other target genes that are clock outputs. PER/CRY heterodimers in turn inhibit the transcriptional activity of CLOCK/BMAL-1, thereby preventing their own transcription. Additionally, *Bmal-1* expression is initiated by RORα/β, but repressed by REV-ERBα. In the cytoplasm, CK-1 and GSK-3β target PER and CRY for degradation, thereby initiating the start of a new transcriptional-translational cycle. Brain and muscle ARNT-like protein 1 (BMAL-1), Casein kinase 1 (CK-1), Circadian locomotor output cycles kaput (CLOCK), Cryptochrome (CRY), Glycogen synthase kinase 3β (GSK-3β), Period (PER), Retinohypothalamic tract (RHT), Reverse erythoblastoma (REV-ERBα), Retinoid orphan receptor (RORα/β), Suprachiasmatic nucleus (SCN).

1.2.1.3. Entrainment signals in circadian clocks

The SCN receives light input directly from melanopsin-containing ganglion cells in the retina of the eyes via the retinohypothalamic tract (RHT) and ultimately synchronises peripheral clocks via circulating humoral factors and autonomic innervation (154-157). Apart from light, other external cues have been proposed to be able to entrain circadian clocks, such as social interactions, exercise and feeding patterns. Interestingly, HFD consumption leads to a disruption of circadian rhythms in the liver and in eating

behaviour of mice after just one week. However, at this point neither the central circadian clock in the SCN nor other peripheral clocks were compromised (158), showing that not only the time of food intake, but also the diet composition affects circadian clocks. Furthermore, these results demonstrated that not all circadian clocks are affected by the same external factors to the same extent and that the brain areas mediating the disruptions in eating behaviour caused by HFD must be located downstream of the SCN. Food intake had already been identified as a powerful SCN-independent entrainment signal for circadian rhythms more than 40 years ago (159, 160). More recently, the existence of a food-entrainable oscillator involving AgRP/NPY neurons in the hypothalamus has been proposed (161). Notably, as discussed in chapter 1.1.1, AgRP/NPY neurons play an important role in the leptin-mediated control of body weight and metabolism.

1.2.1.4. Circadian clock and metabolism

Over the last 15 years, a close link of the circadian clock and metabolism has been demonstrated in numerous studies (162-167). In mice, SCN lesions as well as various clock gene mutations were shown to cause metabolic disorders, including obesity, hyperlipidaemia, hyperglycaemia and an impairment of glucose homeostasis and insulin signalling (163, 168-171). The research group of Joseph Takahashi discovered that a missense mutation in the murine *Clock* gene results in the loss of rhythmic expression of metabolic genes in liver, pancreas and muscle as well as a disruption of glucose and lipid homeostasis, ultimately leading to the development of obesity (170, 171). Similar metabolic syndrome phenotypes occur after mutations in other clock genes, such as *Bmal-1* and *Per2* (164, 172-176). In humans, circadian disruptions such as continuous shift-work and social jet lag have been shown to result in symptoms of the metabolic syndrome. These include impaired glucose tolerance, serving as an indicator for prediabetes, as well as decreased insulin sensitivity, increased body mass index (BMI) and increased mean arterial blood pressure, indicating cardiovascular complications (177, 178). Results from our laboratory and from others demonstrate that chronic circadian misalignment, evoked by continuous exposure to jet lags, causes reduced hypothalamic leptin sensitivity and elevated body weight in mice [(179) and our own unpublished observations]. This offers a potential explanation for the

prominent correlation between circadian misalignment and obesity as observed in humans (177). While circadian misalignment was shown to cause metabolic dysfunctions in both rodents and humans, HFD feeding was in return shown to disrupt behavioural and molecular circadian rhythms. Consumption of HFD leads to arrhythmic feeding patterns, locomotor activity and expression of circadian clock genes (158, 180, 181). As mentioned above, AgRP/NPY-expressing neurons in the hypothalamus were shown to play an important role as a component of a food-entrainable oscillator (161). These neurons express leptin receptors and are crucial for the maintenance of metabolism and body weight. Interestingly, ARC-targeted ablation of leptin-sensitive neurons in rats leads not only to the development of obesity, but also to an attenuation of feeding rhythms. Ablation of leptin-sensitive neurons in other nuclei of the hypothalamus, on the other hand, did not cause arrhythmic feeding (182). This suggests a unique involvement of the ARC in generating feeding rhythms over other hypothalamic areas involved in metabolic control. Whether leptin signal transduction in the ARC is controlled by a circadian rhythm and how HFD feeding interferes with central leptin sensitivity at different times throughout the day has not been investigated to date.

1.2.2. Time-restricted food intake has beneficial effects on metabolic health

Time-restricted feeding (TRF) is a new diet strategy with apparent efficacy in promoting weight loss and preventing metabolic diseases in both fruit flies and rodents (183, 184). In many organisms, including bacteria, yeast, nematodes, fruit flies and mice, temporary caloric restrictions lead to an extension of lifespan (185). TRF limits energy intake to certain times each day, followed by an extended period of food deprivation. This feeding regimen has been shown to attenuate peripheral inflammation by reducing circulating levels of pro-inflammatory cytokines in mice (185, 186). Two recent studies suggested that the beneficial effects of TRF on health seem to depend on the time of food access throughout the day. Time-restricted access to HFD exclusively during the inactive phase of mice (light phase) leads to increased body weight compared with mice that have access to HFD exclusively during their active phase (dark phase), even though both groups have the same overall caloric intake (181). In line with these results, access to HFD exclusively during their active phase prevents

mice from developing symptoms of metabolic disease, such as obesity, hyperinsulinemia, glucose intolerance and inflammation compared with mice with *ad libitum* access to HFD, while both groups consume a similar amount of calories (184). In humans, restriction of food intake to a maximum of 12 hours per day leads to weight loss in overweight individuals (187). Notably, in this study food access was only restricted to a certain amount of time each day, but not strictly to the participants' active (light) phase. Additionally, while body weight was monitored during this study, caloric intake was not and the observed weight loss might be due to reduced caloric intake instead of a sole effect of circadian timing of food intake. The importance of circadian timing of TRF has so far mainly distinguished between the active and inactive phase in rodent studies. To what extent beneficial effects of TRF on metabolic health depend on circadian timing and during which specific periods throughout the 24-hour cycle TRF can reverse detrimental effects of HFD remains to be examined further.

1.2.3. Seasonal rhythmicity

Many organisms use the annual progression of day length as a cue to anticipate upcoming seasonal changes in environmental factors. This ability to adapt their phenotype accordingly is called photoperiodism and has first been described in conjunction with the seasonal flowering of tobacco plants and was since discovered in a wide variety of species (188). Not all animals are influenced by photoperiod to the same extent. Therefore, only species whose phenotype significantly depends on the photoperiod are considered as photoperiodic, or seasonal. In humans, mice and rats, for instance, reproduction and other physiological processes are less dictated by seasons and therefore those are not considered as photoperiodic species. In animals such as sheep and Djungarian hamsters, on the other hand, reproduction is highly seasonal.

1.2.3.1. Seasonal encoding via circadian oscillation

Melatonin is a crucial hormone for the regulation of circadian rhythmicity of sleep and wakefulness and other physiological functions (189). It is produced exclusively during the dark phase by the pineal gland and its secretion is controlled by a neural pathway originating from the SCN (190). At night, the SCN stimulates norepinephrine release in

the pineal gland, resulting in increased activity of the melatonin synthesis enzyme arylalkylamine N-acetyltransferase (AANAT) (191, 192). The duration of melatonin production during night-time is dependent on the photoperiod, with gradually prolonged production from summer to winter and shortening production from winter to summer. This led to the assumption that changes in photoperiod are mediated through the circadian oscillation of melatonin production (192-194). Furthermore, the electrical activity pattern of the SCN is compressed during short day photoperiod (resembles winter) and extended during long day photoperiod (resembles summer), resulting in changes in the duration of behavioural activity and other physiological processes between those photoperiods (195, 196).

1.2.3.2. Seasonal adaptation of **Phodopus sungorus**

Seasonal mammals have developed different adaptive mechanisms to survive in a seasonally changing environment. Winter-specific strategies include accumulation of large fat deposits or hibernation, methods that are mainly used by larger mammals. Small mammals, on the other hand, decrease their body weight in order to reduce their energy requirements (197). Since a reduction in body mass leads to a relatively larger surface area and increased heat loss (198), this strategy has to be accompanied by other morphological and physiological adaptations. The Djungarian hamster, *Phodopus sungorus*, is a powerful model organism to study seasonal adaptations in mammals. Originating from the steppes of Siberia and the region of Djungaria, this small rodent reduces its body weight by up to 40% during winter. This reduction of body mass is mainly due to a loss of white adipose tissue (199-201). During winter, male hamsters undergo testicular regression and become infertile. To compensate for the loss of body mass and thereby the increased heat loss, hamsters grow a more thermally insulated winter pelage, which turns white compared with their grey-tinged summer pelage and thereby also improves their camouflage (202, 203). Additionally, the cold tolerance of winter-adapted hamsters is improved due to nonshivering thermogenesis in brown adipose tissue (203). The annual cycle of body weight is accompanied by a seasonal, reversible switch in hypothalamic leptin sensitivity. Under laboratory conditions, the summer-like photoperiod is mimicked by an exposure to 16 hours of light and 8 hours of dark (long day, LD), whereas the winter-like photoperiod is mimicked by an

exposure to 8 hours of light and 16 hours of dark (short day, SD). During LD, hamsters have high circulating concentrations of leptin, but are resistant to the central effects of the hormone, whereas they have lower circulating concentrations and are highly leptin sensitive during SD (201, 204, 205). The expression of *Socs-3* in the ARC of hamsters seems to play a crucial role in this cyclic leptin sensitivity (48, 206). After a switch from LD to SD, *Socs-3* gene expression decreases promptly, long before the amount of white adipose tissue and circulating concentrations of leptin change (48). This leads to an increase in leptin sensitivity during SD and due to the yet high leptin levels results in the mediation of anorexigenic and catabolic effects.

1.3. Aims and objectives

Development of hypothalamic leptin resistance is a key event in the manifestation of obesity and related metabolic diseases, such as type 2 diabetes. Over the last decades, significant process has been made in uncovering the neuroendocrine mechanisms that link these metabolic disorders. However, the environmental incitements of our modern age that trigger the disruption of molecular mechanisms underlying leptin resistance are still not entirely understood. The aim of this doctoral research study was to gain new insights into regulatory processes that lead to the development of leptin resistance and the disruption of energy metabolism. In this regard, the main objectives were to determine:

1. Whether other adipocyte-derived hormones, beside leptin, are involved in the neuroendocrine control of energy metabolism.

2. Whether WNT signalling is involved in the neuroendocrine control of energy metabolism in the seasonal rodent *Phodopus sungorus*.

3. Whether hypothalamic leptin signalling and whole body metabolism are modulated by a 24-hour rhythm.

4. How DIO interferes with hypothalamic leptin signalling and whole body metabolism throughout the course of the day.

5. Whether TRF can reverse the detrimental effects of DIO on metabolic health.

1. To examine whether other adipocyte-derived hormones, beside leptin, are involved in the neuroendocrine control of energy metabolism, the adipokine adiponectin was investigated. Therefore, its hypothalamic expression profile was examined and the effects of central adiponectin on glucose homeostasis as well as its implication in other neuroendocrine signalling pathways in lean wildtype and obese mice were analysed (207).

2. To determine whether WNT signalling is involved in the neuroendocrine control of energy metabolism in the seasonal rodent *Phodopus sungorus*, the hypothalamic expression profile of WNT pathway-related genes was examined at specific times throughout the 24-hour cycle in adult LD and SD acclimated hamsters. Next, the effect of leptin on hypothalamic WNT pathway activation was analysed (208).

3. To determine whether hypothalamic leptin signalling and whole body metabolism are modulated by a 24-hour rhythm, the activation of the leptin signal transduction marker STAT3 was analysed every 3 hours throughout the 24-hour cycle in wildtype mice. Furthermore, circulating metabolic markers were examined at these time points.

4. To investigate how DIO interferes with hypothalamic leptin signalling and whole body metabolism throughout the course of the 24-hour cycle, the same markers as described above were analysed every 3 hours throughout the day in DIO mice that received HFD.

5. To determine whether TRF has beneficial effects on metabolic health and can reverse the detrimental impairment of normal energy metabolism caused by DIO, mice received *ad libitum* access to low-fat diet (LFD) or HFD (control groups) or time-restricted access to HFD during different 6-hour periods throughout the 24-hour cycle. Metabolic measurements of energy metabolism and behaviour were examined and circulating metabolic markers were analysed.

2. General methods

2.1. Animals

All experimental protocols involving animals were performed in accordance with the German animal ethics legislation or the New Zealand Animal Welfare Act and associated guidelines, as appropriate, and received approval by the respective authorities for animal ethics.

2.1.1. Djungarian hamsters, *Phodopus sungorus*

Adult female Djungarian hamsters were used for the experiments described in chapter 4.2. Hamsters were bred within the Department of Biology at the Philipps University of Marburg in Germany and were randomised and housed individually at an ambient temperature of 21 ± 1˚C with *ad libitum* access to a hamster-specific standard chow diet and water. Hamsters were maintained either under LD (16:8 hours light/dark cycle) or SD (8:16 hours light/dark cycle) conditions for eight weeks prior to experiments to ensure full adaptation to the respective photoperiods.

2.1.2. Mice

For experiments described in chapter 4.1, adult male C57BL/6J wild-type ($Lep^{+/+}$) and leptin-deficient $Lep^{ob/ob}$ mice were purchased from Janvier (France). They were randomised and housed individually under a 12:12 hours light/dark cycle at an ambient temperature of 22 ± 1˚C with *ad libitum* access to food and water. Mice received either LFD with 10% energy from fat (kcal), moderate HFD (mHFD) with 45% energy from fat (kcal) or HFD with 60% energy from fat (kcal).

Adult male C57BL/6J mice bred at the University of Otago Taieri Resource Unit were used for experiments described in chapter 4.3. Animals were randomised and housed individually under a 12:12 hours light/dark cycle at an ambient temperature of 22 ± 1˚C

with *ad libitum* access to food and water, aside from mice that received time-restricted access to food during the TRF regimen, as described in chapter 4.3. The time periods for TRF were based on our findings about the circadian rhythmicity of leptin sensitivity in lean and DIO mice, as presented in chapter 4.3. Four groups received access to HFD for 6 hours per day, each group during a different period. Thereby, one group had access to food solely during the light (inactive) phase from *Zeitgeber time* (ZT) 3 – ZT9, one group solely during the dark (active) phase from ZT15 – ZT21 and two groups each during equal times of light and dark (both inactive and active) phase. In those activity-independent groups, mice received HFD either during their relative leptin sensitive phase from ZT9 – ZT15 or their relative leptin resistant phase from ZT21 – ZT3. Mice received either LFD with 10% energy from fat (kcal) or HFD with 60% energy from fat (kcal).

2.2. Immunohistochemistry

2.2.1. Collection of brain tissue for immunohistochemistry

Treatment of animals prior to transcardial perfusions is described in the respective subchapters in chapter 4. Animals were deeply anaesthetised with an overdosed intraperitoneal (ip) injection of sodium pentobarbital (200 mg/kg body weight) with heparin to prevent blood clotting. Upon confirmation of deep anaesthesia by testing the pedal withdrawal reflex animals were transcardially perfused. Therefore, the chest cavity was opened, a needle was inserted into the left ventricle of the heart and the right atrium was cut open. Animals were perfused with saline, followed by perfusion with ~20 mL of 4% paraformaldehyde in 0.1 M phosphate buffer (PFA; pH 7.5). Brains were dissected and post-fixed in 4% PFA for 4 hours, followed by 48 hours storage in 30% sucrose solution in 0.1 M phosphate buffer at 4˚C for osmotic dehydration of brains. Brains were then rapidly frozen in 2-methylbutane at -40˚C and stored at -80˚C. Coronal brain sections (30 µm) were collected throughout the extent of the ARC, spanning the hypothalamic region from approximately -2.7 to -0.8 mm relative to Bregma according to the atlas of the mouse brain (209). Sections were stored in

cryoprotectant (30% sucrose, 30% ethylene glycol, 1% polyvinylpyrrolidone, in 0.2 M phosphate-buffered saline) at -20˚C.

2.2.2. Antigen retrieval immunohistochemistry

Antigen retrieval steps were performed to break aldehyde bonds between proteins that were formed in the fixation process during perfusion. This increases immunoreactivity of the brain tissue. Unless stated otherwise, all reagents were diluted in 0.1 M Tris-buffered saline (TBS) and incubation steps were performed at room temperature.

Free-floating brain sections were rinsed three times in 0.1 M TBS to remove cryoprotectant. This step was carried out between all subsequent incubations. For antigen retrieval and blocking of endogenous peroxidase activity, sections were treated with 10% methanol, 1% sodium hydroxide and 1% hydrogen peroxide in water for 20 minutes, followed by incubation in 0.3% glycine for 10 minutes as well as 0.03% sodium dodecyl sulphate for 10 minutes. Next, brain sections were incubated for 1 hour in blocking solution consisting of 1% normal goat serum and 5% bovine serum albumin in TBS with 0.5% Triton-X (TBS-TX) to prevent non-specific binding of the antibody to tissue, followed by incubation in the respective primary antibody (diluted in blocking solution) for 16 hours at 4˚C. Triton-X is used to increase cell membrane permeability and improve the penetration of the primary antibody into the cytoplasm. On the next day, sections were incubated for 1 hour with the biotinylated secondary antibody (diluted in blocking solution), which was targeted against the primary antibody host species. This was followed by 1 hour of incubation in avidin-biotin complex solution. Finally, the signal was developed with diaminobenzidine solution, giving a grey precipitate. Stained brain sections were mounted onto gelatinised object slides and dehydrated in a series of ethanol solutions of increasing concentrations (50% - 100% ethanol), followed by a final wash in xylene. Sections were then coverslipped, using DPX mounting medium.

2.3. Analysis of hypothalamic gene expression

2.3.1. Collection of brain tissue for *in situ* hybridization

Treatment of animals prior to tissue collection is described in the respective subchapters in chapter 4. For *in situ* hybridization, animals were decapitated and brains were rapidly frozen on dry ice. Coronal brain sections (16 µm) were collected throughout the extent of the ARC, spanning the hypothalamic region from approximately -2.7 to -0.8 mm relative to Bregma according to the atlas of the mouse brain (209). Sections were mounted onto object slides and stored at -80˚C.

2.3.2. Preparation of riboprobes

To create riboprobes specific for the genes of interest, the hypothalamus of a hamster or mouse, respectively, was homogenised and ribonucleic acid (RNA) was extracted. Using reverse transcriptase, an enzyme functioning as a RNA-dependent deoxyribonucleic acid (DNA) polymerase, hypothalamic RNA was transcribed into complementary DNA (cDNA). In the next step, polymerase chain reaction (PCR) was performed to amplify cDNA fragments of interest. Therefore, specific primers were used, resulting in the amplification of specific genes sections. The primers used for each study are listed in the respective subchapters in chapter 4. Amplified cDNA fragments were purified and extracted with an agarose gel and via ligation into pGEM®-T Easy vector (Promega Corp.) and subsequent transformation into competent DH5-α *Escherichia coli* cells, cDNA was replicated to a great extent. The replicated DNA of interest was separated from the cells' own structures by minipreparation, followed by sequencing and linearization of the plasmid DNA. To create radioactive RNA that is able to bind to its complementary messenger RNA (mRNA) in tissue, the generated cDNA was used as a template and *in vitro* transcription was performed, using a DNA-dependent RNA polymerase. This polymerase synthesises RNA with provided ribonucleoside triphosphates, including (^{35}S)-radiolabelled uracil triphosphates.

2.3.3. *In situ* hybridization

Brain sections were fixed in 4% PFA for 20 minutes followed by acetylation in 0.1 M triethanolamine and acetic anhydride in order to block non-specific binding sites. Next, sections were dehydrated in a series of ethanol solutions of increasing concentrations. This was followed by a 16-hour hybridization reaction at 58˚C. Therefore, object slides were covered with a hybridization solution containing radiolabelled riboprobes. On the next day, sections were treated with ribonuclease A, leading to the degradation of unbound radiolabelled RNA fragments and preventing false positive detection of tissue-specific mRNA. Subsequently, brain sections were desalted, dehydrated and exposed to an X-ray film sensitive to decay emissions, giving a black precipitation on the radiograph.

2.4. Respirometry

Metabolic measurements were performed using a multichannel respirometry system (Promethion, Sable Systems International), allowing synchronised monitoring of energy metabolism and behaviour. The Promethion system used in this study is an open-flow multiplexed system, with up to eight cages sharing one gas analyser. This allows the gas analyser to take brief metabolic measurements of the animal in each cage at intervals of a few minutes. To accurately determine the effect each animal has on air analysed from its cage relative to background air around the cage, continuous baseline measurements of the surrounding air are required (210). Energy expenditure was determined by indirect calorimetry, a method by which oxygen consumption and carbon dioxide production are synchronously measured, thereby accurately evaluating an endothermic animal's metabolic rate. The air flow rate was adjusted to 2000 mL/min, guaranteeing complete air exchange of 15 times per hour in compliance with Institutional Animal Care and Use Committee mouse calorimetry standards. The system synchronously measured oxygen consumption, carbon dioxide production, energy expenditure, food intake, body weight and locomotor activity. Access to food was restricted to defined 6-hour periods each day (specified in chapter 2.1.2) by

programming the food hopper doors in each individual cage to open and close at specific times. To compare metabolic parameters specific for the different feeding periods of the TRF groups, raw data were binned into the defined 6-hour periods using a customized automated analysis script kindly created and provided by Sable Systems International. The average of each of the four 6-hour periods recorded over three consecutive days was then assessed and compared between the different animal groups.

2.5. Analysis of blood-borne metabolic signals

Circulating levels of leptin, insulin and glucose were measured using enzyme-linked immunosorbent assays (ELISA) and glucose assays. Therefore, animals were decapitated; blood was collected and immediately placed on ice to allow coagulation, followed by centrifugation for 20 minutes at 4 °C and 13000 rpm. Extracted serum and plasma were stored at -80˚C. Assays were carried out using 96 well microplates and all samples were assayed in duplicate.

2.5.1. Leptin ELISA

Because circulating leptin levels of mice fed HFD were expected to be above the sensitivity range of the leptin ELISA (0.2 to 12.8 ng/mL), serum and plasma samples of those mice were diluted using sample diluent provided within the ELISA kit prior to performing the assay. To measure circulating leptin concentrations, a sandwich ELISA was performed. Here, two sets of antibodies are used to detect mouse leptin in the samples. Mouse serum or plasma samples as well as predefined mouse leptin standards were dispensed into wells together with sample diluent and guinea pig anti-leptin serum and incubated for 20 hours at 4˚C. During this first reaction, mouse leptin in the serum or plasma samples is simultaneously bound to the rabbit anti-leptin antibody coated on the microplate well and the anti-leptin antibody of the guinea pig serum. On the next day, wells were washed using washing buffer to remove unbound material. This step was carried out between all subsequent incubations. For the next step, horseradish

peroxidase (HRP)-conjugated anti-guinea pig antibody was added and incubated for 3 hours at 4˚C to allow binding of the HRP-conjugated antibody to the immobilized complex on the microplate well. This was followed by 30 minutes of incubation with tetramethylbenzidine (TMB) enzyme substrate solution to chromogenically detect the HRP-conjugated antibody. Finally, the enzyme reaction was stopped with sulfuric acid and absorbance was measured using a plate reader. Leptin concentrations in the samples were interpolated using the standard curve and mean absorbance values for each sample.

2.5.2. Insulin ELISA

To determine circulating insulin concentrations, a sandwich ELISA was performed. Mouse serum or plasma samples as well as predefined mouse insulin standards were dispensed into wells together with sample diluent and incubated for 2 hours at 4˚C. During this first reaction, mouse insulin in the serum or plasma samples binds to the guinea pig anti-insulin antibody coated on the microplate well. Subsequently, wells were washed using washing buffer to remove unbound material. This step was carried out between all subsequent incubations. Next, HRP-conjugated anti-insulin antibody was dispensed into the wells and incubated for 30 minutes at room temperature to allow binding of the HRP-conjugated antibody to the immobilized complex on the microplate well. This was followed by 40 minutes of incubation with TMB enzyme substrate solution. Finally, the enzyme reaction was stopped with sulfuric acid and absorbance was measured using a plate reader. Insulin concentrations in the samples were determined by interpolation using the standard curve and mean absorbance values for each sample.

2.5.3. Glucose assay

Serum glucose concentrations were measured performing a multi-step glucose assay. Therefore, mouse serum samples as well as predefined glucose standards were incubated with an enzyme solution containing mutarotase for 5 minutes at 37˚C, leading to the rapid conversion of α-D-glucose to β-D-glucose. The β-D-glucose is then

oxidised and releases hydrogen peroxide, which reacts with the enzyme solution to yield a red dye. Absorbance was measured and serum glucose concentrations were determined by interpolation using the standard curve and mean absorbance values for each sample.

2.6. Analysis of glucose metabolism

To measure glucose tolerance and insulin sensitivity in mice, intraperitoneal glucose tolerance tests (ipGTT) were performed. For respective treatments prior to the ipGTT, see chapter 4.1. Fasted animals received an ip injection of glucose solution (0.75 – 1.0 g glucose/kg body weight) and blood glucose concentration was measured at defined time points (0, 15, 30, 60, 90, 120, 150 and 180 minutes after glucose injection) using a glucometer. Blood was collected by puncturing the facial vein.

Furthermore, hepatic glucose production was analysed by performing an ip pyruvate tolerance test (ipPTT). Pyruvate is an intermediate of gluconeogenesis and the conversion of pyruvate to glucose reflects hepatic glucose production. Mice received an ip pyruvate injection (1.5 g/kg) and blood glucose concentration was detected at defined time points (0, 15, 30, 45, 60, 90, 120, 150 and 180 minutes after pyruvate injection) as described above.

3. General results and discussion

3.1. The role of adiponectin in the central regulation of energy metabolism

Peripheral effects of adiponectin on energy metabolism have been demonstrated to possess anabolic and orexigenic properties (83), whereas the opposite appears to apply to its central effects (78, 82). Adiponectin receptors have been found to be expressed on energy homeostasis-regulating neurons in the ARC (84, 86, 87). However, the role of central adiponectin has been insufficiently studied to date.

3.1.1. Central expression profile of genes involved in adiponectin signal transduction

Whether adiponectin is expressed in the CNS and whether it is able to cross the blood-brain-barrier has so far been discussed controversially. While some studies suggest that adiponectin is expressed in brain tissue (79), others rebut that adiponectin has any direct central effect at all (81).

By performing *in situ* hybridization, we found central expression of *adiponectin*, *APPL1*, *AdipoR1* and *AdipoR2* in the mediobasal hypothalamus of mice, specifically in the ARC (chapter 4.1, figure 1). The gene expression of all investigated genes was dependent on the nutritional state of mice. We detected markedly reduced *adiponectin* mRNA levels in the ARC after 16 hours of food deprivation compared with *ad libitum* fed mice. This regulatory mechanism might compensate for the catabolic and anorexigenic properties described for central adiponectin (78, 82), in order to prevent further body weight loss. In the periphery, on the other hand, circulating adiponectin concentrations are inversely correlated with adipose tissue mass and food deprivation leads to elevated adiponectin secretion (75-77). Regarding the anti-inflammatory and insulin-sensitizing effects described for peripheral adiponectin (73, 74), this increase might be a potential explanation for the beneficial effects of periodic fasting on

metabolic health. Furthermore, due to the anabolic and orexigenic effects of peripheral adiponectin the up-regulation of adiponectin secretion might be a mechanism to antagonize further body weight loss during food deprivation. The down-regulation of *adiponectin* gene expression during fasting might also explain contradictory results from prior studies regarding adiponectin action in the CNS (79, 81). Spranger and colleagues reported that adiponectin does not cross the brain-blood-barrier in either mice or humans, nor did they detect *adiponectin* gene expression in the brain. However, in their study, cerebrospinal fluid (CSF) was sampled from human subjects that had fasted overnight prior to the surgical intervention. Unfortunately, no information about the nutritional state of mice used in those experiments was provided (81).

Interestingly, we found increased *APPL1* and *AdipoR1* gene expression in the ARC of food deprived compared with *ad libitum* fed mice. This might be an adaptive mechanism to ensure sufficient hypothalamic adiponectin signal transduction to compensate for decreased levels of adiponectin. *AdipoR2* showed a trend towards lower gene expression after fasting, although this decrease did not reach significance. However, in both *ad libitum* fed and fasted mice, *AdipoR2* gene expression in the ARC was considerably low suggesting that adiponectin signal transduction via this receptor plays only a minor role in central regulation of metabolism. Furthermore, *AdipoR1* gene expression was increased in mice that received mHFD and HFD, whereas *AdipoR2* gene expression was only elevated in mHFD mice. Leptin-deficient $Lep^{ob/ob}$ mice showed no change in gene expression of both receptors (chapter 4.1, figure 2). These results suggest that hypothalamic adiponectin signal transduction is compromised by DIO, but is independent of functional leptin signal transduction.

3.1.2. Central adiponectin has insulin-sensitizing and anti-inflammatory effects

By performing ipGTTs, we next analysed the effects of centrally administered adiponectin on glucose homeostasis in mice with genetically or diet-induced obesity. Central adiponectin proved to have the same blood glucose-lowering effects as described for peripherally administered adiponectin (74). This was not only the case in leptin-deficient $Lep^{ob/ob}$ mice on LFD and DIO mice that received HFD, but even in

$Lep^{ob/ob}$ mice on HFD, an extremely severe model of obesity (chapter 4.1, figure 3). To determine via which neuroendocrine pathways these beneficial effects on metabolic health are mediated, we measured the activation of several signalling markers of hormone pathways in the hypothalamus (chapter 4.1, figures 4 and 5c, d). Central adiponectin led to an activation of insulin signal transduction as demonstrated by activated pAKT in the VMH of $Lep^{ob/ob}$ mice, while the increase in pAKT immunoreactivity in the ARC only showed a trend towards elevated insulin signalling activation. Inhibition of the negative insulin signalling modulator GSK-3β was also increased in both ARC and VMH after adiponectin administration during DIO. Additionally, central adiponectin led to a decrease in pAMPK immunoreactivity in both ARC and VMH, whereas no effect was observed for the activation of leptin signal transduction in either ARC or VMH after icv adiponectin administration in leptin deficient $Lep^{ob/ob}$ mice. These results suggest that adiponectin mediates its glucose-lowering effects by interacting with hypothalamic insulin signal transduction, without affecting leptin signalling in the hypothalamus as observed in both leptin deficient $Lep^{ob/ob}$ mice and leptin resistant DIO mice. Furthermore, we confirmed the catabolic and anorexigenic properties of central adiponectin (78, 82), as shown by the decrease of AMPK activation, since phosphorylation of AMPK leads to increased food intake (85).

Anti-inflammatory effects have previously been described for peripheral adiponectin (73). By measuring the activation of pro-inflammatory markers in DIO mice, which have been demonstrated to have increased hypothalamic inflammation (211), we found ameliorated hypothalamic inflammation after central adiponectin administration (chapter 4.1, figure 5). These results provide evidence for anti-inflammatory properties of central adiponectin.

3.2. Central WNT signal transduction and its role in the neuroendocrine control of seasonal energy metabolism

The evolutionary highly conserved WNT signalling pathway is best studied for its role in embryogenesis and tumorigenesis (88-90). Recent findings suggest an important role of this pathway in adult neurogenesis and the neuroendocrine control of energy metabolism, in particular in hypothalamic leptin signalling in obese mice (119, 120, 124, 125). Furthermore, hypothalamic WNT signalling is involved in seasonal physiology in photoperiod-responsive rats (125-127). Here, we examined the implication of WNT signalling in the neuroendocrine control of seasonal body weight regulation and annual changes in leptin sensitivity exhibited by *Phodopus sungorus*. Furthermore, we examined whether hypothalamic WNT signalling is regulated by a 24-hour rhythm.

3.2.1. Central expression profile of WNT genes and the effect of photoperiod and time of day on WNT signal transduction in adult *Phodopus sungorus*

We first characterised the hypothalamic expression profile of genes encoding components involved in the WNT pathway by performing *in situ* hybridization. We found gene expression of the WNT pathway ligands *WNT-4, SFRP-2* and *DKK-3*, the key enzyme *GSK-3β* and the WNT pathway target genes *Axin-2* and *Cyclin-D1* in the mediobasal hypothalamus of adult Djungarian hamsters, specifically in the ARC (chapter 4.2, figure 1). Interestingly, gene expression of all investigated ligands as well as target genes was dependent on the photoperiod (chapter 4.2, figures 2 and 3a, b). The up-regulation of *WNT-4*, a WNT/β-catenin pathway agonist (212), together with increased levels of *Axin-2* and *Cyclin-D1* mRNA in the hypothalami of LD compared with SD hamsters, indicates enhanced activation of the canonical WNT/β-catenin pathway during LD conditions. Nonetheless, these data solely stem from observations of WNT signalling on a transcriptional level.

To provide further evidence for increased hypothalamic WNT/β-catenin signalling in LD relative to SD hamsters, we next examined the canonical WNT/β-catenin pathway on a posttranslational level. Indeed, by performing immunohistochemistry we found

elevated phosphorylation of the WNT co-receptor LRP-6 at serine 1490 in the ARC of LD hamsters in comparison with SD hamsters (chapter 4.2, figure 4). Phosphorylation at this serine residue leads to activation of LRP-6, which is required for the initiation of canonical WNT/β-catenin signal transduction (106, 107). These data provide strong evidence for elevated WNT/β-catenin signalling in the ARC of Djungarian hamsters during LD relative to SD conditions.

Additionally, *SFRP-2* mRNA levels were increased in LD hamsters. In light of the proposed increased WNT/β-catenin pathway activation during LD this appears paradoxical at first, due to the general antagonizing effect on both canonical and non-canonical WNT signalling described for members of the SFRP family (110, 111). However, SFRP-2 has been demonstrated to particularly facilitate the activity of WNT-4 during kidney development (213). Thereby, the increase in *SFRP-2* mRNA observed in our study might illustrate a regulatory mechanism to prevent aberrant activation of non-canonical WNT signalling, while at the same time allowing enhanced activation of canonical WNT/β-catenin signalling via WNT-4 in the ARC of LD hamsters.

A key regulatory enzyme of the WNT/β-catenin pathway is GSK-3β, being responsible for the phosphorylation and subsequent proteasomal degradation of the co-transcription factor β-catenin (115, 116). In the present study, *GSK-3β* gene expression was regulated by neither photoperiod nor time of day (chapter 4.2, figure 3c). The WNT/β-catenin pathway-inhibiting activity of GSK-3β is, however, altered by phosphorylation at serine 9, which results in the inhibition of this kinase (117). We performed immunohistochemistry to evaluate the number of pGSK-3β (serine 9)-immunoreactive cells in the ARC of hamsters from LD or SD and at different times throughout the 24-hour period. Unfortunately, commercially available antibodies used in this study did not cross-react with hamster tissue. Therefore, no definite prediction can be made as to how GSK-3β activity is regulated by seasonal adaptations or during day and night in Djungarian hamsters. However, in light of our findings regarding increased WNT/β-catenin pathway activation and elevated target gene expression during LD relative to SD, a probable reduction in GSK-3β activity in the ARC of LD hamsters can be proposed. Interestingly, SD compared with LD photoperiod was shown to induce deteriorated insulin signalling in the ARC of Djungarian hamsters (214). GSK-3β is a potent inhibitor of insulin signal transduction. The reduction in hypothalamic insulin signalling detected in SD hamsters may therefore result from ameliorated GSK-3β

activity as a consequence of reduced WNT/β-catenin pathway activation during SD compared with LD. In line with this, Benzler *et al.* demonstrated that blockade of canonical WNT/β-catenin signalling in diabetic $Lep^{ob/ob}$ mice inhibits the glucose-lowering effects of exogenous leptin (119). This suggests that WNT/β-catenin signalling is an important mediator of leptin-induced attenuation of glucose homeostasis and provides further evidence for a crucial role of hypothalamic WNT/β-catenin signal transduction in the neuroendocrine control of metabolism.

Furthermore, we investigated the 24-hour profile of hypothalamic WNT component gene expression. Overall, the effects of time of day on gene expression were limited, with no rhythmic regulation for *WNT-4, SFRP-2* and *GSK-3β* (chapter 4.2, figure 3). On the other hand, *DKK-3, Axin-2* and *Cyclin-D1* revealed rhythmic regulation of hypothalamic gene expression throughout the 24-hour cycle (chapter 4.2, figure 2). In both LD and SD hamsters, expression of the two WNT target genes *Axin-2* and *Cyclin-D1* appeared to decline throughout the light phase and increase throughout the dark phase. In LD hamsters, this was accompanied by increasing expression of the WNT/β-catenin signalling antagonist *DKK-3* throughout the light phase and decreasing expression throughout the dark phase, potentially resulting in the reciprocal expression profile of WNT target genes that we observed in the present study. Other than in LD hamsters, the 24-hour expression profile of *DKK-3* did not justify the rhythmic regulation of *Axin-2* and *Cyclin-D1* mRNA in SD hamsters. Interestingly, several WNT gene promotors were shown to exhibit BMAL-1 occupancy, suggesting direct circadian regulation of expression of genes encoding components involved in the WNT pathway. Guo and colleagues demonstrated that overexpression of BMAL-1 resulted in enhanced WNT/β-catenin signal activity. Disruption of BMAL-1 function, on the other hand, led to down-regulation of genes involved in the canonical WNT/β-catenin pathway, accompanied by increased adipogenesis and the development of obesity in mice (215). Furthermore, BMAL-1 has been shown to be a prominent transcription factor for genes encoding central regulators of metabolism (216). These results, together with our findings in the Djungarian hamster, support an important role of canonical WNT/β-catenin signalling in the seasonal as well as 24-hour-rhythmic hypothalamic regulation of cell differentiation as well as energy metabolism, as further discussed below.

3.2.2. The potential role of canonical WNT/β-catenin signalling in cell differentiation processes in *Phodopus sungorus*

WNT/β-catenin signalling has been shown to control adipogenesis; it prevents differentiation of preadipocytes by inhibition of adipogenic transcription factors, namely CCAAT-enhancer binding protein α (C/EBPα) and peroxisome proliferator-activated receptor γ (PPARγ), whereas disruption of WNT signal transduction in preadipocytes causes these cells to differentiate into adipocytes (217, 218). Interestingly, C/EBPα disruption in knockout mice causes a major reduction in lipid content and adipose cell size, while adipocyte differentiation still occurs (219). We found elevated WNT/β-catenin pathway activity during LD compared with SD, pointing to reduced adipogenesis in LD hamsters. However, LD hamsters possess larger body fat stores than SD hamsters (199, 200). This is primarily due to increased adipose hypertrophy, but not adipose hyperplasia (220). Therefore, the adipogenesis-inhibiting role of canonical WNT/β-catenin signalling appears to play only a minor role in the seasonal regulation of fat pad mass in Djungarian hamsters. However, it is important to consider that we examined WNT/β-catenin signal transduction only in brain tissue, but not in the periphery. In peripheral tissues it might be regulated conversely depending on photoperiodic background and still contribute to the seasonal changes in adipose mass observed in Djungarian hamsters.

The importance of neural WNT signalling has been extensively described in embryonic development. For a long time, neurogenesis in the adult mammalian brain was considered to be restricted to two distinct regions: the dentate gyrus in the hippocampus and the subventricular zone of the lateral ventricles in the forebrain, linked to learning, memory formation, olfaction and mood modulation (221-225). In these brain regions, canonical WNT signalling promotes neurogenesis (226). Recently, accumulating evidence suggests that adult neurogenesis also appears in other brain regions, such as the hypothalamus (227, 228). It was demonstrated that WNT signalling is required in the developed hypothalamus of both zebrafish and mice (227). Furthermore, there is a large body of evidence showing photoperiodic control of hypothalamic WNT signalling in photoperiod-sensitive F344 rats (125, 126, 229), and various members of the canonical WNT/β-catenin pathway were up-regulated in LD-acclimated F344 rats (127). In line with these findings, we demonstrated elevated canonical WNT pathway activity in the Djungarian hamster during LD. It is tempting to speculate that this

increased pathway activation in LD hamsters entails increased neurogenesis. However, a study conducted in another hamster species, the adult Syrian hamster (*Mesocricetus auratus*), found contradictory results. There, higher numbers of newly incorporated neurons were detected in the hypothalamus of SD hamsters. It was unclear whether this was due to increased cell birth or reduced cell death, but the authors concluded that LD-acclimated Syrian hamsters exhibit reduced neuronal cell proliferation compared with SD hamsters (230). Whether this is regulated similarly in Djungarian hamsters is unclear. While both hamster species are long day-breeders, there are numerous differences in regards to their photoperiodic adaptations. While Djungarian hamsters exhibit an increase in body weight, adipose tissue mass and circulating leptin levels during LD compared with SD, these effects are absent or very limited in Syrian hamsters (231-233). Additionally, Djungarian hamsters exhibit increased *Socs-3* mRNA levels during LD relative to SD conditions, accompanied by deteriorated hypothalamic leptin sensitivity (48). In Syrian hamsters, on the other hand, photoperiod had no effect on *Socs-3* gene expression (206). Therefore, neurogenesis might also be regulated differently in these two hamster species.

Studies conducted in photoperiod-responsive hamsters as well as sheep suggest photoperiod-induced alterations in the morphology of the mediobasal hypothalamus (230, 234-236). Neurogenesis in the adult murine hypothalamus has been demonstrated to play an important role in the regulation of neuroendocrine pathways that are in control of energy metabolism (237, 238). The increase in WNT/β-catenin signalling in the ARC of LD hamsters demonstrated in the present study potentially represents a mechanism for cellular and structural remodelling of neurocircuits that mediate photoperiodic alterations in energy balance in the Djungarian hamster. Further investigation into the effects of photoperiod on neurogenesis and morphological remodelling of the adult Djungarian hamster's hypothalamus with a focus on signalling pathways regulating energy homeostasis is required.

3.2.3. Leptin activates the canonical WNT/β-catenin signalling pathway in *Phodopus sungorus*

Recently, our group demonstrated that hypothalamic WNT/β-catenin signalling is disrupted in obese leptin-deficient $Lep^{ob/ob}$ mice and is reinstated by leptin administration (119). Therefore, we next wanted to investigate whether leptin administration in Djungarian hamsters leads to an activation of the canonical WNT pathway and whether this effect is photoperiod-dependent. By using immunohistochemistry to determine the number of pLRP-6 (serine 1490)-immunoreactive cells, we found increased activation of the canonical WNT co-receptor LRP-6 in the ARC of hamsters that were challenged with leptin compared with vehicle-treated control animals (chapter 4.2, figure 4). Interestingly, leptin led to activation of the WNT/β-catenin pathway in Djungarian hamsters from LD as well as SD. This finding was surprising, since LD hamsters are leptin resistant relative to SD hamsters (201, 204, 205, 239). In Djungarian hamsters, hypothalamic leptin resistance during LD was shown to be mediated by reduced translocation of activated STAT3 into the nucleus and as a consequence of up-regulated *Socs-3* expression, leading to an inhibition of intracellular signal transduction via JAK2/STAT3 signalling (28, 29, 48, 206, 240). Therefore, it is probable that the leptin-induced activation of the WNT/β-catenin pathway is independent of the JAK2/STAT3 pathway. Instead, signal transduction via an indirect mechanism could be possible. However, the rapid activation of the WNT/β-catenin co-receptor LRP-6 only 15 minutes after intraperitoneal leptin administration suggests a direct effect of leptin. Therefore, the exact mechanism via which leptin mediates its WNT pathway-activating effects in the hypothalamus remains to be further investigated. A very recent study conducted in *Xenopus laevis* tadpoles confirmed our finding that leptin is able to activate WNT/β-catenin signalling in the hypothalamus of yet another species (241), indicating that this particular effect of leptin is conserved throughout several taxonomic classes of the animal kingdom.

Intriguingly, Ellis *et al*. reported a time of day-dependent effect on *LepRb* gene expression in the ARC of Djungarian hamsters acclimated to LD, but this rhythm was not present in SD animals (242). In LD hamsters, *LepRb* mRNA levels are elevated during the dark phase relative to the light phase. It is interesting to note that *LepRb* gene expression in LD hamsters peaks in the middle of the dark phase at ZT21 (242).

We found that at this exact time mRNA levels of the WNT target genes *Axin-2* and *Cyclin-D1* reach their nadir in LD hamsters, followed by an abrupt increase in gene expression. This may be a consequence of enhanced leptin signalling due to increased leptin receptor levels. It appears that the 24-hour rhythm in *LepRb* gene expression and, as a potential consequence, leptin sensitivity is revealed under conditions of leptin resistance and high levels of the hormone during LD, whereas this does not apply to leptin sensitive SD hamsters with low hormone levels (242). Furthermore, these data suggest that hypothalamic leptin resistance does not persist throughout the entire day once it is established, but may be subject to daily variations.

3.3. Influence of the time of day on the control of energy metabolism

It is well established that circadian clocks play an important role in the maintenance of energy metabolism. Disruptions of circadian rhythms lead to metabolic disorders in both rodents and humans (177-179) and HFD feeding has been shown to interfere with circadian rhythms (158, 180, 181). However, whether leptin signal transduction in the ARC, a key region in neuronal control of body weight and overall energy metabolism, is rhythmically regulated throughout the day has not yet been examined. Furthermore, the suggestion that physiological leptin resistance in LD-acclimated Djungarian hamsters may underlie a 24-hour rhythm, as discussed above (chapter 3.2.3), brings about the question as to whether this also applies to the pathological model of leptin resistance during DIO. In the present study, we therefore investigated how activation of the leptin signalling pathway is modulated over the course of the day *per se* and whether HFD-induced obesity interferes with this. We also examined the effects of time-restricted access to HFD on metabolic markers and whether the time of TRF has an influence on the amelioration of metabolic health. For an overview of the experimental designs of this study, see chapter 4.3, supplementary figure 1.

3.3.1. Time of day-dependent action of hypothalamic leptin signalling

3.3.1.1. Rhythmic regulation of basal leptin signal transduction is disrupted by HFD feeding

By performing immunohistochemistry, we examined the activation of the transcription factor STAT3 at its phosphorylation site tyrosine 705 as a marker for leptin's intracellular signalling action over the course of an entire day in mice that had been fasted for 24 hours prior to perfusion (chapter 4.3, figure 1a, b). We discovered a 24-hour rhythm of leptin pathway activation, as demonstrated by the number of pSTAT3 (tyrosine 705)-immunoreactive cells, in the ARC of vehicle-treated mice that were fed with LFD, as well as both mice fed with LFD and HFD after leptin treatment. Although three-way ANOVA detected an overall rhythmicity of basal pSTAT3 immunoreactivity in vehicle-treated mice fed HFD, the subsequent post hoc test did not reveal significant differences between the individual time points. Instead, these mice showed a consistent

number of basal pSTAT3-immunoreactive cells throughout the entire 24-hour cycle. We therefore concluded that no physiologically relevant 24-hour rhythm of endogenous leptin pathway activation is present in mice fed HFD, showing that HFD feeding leads to a disruption of the rhythmic regulation of basal leptin pathway activity.

In vehicle-treated mice fed LFD, basal leptin pathway activity was at a maximum at the beginning of the light phase at ZT0 and at a minimum at ZT6 with continuously increasing pSTAT3 activation from the middle of the light phase to the end of the dark phase. This rhythmic regulation of basal leptin pathway activity occurred despite an extended fasting period of 24 hours prior to tissue sampling and therefore indicates a physiological role that is independent of preceding food intake. Furthermore, this rhythmic oscillation of basal pSTAT3 activation is also independent of variations in serum leptin concentrations, which revealed no rhythmic regulation over 24 hours in fasted vehicle-treated mice fed LFD (chapter 4.3, figure 2a). These results indicate that the elevated number of pSTAT3-immunoreactive cells during the dark compared with the light phase is due to enhanced leptin sensitivity caused by mechanisms independent of the short-term factors food intake and circulating leptin levels.

The majority of studies that investigated the effect of HFD feeding on leptin sensitivity in the ARC so far reported similar numbers of basal pSTAT3-immunoreactive cells in wild-type mice as well as in rats fed either LFD or HFD (12, 243, 244). By rigorous tissue sampling every 3 hours throughout the 24-hour cycle, we discovered that the effect of the diet on pSTAT3 activation is dependent on the time of day. Mice fed LFD compared with HFD had similar levels of pSTAT3 activation exclusively during the second part of the dark phase and the first part of the light phase from ZT21 – ZT3. However, HFD feeding led to an increase in pSTAT3 activation during the second part of the light phase and the first part of the dark phase from ZT6 – ZT18 (chapter 4.3, figure 1b). The discrepant results between our and the above-mentioned studies can be explained by the time of tissue sampling, which is typically performed in the early morning as has been specified in at least one of these studies (243). To our knowledge, there is only one other study that demonstrates elevated basal pSTAT3 activation during DIO. This study was conducted in rats that were fed either chow or HFD and received an icv injection of artificial cerebrospinal fluid (ACSF) and pSTAT3 immunoreactivity was measured in the entire hypothalamus (245). Unfortunately, the authors did not indicate at what time of day brains were harvested.

A plausible explanation for this HFD-induced activation of pSTAT3 at specific times during the day compared with basal pathway activation in mice on LFD might be hypothalamic inflammation. Obesity is associated with chronic low-grade systemic and central inflammation (50, 246, 247). Pro-inflammatory cytokines such as interleukin 6 (IL-6) and tumour necrosis factor α (TNFα) are secreted by white adipose and brain tissue, amongst a variety of other cell types, and circulating levels of IL-6 as well as TNFα were shown to be elevated during obesity (248-250). Interestingly, the role of IL-6 in inflammatory responses is complex and appears to be tissue-dependent. While myocyte-derived IL-6 has been shown to improve glucose metabolism and to have anti-inflammatory functions (251, 252), these effects appear to be specific for its role as a myokine. Pro-inflammatory effects have been demonstrated for IL-6 in the majority of other tissues. Both IL-6 and TNFα mediate their effects via actions in the CNS, specifically the hypothalamus (253, 254), and hypothalamic inflammation via these cytokines has been implicated in the development of leptin as well as insulin resistance and type 2 diabetes (50, 248, 255, 256). Both cytokines have been shown to be able to mediate their pro-inflammatory effects via activation of the intracellular JAK2/STAT3 pathway (257, 258). In line with this, our research group recently demonstrated that pSTAT3 is equally activated in leptin-deficient $Lep^{ob/ob}$ mice fed HFD and treated with vehicle and mice fed LFD and treated with leptin (51). Since these mice lack endogenous leptin, the activation of pSTAT3 observed in vehicle-treated mice on HFD must be due to mechanisms other than leptin signalling. Furthermore, inhibition of the pro-inflammatory c-Jun N-terminal kinase (JNK) pathway in the hypothalamus of $Lep^{ob/ob}$ mice reversed the HFD-induced resistance to the glucose-lowering effects of leptin (51). These results suggest that hypothalamic inflammation due to HFD-induced elevation of pro-inflammatory cytokine levels, but not the occurrence of hyperleptinemia, causes leptin resistance in leptin-deficient $Lep^{ob/ob}$ mice. Therefore, it is possible that the increase in pSTAT3 activation in vehicle-treated wild-type mice fed HFD compared with LFD at particular times of the day demonstrated in the current study is a direct effect of pro-inflammatory cytokines leading to pSTAT3 activation.

Notably, in the current study we used a mouse model of DIO typically associated with high circulating levels of leptin. Nonetheless, hypothalamic inflammation has been shown to interfere with leptin signalling in this mouse model and is causative for the development of HFD-induced obesity and related metabolic disorders (246, 259).

Hypothalamic inflammation is already altered within just hours of HFD consumption (247). By central inhibition of pro-inflammatory inhibitor of nuclear factor-κB kinase β (IKKβ)/nuclear factor-κ-light-chain-enhancer of B-cells (NF-κB) signal transduction in mice fed HFD, our research group recently confirmed that this pathway is involved in the development of DIO (52). Mice subjected to ARC-directed genetic inhibition of IKKβ/NF-κB signalling experienced an amelioration of the detrimental effects of HFD on body weight gain, body fat mass, energy expenditure, *Socs3* gene expression in the ARC, as well as glucose tolerance. Since all of these factors are regulated by hypothalamic leptin signalling, these results provide evidence that the central pro-inflammatory IKKβ/NF-κB pathway is involved in the development of arcuate leptin resistance during DIO (52). Indeed, a prominent target of the IKKβ/NF-κB signalling cascade is the expression of SOCS3, a potent inhibitor of leptin signalling (49). Gao and colleagues demonstrated similar effects for the JNK pathway. They found enhanced hypothalamic leptin signalling as well as decreased body weight gain and food intake in DIO mice after pharmacological inhibition of JNK signal transduction (260). Based on these findings, the elevated activation of pSTAT3 in HFD-induced obese mice at specific times, as observed in the current study, might result from a rhythmic occurrence of hypothalamic inflammation and thus rhythmic appearance and abatement of leptin signal transduction-inhibiting inflammatory effects, rather than from a direct effect of pro-inflammatory cytokines.

3.3.1.2. Rhythmic regulation of leptin-induced leptin signal transduction is disrupted by HFD feeding

This phenomenon would also explain our findings of leptin-induced pSTAT3 activation over the course of a day in mice that were fasted for 24 hours prior to leptin injections. Mice fed LFD displayed a 24-hour rhythm in arcuate pSTAT3 levels, with maximum activation at ZT0 and declining levels throughout the light phase, reaching a minimum at ZT9 (chapter 4.3, figure 1a, b). These findings suggest rhythmic regulation of leptin signal transduction in the hypothalamic ARC of mice independent of food intake, with highest leptin sensitivity at the end of their active phase and lowest sensitivity before the onset of their active phase. Interestingly, basal pSTAT3 activation in vehicle-treated mice fed LFD follows the same daily pattern, even though baseline levels are

significantly lower at all investigated time points compared with leptin-induced pSTAT3 activation (chapter 4.3, figure 1a, b).

On the other hand, HFD feeding led to a disruption of the 24-hour rhythm of leptin-induced pSTAT3 activation that we observed in mice fed LFD. Leptin-treated mice fed HFD showed pSTAT3 levels that were at a minimum at ZT0 and continuously increasing throughout the light as well as the first half of the dark phase, reaching maximum levels at ZT18. Intriguingly, mice fed HFD showed lower levels of leptin-induced pSTAT3 activation only during the second part of the dark and the first part of the light phase from ZT21 – ZT6 compared with mice fed LFD. At all other time points, pSTAT3 levels were similar between mice fed HFD and LFD (chapter 4.3, figure 1a, b). To our knowledge, this is the first description of this time of day-dependent occurrence of leptin resistance in response to HFD feeding. Other studies so far reported decreased leptin-induced pSTAT3 activation and thus impaired leptin sensitivity in rodents fed HFD as a temporally omnipresent phenomenon (12, 243, 244). As discussed above for basal pSTAT3 activation, this discrepancy most likely arises from the limited number of time points of tissue sampling in those studies.

Taken together, our results demonstrate that DIO leads to a disruption of the 24-hour rhythm in the control of both basal as well as leptin-induced leptin signalling and furthermore suggest that DIO-induced leptin resistance is restricted to specific times of the day. In vehicle-treated mice fed HFD, which have higher circulating leptin concentrations relative to LFD throughout the entire day (chapter 4.3, figure 2a), we report increased leptin pathway activity, exemplified by the number of pSTAT3-immunoreactive cells, exclusively from ZT6 – ZT18. In line with this, leptin-treated mice fed HFD show leptin sensitivity similar to mice fed LFD exclusively from ZT9 – ZT18, whereas pSTAT3 activation is deteriorated at all other times. A DIO-induced increase in hypothalamic inflammatory activity during the second half of the dark (active) and the first half of the light (inactive) phase, evoking impaired leptin signalling, might be causative for this time of day-dependent impairment of leptin signal transduction as observed in both vehicle- and leptin-treated mice fed HFD compared with LFD.

Although a large body of evidence demonstrates circadian regulation of central inflammation in rodents, only few of these studies concentrated on the hypothalamus

and results are contradictory. Some studies report that *Tnfα* gene expression in the hypothalamus is increased in the light phase compared with the dark phase (261), with peak mRNA levels at ZT0 and lowest levels at ZT18 (262), while others found relatively low *Tnfα* gene expression during the light phase and highest mRNA levels during the middle of the dark phase (263). Notably, only the latter study was conducted in mice, whereas all other studies used rats. These discrepancies could be due to differences between species or to different experimental conditions. Cytokines and other immune mediators have been shown to be directly influenced by circadian timekeeping processes in various tissues (264). For example, CLOCK can directly interact with the pro-inflammatory transcription factor NF-κB, leading to elevated transcriptional activity, whereas the heterodimerisation of CLOCK and BMAL-1 results in rhythmic repression of inflammatory genes (265). Furthermore, REV-ERBα represses a distinct subset of inflammatory genes in macrophages (266) and loss of CRY proteins results in constitutive NF-κB activation (267). These studies show that the rhythmic regulation of inflammatory responses is intricately arranged. Characteristically, a peak in circulating cytokines during the onset of an animal's active phase has been described for humans as well as mice (268, 269). Of great importance is that all above-mentioned studies examining rhythmic regulation of inflammatory activity focused on non-obese subjects (261-263, 268, 269). Therefore, it is rather possible that the daily rhythm of hypothalamic inflammation in DIO mice, which show an increase in pro-inflammatory markers, is regulated differently. Unfortunately, commercially available ELISA kits for the analysis of circulating cytokines required too large serum sample volumes and we were therefore unable to measure circulating levels of IL-6 and TNFα throughout the 24-hour cycle in mice used in our study.

3.3.1.3. Leptin sensitivity on a behavioural level is dependent on the time of day

After we had established that arcuate leptin sensitivity on a molecular level exhibits a 24-hour rhythm in mice, we next analysed whether this rhythmicity also applies to the behavioural response to exogenous leptin. Mice fed either LFD or HFD were injected at either ZT0, when leptin sensitivity on a molecular level was at a maximum in LFD mice, or at ZT12. Subsequently, accumulated caloric intake was measured 4 hours and 24 hours post injections to assess the anorexigenic effects of the hormone (chapter 4.3,

figure 1b, c). Compared with their vehicle-treated counterparts, mice fed LFD showed a significant reduction in caloric intake after both 4 hours and 24 hours when leptin was administered at ZT0, whereas injections at ZT12 had no effect on caloric intake. In mice fed HFD, on the other hand, exogenous leptin at either time point did not result in decreased caloric intake, suggesting that on a behavioural level these mice are resistant to the anorexigenic effects of leptin throughout the entire 24-hour cycle.

3.3.1.4. 24-hour profile of blood-borne metabolic markers

To further investigate the impact of DIO on physiological rhythms, we next analysed circulating metabolic markers throughout the 24-hour cycle. Vehicle-treated mice fed LFD showed consistently low levels of circulating leptin. The absence of a 24-hour rhythm in these mice is most likely due to the extended fasting period prior to blood sampling. Non-fasted male mice on a control diet have been shown to exhibit a 24-hour rhythm of endogenous leptin, with elevated levels during the dark and reduced levels during the light phase (270). Intriguingly, vehicle-treated mice fed HFD displayed a prominent rhythm in serum leptin concentrations, despite the preceding 24-hour fasting period (chapter 4.3, figure 2a). Leptin concentrations were elevated during the light phase, reaching a maximum at ZT6, and reduced during the dark phase. This peak in endogenous leptin levels coincides with reduced pSTAT3 activation in mice fed HFD on a molecular level, indicating an inhibitory effect of leptin on leptin pathway activation during DIO. This finding furthermore corroborates that hyperleptinemia is required for the development of hypothalamic leptin resistance (271).

Indeed, in a series of elegant studies, Scarpace and colleagues demonstrated that elevated central leptin levels are causative for hypothalamic leptin resistance. Rats received a chronic virus-mediated leptin transgene overexpression directly into the third ventricle of the brain, resulting in elevated hypothalamic but not systemic leptin levels (272). These rats developed impaired leptin responsiveness despite lower body mass and serum leptin levels compared with control rats, demonstrating hypothalamic leptin-induced leptin resistance independent of other detrimental effects typically associated with DIO, such as elevated hypothalamic inflammation (272). In a follow-up study, hypothalamic leptin resistance was induced as described above and rats received a HFD after hypothalamic leptin resistance was established (273). Leptin-vector-treated

rats fed HFD consumed significantly more calories and gained more body weight and fat mass than rats that were treated with a control virus and fed HFD. These results indicate that hypothalamic leptin resistance provokes increased susceptibility to DIO, proposing the fascinating notion that leptin resistance is both a cause and a consequence of obesity (273). As discussed above, the involvement of hypothalamic inflammation has also been shown to contribute to the development of leptin resistance and obesity (52, 260). Taken together, these findings provide evidence that not one single cause underlies these metabolic derangements, but rather the conjoined occurrence of both hyperleptinemia and elevated hypothalamic inflammation is causative for their development.

To further examine the hypothesis that leptin has an inhibitory effect on hypothalamic leptin signal transduction in states of DIO, we conducted another study with the same experimental setup as described above in which mice were injected at either ZT0 or ZT12. This time mice received an ip injection of a potent short-acting leptin antagonist (LAN; 1.0 mg/kg in PBS; Protein Laboratories Rehovot Ltd.) with the same half-life as recombinant mouse leptin, to assess whether acute targeted inhibition of leptin action at specific time points leads to an increased anorexigenic response on a behavioural level in mice fed HFD. Unfortunately, we found no effect of acute LAN administration on caloric intake in either mice fed LFD or HFD, potentially because the applied dose was insufficient to entirely antagonise leptin binding to its receptor and activating downstream pathway signalling.

Circulating insulin concentrations displayed no rhythmic oscillation over the 24-hour cycle in either mice fed LFD or HFD, but three-way ANOVA revealed an overall increase of serum insulin levels in mice fed HFD compared with LFD, independent of leptin administration (chapter 4.3, figure 2b). Increased insulin levels during DIO have been reported previously and are an indicator for disrupted insulin signal transduction, eventually resulting in the manifestation of type 2 diabetes (23).

In line with the consistently low levels of leptin and insulin, mice that were fed LFD and fasted for 24 hours prior to blood sampling showed no rhythmic regulation of serum glucose levels throughout the day. In contrast, mice fed HFD displayed rhythmic levels of circulating glucose with concentrations similar to those observed in mice fed LFD during the light phase and elevated levels during the dark phase (chapter 4.3,

figure 2c). Notably, this peak occurs independently of food intake, but simultaneously with reduced levels of serum leptin, suggesting a correlation between circulating leptin and glucose levels. Indeed, obese leptin-deficient $Lep^{ob/ob}$ mice display severe hyperglycaemia despite increased levels of circulating insulin. In these mice, even low doses of exogenous leptin restore normal glucose homeostasis without leptin eliciting its anorexigenic properties on food intake and body weight, demonstrating a profound blood glucose-lowering effect of the hormone and highlighting the importance of leptin signalling on functional insulin signal transduction (271). On a molecular level, leptin injections lead to increased activation of IRS1 (71). This is most likely achieved by leptin activating the WNT/β-catenin pathway and subsequent inhibition of GSK3β [chapter 3.2 and (119)]. Since GSK3β is a potent inhibitor of insulin signalling, this decrease in GSK3β activity might be causative for the leptin-mediated sensitisation of insulin pathway activation.

Taken together, our and the above-mentioned studies suggest that leptin in more efficient in regulating glucose homeostasis than in mediating its anorexigenic effects on food intake and body weight. Furthermore, no difference in serum glucose levels throughout the day was observed between vehicle- and leptin-treated mice in either mice fed LFD or HFD. This indicates that in mice fed LFD, glucose homeostasis is fully functional and additional leptin administration does not improve glucose tolerance any further. On the other hand, in mice fed HFD that exhibit responsiveness to the glucose-lowering effects of endogenous leptin during the light phase, exogenous leptin seems unable to counteract the deteriorated glucose homeostasis displayed during the dark phase. These findings suggest an intricately regulated mechanism discriminating between effects of endogenous versus exogenous leptin. Indeed, Ottaway *et al.* reported that repeated administration of high doses of a long-acting leptin antagonist leads to an increase in caloric intake in mice fed HFD relative to vehicle-treated animals, suggesting that on a behavioural level DIO mice are still responsive to endogenous leptin to some extent, despite impaired leptin signalling and resistance to exogenous leptin (274).

In conclusion, we demonstrate a time of day-dependent regulation of leptin action that is disrupted by the consumption of HFD. Physiologically, the elevated responsiveness to leptin on both the molecular and behavioural level at the beginning of the light phase as observed in mice fed LFD might present a regulatory mechanism that inhibits the

drive to eat and ultimately prevents food seeking behaviour during the animals' inactive phase. The disruption of this physiological rhythm during DIO might be causative for the arrhythmic behavioural patterns observed during obesity. Mice subjected to HFD were shown to have increased relative locomotor activity and food intake during the light phase (158, 181), coinciding with decreased leptin sensitivity as demonstrated in our study.

3.3.2. Effects of time-restricted feeding on energy metabolism

We next examined whether the beneficial effects on metabolic health that have been described for TRF regimens depend on the rhythmic control of hypothalamic leptin sensitivity. Based on our observations about the DIO-induced disruption of this rhythm on a molecular level, we restricted access to HFD to four defined 6-hour intervals each day, thereby covering the entire 24-hour cycle. One group of mice subjected to the TRF regimen received HFD during the interval when mice fed HFD displayed leptin resistance on a molecular level compared with mice fed LFD (ZT21 – ZT3). A second group received HFD during the interval when both mice fed LFD and HFD showed identical responsiveness to exogenous leptin (ZT9 – ZT15). Because these two groups had access to HFD for 3 hours during both the light and the dark phase, effects observed between these groups can be regarded as activity-independent. Two more groups had access to HFD during either the light (resting) phase (ZT3 – ZT9) or the dark (active) phase (ZT15 – ZT21).

3.3.2.1. Effect of time-restricted feeding on body weight and behaviour

Mice showed increased body weight as early as nine days after the start of HFD feeding relative to mice fed LFD (chapter 4.3, figure 3). After four weeks of *ad libitum* HFD feeding, these mice were separated into five groups of which one continued to receive *ad libitum* HFD and the other animals were subjected to the TRF regimen as described above. By the end of the experiment, all TRF mice had significantly reduced body weight as well as circulating leptin concentrations (chapter 4.3, figure 5a) relative to mice fed HFD *ad libitum*, with values similar to those detected in mice fed LFD. We observed no differences of these parameters between the TRF groups. The reduction in

body weight of TRF mice can be accounted for by reduced daily caloric intake compared with mice fed HFD *ad libitum* (chapter 4.3, supplementary figure 2a), however, this was not accompanied by a reduction of daily locomotor activity (chapter 4.3, supplementary figure 2b). Notably, since circulating leptin levels are proportional to body fat mass (275), the reduction in body weight together with decreased plasma leptin levels observed in TRF mice relative to mice fed HFD *ad libitum* indicates a reduction in fat mass but not lean mass. Indeed, this effect on body fat content has recently been described for a TRF regimen (276).

3.3.2.2. Effect of time-restricted feeding on markers of metabolic health

We monitored parameters of energy metabolism and behaviour of mice from this study using a respirometry system. By analysing data that were binned into 6-hour intervals, we found that locomotor activity as well as average metabolic rate and energy expenditure followed a clear daily rhythm in mice fed LFD and HFD *ad libitum* (chapter 4.3, figure 4b, c, d). These parameters were lowest during the animals' resting phase from ZT3 – ZT9 and highest during their active phase from ZT15 – ZT21, whereas they exhibited similar values during both activity-independent intervals (ZT9 – ZT15 and ZT21 – ZT3) that were situated medially between these two extremes. However, mice fed HFD showed a reduction in these parameters during one or more 6-hour intervals compared with mice fed LFD (chapter 4.3, figure 4b, c, d). This is in accordance with previous studies revealing impaired locomotor activity and energy metabolism during DIO (181). Here, we demonstrate that these impairments occur during phases when mice are active, but not during their exclusive resting phase.

Feeding behaviour exhibited a slight variation from this clear daily rhythm (chapter 4.3, figure 4a). In mice fed LFD, caloric intake was minimal during their inactive phase and maximal during their active phase. Concerning the two activity-independent intervals, caloric intake was significantly higher during ZT9 – ZT15 relative to ZT21 – ZT3. We found similar results in mice fed HFD. Here, caloric intake was lowest during their inactive phase and highest during the two following intervals. However, this was not followed by a reduction in caloric intake as observed in mice fed LFD, but remained significantly increased during ZT21 – ZT3. The caloric overconsumption exclusively during this interval was sufficient to result in the overall increase in daily caloric intake

relative to mice fed LFD (chapter 4.3, supplementary figure 2a). A relative increase in caloric intake during the light relative to the dark phase has been reported previously in mice fed HFD (181). Here, we show that this increase is linked to the animals' responsiveness to leptin. Intriguingly, in mice fed LFD caloric intake is increased at times when leptin sensitivity on a molecular level is at a minimum, and decreases when leptin sensitivity is at a maximum. Moreover, mice fed HFD show abnormally elevated caloric intake exclusively at times when leptin sensitivity on a molecular level is impaired relative to control mice. These findings provide further evidence for an important impact of this 24-hour rhythm of leptin signal transduction on physiological and behavioural responses.

In TRF mice, access to HFD during either the inactive (ZT3 – ZT9) or active (ZT15 – ZT21) phase resulted in a slight dampening of the daily rhythm of locomotor activity, whereas mice with access to HFD exclusively during their leptin sensitive interval from ZT9 – ZT15 retained a robust locomotor activity rhythm relative to mice fed LFD *ad libitum*. In contrast, while mice that consumed HFD exclusively during their relative leptin resistant interval from ZT21 – ZT3 still showed lowest activity during the light phase, these animals lost the daily rhythm in locomotor activity observed in mice fed LFD and HFD *ad libitum* and displayed no variations between any of the subsequent intervals (chapter 4.3, figure 4b).

The daily rhythms in average metabolic rate as well as energy expenditure that were displayed by *ad libitum* fed mice were affected in all TRF mice. To account for the differences in body mass between the experimental groups, we evaluated these parameters based on body weight. Mice with access to HFD during either their leptin sensitive or active phase retained the most robust rhythm relative to animals with *ad libitum* access to food, even though mice with access to food exclusively during their leptin sensitive phase showed no differences in both metabolic rate and energy expenditure between the feeding phase and the subsequent active phase. Notably, an animals' metabolic rate is elevated during times of food intake and this finding can therefore be accounted for by the food intake-mediated increase in oxygen consumption. HFD feeding during either the animals' inactive or leptin resistant phase, on the other hand, led to a loss of the daily rhythms in metabolic rate as well as energy expenditure, with energy expenditure being most severely impaired in mice that had food during the leptin resistant phase (chapter 4.3, figure 4c, d).

Furthermore, mice fed during the leptin resistant interval displayed elevated circulating insulin concentrations compared with mice fed LFD, independent of leptin treatment prior to blood sampling (chapter 4.3, figure 5b). Unfortunately, we were unable to analyse blood glucose concentrations in these mice, which could have revealed the severity of the metabolic derailment. Nonetheless, the increase in plasma insulin levels suggests disrupted insulin signal transduction that may eventually result in the manifestation of type 2 diabetes (23).

Taken together, we demonstrate that the detrimental effects of HFD on metabolic health are dependent on when throughout the day the diet is consumed. HFD feeding at times when mice are unresponsive to the anorexigenic effects of leptin leads to symptoms of metabolic disease, whereas HFD at times when mice are sensitive to leptin protects from these detrimental health outcomes (Figure 4).

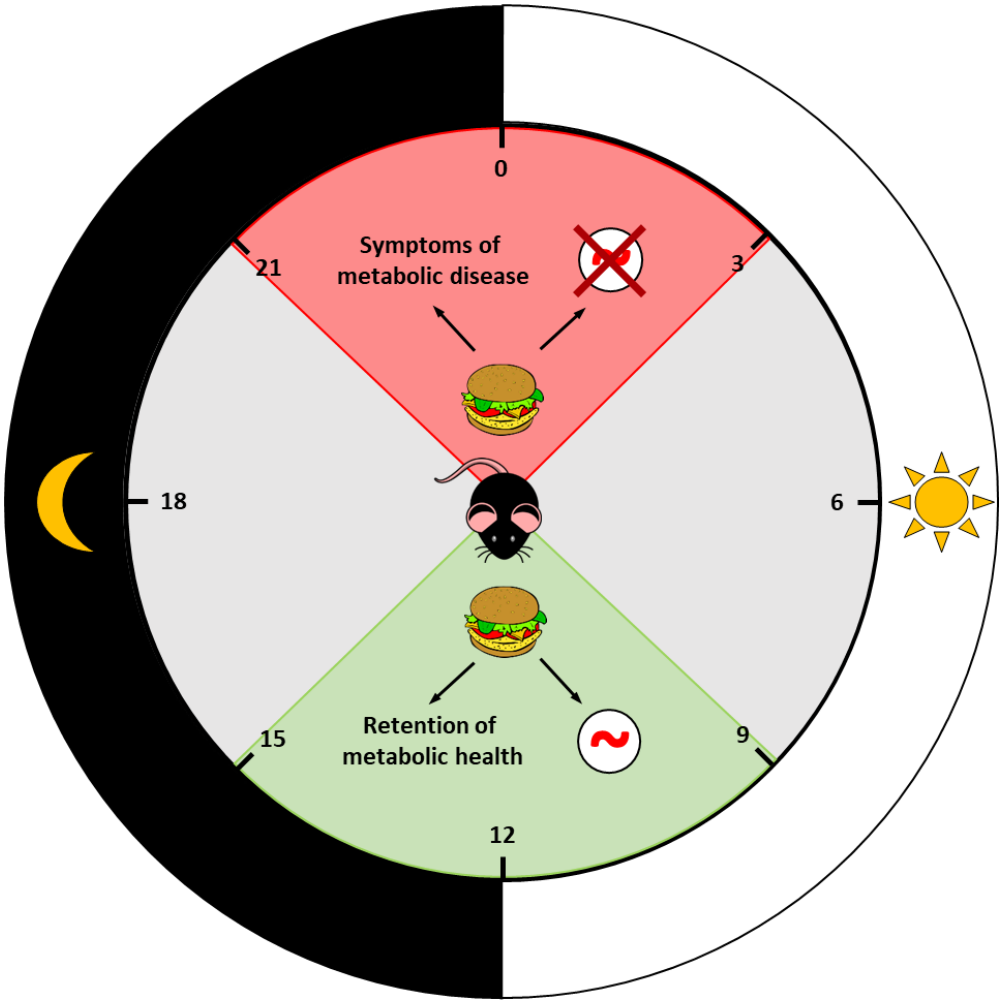

Figure 4: Effects of time-restricted feeding on metabolic health are dependent on the time of day. In mice, restricted access to HFD exclusively from ZT21 – ZT3, coinciding with their relative leptin resistant interval, leads to the manifestation of symptoms of metabolic disease such as compromised daily rhythms of locomotor activity, metabolic rate, and energy expenditure as well as increased circulating insulin levels. On the other hand, restricted access to HFD exclusively from ZT9 – ZT15, coinciding with their relative leptin sensitive interval, protects from the manifestation of these metabolic impairments. These effects on metabolic health are independent of activity states, since both TRF regimens allowed access to HFD for 3 hours during the light and 3 hours during the dark phase each day. High-fat diet (HFD), Time-restricted feeding (TRF), Zeitgeber time (ZT).

3.4. Future perspectives

In this thesis, we revealed a 24-hour rhythm of hypothalamic leptin sensitivity that plays a crucial role in the regulation of whole body energy homeostasis. We furthermore demonstrated that HFD-induced obesity leads to a disruption of this rhythm, which in turn underlies the metabolic derangements observed in obese mice. The underlying molecular mechanism, by which obesity leads to this breakdown of physiological rhythmicity, is yet to be determined. Alterations in the secretion of circulating inflammatory cytokines or expression patterns of other leptin pathway-inhibiting signals could be a plausible explanation for this phenomenon. Therefore, the investigation of 24-hour rhythms in hypothalamic gene expression of leptin inhibitors such as SOCS3 and the effect of HFD feeding on these patterns are to be considered in future experiments, as well as a potential rhythmic regulation of circulating pro-inflammatory cytokines such as TNFα and IL-6.

To assess whether elevated hypothalamic inflammation causes the disruption of leptin sensitivity at specific times during the day as observed in DIO mice, it would be of great interest to examine how inhibition of inflammation at defined times affects this phenomenon. Administration of short-acting pharmacological inhibitors of the pro-inflammatory NFκB and JNK pathways in the middle of the dark phase, when reduced responsiveness to leptin in mice fed HFD first appears, and a potential reversal of HFD-induced disruptions of metabolic rhythms on the molecular as well as behavioural level would determine the implication of hypothalamic inflammation in this metabolic derangement.

Additionally, a closer investigation of the long-term effects of TRF on metabolic health could help develop better strategies for therapeutic interventions on a behavioural level, which could circumvent the side effects that often accompany pharmacological interventions. For example, it needs to be determined whether TRF at defined times during the day maintains its beneficial effects on metabolic health independent of the patients' age and baseline health status, and how these positive health outcomes are affected by prolonged periods of unrestricted food consumption after periods of TRF.

3.5. Abstract

3.5.1. Abstract (English)

Obesity and related metabolic disorders such as type 2 diabetes are a major health issue of our modern society. The brain has been identified to play an essential role in the pathogenesis of these diseases. Disruptions of the neuroendocrine system, such as the development of hypothalamic leptin resistance, are strongly correlated with the manifestation of diet-induced obesity (DIO). To date, the molecular mechanisms underlying these metabolic derangements are incompletely understood. Over the last decade, a close connection of energy metabolism and the circadian clock has been established, but the link between DIO and disruptions of physiological rhythms still needs further investigation. Therefore, the aim of this thesis was to gain new insights into neuroendocrine mechanisms that lead to the development of leptin resistance and the role of physiological rhythms in the disruption of energy metabolism.

In this study, we investigated the implication of the adipocyte-derived hormone adiponectin in neuroendocrine control of energy metabolism. We detected expression of all investigated genes involved in the adiponectin signalling pathway in the hypothalamus of mice. Expression levels of *adiponectin* were reduced during states of food deprivation, potentially presenting a regulatory mechanism to counteract the anorexigenic traits that had been previously described for central adiponectin signalling and that were confirmed by us in this study, in order to prevent further reduction in body weight. In both fasted control mice as well as DIO mice, gene expression of the adiponectin receptor *AdipoR1* was elevated, suggesting multiple regulatory mechanisms to maintain sufficient adiponectin signal transduction. The upregulation of *AdipoR1* during DIO might be an attempt to support the beneficial effects of the hormone on metabolic health that have been reported for peripheral adiponectin. In line with this, we demonstrated that adiponectin holds insulin-sensitising, blood glucose-lowering and anti-inflammatory properties in control as well as DIO mice and that these effects are mediated via central signal transduction.

We furthermore investigated the role of the WNT/β-catenin pathway in the neuroendocrine control of energy metabolism. Here, we found gene expression of members of the WNT pathway on all regulatory levels (ligands, intracellular pathway

enzymes, target genes) in the hypothalamus of adult Djungarian hamsters, *Phodopus sungorus*, a seasonal rodent that exhibits profound annual changes in body weight and leptin sensitivity. Expression of all ligands as well as target genes was upregulated in hamsters acclimated to long day (LD) relative to short day (SD) conditions. Confirming our results from these transcriptional studies, we furthermore found increased phosphorylation of the WNT pathway co-receptor LRP-6, demonstrating elevated activation of canonical WNT signalling, in LD hamsters. These findings provide strong evidence for increased WNT signalling during LD compared with SD photoperiod. We found a 24-hour rhythm in the hypothalamic expression of WNT target genes, with decreasing levels during the light and increasing levels during the dark phase in both LD and SD hamsters. Moreover, leptin administration led to a further increase in LRP-6 activation in hamsters from both photoperiods. Taken together, we demonstrate a novel integration site for the leptin signal in the hypothalamus, potentially linking the WNT pathway to body weight regulation. Furthermore, our results suggest an important role of canonical WNT signalling in the seasonal as well as daily neuroendocrine control of energy metabolism in Djungarian hamsters.

By examining whether hypothalamic leptin signalling and whole body metabolism are modulated by a daily rhythm, we detected a 24-hour rhythm of STAT3 phosphorylation, a marker for activated leptin signalling on a molecular level, in the hypothalamus of wild-type mice. Both basal as well as leptin-induced leptin sensitivity were highest at the end of the dark (active) phase and lowest at the end of the light (inactive) phase. Furthermore, we found that leptin sensitivity on a behavioural level followed the same rhythm, with mice showing a greater response to exogenous leptin at the end of the dark phase at Zeitgeber time (ZT) 0 compared with the end of the light phase at ZT12. Throughout the 24-hour cycle, mice displayed a robust rhythm in food intake, locomotor activity as well as oxygen consumption and energy expenditure, with reduced whole body metabolism during their inactive and increased metabolic rate during their active phase. In DIO mice that were subjected to high-fat diet (HFD) feeding, we found a disruption of the 24-hour rhythmic regulation of leptin pathway activation on a molecular level for both basal and leptin-induced leptin sensitivity. Intriguingly, we demonstrated that this hypothalamic leptin resistance is a temporary phenomenon that persists only at specific times during the day. Responsiveness to leptin was deteriorated during the second part of the dark and the first half of the light

phase (ZT21 – ZT6), but identical to mice fed low-fat diet (LFD) at all other times on both the molecular and behavioural level. Furthermore, DIO mice displayed a disruption of the daily rhythms in food intake, locomotor activity, oxygen consumption and energy expenditure. We found that the daily caloric overconsumption observed in mice fed HFD was restricted to the phase when DIO mice were leptin resistant relative to mice fed LFD. In conclusion, these findings provide strong evidence for a crucial role of the 24-hour rhythm of leptin sensitivity in the control of energy metabolism.

We furthermore demonstrated that mice with access to HFD exclusively during their leptin resistant phase (ZT21 – ZT3) displayed impairments in a variety of parameters that indicate metabolic health, such as compromised rhythms of locomotor activity, metabolic rate, and energy expenditure as well as increased circulating insulin levels. Restricting HFD exclusively to the leptin sensitive phase (ZT9 – ZT15), on the other hand, protected mice from the development of these severe metabolic impairments. To date it is still largely unknown whether HFD-induced development of metabolic diseases results from an increase in body fat content, diet composition or disrupted circadian rhythms. We observed these differences between TRF groups despite an identical reduction in body weight and plasma leptin levels in all TRF mice, suggesting that they are based on the time of food intake during the 24-hour rhythm of leptin sensitivity, but independent from factors such as body composition or HFD content. Nonetheless, all mice fed HFD displayed a reduction in the absolute values of average metabolic rate and energy expenditure relative to mice fed LFD, demonstrating that also the HFD itself affects energy metabolism. In conclusion, these results demonstrate that TRF is efficient in the reduction of body weight and the amelioration of metabolic health. However, our findings also highlight the importance of synchronising food intake with daily physiological rhythms to maintain metabolic health.

Taken together, this thesis identifies novel pathways that are involved in the neuroendocrine regulation of energy metabolism and provides new insights into the connection between physiological rhythms and the development of metabolic diseases.

3.5.2. Zusammenfassung (Deutsch)

Adipositas und damit einhergehende Folgeerkrankungen, wie zum Beispiel Diabetes mellitus Typ 2, stellen ein enormes Gesundheitsproblem in unserer modernen Wohlstandsgesellschaft dar. Dem zentralen Nervensystem wurde dabei eine wesentliche Rolle in der Pathogenese dieser Erkrankungen nachgewiesen. Störungen des neuroendokrinen Systems, im Besonderen die Entstehung von hypothalamischer Leptinresistenz, korrelieren stark mit dem Auftreten von diätinduzierter Adipositas. Die molekularen Mechanismen, die diesen metabolischen Störungen zugrunde liegen, sind noch immer unzureichend erforscht. Zudem wurde gezeigt, dass die Regulierung des Energiemetabolismus eng mit der circadianen Uhr in Verbindung steht. Der Zusammenhang zwischen Adipositas und der Störung physiologischer Rhythmen bedarf jedoch noch weiterer Untersuchungen, um ausreichend verstanden zu werden. Das Ziel der vorliegenden Arbeit war es daher, sowohl neue Einblicke in die neuroendokrinen Mechanismen zu erlangen, die zur Entstehung von Leptinresistenz führen, als auch die Rolle physiologischer Rhythmen in der Entgleisung des Energiemetabolismus zu entschlüsseln.

In dieser Arbeit konnte die Expression von Genen des Adiponektinsignalweges im Hypothalamus von Mäusen sowie eine Reduktion der *adiponektin*-Konzentration bei gefasteten Tieren nachgewiesen werden. Dies dient möglicherweise dazu, den katabolen Eigenschaften von Adiponektin entgegenzuwirken und verhindert somit einen weiteren Verlust an Körpergewicht. Die Erhöhung der Genexpression des Adiponektinrezeptors, die wir in adipösen Mäusen nachweisen konnten, könnte einen Regulationsmechanismus darstellen, um den gesundheitsschädlichen Auswirkungen von Adipositas entgegenzuwirken. Dazu passen unsere Ergebnisse, die zeigen, dass zentral appliziertes Adiponektin zu einer Sensitisierung des Insulinsignalweges, einer Verbesserung der Glucosehomöostase sowie einem antiinflammatorischen Effekt führt.

Des Weiteren wurde die Rolle des WNT/β-catenin-Signalweges in der neuroendokrinen Regulation des Energiemetabolismus untersucht. Hierbei konnten wir die Expression aller untersuchten Gene des WNT-Signalweges im Gehirn von adulten Dsungarischen Zwerghamstern, deren Körpergewicht und Leptinsensitivität einer strengen jahreszeitlichen Regulation unterliegen, nachweisen. Zudem zeigten Zielgene des WNT-Signalweges eine tagesrhythmische Oszillation mit abfallenden Konzentrationen

während des Tages und ansteigenden Konzentrationen während der Nacht. Dies traf sowohl auf Langtag- (LT)- als auch auf Kurztag- (KT)-akklimatisierte Hamster zu. Die Genexpression bei LT-Hamstern war im Vergleich zu der bei KT-Hamstern ebenso erhöht wie die Phosphorylierung des WNT-Korezeptors LRP-6, ein Zeichen für die Aktivierung des WNT-Signalweges. Diese Ergebnisse deuten auf eine erhöhte WNT-Signaltransduktion in LT-Hamstern hin. Zudem führte die Gabe von Leptin zu einer zusätzlichen Aktivierung des WNT-Signalweges in Hamstern aus beiden Photoperioden. Zusammenfassend legen diese Daten nahe, dass der WNT-Signalweg an der saisonalen sowie tagesrhythmischen Regulation des Energiestoffwechsels und des Körpergewichts des Dsungarischen Zwerghamsters beteiligt ist.

Zusätzlich konnten wir einen 24-Stunden-Rhythmus bei der Aktivierung des Leptinsignalweges im Hypothalamus von schlanken Kontrollmäusen auf molekularer Ebene nachweisen. Sowohl die basale als auch die leptininduzierte Leptinsensitivität waren am Ende der aktiven Phase (Zeitgeber time; ZT0) der Tiere am höchsten und am Ende der inaktiven Phase am niedrigsten. Auch auf der Verhaltensebene zeigten die Mäuse zu ZT0 eine höhere Empfindlichkeit gegenüber Leptin als zu ZT12. Futteraufnahme, Bewegungsaktivität, Stoffwechselrate und Energieverbrauch unterlagen ebenfalls einem tagesrhythmischen Verlauf und waren während der inaktiven Phase reduziert und während der aktiven Phase erhöht.

Adipöse Mäuse wiesen im Vergleich dazu eine Störung des 24-Stunden-Rhythmus der Leptinsensitivität auf molekularer Ebene auf. Überraschenderweise bestand diese Leptinresistenz allerdings nicht während des gesamten Tagesverlaufs, sondern ausschließlich von ZT21 – ZT6. Zu allen anderen Zeitpunkten wiesen schlanke und adipöse Mäuse sowohl auf molekularer als auch auf Verhaltensebene die gleiche Sensitivität gegenüber Leptin auf. Zudem waren die Tagesrhythmen von Futteraufnahme, Bewegungsaktivität, Stoffwechselrate und Energieverbrauch bei Mäusen auf hochkalorischer Diät gestört. Die gesteigerte Kalorienaufnahme dieser Mäuse im Vergleich zu der von Kontrollmäusen fand ausschließlich während deren leptinresistenter Phase statt. Diese Ergebnisse zeigen, dass die rhythmische Oszillation der hypothalamischen Leptinsensitivität eine wichtige Rolle in der Regulation des Energiestoffwechsels spielt.

Des Weiteren konnten wir in dieser Arbeit nachweisen, dass der Verzehr einer hochkalorischen Diät ausschließlich während der leptinresistenen Phase adipöser Mäuse (ZT21 – ZT3) zu einer Beeinträchtigung verschiedener Parameter führt, die einen gesunden Stoffwechsel anzeigen. Dies traf auf die Tagesrhythmik von Bewegungsaktivität, Stoffwechselrate und Energieverbrauch sowie auf die zirkulierenden Insulinkonzentrationen zu. Mäuse, deren Futteraufnahme ausschließlich während ihrer leptinsensitiven Phase (ZT9 – ZT15) erfolgte, waren im Gegensatz dazu vor diesen negativen Auswirkungen auf den Energiemetabolismus geschützt. Ob die Entgleisung des Energiestoffwechsels, die durch den Konsum einer hochkalorischen Diät hervorgerufen wird, durch erhöhte Körperfettmasse, die Zusammensetzung der Diät oder Störungen der circadianen Rhythmen bedingt ist, ist noch immer weitgehend unklar. Die Unterschiede im Energiestoffwechsel traten ungeachtet einer identischen Abnahme an Körpergewicht sowie von zirkulierenden Leptinkonzentrationen bei allen Mäusen auf, deren Zugang zu hochkalorischer Diät auf verschiedene Zeiträume während des Tages (inaktive, leptinsensitive, aktive, leptinresistente Phase) beschränkt war. Dies deutet darauf hin, dass der Einfluss der Futteraufnahme auf die metabolische Gesundheit hauptsächlich von der Tageszeit und dem Status der Leptinsensitivität abhängt, weniger jedoch von anderen Faktoren wie Körperfettgehalt oder Zusammensetzung der Diät. Trotzdessen wiesen alle Mäuse, die eine hochkalorische Diät erhielten, im Vergleich zu Kontrollmäusen eine Beeinträchtigung der absoluten Werte für Stoffwechselrate und Energieverbrauch auf, was zusätzlich auf einen metabolischen Effekt der hochkalorischen Diät selbst hindeutet. Zusammengefasst konnten wir mit dieser Studie nachweisen, dass Varianten des intermittierenden Fastens, in diesem Fall die sogenannte 16/8-Variante mit 16 Stunden Fasten und 8 Stunden Nahrungsaufnahme pro Tag, bei einer Gewichtsabnahme und der Verbesserung der metabolischen Gesundheit helfen können. Allerdings ist hierbei zu beachten, dass der Zeitraum der Nahrungsaufnahme kritisch ist, um die positiven Auswirkungen auf den Stoffwechsel zu garantieren.

Mit der vorliegenden Arbeit konnten neue Einblicke in die neuroendokrine Regulation des Energiestoffwechsels gewonnen und weitere Signalwege identifiziert werden, die an dieser Regulation beteiligt sind. Zusätzlich konnten wir eine wichtige Rolle der rhythmischen Oszillation der hypothalamischen Leptinsensitivität bei der Entstehung von Stoffwechselentgleisungen nachweisen.

3.6. References

1. Edholm OG. Energy balance in man studies carried out by the Division of Human Physiology, National Institute for Medical Research. J Hum Nutr. 1977;31(6):413-31.

2. Harris RB, Kasser TR, Martin RJ. Dynamics of recovery of body composition after overfeeding, food restriction or starvation of mature female rats. J Nutr. 1986;116(12):2536-46.

3. Kennedy GC. The role of depot fat in the hypothalamic control of food intake in the rat. Proc R Soc Lond B Biol Sci. 1953;140(901):578-96.

4. Zhang Y, Proenca R, Maffei M, Barone M, Leopold L, Friedman JM. Positional cloning of the mouse obese gene and its human homologue. Nature. 1994;372(6505):425-32.

5. Halaas JL, Gajiwala KS, Maffei M, Cohen SL, Chait BT, Rabinowitz D, et al. Weight-reducing effects of the plasma protein encoded by the obese gene. Science. 1995;269(5223):543-6.

6. Considine RV, Sinha MK, Heiman ML, Kriauciunas A, Stephens TW, Nyce MR, et al. Serum immunoreactive-leptin concentrations in normal-weight and obese humans. N Engl J Med. 1996;334(5):292-5.

7. Farooqi IS, Jebb SA, Langmack G, Lawrence E, Cheetham CH, Prentice AM, et al. Effects of recombinant leptin therapy in a child with congenital leptin deficiency. N Engl J Med. 1999;341(12):879-84.

8. Campfield LA, Smith FJ, Guisez Y, Devos R, Burn P. Recombinant mouse OB protein: evidence for a peripheral signal linking adiposity and central neural networks. Science. 1995;269(5223):546-9.

9. Pelleymounter MA, Cullen MJ, Baker MB, Hecht R, Winters D, Boone T, et al. Effects of the obese gene product on body weight regulation in ob/ob mice. Science. 1995;269(5223):540-3.

10. Frederich RC, Lollmann B, Hamann A, Napolitano-Rosen A, Kahn BB, Lowell BB, et al. Expression of ob mRNA and its encoded protein in rodents. Impact of nutrition and obesity. J Clin Invest. 1995;96(3):1658-63.

11. Westerterp-Plantenga MS, Saris WH, Hukshorn CJ, Campfield LA. Effects of weekly administration of pegylated recombinant human OB protein on appetite profile and energy metabolism in obese men. Am J Clin Nutr. 2001;74(4):426-34.

12. Munzberg H, Flier JS, Bjorbaek C. Region-specific leptin resistance within the hypothalamus of diet-induced obese mice. Endocrinology. 2004;145(11):4880-9.

13. Smith PM, Ferguson AV. Neurophysiology of hunger and satiety. Dev Disabil Res Rev. 2008;14(2):96-104.

14. Coll AP, Yeo GS. The hypothalamus and metabolism: integrating signals to control energy and glucose homeostasis. Curr Opin Pharmacol. 2013;13(6):970-6.

15. Mistry AM, Swick AG, Romsos DR. Leptin rapidly lowers food intake and elevates metabolic rates in lean and ob/ob mice. J Nutr. 1997;127(10):2065-72.

16. Kastin AJ, Pan W, Maness LM, Koletsky RJ, Ernsberger P. Decreased transport of leptin across the blood-brain barrier in rats lacking the short form of the leptin receptor. Peptides. 1999;20(12):1449-53.

17. Schwartz MW, Peskind E, Raskind M, Boyko EJ, Porte D, Jr. Cerebrospinal fluid leptin levels: relationship to plasma levels and to adiposity in humans. Nat Med. 1996;2(5):589-93.

18. Bjorbaek C, Elmquist JK, Michl P, Ahima RS, van Bueren A, McCall AL, et al. Expression of leptin receptor isoforms in rat brain microvessels. Endocrinology. 1998;139(8):3485-91.

19. Tartaglia LA, Dembski M, Weng X, Deng N, Culpepper J, Devos R, et al. Identification and expression cloning of a leptin receptor, OB-R. Cell. 1995;83(7):1263-71.

20. Mercer JG, Hoggard N, Williams LM, Lawrence CB, Hannah LT, Trayhurn P. Localization of leptin receptor mRNA and the long form splice variant (Ob-Rb) in mouse hypothalamus and adjacent brain regions by in situ hybridization. FEBS letters. 1996;387(2-3):113-6.

21. Tang-Christensen M, Holst JJ, Hartmann B, Vrang N. The arcuate nucleus is pivotal in mediating the anorectic effects of centrally administered leptin. Neuroreport. 1999;10(6):1183-7.

22. Dawson R, Pelleymounter MA, Millard WJ, Liu S, Eppler B. Attenuation of leptin-mediated effects by monosodium glutamate-induced arcuate nucleus damage. The American journal of physiology. 1997;273(1 Pt 1):E202-6.

23. Schwartz MW, Woods SC, Porte D, Jr., Seeley RJ, Baskin DG. Central nervous system control of food intake. Nature. 2000;404(6778):661-71.

24. Morton GJ, Cummings DE, Baskin DG, Barsh GS, Schwartz MW. Central nervous system control of food intake and body weight. Nature. 2006;443(7109):289-95.

25. Bjorbaek C, Uotani S, da Silva B, Flier JS. Divergent signaling capacities of the long and short isoforms of the leptin receptor. The Journal of biological chemistry. 1997;272(51):32686-95.

26. Banks AS, Davis SM, Bates SH, Myers MG, Jr. Activation of downstream signals by the long form of the leptin receptor. The Journal of biological chemistry. 2000;275(19):14563-72.

27. Bjorbaek C, Kahn BB. Leptin signaling in the central nervous system and the periphery. Recent Prog Horm Res. 2004;59:305-31.

28. Bjorbaek C, Elmquist JK, Frantz JD, Shoelson SE, Flier JS. Identification of SOCS-3 as a potential mediator of central leptin resistance. Molecular cell. 1998;1(4):619-25.

29. Bjorbaek C, El-Haschimi K, Frantz JD, Flier JS. The role of SOCS-3 in leptin signaling and leptin resistance. The Journal of biological chemistry. 1999;274(42):30059-65.

30. Elmquist JK, Coppari R, Balthasar N, Ichinose M, Lowell BB. Identifying hypothalamic pathways controlling food intake, body weight, and glucose homeostasis. J Comp Neurol. 2005;493(1):63-71.

31. Schwartz MW, Baskin DG, Bukowski TR, Kuijper JL, Foster D, Lasser G, et al. Specificity of leptin action on elevated blood glucose levels and hypothalamic neuropeptide Y gene expression in ob/ob mice. Diabetes. 1996;45(4):531-5.

32. Baskin DG, Breininger JF, Schwartz MW. Leptin receptor mRNA identifies a subpopulation of neuropeptide Y neurons activated by fasting in rat hypothalamus. Diabetes. 1999;48(4):828-33.

33. Cheung CC, Clifton DK, Steiner RA. Proopiomelanocortin neurons are direct targets for leptin in the hypothalamus. Endocrinology. 1997;138(10):4489-92.

34. Cowley MA, Smart JL, Rubinstein M, Cerdan MG, Diano S, Horvath TL, et al. Leptin activates anorexigenic POMC neurons through a neural network in the arcuate nucleus. Nature. 2001;411(6836):480-4.

35. Stanley BG, Kyrkouli SE, Lampert S, Leibowitz SF. Neuropeptide Y chronically injected into the hypothalamus: a powerful neurochemical inducer of hyperphagia and obesity. Peptides. 1986;7(6):1189-92.

36. Billington CJ, Briggs JE, Grace M, Levine AS. Effects of intracerebroventricular injection of neuropeptide Y on energy metabolism. The American journal of physiology. 1991;260(2 Pt 2):R321-7.

37. Zarjevski N, Cusin I, Vettor R, Rohner-Jeanrenaud F, Jeanrenaud B. Chronic intracerebroventricular neuropeptide-Y administration to normal rats mimics hormonal and metabolic changes of obesity. Endocrinology. 1993;133(4):1753-8.

38. Hagan MM, Rushing PA, Benoit SC, Woods SC, Seeley RJ. Opioid receptor involvement in the effect of AgRP- (83-132) on food intake and food selection. American journal of physiology Regulatory, integrative and comparative physiology. 2001;280(3):R814-21.

39. Rossi M, Kim MS, Morgan DG, Small CJ, Edwards CM, Sunter D, et al. A C-terminal fragment of Agouti-related protein increases feeding and antagonizes the effect of alpha-melanocyte stimulating hormone in vivo. Endocrinology. 1998;139(10):4428-31.

40. Cone RD, Lu D, Koppula S, Vage DI, Klungland H, Boston B, et al. The melanocortin receptors: agonists, antagonists, and the hormonal control of pigmentation. Recent Prog Horm Res. 1996;51:287-317; discussion 8.

41. Fan W, Boston BA, Kesterson RA, Hruby VJ, Cone RD. Role of melanocortinergic neurons in feeding and the agouti obesity syndrome. Nature. 1997;385(6612):165-8.

42. Kristensen P, Judge ME, Thim L, Ribel U, Christjansen KN, Wulff BS, et al. Hypothalamic CART is a new anorectic peptide regulated by leptin. Nature. 1998;393(6680):72-6.

43. Elmquist JK, Maratos-Flier E, Saper CB, Flier JS. Unraveling the central nervous system pathways underlying responses to leptin. Nat Neurosci. 1998;1(6):445-50.

44. Elmquist JK, Elias CF, Saper CB. From lesions to leptin: hypothalamic control of food intake and body weight. Neuron. 1999;22(2):221-32.

45. Stanley BG, Willett VL, 3rd, Donias HW, Ha LH, Spears LC. The lateral hypothalamus: a primary site mediating excitatory amino acid-elicited eating. Brain research. 1993;630(1-2):41-9.

46. Banks WA, Kastin AJ, Huang W, Jaspan JB, Maness LM. Leptin enters the brain by a saturable system independent of insulin. Peptides. 1996;17(2):305-11.

47. Burguera B, Couce ME, Curran GL, Jensen MD, Lloyd RV, Cleary MP, et al. Obesity is associated with a decreased leptin transport across the blood-brain barrier in rats. Diabetes. 2000;49(7):1219-23.

48. Tups A, Ellis C, Moar KM, Logie TJ, Adam CL, Mercer JG, et al. Photoperiodic regulation of leptin sensitivity in the Siberian hamster, Phodopus

sungorus, is reflected in arcuate nucleus SOCS-3 (suppressor of cytokine signaling) gene expression. Endocrinology. 2004;145(3):1185-93.

49. Zhang X, Zhang G, Zhang H, Karin M, Bai H, Cai D. Hypothalamic IKKbeta/NF-kappaB and ER stress link overnutrition to energy imbalance and obesity. Cell. 2008;135(1):61-73.

50. De Souza CT, Araujo EP, Bordin S, Ashimine R, Zollner RL, Boschero AC, et al. Consumption of a fat-rich diet activates a proinflammatory response and induces insulin resistance in the hypothalamus. Endocrinology. 2005;146(10):4192-9.

51. Koch CE, Lowe C, Pretz D, Steger J, Williams LM, Tups A. High-fat diet induces leptin resistance in leptin-deficient mice. Journal of neuroendocrinology. 2014;26(2):58-67.

52. Benzler J, Ganjam GK, Pretz D, Oelkrug R, Koch CE, Legler K, et al. Central inhibition of IKKbeta/NF-kappaB signaling attenuates high-fat diet-induced obesity and glucose intolerance. Diabetes. 2015;64(6):2015-27.

53. Bagdade JD, Bierman EL, Porte D, Jr. The significance of basal insulin levels in the evaluation of the insulin response to glucose in diabetic and nondiabetic subjects. J Clin Invest. 1967;46(10):1549-57.

54. Bernard C. Leçons de physiologie expérimentale appliquée à la médecine, faites au Collège de France. Paris: J.B. Baillière et fils; 1854

55. Woods SC, Lotter EC, McKay LD, Porte D, Jr. Chronic intracerebroventricular infusion of insulin reduces food intake and body weight of baboons. Nature. 1979;282(5738):503-5.

56. Ikeda H, West DB, Pustek JJ, Figlewicz DP, Greenwood MR, Porte D, Jr., et al. Intraventricular insulin reduces food intake and body weight of lean but not obese Zucker rats. Appetite. 1986;7(4):381-6.

57. Bruning JC, Gautam D, Burks DJ, Gillette J, Schubert M, Orban PC, et al. Role of brain insulin receptor in control of body weight and reproduction. Science. 2000;289(5487):2122-5.

58. Baura GD, Foster DM, Porte D, Jr., Kahn SE, Bergman RN, Cobelli C, et al. Saturable transport of insulin from plasma into the central nervous system of dogs in vivo. A mechanism for regulated insulin delivery to the brain. J Clin Invest. 1993;92(4):1824-30.

59. Marks JL, Porte D, Jr., Stahl WL, Baskin DG. Localization of insulin receptor mRNA in rat brain by in situ hybridization. Endocrinology. 1990;127(6):3234-6.

60. Cheatham B, Kahn CR. Insulin action and the insulin signaling network. Endocr Rev. 1995;16(2):117-42.

61. Sutherland C, Leighton IA, Cohen P. Inactivation of glycogen synthase kinase-3 beta by phosphorylation: new kinase connections in insulin and growth-factor signalling. The Biochemical journal. 1993;296 (Pt 1):15-9.

62. Stambolic V, Woodgett JR. Mitogen inactivation of glycogen synthase kinase-3 beta in intact cells via serine 9 phosphorylation. The Biochemical journal. 1994;303 (Pt 3):701-4.

63. Cross DA, Alessi DR, Cohen P, Andjelkovich M, Hemmings BA. Inhibition of glycogen synthase kinase-3 by insulin mediated by protein kinase B. Nature. 1995;378(6559):785-9.

64. Cline GW, Johnson K, Regittnig W, Perret P, Tozzo E, Xiao L, et al. Effects of a novel glycogen synthase kinase-3 inhibitor on insulin-stimulated glucose metabolism in Zucker diabetic fatty (fa/fa) rats. Diabetes. 2002;51(10):2903-10.

65. Kaidanovich-Beilin O, Eldar-Finkelman H. Long-term treatment with novel glycogen synthase kinase-3 inhibitor improves glucose homeostasis in ob/ob mice: molecular characterization in liver and muscle. J Pharmacol Exp Ther. 2006;316(1):17-24.

66. Rao R, Hao CM, Redha R, Wasserman DH, McGuinness OP, Breyer MD. Glycogen synthase kinase 3 inhibition improves insulin-stimulated glucose metabolism but not hypertension in high-fat-fed C57BL/6J mice. Diabetologia. 2007;50(2):452-60.

67. Feve B, Bastard JP, Vidal H. [Relationship between obesity, inflammation and insulin resistance: new concepts]. C R Biol. 2006;329(8):587-97; discussion 653-5.

68. Kahn SE, Prigeon RL, McCulloch DK, Boyko EJ, Bergman RN, Schwartz MW, et al. Quantification of the relationship between insulin sensitivity and beta-cell function in human subjects. Evidence for a hyperbolic function. Diabetes. 1993;42(11):1663-72.

69. Diabetes Deutschland. [15.02.2018]. Available from: http://www.diabetes-deutschland.de/diabetesinzahlen.html.

70. Segal KR, Landt M, Klein S. Relationship between insulin sensitivity and plasma leptin concentration in lean and obese men. Diabetes. 1996;45(7):988-91.

71. Koch C, Augustine RA, Steger J, Ganjam GK, Benzler J, Pracht C, et al. Leptin rapidly improves glucose homeostasis in obese mice by increasing hypothalamic insulin sensitivity. The Journal of neuroscience : the official journal of the Society for Neuroscience. 2010;30(48):16180-7.

72. Zhao AZ, Huan JN, Gupta S, Pal R, Sahu A. A phosphatidylinositol 3-kinase phosphodiesterase 3B-cyclic AMP pathway in hypothalamic action of leptin on feeding. Nat Neurosci. 2002;5(8):727-8.

73. Dridi S, Taouis M. Adiponectin and energy homeostasis: consensus and controversy. J Nutr Biochem. 2009;20(11):831-9.

74. Yamauchi T, Kamon J, Waki H, Terauchi Y, Kubota N, Hara K, et al. The fat-derived hormone adiponectin reverses insulin resistance associated with both lipoatrophy and obesity. Nat Med. 2001;7(8):941-6.

75. Arita Y, Kihara S, Ouchi N, Takahashi M, Maeda K, Miyagawa J, et al. Paradoxical decrease of an adipose-specific protein, adiponectin, in obesity. Biochemical and biophysical research communications. 1999;257(1):79-83.

76. Hotta K, Funahashi T, Bodkin NL, Ortmeyer HK, Arita Y, Hansen BC, et al. Circulating concentrations of the adipocyte protein adiponectin are decreased in parallel with reduced insulin sensitivity during the progression to type 2 diabetes in rhesus monkeys. Diabetes. 2001;50(5):1126-33.

77. Hu E, Liang P, Spiegelman BM. AdipoQ is a novel adipose-specific gene dysregulated in obesity. The Journal of biological chemistry. 1996;271(18):10697-703.

78. Qi Y, Takahashi N, Hileman SM, Patel HR, Berg AH, Pajvani UB, et al. Adiponectin acts in the brain to decrease body weight. Nat Med. 2004;10(5):524-9.

79. Wilkinson M, Brown R, Imran SA, Ur E. Adipokine gene expression in brain and pituitary gland. Neuroendocrinology. 2007;86(3):191-209.

80. Neumeier M, Weigert J, Buettner R, Wanninger J, Schaffler A, Muller AM, et al. Detection of adiponectin in cerebrospinal fluid in humans. Am J Physiol Endocrinol Metab. 2007;293(4):E965-9.

81. Spranger J, Verma S, Gohring I, Bobbert T, Seifert J, Sindler AL, et al. Adiponectin does not cross the blood-brain barrier but modifies cytokine expression of brain endothelial cells. Diabetes. 2006;55(1):141-7.

82. Coope A, Milanski M, Araujo EP, Tambascia M, Saad MJ, Geloneze B, et al. AdipoR1 mediates the anorexigenic and insulin/leptin-like actions of adiponectin in the hypothalamus. FEBS letters. 2008;582(10):1471-6.

83. Yamauchi T, Kamon J, Minokoshi Y, Ito Y, Waki H, Uchida S, et al. Adiponectin stimulates glucose utilization and fatty-acid oxidation by activating AMP-activated protein kinase. Nat Med. 2002;8(11):1288-95.

84. Yamauchi T, Nio Y, Maki T, Kobayashi M, Takazawa T, Iwabu M, et al. Targeted disruption of AdipoR1 and AdipoR2 causes abrogation of adiponectin binding and metabolic actions. Nat Med. 2007;13(3):332-9.

85. Minokoshi Y, Alquier T, Furukawa N, Kim YB, Lee A, Xue B, et al. AMP-kinase regulates food intake by responding to hormonal and nutrient signals in the hypothalamus. Nature. 2004;428(6982):569-74.

86. Kos K, Harte AL, da Silva NF, Tonchev A, Chaldakov G, James S, et al. Adiponectin and resistin in human cerebrospinal fluid and expression of adiponectin receptors in the human hypothalamus. J Clin Endocrinol Metab. 2007;92(3):1129-36.

87. Guillod-Maximin E, Roy AF, Vacher CM, Aubourg A, Bailleux V, Lorsignol A, et al. Adiponectin receptors are expressed in hypothalamus and colocalized with proopiomelanocortin and neuropeptide Y in rodent arcuate neurons. J Endocrinol. 2009;200(1):93-105.

88. Hoppler S, Kavanagh CL. Wnt signalling: variety at the core. Journal of cell science. 2007;120(Pt 3):385-93.

89. Moon RT, Brown JD, Torres M. WNTs modulate cell fate and behavior during vertebrate development. Trends in genetics : TIG. 1997;13(4):157-62.

90. Peifer M, Polakis P. Wnt signaling in oncogenesis and embryogenesis--a look outside the nucleus. Science. 2000;287(5458):1606-9.

91. Nusse R. Wnt signaling in disease and in development. Cell Res. 2005;15(1):28-32.

92. Nusse R, van Ooyen A, Cox D, Fung YK, Varmus H. Mode of proviral activation of a putative mammary oncogene (int-1) on mouse chromosome 15. Nature. 1984;307(5947):131-6.

93. Adler PN. Planar signaling and morphogenesis in Drosophila. Developmental cell. 2002;2(5):525-35.

94. Veeman MT, Axelrod JD, Moon RT. A second canon. Functions and mechanisms of beta-catenin-independent Wnt signaling. Developmental cell. 2003;5(3):367-77.

95. Kohn AD, Moon RT. Wnt and calcium signaling: beta-catenin-independent pathways. Cell Calcium. 2005;38(3-4):439-46.

96. Montcouquiol M, Crenshaw EB, 3rd, Kelley MW. Noncanonical Wnt signaling and neural polarity. Annu Rev Neurosci. 2006;29:363-86.

97. Giles RH, van Es JH, Clevers H. Caught up in a Wnt storm: Wnt signaling in cancer. Biochim Biophys Acta. 2003;1653(1):1-24.

98. Jope RS, Johnson GV. The glamour and gloom of glycogen synthase kinase-3. Trends Biochem Sci. 2004;29(2):95-102.

99. Florez JC, Jablonski KA, Bayley N, Pollin TI, de Bakker PI, Shuldiner AR, et al. TCF7L2 polymorphisms and progression to diabetes in the Diabetes Prevention Program. N Engl J Med. 2006;355(3):241-50.

100. Grant SF, Thorleifsson G, Reynisdottir I, Benediktsson R, Manolescu A, Sainz J, et al. Variant of transcription factor 7-like 2 (TCF7L2) gene confers risk of type 2 diabetes. Nat Genet. 2006;38(3):320-3.

101. Kiessling A, Ehrhart-Bornstein M. Transcription factor 7-like 2 (TCFL2) - a novel factor involved in pathogenesis of type 2 diabetes. Comment on: Grant et al., Nature Genetics 2006, Published online 15 January 2006. Horm Metab Res. 2006;38(2):137-8.

102. Mani A, Radhakrishnan J, Wang H, Mani A, Mani MA, Nelson-Williams C, et al. LRP6 mutation in a family with early coronary disease and metabolic risk factors. Science. 2007;315(5816):1278-82.

103. Bhanot P, Brink M, Samos CH, Hsieh JC, Wang Y, Macke JP, et al. A new member of the frizzled family from Drosophila functions as a Wingless receptor. Nature. 1996;382(6588):225-30.

104. Rulifson EJ, Wu CH, Nusse R. Pathway specificity by the bifunctional receptor frizzled is determined by affinity for wingless. Molecular cell. 2000;6(1):117-26.

105. van Amerongen R, Mikels A, Nusse R. Alternative wnt signaling is initiated by distinct receptors. Science signaling. 2008;1(35):re9.

106. Tamai K, Semenov M, Kato Y, Spokony R, Liu C, Katsuyama Y, et al. LDL-receptor-related proteins in Wnt signal transduction. Nature. 2000;407(6803):530-5.

107. Wehrli M, Dougan ST, Caldwell K, O'Keefe L, Schwartz S, Vaizel-Ohayon D, et al. arrow encodes an LDL-receptor-related protein essential for Wingless signalling. Nature. 2000;407(6803):527-30.

108. Mao J, Wang J, Liu B, Pan W, Farr GH, 3rd, Flynn C, et al. Low-density lipoprotein receptor-related protein-5 binds to Axin and regulates the canonical Wnt signaling pathway. Molecular cell. 2001;7(4):801-9.

109. Mao B, Wu W, Li Y, Hoppe D, Stannek P, Glinka A, et al. LDL-receptor-related protein 6 is a receptor for Dickkopf proteins. Nature. 2001;411(6835):321-5.

110. Finch PW, He X, Kelley MJ, Uren A, Schaudies RP, Popescu NC, et al. Purification and molecular cloning of a secreted, Frizzled-related antagonist of Wnt action. Proceedings of the National Academy of Sciences of the United States of America. 1997;94(13):6770-5.

111. Rattner A, Hsieh JC, Smallwood PM, Gilbert DJ, Copeland NG, Jenkins NA, et al. A family of secreted proteins contains homology to the cysteine-rich ligand-binding domain of frizzled receptors. Proceedings of the National Academy of Sciences of the United States of America. 1997;94(7):2859-63.

112. Schwarz-Romond T, Metcalfe C, Bienz M. Dynamic recruitment of axin by Dishevelled protein assemblies. Journal of cell science. 2007;120(Pt 14):2402-12.

113. Cliffe A, Hamada F, Bienz M. A role of Dishevelled in relocating Axin to the plasma membrane during wingless signaling. Curr Biol. 2003;13(11):960-6.

114. Gao C, Chen YG. Dishevelled: The hub of Wnt signaling. Cell Signal. 2010;22(5):717-27.

115. Aberle H, Bauer A, Stappert J, Kispert A, Kemler R. beta-catenin is a target for the ubiquitin-proteasome pathway. EMBO J. 1997;16(13):3797-804.

116. Liu C, Li Y, Semenov M, Han C, Baeg GH, Tan Y, et al. Control of beta-catenin phosphorylation/degradation by a dual-kinase mechanism. Cell. 2002;108(6):837-47.

117. Diehn M, Alizadeh AA, Rando OJ, Liu CL, Stankunas K, Botstein D, et al. Genomic expression programs and the integration of the CD28 costimulatory signal in T cell activation. Proceedings of the National Academy of Sciences of the United States of America. 2002;99(18):11796-801.

118. MacDonald BT, Tamai K, He X. Wnt/beta-catenin signaling: components, mechanisms, and diseases. Developmental cell. 2009;17(1):9-26.

119. Benzler J, Andrews ZB, Pracht C, Stohr S, Shepherd PR, Grattan DR, et al. Hypothalamic WNT signalling is impaired during obesity and reinstated by leptin treatment in male mice. Endocrinology. 2013;154(12):4737-45.

120. Benzler J, Ganjam GK, Kruger M, Pinkenburg O, Kutschke M, Stohr S, et al. Hypothalamic glycogen synthase kinase 3beta has a central role in the regulation of food intake and glucose metabolism. The Biochemical journal. 2012;447(1):175-84.

121. Lattanzio S, Santilli F, Liani R, Vazzana N, Ueland T, Di Fulvio P, et al. Circulating dickkopf-1 in diabetes mellitus: association with platelet activation and effects of improved metabolic control and low-dose aspirin. J Am Heart Assoc. 2014;3(4).

122. Li X, Shan J, Chang W, Kim I, Bao J, Lee HJ, et al. Chemical and genetic evidence for the involvement of Wnt antagonist Dickkopf2 in regulation of glucose metabolism. Proceedings of the National Academy of Sciences of the United States of America. 2012;109(28):11402-7.

123. Ohba S, Lanigan TM, Roessler BJ. Leptin receptor JAK2/STAT3 signaling modulates expression of Frizzled receptors in articular chondrocytes. Osteoarthritis and cartilage / OARS, Osteoarthritis Research Society. 2010;18(12):1620-9.

124. Inestrosa NC, Arenas E. Emerging roles of Wnts in the adult nervous system. Nature reviews Neuroscience. 2010;11(2):77-86.

125. Helfer G, Ross AW, Russell L, Thomson LM, Shearer KD, Goodman TH, et al. Photoperiod regulates vitamin A and Wnt/beta-catenin signaling in F344 rats. Endocrinology. 2012;153(2):815-24.

126. Ross AW, Helfer G, Russell L, Darras VM, Morgan PJ. Thyroid hormone signalling genes are regulated by photoperiod in the hypothalamus of F344 rats. PloS one. 2011;6(6):e21351.

127. Helfer G, Ross AW, Morgan PJ. Neuromedin U partly mimics thyroid-stimulating hormone and triggers Wnt/beta-catenin signalling in the photoperiodic response of F344 rats. Journal of neuroendocrinology. 2013;25(12):1264-72.

128. Mairan J-JDd. Observation botanique. Histoire de l'Academie royale des sciences. Paris 1729. p. 35.

129. Candolle APd. Physiologie végétale, ou Exposition des forces et des fonctions vitales des végétaux. Paris: Béchet jeune; 1832.

130. Halberg F. [Physiologic 24-hour periodicity; general and procedural considerations with reference to the adrenal cycle]. Int Z Vitaminforsch Beih. 1959;10:225-96.

131. Loudon AS. Circadian biology: a 2.5 billion year old clock. Curr Biol. 2012;22(14):R570-1.

132. Stephan FK, Zucker I. Circadian rhythms in drinking behavior and locomotor activity of rats are eliminated by hypothalamic lesions. Proceedings of the National Academy of Sciences of the United States of America. 1972;69(6):1583-6.

133. Moore RY, Eichler VB. Loss of a circadian adrenal corticosterone rhythm following suprachiasmatic lesions in the rat. Brain research. 1972;42(1):201-6.

134. Ralph MR, Foster RG, Davis FC, Menaker M. Transplanted suprachiasmatic nucleus determines circadian period. Science. 1990;247(4945):975-8.

135. Takahashi JS, Hong HK, Ko CH, McDearmon EL. The genetics of mammalian circadian order and disorder: implications for physiology and disease. Nat Rev Genet. 2008;9(10):764-75.

136. Yamazaki S, Yoshikawa T, Biscoe EW, Numano R, Gallaspy LM, Soulsby S, et al. Ontogeny of circadian organization in the rat. J Biol Rhythms. 2009;24(1):55-63.

137. Yoo SH, Yamazaki S, Lowrey PL, Shimomura K, Ko CH, Buhr ED, et al. PERIOD2::LUCIFERASE real-time reporting of circadian dynamics reveals persistent circadian oscillations in mouse peripheral tissues. Proceedings of the National Academy of Sciences of the United States of America. 2004;101(15):5339-46.

138. Inouye ST, Kawamura H. Persistence of circadian rhythmicity in a mammalian hypothalamic "island" containing the suprachiasmatic nucleus. Proceedings of the National Academy of Sciences of the United States of America. 1979;76(11):5962-6.

139. Shibata S, Oomura Y, Kita H, Hattori K. Circadian rhythmic changes of neuronal activity in the suprachiasmatic nucleus of the rat hypothalamic slice. Brain research. 1982;247(1):154-8.

140. Honma S, Honma K, Hiroshige T. Dissociation of circadian rhythms in rats with a hypothalamic island. The American journal of physiology. 1984;246(6 Pt 2):R949-54.

141. Eskes GA, Rusak B. Horizontal knife cuts in the suprachiasmatic area prevent hamster gonadal responses to photoperiod. Neuroscience letters. 1985;61(3):261-6.

142. Panda S, Hogenesch JB. It's all in the timing: many clocks, many outputs. J Biol Rhythms. 2004;19(5):374-87.

143. Abrahamson EE, Moore RY. Lesions of suprachiasmatic nucleus efferents selectively affect rest-activity rhythm. Mol Cell Endocrinol. 2006;252(1-2):46-56.

144. Pittendrigh CS. Circadian rhythms and the circadian organization of living systems. Cold Spring Harb Symp Quant Biol. 1960;25:159-84.

145. Daan S. Tonic and phasic effects of light in the entrainment of circadian rhythms. Ann N Y Acad Sci. 1977;290:51-9.

146. Pilorz V, Helfrich-Forster C, Oster H. The role of the circadian clock system in physiology. Pflugers Arch. 2018;470(2):227-39.

147. Konopka RJ, Benzer S. Clock mutants of Drosophila melanogaster. Proceedings of the National Academy of Sciences of the United States of America. 1971;68(9):2112-6.

148. Vitaterna MH, King DP, Chang AM, Kornhauser JM, Lowrey PL, McDonald JD, et al. Mutagenesis and mapping of a mouse gene, Clock, essential for circadian behavior. Science. 1994;264(5159):719-25.

149. Huang N, Chelliah Y, Shan Y, Taylor CA, Yoo SH, Partch C, et al. Crystal structure of the heterodimeric CLOCK:BMAL1 transcriptional activator complex. Science. 2012;337(6091):189-94.

150. Koike N, Yoo SH, Huang HC, Kumar V, Lee C, Kim TK, et al. Transcriptional architecture and chromatin landscape of the core circadian clock in mammals. Science. 2012;338(6105):349-54.

151. Buhr ED, Takahashi JS. Molecular components of the Mammalian circadian clock. Handb Exp Pharmacol. 2013(217):3-27.

152. Etchegaray JP, Machida KK, Noton E, Constance CM, Dallmann R, Di Napoli MN, et al. Casein kinase 1 delta regulates the pace of the mammalian circadian clock. Molecular and cellular biology. 2009;29(14):3853-66.

153. Meng QJ, Logunova L, Maywood ES, Gallego M, Lebiecki J, Brown TM, et al. Setting clock speed in mammals: the CK1 epsilon tau mutation in mice accelerates circadian pacemakers by selectively destabilizing PERIOD proteins. Neuron. 2008;58(1):78-88.

154. Gooley JJ, Lu J, Chou TC, Scammell TE, Saper CB. Melanopsin in cells of origin of the retinohypothalamic tract. Nat Neurosci. 2001;4(12):1165.

155. Hattar S, Liao HW, Takao M, Berson DM, Yau KW. Melanopsin-containing retinal ganglion cells: architecture, projections, and intrinsic photosensitivity. Science. 2002;295(5557):1065-70.

156. Morin LP, Allen CN. The circadian visual system, 2005. Brain Res Rev. 2006;51(1):1-60.

157. Froy O, Miskin R. Effect of feeding regimens on circadian rhythms: implications for aging and longevity. Aging (Albany NY). 2010;2(1):7-27.

158. Pendergast JS, Branecky KL, Yang W, Ellacott KL, Niswender KD, Yamazaki S. High-fat diet acutely affects circadian organisation and eating behavior. Eur J Neurosci. 2013;37(8):1350-6.

159. Krieger DT, Hauser H, Krey LC. Suprachiasmatic nuclear lesions do not abolish food-shifted circadian adrenal and temperature rhythmicity. Science. 1977;197(4301):398-9.

160. Stephan FK, Swann JM, Sisk CL. Entrainment of circadian rhythms by feeding schedules in rats with suprachiasmatic lesions. Behav Neural Biol. 1979;25(4):545-54.

161. Tan K, Knight ZA, Friedman JM. Ablation of AgRP neurons impairs adaption to restricted feeding. Molecular metabolism. 2014;3(7):694-704.

162. Rutter J, Reick M, McKnight SL. Metabolism and the control of circadian rhythms. Annu Rev Biochem. 2002;71:307-31.

163. Green CB, Takahashi JS, Bass J. The meter of metabolism. Cell. 2008;134(5):728-42.

164. Lamia KA, Sachdeva UM, DiTacchio L, Williams EC, Alvarez JG, Egan DF, et al. AMPK regulates the circadian clock by cryptochrome phosphorylation and degradation. Science. 2009;326(5951):437-40.

165. Bass J, Takahashi JS. Circadian integration of metabolism and energetics. Science. 2010;330(6009):1349-54.

166. Asher G, Schibler U. Crosstalk between components of circadian and metabolic cycles in mammals. Cell metabolism. 2011;13(2):125-37.

167. Gerhart-Hines Z, Lazar MA. Circadian metabolism in the light of evolution. Endocr Rev. 2015;36(3):289-304.

168. Coomans CP, van den Berg SA, Lucassen EA, Houben T, Pronk AC, van der Spek RD, et al. The suprachiasmatic nucleus controls circadian energy metabolism and hepatic insulin sensitivity. Diabetes. 2013;62(4):1102-8.

169. Shi SQ, Ansari TS, McGuinness OP, Wasserman DH, Johnson CH. Circadian disruption leads to insulin resistance and obesity. Curr Biol. 2013;23(5):372-81.

170. Marcheva B, Ramsey KM, Buhr ED, Kobayashi Y, Su H, Ko CH, et al. Disruption of the clock components CLOCK and BMAL1 leads to hypoinsulinaemia and diabetes. Nature. 2010;466(7306):627-31.

171. Turek FW, Joshu C, Kohsaka A, Lin E, Ivanova G, McDearmon E, et al. Obesity and metabolic syndrome in circadian Clock mutant mice. Science. 2005;308(5724):1043-5.

172. McCarthy JJ, Andrews JL, McDearmon EL, Campbell KS, Barber BK, Miller BH, et al. Identification of the circadian transcriptome in adult mouse skeletal muscle. Physiol Genomics. 2007;31(1):86-95.

173. Shimba S, Ishii N, Ohta Y, Ohno T, Watabe Y, Hayashi M, et al. Brain and muscle Arnt-like protein-1 (BMAL1), a component of the molecular clock, regulates adipogenesis. Proceedings of the National Academy of Sciences of the United States of America. 2005;102(34):12071-6.

174. Carvas JM, Vukolic A, Yepuri G, Xiong Y, Popp K, Schmutz I, et al. Period2 gene mutant mice show compromised insulin-mediated endothelial nitric oxide release and altered glucose homeostasis. Front Physiol. 2012;3:337.

175. So AY, Bernal TU, Pillsbury ML, Yamamoto KR, Feldman BJ. Glucocorticoid regulation of the circadian clock modulates glucose homeostasis. Proceedings of the National Academy of Sciences of the United States of America. 2009;106(41):17582-7.

176. Yang S, Liu A, Weidenhammer A, Cooksey RC, McClain D, Kim MK, et al. The role of mPer2 clock gene in glucocorticoid and feeding rhythms. Endocrinology. 2009;150(5):2153-60.

177. Roenneberg T, Allebrandt KV, Merrow M, Vetter C. Social jetlag and obesity. Curr Biol. 2012;22(10):939-43.

178. Scheer FA, Hilton MF, Mantzoros CS, Shea SA. Adverse metabolic and cardiovascular consequences of circadian misalignment. Proceedings of the National Academy of Sciences of the United States of America. 2009;106(11):4453-8.

179. Kettner NM, Mayo SA, Hua J, Lee C, Moore DD, Fu L. Circadian Dysfunction Induces Leptin Resistance in Mice. Cell metabolism. 2015;22(3):448-59.

180. Branecky KL, Niswender KD, Pendergast JS. Disruption of Daily Rhythms by High-Fat Diet Is Reversible. PloS one. 2015;10(9):e0137970.

181. Kohsaka A, Laposky AD, Ramsey KM, Estrada C, Joshu C, Kobayashi Y, et al. High-fat diet disrupts behavioral and molecular circadian rhythms in mice. Cell metabolism. 2007;6(5):414-21.

182. Li AJ, Wiater MF, Oostrom MT, Smith BR, Wang Q, Dinh TT, et al. Leptin-sensitive neurons in the arcuate nuclei contribute to endogenous feeding rhythms. American journal of physiology Regulatory, integrative and comparative physiology. 2012;302(11):R1313-26.

183. Chaix A, Zarrinpar A, Miu P, Panda S. Time-restricted feeding is a preventative and therapeutic intervention against diverse nutritional challenges. Cell metabolism. 2014;20(6):991-1005.

184. Hatori M, Vollmers C, Zarrinpar A, DiTacchio L, Bushong EA, Gill S, et al. Time-restricted feeding without reducing caloric intake prevents metabolic diseases in mice fed a high-fat diet. Cell metabolism. 2012;15(6):848-60.

185. Longo VD, Mattson MP. Fasting: molecular mechanisms and clinical applications. Cell metabolism. 2014;19(2):181-92.

186. Arumugam TV, Phillips TM, Cheng A, Morrell CH, Mattson MP, Wan R. Age and energy intake interact to modify cell stress pathways and stroke outcome. Ann Neurol. 2010;67(1):41-52.

187. Gill S, Panda S. A Smartphone App Reveals Erratic Diurnal Eating Patterns in Humans that Can Be Modulated for Health Benefits. Cell metabolism. 2015;22(5):789-98.

188. Garner WW, Allard, HA. Flowering and Fruiting of Plants as Controlled by the Lenght of Day. Yearbook of the US Dept of Agr 1920. p. 377-400.

189. Hardeland R, Pandi-Perumal SR, Cardinali DP. Melatonin. Int J Biochem Cell Biol. 2006;38(3):313-6.

190. Moore RY. Neural control of the pineal gland. Behav Brain Res. 1996;73(1-2):125-30.

191. Klein DC, Moore RY. Pineal N-acetyltransferase and hydroxyindole-O-methyltransferase: control by the retinohypothalamic tract and the suprachiasmatic nucleus. Brain research. 1979;174(2):245-62.

192. Schwartz WJ, de la Iglesia HO, Zlomanczuk P, Illnerova H. Encoding le quattro stagioni within the mammalian brain: photoperiodic orchestration through the suprachiasmatic nucleus. J Biol Rhythms. 2001;16(4):302-11.

193. Bartness TJ, Goldman BD. Mammalian pineal melatonin: a clock for all seasons. Experientia. 1989;45(10):939-45.

194. Pevet P, Jacob N, Lakhdar-Ghazal N, Vuillez P. How do the suprachiasmatic nuclei of the hypothalamus integrate photoperiodic information? Biol Cell. 1997;89(9):569-77.

195. Mrugala M, Zlomanczuk P, Jagota A, Schwartz WJ. Rhythmic multiunit neural activity in slices of hamster suprachiasmatic nucleus reflect prior photoperiod. American journal of physiology Regulatory, integrative and comparative physiology. 2000;278(4):R987-94.

196. Meijer JH, Michel S, Vanderleest HT, Rohling JH. Daily and seasonal adaptation of the circadian clock requires plasticity of the SCN neuronal network. Eur J Neurosci. 2010;32(12):2143-51.

197. Heldmaier G. Seasonal acclimatization of energy requirements in mammals: functional significance of body weight control, hypothermia, torpor and hibernation. In: Wieser W, Gnaiger E, Energy Transformations in Cells and Organisms. Stuttgart: Georg Thieme; 1989 p. 130-9.

198. Bergmann C. Über die Verhältnisse der Wärmeökonomie der Thiere zu ihrer Grösse. Göttinger Studien 1847 p. 595-708.

199. Wade GN, Bartness TJ. Effects of photoperiod and gonadectomy on food intake, body weight, and body composition in Siberian hamsters. The American journal of physiology. 1984;246(1 Pt 2):R26-30.

200. Gorman MR, Zucker I. Seasonal adaptations of Siberian hamsters. II. Pattern of change in daylength controls annual testicular and body weight rhythms. Biology of reproduction. 1995;53(1):116-25.

201. Klingenspor M, Niggemann H, Heldmaier G. Modulation of leptin sensitivity by short photoperiod acclimation in the Djungarian hamster, Phodopus sungorus. Journal of comparative physiology B, Biochemical, systemic, and environmental physiology. 2000;170(1):37-43.

202. Figala J, Hoffmann K, Goldau G. [The annual cycle in the Djungarian Hamster Phodopus sungorus Pallas]. Oecologia. 1973;12(2):89-118.

203. Heldmaier GS, S. . Seasonal control of energy requirements for thermoregulation in the djungarian hamster (*Phodopus sungorus*), living in natural photoperiod. Journal of comparative physiology. 1981 (142):429-37.

204. Atcha Z, Cagampang FR, Stirland JA, Morris ID, Brooks AN, Ebling FJ, et al. Leptin acts on metabolism in a photoperiod-dependent manner, but has no effect on reproductive function in the seasonally breeding Siberian hamster (Phodopus sungorus). Endocrinology. 2000;141(11):4128-35.

205. Rousseau K, Atcha Z, Cagampang FR, Le Rouzic P, Stirland JA, Ivanov TR, et al. Photoperiodic regulation of leptin resistance in the seasonally breeding Siberian hamster (Phodopus sungorus). Endocrinology. 2002;143(8):3083-95.

206. Tups A, Barrett P, Ross AW, Morgan PJ, Klingenspor M, Mercer JG. The suppressor of cytokine signalling 3, SOCS3, may be one critical modulator of seasonal body weight changes in the Siberian hamster, Phodopus sungorus. Journal of neuroendocrinology. 2006;18(2):139-45.

207. Koch CE, Lowe C, Legler K, Benzler J, Boucsein A, Bottiger G, et al. Central adiponectin acutely improves glucose tolerance in male mice. Endocrinology. 2014;155(5):1806-16.

208. Boucsein A, Benzler J, Hempp C, Stohr S, Helfer G, Tups A. Photoperiodic and Diurnal Regulation of WNT Signaling in the Arcuate Nucleus of the Female Djungarian Hamster, Phodopus sungorus. Endocrinology. 2016;157(2):799-809.

209. Paxinos G, Franklin KBJ, Franklin KBJ. The mouse brain in stereotaxic coordinates. 2nd ed. San Diego: Academic Press; 2001.

210. Lighton JR, Turner RJ. The hygric hypothesis does not hold water: abolition of discontinuous gas exchange cycles does not affect water loss in the ant Camponotus vicinus. J Exp Biol. 2008;211(Pt 4):563-7.

211. Benzler J, Ganjam GK, Legler K, Stohr S, Kruger M, Steger J, et al. Acute inhibition of central c-Jun N-terminal kinase restores hypothalamic insulin signalling and alleviates glucose intolerance in diabetic mice. Journal of neuroendocrinology. 2013;25(5):446-54.

212. Lyons JP, Mueller UW, Ji H, Everett C, Fang X, Hsieh JC, et al. Wnt-4 activates the canonical beta-catenin-mediated Wnt pathway and binds Frizzled-6 CRD: functional implications of Wnt/beta-catenin activity in kidney epithelial cells. Experimental cell research. 2004;298(2):369-87.

213. Yoshino K, Rubin JS, Higinbotham KG, Uren A, Anest V, Plisov SY, et al. Secreted Frizzled-related proteins can regulate metanephric development. Mechanisms of development. 2001;102(1-2):45-55.

214. Tups A, Helwig M, Stohr S, Barrett P, Mercer JG, Klingenspor M. Photoperiodic regulation of insulin receptor mRNA and intracellular insulin signaling in the arcuate nucleus of the Siberian hamster, Phodopus sungorus. American journal of physiology Regulatory, integrative and comparative physiology. 2006;291(3):R643-50.

215. Guo B, Chatterjee S, Li L, Kim JM, Lee J, Yechoor VK, et al. The clock gene, brain and muscle Arnt-like 1, regulates adipogenesis via Wnt signaling pathway. FASEB journal : official publication of the Federation of American Societies for Experimental Biology. 2012;26(8):3453-63.

216. Hatanaka F, Matsubara C, Myung J, Yoritaka T, Kamimura N, Tsutsumi S, et al. Genome-wide profiling of the core clock protein BMAL1 targets reveals a strict relationship with metabolism. Molecular and cellular biology. 2010;30(24):5636-48.

217. Ross SE, Hemati N, Longo KA, Bennett CN, Lucas PC, Erickson RL, et al. Inhibition of adipogenesis by Wnt signaling. Science. 2000;289(5481):950-3.

218. Bennett CN, Ross SE, Longo KA, Bajnok L, Hemati N, Johnson KW, et al. Regulation of Wnt signaling during adipogenesis. The Journal of biological chemistry. 2002;277(34):30998-1004.

219. Wang ND, Finegold MJ, Bradley A, Ou CN, Abdelsayed SV, Wilde MD, et al. Impaired energy homeostasis in C/EBP alpha knockout mice. Science. 1995;269(5227):1108-12.

220. Bartness TJ. Photoperiod, sex, gonadal steroids, and housing density affect body fat in hamsters. Physiol Behav. 1996;60(2):517-29.

221. Ming GL, Song H. Adult neurogenesis in the mammalian brain: significant answers and significant questions. Neuron. 2011;70(4):687-702.

222. Duan X, Kang E, Liu CY, Ming GL, Song H. Development of neural stem cell in the adult brain. Curr Opin Neurobiol. 2008;18(1):108-15.

223. Lie DC, Song H, Colamarino SA, Ming GL, Gage FH. Neurogenesis in the adult brain: new strategies for central nervous system diseases. Annu Rev Pharmacol Toxicol. 2004;44:399-421.

224. Alvarez-Buylla A, Lim DA. For the long run: maintaining germinal niches in the adult brain. Neuron. 2004;41(5):683-6.

225. Fortress AM, Frick KM. Hippocampal Wnt Signaling: Memory Regulation and Hormone Interactions. Neuroscientist. 2016;22(3):278-94.

226. Wang YZ, Yamagami T, Gan Q, Wang Y, Zhao T, Hamad S, et al. Canonical Wnt signaling promotes the proliferation and neurogenesis of peripheral olfactory stem cells during postnatal development and adult regeneration. Journal of cell science. 2011;124(Pt 9):1553-63.

227. Wang X, Kopinke D, Lin J, McPherson AD, Duncan RN, Otsuna H, et al. Wnt signaling regulates postembryonic hypothalamic progenitor differentiation. Developmental cell. 2012;23(3):624-36.

228. Wang X, Lee JE, Dorsky RI. Identification of Wnt-responsive cells in the zebrafish hypothalamus. Zebrafish. 2009;6(1):49-58.

229. Tavolaro FM, Thomson LM, Ross AW, Morgan PJ, Helfer G. Photoperiodic effects on seasonal physiology, reproductive status and hypothalamic gene expression in young male F344 rats. Journal of neuroendocrinology. 2015;27(2):79-87.

230. Huang L, DeVries GJ, Bittman EL. Photoperiod regulates neuronal bromodeoxyuridine labeling in the brain of a seasonally breeding mammal. J Neurobiol. 1998;36(3):410-20.

231. Horton TH, Buxton OM, Losee-Olson S, Turek FW. Twenty-four-hour profiles of serum leptin in siberian and golden hamsters: photoperiodic and diurnal variations. Hormones and behavior. 2000;37(4):388-98.

232. Weitten M, Robin JP, Oudart H, Pevet P, Habold C. Hormonal changes and energy substrate availability during the hibernation cycle of Syrian hamsters. Hormones and behavior. 2013;64(4):611-7.

233. Bartness TJ, Wade GN. Photoperiodic control of body weight and energy metabolism in Syrian hamsters (Mesocricetus auratus): role of pineal gland, melatonin, gonads, and diet. Endocrinology. 1984;114(2):492-8.

234. Bolborea M, Laran-Chich MP, Rasri K, Hildebrandt H, Govitrapong P, Simonneaux V, et al. Melatonin controls photoperiodic changes in tanycyte vimentin and neural cell adhesion molecule expression in the Djungarian hamster (Phodopus sungorus). Endocrinology. 2011;152(10):3871-83.

235. Hazlerigg DG, Wyse CA, Dardente H, Hanon EA, Lincoln GA. Photoperiodic variation in CD45-positive cells and cell proliferation in the mediobasal hypothalamus of the Soay sheep. Chronobiol Int. 2013;30(4):548-58.

236. Herwig A, de Vries EM, Bolborea M, Wilson D, Mercer JG, Ebling FJ, et al. Hypothalamic ventricular ependymal thyroid hormone deiodinases are an important element of circannual timing in the Siberian hamster (Phodopus sungorus). PloS one. 2013;8(4):e62003.

237. Lee DA, Bedont JL, Pak T, Wang H, Song J, Miranda-Angulo A, et al. Tanycytes of the hypothalamic median eminence form a diet-responsive neurogenic niche. Nat Neurosci. 2012;15(5):700-2.

238. Kokoeva MV, Yin H, Flier JS. Neurogenesis in the hypothalamus of adult mice: potential role in energy balance. Science. 2005;310(5748):679-83.

239. Mercer JG, Tups A. Neuropeptides and anticipatory changes in behaviour and physiology: seasonal body weight regulation in the Siberian hamster. Eur J Pharmacol. 2003;480(1-3):43-50.

240. Tups A, Stohr S, Helwig M, Barrett P, Krol E, Schachtner J, et al. Seasonal leptin resistance is associated with impaired signalling via JAK2-STAT3 but not ERK, possibly mediated by reduced hypothalamic GRB2 protein. Journal of comparative physiology B, Biochemical, systemic, and environmental physiology. 2012;182(4):553-67.

241. Bender MC, Sifuentes CJ, Denver RJ. Leptin Induces Mitosis and Activates the Canonical Wnt/beta-Catenin Signaling Pathway in Neurogenic Regions of Xenopus Tadpole Brain. Front Endocrinol (Lausanne). 2017;8:99.

242. Ellis C, Moar KM, Logie TJ, Ross AW, Morgan PJ, Mercer JG. Diurnal profiles of hypothalamic energy balance gene expression with photoperiod manipulation in the Siberian hamster, Phodopus sungorus. American journal of physiology Regulatory, integrative and comparative physiology. 2008;294(4):R1148-53.

243. Rizwan MZ, Mehlitz S, Grattan DR, Tups A. Temporal and regional onset of leptin resistance in diet-induced obese mice. Journal of neuroendocrinology. 2017;29(10).

244. Matheny M, Shapiro A, Tumer N, Scarpace PJ. Region-specific diet-induced and leptin-induced cellular leptin resistance includes the ventral tegmental area in rats. Neuropharmacology. 2011;60(2-3):480-7.

245. Wilsey J, Scarpace PJ. Caloric restriction reverses the deficits in leptin receptor protein and leptin signaling capacity associated with diet-induced obesity: role of leptin in the regulation of hypothalamic long-form leptin receptor expression. J Endocrinol. 2004;181(2):297-306.

246. Hotamisligil GS. Inflammation and metabolic disorders. Nature. 2006;444(7121):860-7.

247. Thaler JP, Yi CX, Schur EA, Guyenet SJ, Hwang BH, Dietrich MO, et al. Obesity is associated with hypothalamic injury in rodents and humans. J Clin Invest. 2012;122(1):153-62.

248. Moller DE. Potential role of TNF-alpha in the pathogenesis of insulin resistance and type 2 diabetes. Trends Endocrinol Metab. 2000;11(6):212-7.

249. Hotamisligil GS, Shargill NS, Spiegelman BM. Adipose expression of tumor necrosis factor-alpha: direct role in obesity-linked insulin resistance. Science. 1993;259(5091):87-91.

250. Fried SK, Bunkin DA, Greenberg AS. Omental and subcutaneous adipose tissues of obese subjects release interleukin-6: depot difference and regulation by glucocorticoid. J Clin Endocrinol Metab. 1998;83(3):847-50.

251. Carey AL, Steinberg GR, Macaulay SL, Thomas WG, Holmes AG, Ramm G, et al. Interleukin-6 increases insulin-stimulated glucose disposal in humans and glucose uptake and fatty acid oxidation in vitro via AMP-activated protein kinase. Diabetes. 2006;55(10):2688-97.

252. Pedersen BK, Febbraio MA. Muscle as an endocrine organ: focus on muscle-derived interleukin-6. Physiol Rev. 2008;88(4):1379-406.

253. Bernardini R, Kamilaris TC, Calogero AE, Johnson EO, Gomez MT, Gold PW, et al. Interactions between tumor necrosis factor-alpha, hypothalamic corticotropin-releasing hormone, and adrenocorticotropin secretion in the rat. Endocrinology. 1990;126(6):2876-81.

254. Wallenius V, Wallenius K, Ahren B, Rudling M, Carlsten H, Dickson SL, et al. Interleukin-6-deficient mice develop mature-onset obesity. Nat Med. 2002;8(1):75-9.

255. Pradhan AD, Manson JE, Rifai N, Buring JE, Ridker PM. C-reactive protein, interleukin 6, and risk of developing type 2 diabetes mellitus. JAMA. 2001;286(3):327-34.

256. Howard JK, Cave BJ, Oksanen LJ, Tzameli I, Bjorbaek C, Flier JS. Enhanced leptin sensitivity and attenuation of diet-induced obesity in mice with haploinsufficiency of Socs3. Nat Med. 2004;10(7):734-8.

257. Romanatto T, Cesquini M, Amaral ME, Roman EA, Moraes JC, Torsoni MA, et al. TNF-alpha acts in the hypothalamus inhibiting food intake and increasing the respiratory quotient--effects on leptin and insulin signaling pathways. Peptides. 2007;28(5):1050-8.

258. Piekorz R, Schlierf B, Burger R, Hocke GM. Reconstitution of IL6-inducible differentiation of a myeloid leukemia cell line by activated Stat factors. Biochemical and biophysical research communications. 1998;250(2):436-43.

259. Velloso LA, Araujo EP, de Souza CT. Diet-induced inflammation of the hypothalamus in obesity. Neuroimmunomodulation. 2008;15(3):189-93.

260. Gao S, Howard S, LoGrasso PV. Pharmacological Inhibition of c-Jun N-terminal Kinase Reduces Food Intake and Sensitizes Leptin's Anorectic Signaling Actions. Sci Rep. 2017;7:41795.

261. Bredow S, Guha-Thakurta N, Taishi P, Obal F, Jr., Krueger JM. Diurnal variations of tumor necrosis factor alpha mRNA and alpha-tubulin mRNA in rat brain. Neuroimmunomodulation. 1997;4(2):84-90.

262. Floyd RA, Krueger JM. Diurnal variation of TNF alpha in the rat brain. Neuroreport. 1997;8(4):915-8.

263. Han C, Wu W, Ale A, Kim MS, Cai D. Central Leptin and Tumor Necrosis Factor-alpha (TNFalpha) in Diurnal Control of Blood Pressure and Hypertension. The Journal of biological chemistry. 2016;291(29):15131-42.

264. Scheiermann C, Kunisaki Y, Frenette PS. Circadian control of the immune system. Nat Rev Immunol. 2013;13(3):190-8.

265. Spengler ML, Kuropatwinski KK, Comas M, Gasparian AV, Fedtsova N, Gleiberman AS, et al. Core circadian protein CLOCK is a positive regulator of NF-kappaB-mediated transcription. Proceedings of the National Academy of Sciences of the United States of America. 2012;109(37):E2457-65.

266. Lam MT, Cho H, Lesch HP, Gosselin D, Heinz S, Tanaka-Oishi Y, et al. Rev-Erbs repress macrophage gene expression by inhibiting enhancer-directed transcription. Nature. 2013;498(7455):511-5.

267. Narasimamurthy R, Hatori M, Nayak SK, Liu F, Panda S, Verma IM. Circadian clock protein cryptochrome regulates the expression of proinflammatory cytokines. Proceedings of the National Academy of Sciences of the United States of America. 2012;109(31):12662-7.

268. Haus E, Lakatua DJ, Swoyer J, Sackett-Lundeen L. Chronobiology in hematology and immunology. Am J Anat. 1983;168(4):467-517.

269. Haus E, Smolensky MH. Biologic rhythms in the immune system. Chronobiol Int. 1999;16(5):581-622.

270. Ahren B. Diurnal variation in circulating leptin is dependent on gender, food intake and circulating insulin in mice. Acta Physiol Scand. 2000;169(4):325-31.

271. Knight ZA, Hannan KS, Greenberg ML, Friedman JM. Hyperleptinemia is required for the development of leptin resistance. PloS one. 2010;5(6):e11376.

272. Scarpace PJ, Matheny M, Zolotukhin S, Tumer N, Zhang Y. Leptin-induced leptin resistant rats exhibit enhanced responses to the melanocortin agonist MT II. Neuropharmacology. 2003;45(2):211-9.

273. Scarpace PJ, Matheny M, Tumer N, Cheng KY, Zhang Y. Leptin resistance exacerbates diet-induced obesity and is associated with diminished maximal leptin signalling capacity in rats. Diabetologia. 2005;48(6):1075-83.

274. Ottaway N, Mahbod P, Rivero B, Norman LA, Gertler A, D'Alessio DA, et al. Diet-induced obese mice retain endogenous leptin action. Cell metabolism. 2015;21(6):877-82.

275. Frederich RC, Hamann A, Anderson S, Lollmann B, Lowell BB, Flier JS. Leptin levels reflect body lipid content in mice: evidence for diet-induced resistance to leptin action. Nat Med. 1995;1(12):1311-4.

276. Delahaye LB, Bloomer RJ, Butawan MB, Wyman JM, Hill JL, Lee HW, et al. Time-restricted feeding of a high fat diet in C57BL/6 male mice reduces adiposity, but does not protect against increased systemic inflammation. Appl Physiol Nutr Metab. 2018.

4. Publications and Manuscripts

4.1. Central adiponectin acutely improves glucose tolerance in male mice

Central Adiponectin Acutely Improves Glucose Tolerance in Male Mice

Christiane E. Koch, Chrishanthi Lowe, Karen Legler, Jonas Benzler, Alisa Boucsein, Gregor Böttiger, David R. Grattan, Lynda M. Williams, and Alexander Tups

Department of Animal Physiology (C.E.K., C.L., K.L., J.B., A.B., G.B., A.T.), Faculty of Biology, Philipps University Marburg, D-35043 Marburg, Germany; Metabolic Health Group (L.M.W.), Rowett Institute of Nutrition and Health, University of Aberdeen, Aberdeen AB21 9SB, United Kingdom; and Centre for Neuroendocrinology and Department of Anatomy and Structural Biology (D.R.G.), University of Otago, Dunedin, New Zealand

Adiponectin, an adipocyte-derived hormone, regulates glucose and lipid metabolism. It is also antiinflammatory. During obesity, adiponectin levels and sensitivity are reduced. Whereas the action of adiponectin in the periphery is well established the neuroendocrine role of adiponectin is largely unknown. To address this we analyzed the expression of adiponectin and the 2 adiponectin receptors (AdipoR1 and AdipoR2) in response to fasting and to diet-induced and genetic obesity. We also investigated the acute impact of adiponectin on central regulation of glucose homeostasis. Adiponectin (1 μg) was injected intracerebroventricularly (ICV), and glucose tolerance tests were performed in dietary and genetic obese mice. Finally, the influence of ICV adiponectin administration on central signaling cascades regulating glucose homeostasis and on markers of hypothalamic inflammation was assessed. Gene expression of *adiponectin* was downregulated whereas *AdipoR1* was up-regulated in the arcuate nucleus of fasted mice. High-fat (HF) feeding increased *AdipoR1* and *AdipoR2* gene expression in this region. In mice on a HF diet and in leptin-deficient mice acute ICV adiponectin improved glucose tolerance 60 minutes after injection, whereas normoglycemia in control mice was unaffected. ICV adiponectin increased pAKT, decreased phospho-AMP-activated protein kinase, and did not change phospho-signal transducer and activator of transcription 3 immunoreactivity. In HF-fed mice, ICV adiponectin reversed parameters of hypothalamic inflammation and insulin resistance as determined by the number of phospho-glycogen synthase kinase 3 β(Ser9) and phospho-c-Jun N-terminal kinase (Thr183/Tyr185) immunoreactive cells in the arcuate nucleus and ventromedial hypothalamus. This study demonstrates that the insulin-sensitizing properties of adiponectin are at least partially based on a neuroendocrine mechanism that involves centrally synthesized adiponectin. **(*Endocrinology* 155: 1806–1816, 2014)**

Obesity and its comorbidities, especially type 2 diabetes, have emerged as major medical problems of modern societies (1). Obesity is associated with a profound drop in circulating adiponectin levels (2). Adiponectin, which is a potent antiinflammatory and insulin-sensitizing hormone, is at present, the only adipokine in which circulating concentrations inversely correlate with the body fat mass (3–5). It has been proposed that the obesity-associated decrease of the insulin-sensitizing hormone adiponectin links obesity with insulin insensitivity and the development of type 2 diabetes. Based on the insulin-sensitizing properties of adiponectin, this hor-

ISSN Print 0013-7227 ISSN Online 1945-7170
Printed in U.S.A.

Received August 5, 2013. Accepted February 17, 2014.
First Published Online February 24, 2014

Abbreviations: AdipoR, adiponectin receptor; AMPK, AMP-activated protein kinase; ARC, arcuate nucleus; CSF, cerebrospinal fluid; DIO, diet-induced obesity; GSK, glycogen synthase kinase; HF, high fat; HFD, high-fat diet; ICV, intracerebroventricular; ipGTT, ip glucose tolerance test; JNK, c-Jun N-terminal kinase; LFD, low-fat diet; MBH, mediobasal hypothalamus; mHF, moderate HF; pAMPK, phospho-AMPK; pGSK3β, phospho-GSK3β; PI3K, phosphoinositide 3-kinase; pJNK, phospho-JNK; pSTAT3, phospho-STAT3; STAT3, signal transducer and activator of transcription 3; VMH, ventromedial hypothalamus.

mone could be an important therapeutic target for metabolic disorders.

Whereas peripheral actions of adiponectin have been thoroughly investigated, studies investigating the central properties of this hormone in mediating the regulation of energy balance and glucose metabolism are rare. Adiponectin is one of the most abundant hormones in the circulation of nonobese individuals and is found in the cerebrospinal fluid (CSF) at a concentration approximately 0.1% of those in the circulation. Nonetheless, in comparison with other circulating fat-derived hormones, such as leptin, this CSF concentration is remarkably high (6–9). Adiponectin is detectable in the serum as full-length trimers and hexamers, as low molecular weight adiponectin (low molecular weight), as high molecular weight adiponectin multimers or globular adiponectin, which is generated by cleavage of the full-length adiponectin monomers (10–13). The globular form of adiponectin has been shown to activate signaling events in hypothalamic neurons and appears to have the highest binding affinity for the adiponectin receptor 1 (AdipoR1) (14). A high binding affinity of AdipoR2 for globular adiponectin has also been found but is lower than that for AdipoR1 (15).

In the periphery adiponectin has been shown to activate AMP-activated protein kinase (AMPK) (14), a master switch involved in the regulation of a number of different metabolic processes, including carbohydrate, lipid, and protein metabolism and aging (16). Emerging evidence suggests that adiponectin acts in the brain to decrease body weight mainly by stimulating energy expenditure and reducing food intake (17, 18). However, together with the origin of adiponectin in the CSF, the nature of signaling pathways involved in this phenomenon remain incompletely understood. It is still a matter of debate as to whether adiponectin reaches the brain via passage through the blood brain barrier or whether it is directly expressed in the brain (8). Several recent studies suggest that adiponectin is biologically active in the brain because intracerebroventricular (ICV) administration leads to an increase in cFos-positive cells in the hypothalamus and activation of signaling typical of insulin stimulation of the PI3K (phosphoinositide 3-kinase) in rats (17). The effects of adiponectin in the central nervous system seem to be mediated via the AdipoR1 (17). Central inhibition of AdipoR1 decreases adiponectin-induced activation of PI3K, whereas inhibition of AdipoR2 appears not to affect insulin signaling in the hypothalamus (17).

Adiponectin has also been described to act as antiinflammatory hormone. We recently demonstrated that diet-induced obesity (DIO) in mice is associated with increased proinflammatory signaling in the mediobasal hypothalamus (MBH) involving phospho-c-Jun N-terminal kinases (pJNK) (19) and phospho-glycogen synthase kinase 3 (pGSK3) (20). We therefore hypothesized that the effect of adiponectin in the hypothalamus may be via an inhibition of hypothalamic inflammation.

Thus, the aim of the current study was to look more closely at the central actions of adiponectin, particularly its glucose-lowering, insulin-sensitizing, and antiinflammatory properties. To measure the effects of obesity on adiponectin and adiponectin receptor expression in the hypothalamus, we used 2 models of obesity: leptin-deficient, $Lep^{ob/ob}$ mice and DIO mice fed a high-fat (HF) diet (HFD) either containing 45% or 60% fat by energy and assessed the effect of nutritional status on the adiponectin system. Using in situ hybridization, we measured gene expression of *adiponectin*, *AdipoR1*, *AdipoR2*, and adaptor protein containing pleckstrin homology domain, phosphotyrosine-binding domain, and leucine zipper motif 1 (*APPL1*), an important mediator linking adiponectin and insulin signaling, in the arcuate nucleus (ARC), a key region in the MBH that is involved in the regulation of energy and glucose homeostasis. The hypothesis tested was whether adiponectin exhibits potent glucose-lowering properties upon central administration involving PI3K and AMPK signaling in the ARC and ventromedial hypothalamus (VMH). Finally, we determined whether ICV adiponectin could acutely reverse the elevated proinflammatory signals seen in DIO mice in the MBH.

Materials and Methods

Animals

All procedures involving animals were carried out under national animal ethics legislation and received approval by the respective authorities for animal ethics. Male C57BL/6JRj wild-type ($Lep^{+/+}$) and $Lep^{ob/ob}$ mice were purchased from Janvier. They were housed individually under a 12-hour light/12-hour dark cycle and an ambient temperature of 23°C. All mice had ad libitum access to food and water. Unless stated otherwise, all mice were food deprived prior to the experiments (overnight fasting for 16 hours). Mice were fed either a low-fat diet (LF); with 10% energy from fat (Kcal), a moderate high-fat diet (mHF) with 45% from fat or a high-fat diet (HF) with 60% from fat (D12450B, D12451, and D12492, respectively; Research Diets).

Analysis of gene expression of the adiponectin system in the mediobasal hypothalamus

Using in situ hybridization (21), we analyzed whether fasting influences central gene expression of *adiponectin* (accession no. NM_145221.2), *AdipoR1* (accession no. NM_028320.3), *AdipoR2* (accession no. NM_197985.3), and the adaptor protein *APPL1* (accession no. AF304466.1). Mice were divided into 2 groups, the first group was fed ad libitum, and the second group was fasted for 16 hours prior to decapitation (n = 6–7).

Additionally, we characterized whether the expression patterns of *AdipoR1*, *AdipoR2*, and *APPL1* were influenced by diet and/or genotype. Eight-week-old wild-type mice were divided into 3 groups and were fed a LF, a mHF (45%), or a HF (60%) diet for 4 weeks. To analyze the influence of genetic obesity, a group of 8-week-old $Lep^{ob/ob}$ mice fed a LF diet were used (n = 4–6 mice per group). Mice were killed, and brains were removed and frozen on dry ice. For in situ hybridization, brains were cryosectioned at 16 μm. The sequences of the primers to generate the specific amplicons are provided in Table 1.

Acute action of centrally administered adiponectin on glucose tolerance and hepatic glucose production

Using 3 different glucose-intolerant and obese mouse models, we investigated whether centrally administered adiponectin improves glucose tolerance in these mice. The procedure was identical in each experiment. One hour prior to an ip glucose tolerance test (ipGTT) all mice received either an ICV injection of adiponectin (1 μg in PBS) or vehicle (PBS). Blood was collected by puncturing the *V. facials*, and glucose concentration was measured at defined time points using a glucometer [Roche; Accu-Check Performa; (22)]. In all experiments globular adiponectin was used (R&D Systems; catalog no. 1119-AC).

In experiment 1 the effect of ICV adiponectin on glucose tolerance of 8-week-old normoglycemic wild-type- (n = 7–8 mice per group) or leptin-deficient, glucose-intolerant $Lep^{ob/ob}$ mice (n = 9–11 mice per group) on low-fat diet (LFD) was analyzed. For the ipGTT, mice received 1 g glucose/kg body weight.

To further asses whether ICV adiponectin alters hepatic glucose output, $Lep^{ob/ob}$ mice received an ip pyruvate injection (1.5 mg/kg) 60 minutes prior to acute ICV injection of either adiponectin (1 μg adiponectin in PBS; n = 5) or vehicle (PBS; n = 6). Blood glucose levels were measured as stated above.

In experiment 2 we analyzed whether ICV adiponectin improves the impaired glucose tolerance during diet-induced obesity. Wild-type mice received either a LFD or a HFD for four weeks (n = 5–7 mice per group). An ipGTT (1 g glucose/kg body weight) was then carried out with either ICV adiponectin or vehicle pretreatment as described above.

In the third experiment, we analyzed the effect of central adiponectin in an extreme setting of obesity; 5-week-old $Lep^{ob/ob}$ mice were fed a 60% HFD for 10 days. An ipGTT (0.75 g glucose/kg body weight) with either adiponectin or vehicle pretreatment was performed as described above (adiponectin, n = 9; vehicle, n = 23).

Acute effects of ICV adiponectin on central signaling cascades involved in energy balance and glucose metabolism

To identify the molecular mechanisms of central adiponectin action, hypothalamic signaling cascades that are involved in the regulation of energy and glucose metabolism were analyzed. $Lep^{ob/ob}$ mice on LFD were treated centrally with either adiponectin or vehicle (n = 5–6 mice per group). One hour after ICV injections, mice were anesthetized with pentobarbital (Narcoren; Merial GmbH) and perfused with 0.9% saline containing heparin followed by 4% paraformaldehyde in 0.1M phosphate buffer, pH 7.4. Brains were removed and stored in the same solution for about 5 hours followed by dehydration (in 30% sucrose/0.1 M phosphate buffer). When brains had sunk, they were frozen in isopentane cooled over dry ice for 1 minute and sectioned coronally at 35 μm. Brain slices were collected in a series of 4 and stored in cryoprotectant at −20°C. Free-floating sections were incubated in H_2O_2 diluted in 0.1 M phosphate buffer followed by incubation in blocking solution (5% normal goat serum, 0.5% Triton X-100 in phosphate buffer) for 60 minutes. Sections were incubated with the primary antibody overnight at 4°C diluted in blocking solution [anti-pAKT(Ser473) 1:500; anti-pAMPK (Thr172) 1:500; Cell Signaling Technology]. After an overnight incubation and rinsing, sections were incubated with a secondary goat antirabbit antibody for 1–2 hours. For pAKT(Ser473) sections were incubated with a biotinylated secondary antibody (1:500 in blocking solution containing 3% normal goat serum, 0.5% Triton X-100) followed by ABC solution (Vector Laboratories) for 1 hour. To detect pAMPK(Thr172), sections were incubated with a horseradish peroxidase-conjugated secondary goat antirabbit antibody overnight (1:500 in blocking solution containing 3% normal goat serum-0.5% Triton X-100). Finally, the signal was developed by nickel-diaminobenzidine solution (Vector Laboratories), giving a gray/black precipitate. Immunoreactive cells in the ARC and the VMH were counted by 2 investigators blinded to the treatments.

For phospho-signal transducer and activator of transcription 3 (pSTAT3) immunostaining an antigen-retrieval step was necessary. Prior to the blocking step detailed above, sections were pretreated with 1% NaOH and 1% H_2O_2 for 20 minutes, followed by 0.3% glycine for 10 minutes and by incubation in 0.03% sodium dodecyl sulfate for 10 minutes (23). The primary antibody for pSTAT3(Tyr705) (Cell Signaling Technology) was diluted 1:3000 in blocking solution followed by a biotinylated secondary antibody diluted 1:1000 using the ABC protocol.

Table 1. Genes With Their Primer Sequences Used for Riboprobe Derivation

Gene	Primer Sequence
AdipoR1 forward:	5′-GGCTGAAAGACAACGACTAC-3′ (20 bp)
AdipoR1 reverse:	5′-GGAAGAACATCCCGAAGAC-3′ (20 bp)
AdipoR2 forward:	5′-GGGCACCAACTTGATGATAC-3′ (20 bp)
AdipoR2 reverse:	5′-CCTTCCCACACCTTACAAAC-3′ (20 bp)
Adiponectin forward:	5′-GGAATGACAGGAGCTGAAGG-3′ (20 bp)
Adiponectin reverse:	5′-GTCCCGGAATGTTGCAGTAG-3′ (20 bp)
APPL1 forward:	5′-CCGATTCCTTGGTTCATATGG-3′ (20 bp)
APPL1 reverse:	5′-CACGGCAATGGAAATGTGAG-3′ (20 bp)

Acute effects of ICV adiponectin on phospho-JNK(Thr183/Tyr185) and phospho-GSK3β(Ser9) immunoreactivity in the MBH in diet-induced obesity

Wild-type mice were divided into 3 groups (n = 5 mice per group). One group was fed a LF diet, and 2 groups were fed a HF diet. After 4 weeks on diet, one group of HF mice was injected centrally, as described above with adiponectin, and the second HF group was injected with vehicle, whereas the LF group received a vehicle injection. One hour after injection, mice were perfused with 4% paraformaldehyde/phosphate buffer under pentobarbital anesthesia, and brains were removed, sectioned, and analyzed by immunohistochemistry as detailed above. A specific antibody against pJNK(Thr183/Tyr185) or pGSK3β(Ser9) (both diluted 1:1000 in blocking solution, anti-pJNK, and anti-pGSK3β [Cell Signaling Technology]) was used, using the protocol specific for the horseradish peroxidase-conjugated secondary antibody as described above.

Results

Central expression pattern of genes involved in adiponectin signal transduction

The level of gene expression of *adiponectin*, *AdipoR1* and *APPL1* in the ARC was dependent on the feeding status of the mice, whereas *AdipoR2* was unchanged (Figure 1). In ad libitum fed wild-type mice, *adiponectin* expression was detected in the hypothalamic ARC. After food deprivation for 16 hours *adiponectin* gene expression was markedly reduced (n = 6–7 mice per group; ad libitum vs food deprived $P < .001$). Gene expression of *AdipoR1* and *APPL1* in the ARC was increased in fasted mice compared with ad libitum fed controls, whereas expression of *AdipoR2* was not affected by diet (n = 7 mice per group; ad libitum vs food deprived $P = .051$). *APPL1* gene expression was also elevated by fasting in the VMH compared with ad libitum fed mice (Supplemental Figure 1; $P = .047$), whereas the hybridization signal for the adiponectin receptors in the VMH could not be analyzed because it was beyond the sensitivity of the assay. The magnitude of changes in mRNA expression was 1.8-fold for *AdipoR1* ($P = .039$; Figure 1b) and 4-fold for *APPL1* ($P = .019$; Figure 1c) in food-deprived mice compared with controls.

We next tested whether diet or genotype may also affect gene expression of adiponectin signaling components (Figure 2; n = 4–6 mice per group). After feeding the respective diets for 4 weeks all mice increased their body weight significantly ($P < .001$; LF mice: 15.1 ± 0.3 g to 21.35 ± 0.4 g; mHF mice: 14.9 ± 0.4 g to 24.3 ± 0.4 g; HF mice: 15 ± 0.3 g to 25.6 ± 0.7 g and $Lep^{ob/ob}$ mice: 21.8 ± 0.6 g to 38.0 ± 0.8 g). After 4 weeks on diet there was a significant increase in body weight between LF mice

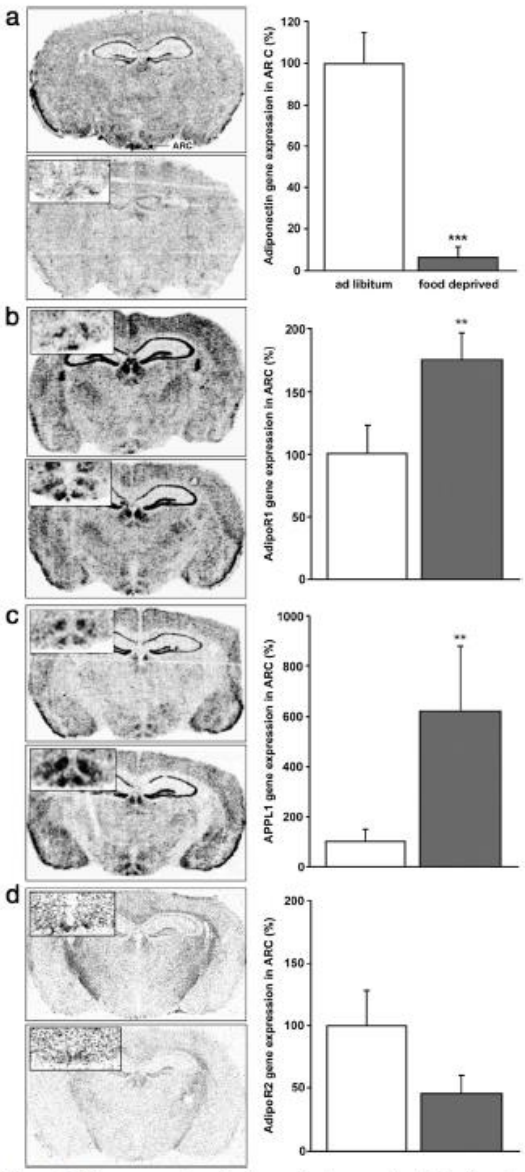

Figure 1. Gene expression of *adiponectin*, the receptor *AdipoR* , and the adaptor protein *APPL1* in the ARC of either ad libitum or food-deprived mice. *Adiponectin*, *AdipoR1*, and *APPL1* gene expression in the ARC is regulated by feeding status whereas *AdipoR2* is unchanged. Autoradiographs depicting in situ hybridization with antisense ^{35}S-labeled riboprobes to *adiponectin* (a), *AdipoR1* (b), *APPL1* (c), and *AdipoR2* (d) mRNA signal in ad libitum-fed (upper left panels) and food-deprived (lower left panels) mice (n = 6–7 mice per group). The right panels show a bar graph generated from quantification of the respective signal in the ARC. Means ± SEM of the quantified signal; **, $P < .01$; ***, $P < .001$

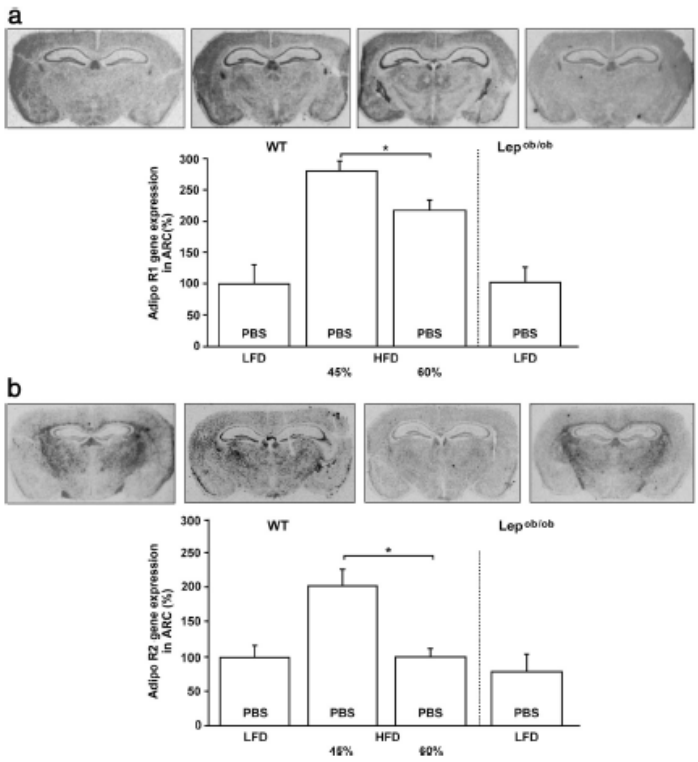

Figure 2. Gene expression pattern of *AdipoR1* and *AdipoR2* in the ARC of wild-type mice fed LFDs and HFDs and leptin-deficient mice on LFD. AdipoR1 and AdipoR2 gene expression in the ARC are affected by dietary fat content. Gene expression of AdipoR1 (a) and AdipoR2 (b) in the ARCs of wild-type mice fed LFDs and HFDs (45% and 60% fat content, for 4 weeks) and $Lep^{ob/ob}$ mice on LFD (n = 4–6 mice per group). Autoradiographs depicting in situ hybridization with antisense ^{35}S-labeled riboprobes to *AdipoR1* and *AdipoR2* refer to the bar graph below the respective image. The bar chart shows the means ± SEM of the quantified in situ hybridization signal; *, $P < .05$; **, $P < .01$; ***, $P < .001$. WT, wild type.

vs mHF ($P < .001$), vs HF ($P < .001$) and vs the ob/ob genotype ($P < .001$). However, there was no significant difference in body weight between mice fed mHF and HF ($P = .089$). Expression of *AdipoR1* in the ARC was increased in mice fed HFD (60%) more than 2-fold compared with LF controls ($P = .008$; Figure 2a). In mice fed mHF (45%), expression of *AdipoR1* was markedly increased in this brain region reaching 3 times that in LF controls (LF vs mHF, $P = .001$; Figure 2a). There was a significant difference in *AdipoR1* gene expression between mice on mHF and HF (mHF vs HF, $P = .025$; Figure 2a). The lack of endogenous leptin had no effect on central *AdipoR1* gene expression in $Lep^{ob/ob}$ mice compared with wild-type controls (Figure 2a).

The gene expression of the second adiponectin receptor *AdipoR2* was unaffected in mice fed the 60% HF diet (Figure 2b); however, gene expression of mice on mHF (45%) was doubled compared with LF mice (LF vs mHF; $P = .007$; Figure 2b). As with *AdipoR1* expression in the ARC, lack of leptin did not affect gene expression of *AdipoR2* (Figure 2b) in this region. *AdipoR2* expression was comparable in wild-type and $Lep^{ob/ob}$ mice on LFD.

The downstream target of adiponectin signaling, *APPL1*, was neither influenced by diet nor by genotype (data not shown).

Acute actions of ICV adiponectin on glucose tolerance and hepatic glucose production

Having established that gene expression of *adiponectin*, its receptors, and the adaptor protein *APPL1* were influenced by feeding status and partially by diet, we next investigated whether ICV adiponectin could modulate impaired glucose tolerance during HF vs LF feeding in wild-type and in $Lep^{ob/ob}$ mice. In all mouse models of obesity used, ICV adiponectin consistently improved the impaired glucose tolerance (Figure 3). In glucose-intolerant $Lep^{ob/ob}$ mice fed a LF diet (n = 9–11 mice per group) acute ICV adiponectin markedly improved glucose tolerance. The area under the curve in these mice was significantly decreased compared with vehicle-treated $Lep^{ob/ob}$ mice ($P = .01$; Figure 3a).

In normoglycemic wild-type mice fed a LF diet, ICV adiponectin had no effect and did not lead to hypoglycemia (Figure 3a; n = 7–8 mice per group).

Additionally, in glucose-intolerant $Lep^{ob/ob}$ mice the effect of ICV adiponectin on hepatic glucose production (n = 5–6 mice per group) using a pyruvate tolerance test was tested. By using pyruvate, a substrate for gluconeogenesis, it is possible to measure the rate of glucose production reflecting hepatic glucose output. Central adiponectin application led to a significantly reduced glucose excursion compared with the vehicle-treated $Lep^{ob/ob}$ mice ($P = .006$; Figure 3b).

Next we investigated whether the glucose-lowering properties of ICV adiponectin are also present in DIO mice. As expected, 4 weeks of HF feeding significantly

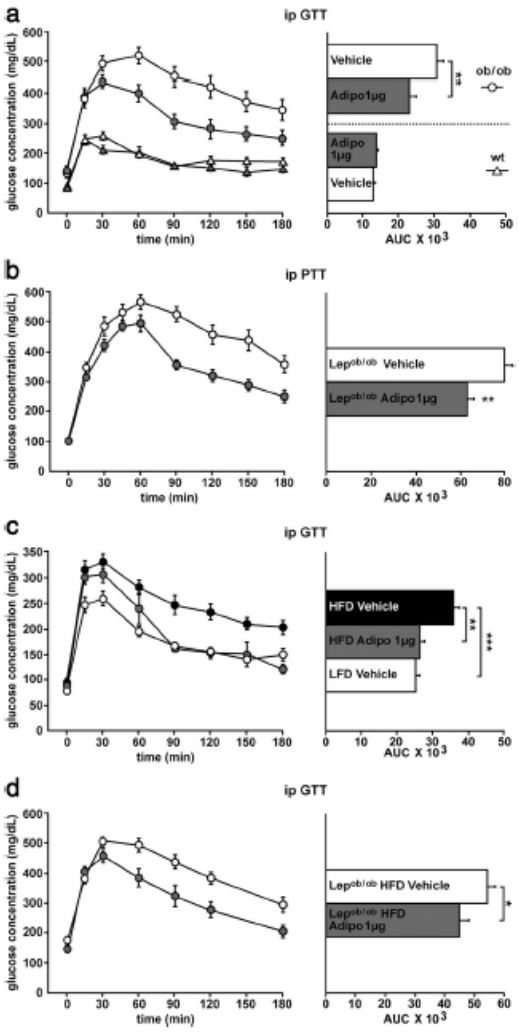

Figure 3. Effect of centrally administered adiponectin on glucose tolerance in mice with genetically and/or diet-induced impaired energy, glucose metabolism, and pyruvate. Central adiponectin lowers peripheral glucose levels. a, ipGTT in $Lep^{ob/ob}$ mice (n = 9–11 mice per group) and respective wild-type controls (n = 7–8 mice per group) that were either ICV injected with adiponectin (1 µg in PBS) or vehicle (PBS). b, Pyruvate tolerance test of $Lep^{ob/ob}$ mice and respective wild-type controls either ICV injected with adiponectin (1 µg in PBS; n = 5) or vehicle (PBS; n = 6). c, ipGTTs of wild-type mice on LFD (ICV injected with vehicle [PBS; n = 7]) and of wild-type mice fed HFD (60% fat; n = 5 mice per group) ICV injected with either adiponectin (1 µg in PBS) or vehicle (PBS). d, ipGTTs after either adiponectin (1 µg in PBS; n = 9) or vehicle (PBS; n = 23) ICV injection in $Lep^{ob/ob}$ mice on HFD (60% fat, 10 days). Adiponection and vehicle were injected 60 minutes prior to all tests. Shown are tolerance test (left panels) and respective AUCs (right panels). Data show means ± SEM; *, $P < .05$; **, $P < .01$; ***, $P < .001$. ipPTT, ip pyruvate tolerance test; wt, wild type.

impaired basal blood glucose levels (LF mice: 74.4 ± 6.6 vs HF mice: 91.3 ± 4.2; $P = .048$) and the glucose tolerance of mice (LF vehicle vs HF vehicle: $P < .001$; Figure 3c). Centrally administered adiponectin 60 minutes prior to an ipGTT acutely improved the impaired glucose tolerance in these mice (HF adiponectin vs HF vehicle: $P = .002$; n = 5–7 mice per group) so that the glucose clearance rate was comparable to that observed in normoglycemic mice on LF diet (LF vehicle vs HF adiponectin = n.s; HF vehicle vs LF vehicle, $P < .001$).

We next tested whether central adiponectin can also improve glucose tolerance in mice in an extreme state of obesity and glucose intolerance; $Lep^{ob/ob}$ mice fed a HF diet for 10 days. HF feeding was associated with an increase in body weight from 27.2 ± 0.9 g to 38.2 ± 0.7g ($P < .001$). Consistent with the findings above, ICV adiponectin, in these mice, robustly improved glucose tolerance. The calculated area under the curve of DIO $Lep^{ob/ob}$ mice treated centrally with adiponectin was significantly decreased compared with vehicle-treated controls ($P = .045$; Figure 3d; n = 9–23 mice per group).

Acute effects of centrally administered adiponectin on central signaling cascades involved in energy regulation and glucose metabolism

Because centrally administered adiponectin exhibited potent glucose-lowering properties, we next investigated the underlying neurochemical mechanism in the glucose-intolerant $Lep^{ob/ob}$ mouse on LF diet. ICV adiponectin led to a nonsignificant 1.7-fold increase in the number of pAKT(Ser473) immunoreactive cells in the ARC of $Lep^{ob/ob}$ mice on LF diet relative to vehicle (vehicle vs adiponectin, $P = .07$; Figure 4a; n = 5–6 mice per group). In the VMH we observed a significant 2.4-fold increase in the number of pAKT(Ser473) immunoreactive cells in adiponectin-treated $Lep^{ob/ob}$ mice compared with controls (vehicle vs adiponectin, $P = .02$; Figure 4b; n = 5–6 mice per group).

The number of pAMPK(Thr172) immunoreactive cells was significantly reduced by 1.5-fold in the ARC ($P = .018$) and by 2.5-fold in the VMH ($P = .005$) after ICV adiponectin treatment compared with vehicle (Figure 4, c and d, n = 13 per group).

In contrast to the rise in pAKT immunoreactivity and the decrease in pAMPK, the number of pSTAT3(Try705) immunoreactive cells in both hypothalamic nuclei was unaffected by adiponectin treatment, and only very few pSTAT3(Try705) immunoreactive cells were detected in

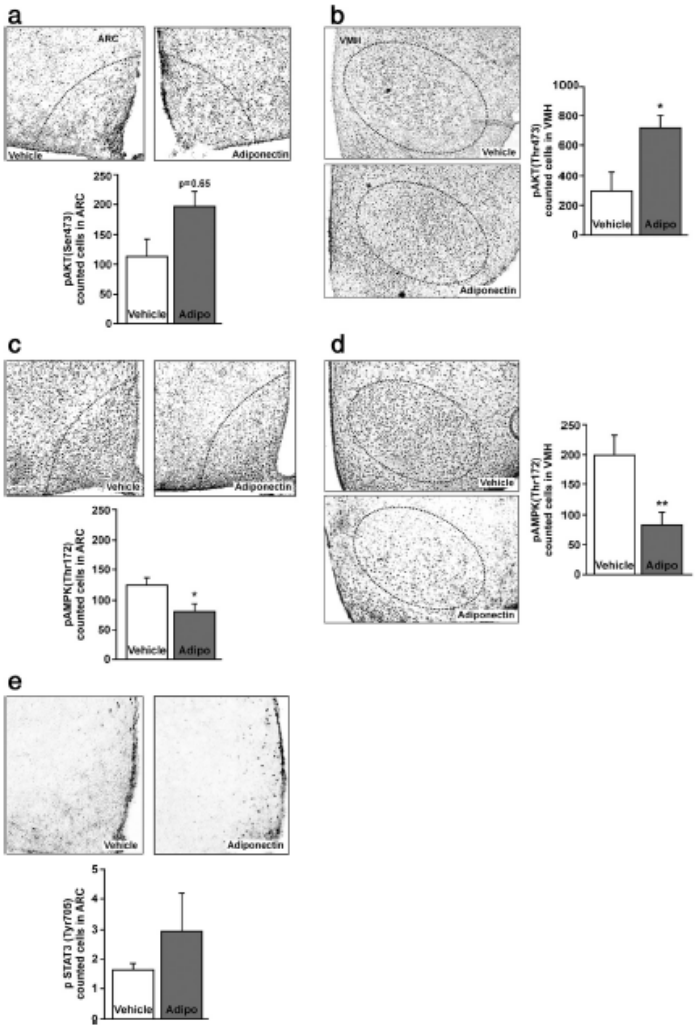

Figure 4. Impact of centrally administered adiponectin on hypothalamic insulin and leptin-signaling pathways. Compared with vehicle-treated controls centrally administered adiponectin (1 μg) partially increases the number of pAKT(Ser473) (a and b) and reduces the number of pAMPK(Thr172) (c and d) immunopositive cells in the ARC and VMH of $Lep^{ob/ob}$ mice whereas pSTAT3(Tyr705) (e) immunoreactivity remains unaltered (n = 5–6 mice per group). Mice received either adiponectin (1 μg in PBS) or vehicle (PBS) 60 minutes prior to transcardial perfusion. Representative images show pAKT(Ser473), pAMPK(Thr172), and pSTAT3(Tyr705) immunoreactivity in the ARC and VMH. Immunoreactive cells counted in the respective region are shown in bar charts. Bar charts show means ± SEM; *, $P < .05$; **, $P < .01$

the ARC (Figure 4c), whereas staining in the VMH was undetectable (data not shown).

Acute effects of ICV adiponectin on proinflammatory signaling in DIO

To identify whether adiponectin affects proinflammatory signaling in the MBH in obesity, we investigated the pattern of pJNK(Thr183/Tyr185) and pGSK3β(Ser9) immunoreactivity after acute ICV adiponectin administration (n = 5 per group). This experiment was performed in DIO wild-type mice that exhibit increased proinflammatory signaling. We previously reported that HF feeding leads to an increase in the number of pJNK(Thr183/Tyr185) and a decrease in the number of pGSK3β(Ser9) immunoreactive cells in regions of the MBH (19, 20), which is associated with activation of proinflammatory signaling pathways.

Consistent with our previous findings (19), HF feeding was associated with an increase in the number of pJNK(Thr183/Tyr185) cells in the ARC ($P = .001$) and VMH ($P = .043$) compared with control mice on LF diet (Figure 5, a and b). ICV adiponectin acutely reduced the elevated number of pJNK(Thr183/Tyr185)-positive cells in the ARC of these mice (HF vehicle vs HF adiponectin, $P = .019$). Notably, in the ARC, the number of pJNK(Thr183/Tyr185)-positive cells was reversed to levels of LFD mice after this treatment (LF vehicle vs HF adiponectin $P = .06$; Figure 5a). In the VMH, centrally administered adiponectin totally reversed the diet-induced increase in pJNK(Thr183/Tyr185) immunoreactive cells to levels exhibited by LF mice (HF vehicle vs HF adiponectin; $P = .045$; Figure 5b). Consistent with previous findings (20), HF feeding led to a decrease in the number of pGSK3β(Ser9) immunoreactive cells in the ARC (HF vehicle vs LF vehicle $P = .026$; Figure 5c) and VMH (HF vehicle vs LF vehicle P = .002; Figure 5d) by approximately 30%, indicating an elevated GSK3 activity in these mice. ICV adiponectin totally reversed these diet-induced alterations in the number of pGSK3β(Ser9)-positive cells in the ARC (HF vehicle vs HF adiponectin, $P < .001$; Figure 5c) and VMH (HF vehicle vs HF adiponectin, $P = .012$; Figure 5d) to levels seen in mice on the LF diet.

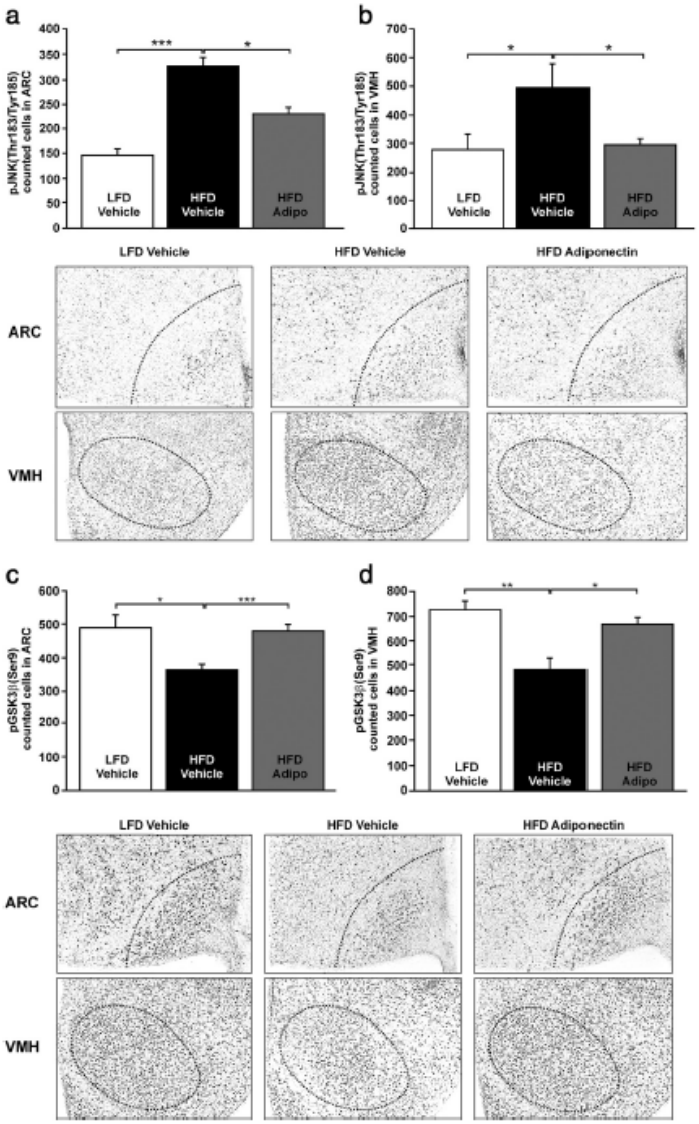

Figure 5. Central adiponectin reduces inflammatory signaling in the MBH during DIO. HF feeding (60% fat) increases the number of pJNK(Thr183/Tyr185) and reduces the number of pGSK3β(Ser9) counted cells in the ARC and VMH of wild-type mice whereas central adiponectin (1 μg in PBS) reverses this effect (n = 5 mice per group). Wild-type mice were fed the HFD for 4 weeks. Mice received either adiponectin (1 μg in PBS) or vehicle (PBS) 60 minutes prior to transcardial perfusion. Representative images show pJNK(Thr183/Tyr185) and pGSK3β(Ser9) and immunoreactivity in the ARC and VMH. Immunoreactive cells counted in the respective region are shown in bar charts. Bar charts show means ± SEM; *, $P < .05$; **, $P < .01$; ***, $P < .001$

Discussion

It is well established that the antiinflammatory hormone adiponectin sensitizes the action of insulin in peripheral tissues (24, 25). Circulating adiponectin levels are inversely correlated with the size of body fat stores, thereby linking obesity to insulin insensitivity and the development of type 2 diabetes (3, 26). Although peripheral effects of adiponectin on glucose- and energy metabolism are well characterized, the precise action of adiponectin in the central nervous system remains uncertain (26). Although some evidence suggests that adiponectin acts centrally to control metabolism, it has not yet been satisfactorily determined whether adiponectin is expressed in the brain. Neumeier et al (8) described adiponectin to be 1000-fold lower in mouse and human CSF than in the peripheral circulation. Compared with other hormones, eg, leptin (~ 100 pg/mL), the absolute adiponectin concentration in CSF (~100 ng/mL) is still about 1000-fold higher, suggesting a potent biological activity of adiponectin in the brain (18). Despite this high concentration of adiponectin in the CSF, *adiponectin* gene expression has not been detected in the human brain, indicating that transport across the blood brain barrier must occur (8). In contrast to humans, emerging evidence suggests that *adiponectin* is expressed in the brain of mice (27). These apparent controversial findings might be explained by the regulation of *adiponectin* gene expression by feeding status. In our experiments, *adiponectin* expression was only detectable in the ARC of ad libitum fed mice, whereas fasting led to a reduction in gene expression levels that was virtually undetectable. The physiological relevance of *adiponectin* expression in the hypothalamus remains uncertain. Bauche et al (28) suggested that adiponectin might regulate its own expression because transient overexpression of adiponectin in young mice was associated with a decreased *adiponectin* gene expression, protein content in fat depots, and serum adiponectin during adulthood. This potential auto-regulation of the adiponectin gene may ac-

count for the down-regulation of central *adiponectin* expression seen after 16 hours of food deprivation in the present study.

It was reported that central injection of adiponectin robustly reduces food intake (17) and increases energy expenditure (18) whereas chronic infusion improved energy and glucose homeostasis but did not affect food intake (29). Thus, down-regulation of *adiponectin* gene expression in the ARC after fasting might compensate for the catabolic action of adiponectin in the MBH. This indicates a regulatory mechanism distinct from the reported peripheral regulation processes. In the periphery, during fasting or caloric restriction, circulating adiponectin and expression in adipose tissue is elevated, which may convey the beneficial properties of adiponectin on whole-body glucose and energy homeostasis (30, 31).

In contrast to *adiponectin*, *AdipoR1* expression appears to be similarly regulated in peripheral and central insulin target regions. Caloric restriction significantly increased the expression of *AdipoR1* in liver and skeletal muscle (32, 33). We found that fasting was also associated with increased *AdipoR1* gene expression in the ARC. HF feeding, however, was also associated with increased *AdipoR1* expression in the ARC; intriguingly this effect was exacerbated in mice on the 45% fat diet compared with those on the 60% fat diet. The 45% fat diet was also effective in increasing *AdipoR2* gene expression in the ARC whereas on the 60% fat diet and after fasting no change was observed compared with the LFD or the ad libitum-fed controls. A DIO-associated increase in central *AdipoR1* is in line with data derived from studies in the periphery, in which HF feeding was associated with an increase in *AdipoR1* expression in liver and skeletal muscle of HF-fed rodents compared with LF controls (34, 35). It is plausible that up-regulation of *AdipoR1* in the ARC might be a compensatory mechanism for the reported reduction in circulating adiponectin levels during DIO. This suggests that the ARC becomes more sensitive to adiponectin during DIO. Apart from nutrition-related regulation of *AdipoR1* and *AdipoR2*, we also investigated whether the central expression of these receptors is regulated by endogenous leptin. Surprisingly, in our study *AdipoR1* and *AdipoR2* expression in the ARC was not different in the ARC of $Lep^{ob/ob}$ compared with wild-type mice, although circulating adiponectin levels and the expression of the peripheral adiponectin receptors have been reported to be significantly reduced in these mice. In contrast, Kubota et al (36) reported that central expression of *AdipoR1* and *AdipoR2* was significantly decreased in $Lep^{ob/ob}$ mice compared with wild-type mice. This apparent discrepancy may be explained by differences in the experimental design (Kubota et al employed a fast refeeding regimen) or by termination of the experiments during a different circadian phase (37, 38). Gene expression of the adaptor protein *APPL1* was only affected by nutritional status. Acute 16-hour fasting increased the expression of *APPL1*, whereas dietary fat content or endogenous leptin levels did not affect the expression, indicating that mRNA expression of this adaptor protein is not affected by HF diet or leptin treatment.

Having established that adiponectin and adiponectin receptor expression are regulated by acute feeding conditions and chronic HF feeding, we hypothesized an important role for central adiponectin in the regulation of whole-body glucose homeostasis. In agreement with this hypothesis, ICV adiponectin acutely improved glucose tolerance in $Lep^{ob/ob}$ mice. This finding is consistent with a study by Qi et al (18) who demonstrated that ICV adiponectin improved basal blood glucose levels in these mice, and agrees with Park et al (29), who infused adiponectin ICV for 4 weeks in rats and detected improvements in glucose homeostasis. Intriguingly, in wild-type mice fed a HF diet that exhibit profound central leptin resistance in terms of its glucose-lowering potential (43), central adiponectin potently improved glucose homeostasis. It has been reported that peripheral adiponectin sensitivity was reduced in mice fed a HF diet. Also in the case of extreme obesity and glucose intolerance, as exhibited by $Lep^{ob/ob}$ mice fed a HFD for 10 days, adiponectin retained its glucose-lowering properties.

We next investigated whether ICV adiponectin affects hypothalamic insulin signaling and proinflammatory pathways. Coope et al (17) had previously shown that central adiponectin elevates protein levels of the insulin-signaling target pAKT(Ser473) in rat hypothalamic lysates. Using immunohistochemistry, we demonstrated that in mice ICV adiponectin increased the number of pAKT(Ser473)-positive cells in the ARC and VMH. Interestingly, the most documented molecular target of adiponectin, pAMPK(Thr172), was inversely regulated by adiponectin, with the number of pAMPK(Thr172) cells decreased in these regions compared with vehicle-treated mice. This down-regulation of pAMPK(Thr172) in response to acute ICV adiponectin in the MBH is in contrast to peripheral action of this hormone and one previous study that investigated the central effects of adiponectin on AMPK after acute peripheral administration of the hormone (36). These differences could be explained by an opposite action of adiponectin in the periphery and in the brain. The dichotomoy of central and peripheral adiponectin action is in line with other peripheral signals such as leptin and thyroid hormone that inhibit the central hypothalamic AMPK pathway but activate it in the periphery (39, 40). The molecular identity underlying these dif-

ferences between central and peripheral action of the hormone remains to be identified. Our findings clearly show reduced AMPK activity after ICV adiponectin administration, which agrees with the general catabolic action of central adiponectin similar to both central insulin and leptin, which have a potent catabolic action and reduce pAMPK(Thr172) in the MBH (41). However, whether central actions of adiponectin are largely mediated via AMPK signaling remains a matter of debate because it has been shown in one study that long-term central infusion of adiponectin improves energy and glucose homeostasis without altering hypothalamic AMPK phosphorylation in rats (29).

The known catabolic action of central adiponectin appears to be independent of the JAK2/STAT3 pathway that mediates the anorexigenic effect of leptin because ICV adiponectin did not affect the number of pSTAT3(Tyr705) immunoreactive cells in the ARC or VMH. Thus, it is likely that the catabolic function of adiponectin is mediated by hypothalamic AMPK, which is known to be involved in the regulation of food intake (41).

As previously described, adiponectin improves glucose tolerance in mice fed a HF diet. Because HF feeding is associated with inflammation in the MBH (42), we hypothesized that central adiponectin may reverse the HFD induction of important proinflammatory markers, such as JNK and GSK3 (19, 20). Consistent with this hypothesis, ICV administration of adiponectin, lowered the HF-induced increase in the number of pJNK-immunoreactive cells in the ARC and VMH. Also the reduced number of pGSK3-immunoreactive cells seen in HFD mice was fully reversed by ICV adiponectin. We have previously shown that increased activity of JNK and GSK3 in the MBH is associated with impaired whole-body glucose homeostasis (19, 20). Therefore, it is plausible that one of the ways in which adiponectin exerts its glucose-lowering properties is by reversing proinflammatory signaling in the MBH. Taken together, these data clearly demonstrate that adiponectin plays a crucial role in the neuroendocrine regulation of glucose homeostasis, providing an important link in the interaction of obesity and insulin insensitivity.

Acknowledgments

Address all correspondence and requests for reprints to: Dr Alexander Tups, Department of Animal Physiology, Faculty of Biology, Philipps University Marburg, Karl-von-Frisch Strasse. 8 D-35043 Marburg, Germany. E-mail: alexander.tups@staff.uni-marburg.de.

This study was funded by the German Ministry of Education and Research (Grant 0315087 to A.T.). L.M.W. was funded by Rural and Environment Science and Analytical Services Division.

Disclosure Summary: The authors have nothing to disclose.

References

1. **Chan JC, Malik V, Jia W, et al.** Diabetes in Asia: epidemiology, risk factors, and pathophysiology. *JAMA*. 2009;301:2129–2140.
2. **Trayhurn P, Beattie JH.** Physiological role of adipose tissue: white adipose tissue as an endocrine and secretory organ. *Proc Nutr Soc*. 2001;60:329–339.
3. **Arita Y, Kihara S, Ouchi N, et al.** Paradoxical decrease of an adipose-specific protein, adiponectin, in obesity. *Biochem Biophys Res Commun*. 1999;257:79–83.
4. **Hotta K, Funahashi T, Bodkin NL, et al.** Circulating concentrations of the adipocyte protein adiponectin are decreased in parallel with reduced insulin sensitivity during the progression to type 2 diabetes in rhesus monkeys. *Diabetes*. 2001;50:1126–1133.
5. **Hu E, Liang P, Spiegelman BM.** AdipoQ is a novel adipose-specific gene dysregulated in obesity. *J Biol Chem*. 1996;271:10697–10703.
6. **Ebinuma H, Miida T, Yamauchi T, et al.** Improved ELISA for selective measurement of adiponectin multimers and identification of adiponectin in human cerebrospinal fluid. *Clin Chem*. 2007;53:1541–1544.
7. **Kusminski CM, McTernan PG, Schraw T, et al.** Adiponectin complexes in human cerebrospinal fluid: distinct complex distribution from serum. *Diabetologia*. 2007;50:634–642.
8. **Neumeier M, Weigert J, Buettner R, et al.** Detection of adiponectin in cerebrospinal fluid in humans. *Am J Physiol Endocrinol Metab*. 2007;293:E965–E969.
9. **Yildiz BO, Suchard MA, Wong ML, McCann SM, Licinio J.** Alterations in the dynamics of circulating ghrelin, adiponectin, and leptin in human obesity. *Proc Natl Acad Sci USA*. 2004;101:10434–10439.
10. **Fruebis J, Tsao TS, Javorschi S, et al.** Proteolytic cleavage product of 30-kDa adipocyte complement-related protein increases fatty acid oxidation in muscle and causes weight loss in mice. *Proc Natl Acad Sci USA*. 2001;98:2005–2010.
11. **Nakano Y, Tobe T, Choi-Miura NH, Mazda T, Tomita M.** Isolation and characterization of GBP28, a novel gelatin-binding protein purified from human plasma. *J Biochem*. 1996;120:803–812.
12. **Waki H, Yamauchi T, Kamon J, et al.** Impaired multimerization of human adiponectin mutants associated with diabetes. Molecular structure and multimer formation of adiponectin. *J Biol Chem*. 2003;278:40352–40363.
13. **Waki H, Yamauchi T, Kamon J, et al.** Generation of globular fragment of adiponectin by leukocyte elastase secreted by monocytic cell line THP-1. *Endocrinology*. 2005;146:790–796.
14. **Yamauchi T, Kamon J, Minokoshi Y, et al.** Adiponectin stimulates glucose utilization and fatty-acid oxidation by activating AMP-activated protein kinase. *Nat Med*. 2002;8:1288–1295.
15. **Kadowaki T, Yamauchi T, Kubota N, Hara K, Ueki K, Tobe K.** Adiponectin and adiponectin receptors in insulin resistance, diabetes, and the metabolic syndrome. *J Clin Invest*. 2006;116:1784–1792.
16. **Minokoshi Y, Alquier T, Furukawa N, et al.** AMP-kinase regulates food intake by responding to hormonal and nutrient signals in the hypothalamus. *Nature*. 2004;428:569–574.
17. **Coope A, Milanski M, Araújo EP, et al.** AdipoR1 mediates the anorexigenic and insulin/leptin-like actions of adiponectin in the hypothalamus. *FEBS Lett*. 2008;582:1471–1476.
18. **Qi Y, Takahashi N, Hileman SM, et al.** Adiponectin acts in the brain to decrease body weight. *Nat Med*. 2004;10:524–529.
19. **Benzler J, Ganjam GK, Legler K, et al.** Acute inhibition of central

c-Jun N-terminal kinase restores hypothalamic insulin signalling and alleviates glucose intolerance in diabetic mice. *J Neuroendocrinol*. 2013;25:446–454.
20. **Benzler J, Ganjam GK, Krüger M, et al.** Hypothalamic glycogen synthase kinase 3β has a central role in the regulation of food intake and glucose metabolism. *Biochem J*. 2012;447:175–184.
21. **Mercer JG, Moar KM, Logie TJ, Findlay PA, Adam CL, Morgan PJ.** Seasonally inappropriate body weight induced by food restriction: effect on hypothalamic gene expression in male Siberian hamsters. *Endocrinology*. 2001;142:4173–4181.
22. **Koch C, Augustine RA, Steger J, et al.** Leptin rapidly improves glucose homeostasis in obese mice by increasing hypothalamic insulin sensitivity. *J Neurosci*. 2010;30:16180–16187.
23. **Münzberg H, Huo L, Nillni EA, Hollenberg AN, Bjørbaek C.** Role of signal transducer and activator of transcription 3 in regulation of hypothalamic proopiomelanocortin gene expression by leptin. *Endocrinology*. 2003;144:2121–2131.
24. **Kubota N, Terauchi Y, Yamauchi T, et al.** Disruption of adiponectin causes insulin resistance and neointimal formation. *J Biol Chem*. 2002;277:25863–25866.
25. **Maeda N, Shimomura I, Kishida K, et al.** Diet-induced insulin resistance in mice lacking adiponectin/ACRP30. *Nat Med*. 2002;8:731–737.
26. **Thundyil J, Pavlovski D, Sobey CG, Arumugam TV.** Adiponectin receptor signalling in the brain. *Br J Pharmacol*. 2012;165:313–327.
27. **Wilkinson M, Brown R, Imran SA, Ur E.** Adipokine gene expression in brain and pituitary gland. *Neuroendocrinology*. 2007;86:191–209.
28. **Bauche IB, Ait El Mkadem S, Rezsohazy R, et al.** Adiponectin downregulates its own production and the expression of its AdipoR2 receptor in transgenic mice. *Biochem Biophys Res Commun*. 2006;345:1414–1424.
29. **Park S, Kim DS, Kwon DY, Yang HJ.** Long-term central infusion of adiponectin improves energy and glucose homeostasis by decreasing fat storage and suppressing hepatic gluconeogenesis without changing food intake. *J Neuroendocrinol*. 2011;23:687–698.
30. **Ding Q, Ash C, Mracek T, Merry B, Bing C.** Caloric restriction increases adiponectin expression by adipose tissue and prevents the inhibitory effect of insulin on circulating adiponectin in rats. *J Nutr Biochem*. 2012;23:867–874.
31. **Niemann B, Silber RE, Rohrbach S.** Age-specific effects of short- and long-term caloric restriction on the expression of adiponectin and adiponectin receptors: influence of intensity of food restriction. *Exp Gerontol*. 2008;43:706–713.
32. **de Oliveira C, de Mattos AB, Biz C, Oyama LM, Ribeiro EB, do Nascimento CM.** High-fat diet and glucocorticoid treatment cause hyperglycemia associated with adiponectin receptor alterations. *Lipids Health Dis*. 2011;10:11.
33. **Huang H, Iida KT, Sone H, Yokoo T, Yamada N, Ajisaka R.** The effect of exercise training on adiponectin receptor expression in KKAy obese/diabetic mice. *J Endocrinol*. 2006;189:643–653.
34. **Bullen JW Jr, Bluher S, Kelesidis T, Mantzoros CS.** Regulation of adiponectin and its receptors in response to development of diet-induced obesity in mice. *Am J Physiol Endocrinol Metab*. 2007;292:E1079–E1086.
35. **Tsuchida A, Yamauchi T, Ito Y, et al.** Insulin/Foxo1 pathway regulates expression levels of adiponectin receptors and adiponectin sensitivity. *J Biol Chem*. 2004;279:30817–30822.
36. **Kubota N, Yano W, Kubota T, et al.** Adiponectin stimulates AMP-activated protein kinase in the hypothalamus and increases food intake. *Cell Metab*. 2007;6:55–68.
37. **Barnea M, Madar Z, Froy O.** High-fat diet followed by fasting disrupts circadian expression of adiponectin signaling pathway in muscle and adipose tissue. *Obesity (Silver Spring)*. 2010;18:230–238.
38. **Blüher M, Fasshauer M, Kralisch S, Schön MR, Krohn K, Paschke R.** Regulation of adiponectin receptor R1 and R2 gene expression in adipocytes of C57BL/6 mice. *Biochem Biophys Res Commun*. 2005;329:1127–1132.
39. **López M, Varela L, Vázquez MJ, et al.** Hypothalamic AMPK and fatty acid metabolism mediate thyroid regulation of energy balance. *Nat Med*. 2010;16:1001–1008.
40. **Martin TL, Alquier T, Asakura K, Furukawa N, Preitner F, Kahn BB.** Diet-induced obesity alters AMP kinase activity in hypothalamus and skeletal muscle. *J Biol Chem*. 2006;281:18933–18941.
41. **Andersson U, Filipsson K, Abbott CR, et al.** AMP-activated protein kinase plays a role in the control of food intake. *J Biol Chem*. 2004;279:12005–12008.
42. **Posey KA, Clegg DJ, Printz RL, et al.** Hypothalamic proinflammatory lipid accumulation, inflammation, and insulin resistance in rats fed a high-fat diet. *Am J Physiol Endocrinol Metab*. 2009;296:E1003–E1012.
43. **Koch CE, Lowe C, Pretz D, Steger J, Williams LM, Tups A.** A High-fat diet induces leptin resistance in leptin-deficient mice. *J Neuroendocrinol*. 2014;26:58–67.

4.2. Photoperiodic and diurnal regulation of WNT signaling in the arcuate nucleus of the female Djungarian hamster, *Phodopus sungorus*

Photoperiodic and Diurnal Regulation of WNT Signaling in the Arcuate Nucleus of the Female Djungarian Hamster, *Phodopus sungorus*

Alisa Boucsein, Jonas Benzler, Cindy Hempp, Sigrid Stöhr, Gisela Helfer, and Alexander Tups

Department of Physiology (A.B., A.T.), Centre for Neuroendocrinology and Brain Health Research Centre, University of Otago, Dunedin 9054, New Zealand; Department of Animal Physiology (A.B., J.B., C.H., S.S., A.T.), Faculty of Biology, Philipps University of Marburg, D-35032 Marburg, Germany; and Rowett Institute of Nutrition and Health (G.H.), University of Aberdeen, Aberdeen AB21 9SB, Scotland, United Kingdom

The WNT pathway was shown to play an important role in the adult central nervous system. We previously identified the WNT pathway as a novel integration site of the adipokine leptin in mediating its neuroendocrine control of metabolism in obese mice. Here we investigated the implication of WNT signaling in seasonal body weight regulation exhibited by the Djungarian hamster (*Phodopus sungorus*), a seasonal mammal that exhibits profound annual changes in leptin sensitivity. We furthermore investigated whether crucial components of the WNT pathway are regulated in a diurnal manner. Gene expression of key components of the WNT pathway in the hypothalamus of hamsters acclimated to either long day (LD) or short day (SD) photoperiod was analyzed by in situ hybridization. We detected elevated expression of the genes *WNT-4*, *Axin-2*, *Cyclin-D1*, and *SFRP-2*, in the hypothalamic arcuate nucleus, a key energy balance integration site, during LD compared with SD as well as a diurnal regulation of *Axin-2*, *Cyclin-D1*, and *DKK-3*. Investigating the effect of photoperiod as well as leptin on the activation (phosphorylation) of the WNT coreceptor LRP-6-(Ser1490) by immunohistochemistry, we found elevated activity in the arcuate nucleus during LD relative to SD as well as after leptin treatment (2 mg/kg body weight). These findings indicate that differential WNT signaling may be associated with seasonal body weight regulation and is partially regulated in a diurnal manner in the adult brain. Furthermore, they suggest that this pathway plays a key role in the neuroendocrine regulation of body weight and integration of the leptin signal. (***Endocrinology* 157: 799–809, 2016)**

Survival in a seasonally changing environment requires physiological adaptations for most animals. In seasonal mammals, these adaptations are driven by photoperiod and exhibit remarkable changes in growth, energy balance and reproduction, resulting from changes in the neuroendocrine axis.

During the last decade, significant progress has been achieved in unraveling the molecular mechanisms underlying these physiological changes. One of the best-characterized seasonal rodent models is the Djungarian hamster (*Phodopus sungorus*), also known as the Siberian hamster, because these mammals show an extensive body weight reduction of about 40% in winter-like conditions (short days [SD]) compared with summer-like conditions (long days [LD]). More than half of this weight loss derives from a reduction of adipose tissue mass (1). This annual body weight cycle is characterized by seasonally regulated leptin sensitivity (1).

Accumulating evidence suggests that the WNT signaling pathway, which has been well characterized in embryogenesis and tumorigenesis (2, 3), can be altered in diverse tissues by the body weight-regulating hormone

ISSN Print 0013-7227 ISSN Online 1945-7170
Printed in USA

Received August 10, 2015. Accepted November 25, 2015.
First Published Online December 8, 2015

Abbreviations: ARC, arcuate nucleus; DG, dentate gyrus; DKK, Dickkopf; Fz, Frizzled; GSK-3β, glycogen synthase kinase-3β; HI, hippocampus; LD, long days; LRP, low-density lipoprotein receptor-related protein; SD, short days; SFRP, secreted Fz-related protein; STAT3, signal transducer and activator of transcription 3; WNT, WNT ligand; ZT, Zeitgeber time.

leptin (4, 5). Additionally, hypothalamic WNT signaling was shown to be implicated in the control of adipogenesis and adult neurogenesis as well as the cellular and structural remodeling of the adult hypothalamus (6–8). Recent findings from our laboratory suggested that the central WNT pathway is crucial for the neuroendocrine control of metabolism in mice (5, 9). Furthermore, several genes involved in WNT signal transduction were shown to be regulated by photoperiod in photoperiod-responsive F344 rats (8, 10, 11).

The canonical, β-catenin-dependent WNT pathway is activated when extracellular WNT ligands bind to Frizzled (Fz) receptors and associated coreceptors, the low-density lipoprotein receptor-related proteins (LRPs). The coreceptor LRP-6 is activated via phosphorylation at Ser1490 (12). Subsequently, the formation of a protein complex including Axin-1, Dishevelled, and adenomatous polyposis coli is prevented, resulting in an inhibition of the key enzyme glycogen synthase kinase-3β (GSK-3β). This leads to the stabilization of the cotranscription factor β-catenin in the cytoplasm and its translocation to the nucleus, in which it promotes binding of the transcription factor T cell-specific transcription factor 7, which then induces the expression of WNT target genes (13). In the absence of WNT ligands (WNTs) or in the presence of WNT antagonists such as Dickkopf (DKK) proteins or secreted Fz-related proteins (SFRPs), GSK-3β lingers in the complex and phosphorylates β-catenin, inducing its proteasomal degradation (13).

Circadian clocks adjust behavioral and physiological processes to the most beneficial time of day in a broad range of species. In mammals, the primary entrainment signal (Zeitgeber) is light, which synchronizes the circadian clock, whose pacemaker resides in the hypothalamic suprachiasmatic nucleus with environmental cues (14). The circadian clock is tightly coupled to metabolism and feeding rhythms (15, 16), and GSK-3β has been described as being a crucial part of the transcriptional-translational feedback loop that comprises the clock because this kinase is responsible for the phosphorylation of key clock components and might thereby directly affect circadian rhythms (17–21). Furthermore, the prominent WNT target gene *Cyclin-D1* was shown to be under the control of the circadian clock in the periphery (22). Most of our knowledge about the circadian regulation of WNT signaling derives from stem cell proliferation and cancer studies. However, whether WNT signaling molecules are regulated in a diurnal manner in the hypothalamus is unknown.

In the current study, we analyzed whether WNT signaling is active in the hypothalamus of adult Djungarian hamsters and is furthermore regulated by photoperiod or in a diurnal manner, potentially implicating a novel regulatory role in the hamsters' profound seasonal alterations in physiology. We therefore examined seasonal as well as diurnal regulation of the WNT pathway by analyzing whether key molecules of the WNT pathway are differentially regulated, on a transcriptional and posttranslational level, between hamsters held in LD and SD at different times throughout the day. Furthermore, we challenged hamsters with leptin administration to corroborate our recent finding that leptin activates the WNT pathway in a different rodent species (5).

Materials and Methods

Animals

All procedures involving animals were performed in accordance with German animal ethics legislation and received approval by the respective authorities for animal ethics. Female Djungarian hamsters (*P sungorus*) were bred under LD conditions (light/dark cycle: 16 h light, 8 h dark) at the Department of Biology of the University of Marburg (Marburg, Germany). At the age of 3 weeks, hamsters were weaned and housed individually at an ambient temperature of 21°C with ad libitum access to standard chow diet and water. Hamsters were maintained in LD or, where specified, transferred to SD conditions (light/dark cycle: 8 h light, 16 h dark) for a further 8 weeks until they were fully adapted to SD. Body weight was recorded weekly during this time. Before the animals were killed, they were food deprived for 16 hours. For in situ hybridization, animals were euthanized by cervical dislocation and brains were rapidly frozen on dry ice. For immunohistochemistry, transcardial perfusion was performed and brains were treated as described elsewhere (23). To characterize the diurnal expression profiles of key WNT genes, adult Djungarian hamsters were used. After weaning, all hamsters were maintained in LD until adulthood (3–5 mo of age), whereupon they either remained in LD or were transferred to SD for a further 8 weeks. During LD, the light period was from Zeitgeber time (ZT) 0 to ZT16 and during SD from ZT0 to ZT8. Hamsters were killed at ZT0, ZT3, ZT6, ZT9, ZT12, ZT15, ZT18, and ZT21 (n = 4–5 animals per photoperiod and time point). Hamsters killed during the dark phase were euthanized under dim red light.

Detection of hypothalamic gene expression by in situ hybridization

In situ hybridization was performed on brains of Djungarian hamsters aged 5–7 months. Coronal brain sections (16 μm) were collected throughout the extent of the arcuate nucleus (ARC) onto a set of 12 slides with 10 sections mounted on each slide, as described previously (24). The slides spanned the hypothalamic region approximately from −2.7 to −0.8 mm relative to Bregma according to the atlas of the mouse brain (25). Riboprobes specific for *WNT-4*, *GSK-3β*, *Axin-2*, *Cyclin-D1*, and *DKK-3* mRNA were prepared as described elsewhere (5). Riboprobes specific for *SFRP-2* mRNA were prepared from a 157-bp DNA template, which was generated from *P sungorus* hypothalamic cDNA by PCR using forward primer 5′-GCC ACG GCA TCG

AGT ACC AGA ACA-3′ and reverse primer 5′-ACA GGG GCG AAG AGC GAG CAC A-3′. Primers used for the amplification of DNA fragments were designed using the Lasergene Primer Select software (DNASTAR, Inc). Amplified DNA fragments were ligated into pGEM-T Easy Vector (Promega Corp), transformed into DH5-α *Escherichia coli*, and sequenced. In situ hybridization and analysis were performed as described previously (24). Briefly, cRNA synthesis was facilitated using SP6-polymerase or T7-polymerase as part of a riboprobe synthesis kit (Promega). Slides were fixed, acetylated, and dehydrated, followed by overnight hybridization at 58°C using [^{35}S]-labeled cRNA probes (1–2 × 10^7 cpm/mL). Subsequently, slides were treated with ribonuclease A, desalted, and dehydrated. For autoradiography, dried slides were exposed to Amersham Hyperfilm MP (GE Healthcare) together with Amersham [^{14}C]-microscale standard. Images were quantified by measurement of OD in a defined area (ARC) using the Image-Pro Plus software (Media Cybernetics), and data were stated as integrated OD.

Immunohistochemistry

To investigate whether leptin regulates the hypothalamic WNT pathway in a photoperiod-dependent manner, the phosphorylation of the Fz coreceptor LRP-6, as the marker of its activation, was analyzed. Therefore, Djungarian hamsters were maintained in LD or transferred to SD immediately after weaning. Hamsters received a single ip injection of either leptin (2 mg/kg body weight) or vehicle (0.9% saline) 15 minutes prior to transcardial perfusion (n = 6–8 animals per each group). Subsequently, immunohistochemistry was performed. Free-floating brain sections were pretreated with 10% methanol, 1% NaOH, and 1% H_2O_2 in H_2O for 20 minutes, 0.3% glycine for 10 minutes, and 0.03% sodium dodecyl sulfate for 10 minutes. Next, sections were blocked with 1% normal goat serum and 5% BSA in sodium phosphate buffer-Triton X-100 (0.5%) for 1 hour, followed by overnight incubation at 4°C using a rabbit antiphospho-LRP-6 (Ser1490) antibody (1:1500 in blocking solution; catalog number 2568; Cell Signaling Technology, Inc). On the next day, sections were rinsed and incubated with biotinylated goat-antirabbit secondary antibody (1:1000 in blocking solution) for 1 hour, followed by avidin biotin complex solution (Vector Laboratories, Inc) for 1 hour. Finally, the signal was developed by diaminobenzidine solution (Vector Laboratories), giving a gray precipitate. Pictures were taken and immunoreactive cells were counted by two investigators blinded to the treatments.

Statistical analysis

Rhythmicity of each gene expression was analyzed using one-way factorial ANOVA with Tukey's honestly significant difference post hoc test. To compare phasing and peak expression times, a polynomial fourth-order nonlinear regression was fitted with GraphPad Prism software (GraphPad Software). The effect of day length on each gene's expression profile was then examined by pairwise comparison. Where polynomial fourth-order nonlinear regression indicated rhythmicity of a gene, the difference at each time point was analyzed by a Student's *t* test. For nonrhythmically expressed genes, the values at the different time points were averaged and the mean expression over 24 hours was compared by a Student's *t* test. Coreceptor modification was analyzed by a two-way ANOVA followed by a Holm-Sidak comparison test, as appropriate, using SigmaStat statistical software (Systat Software; Jandel). Results are presented as mean ± SEM, and differences were considered significant if $P \leq .05$.

Results

Localization of WNT signaling gene expression in the brain of Djungarian hamsters

To explore whether WNT signaling is active in the hypothalamus of adult Djungarian hamsters, we analyzed the expression patterns of genes encoding components of the WNT pathway. By performing in situ hybridization, we found that all investigated genes were expressed in the mediobasal hypothalamus, especially in the ARC. Additionally, expression of all genes occurred in extrahypothalamic regions such as the cortex, the thalamus, and the dentate gyrus (DG) as well as the CA1, CA2, and CA3 fields of the hippocampus (HI). The riboprobe specific for *WNT-4* hybridized also to the choroid plexus. Expression of *GSK-3β* and *Axin-2* was relatively intense in the DG and HI and also occurred in the medial habenula and the ventromedial hypothalamus. Both *Cyclin-D1* and *DKK-3* mRNAs were mainly expressed in the ARC, HI, and DG, *DKK-3* additionally in the medial habenula. *SFRP-2* mRNA was intensely concentrated in the thalamus and showed a weaker signal in the ventromedial hypothalamus (Figure 1). Hybridization signals did not occur using the respective sense riboprobes (Figure 1, *DKK-3* sense riboprobe is shown as an example).

Temporal expression pattern of WNT signaling genes in the hypothalamus under long and short photoperiod

Temporal expression patterns of WNT signaling genes in the hypothalamus were examined in the LD or SD photoperiod. Nonlinear regression analysis revealed a trend for diurnal rhythmicity of *Axin-2* expression (Figure 2A; $P = .098$) as well as different amplitude and peak expression times of *Cyclin-D1* and *DKK-3* (Figure 2, B and C), exposing diurnal rhythmicity of both genes. In contrast, no evidence for the rhythmic expression of *WNT-4*, *GSK-3β*, and *SFRP-2* (Figure 3) over 24 hours was obtained. *Axin-2* gene expression showed similar expression patterns between the two photoperiods. The differential expression of mRNA levels appeared to increase during the dark phase and seemed to decline during the light phase. For both LD and SD, *Axin-2* showed the lowest expression levels around the first half of the subjective night (ZT21 and ZT12, respectively).

Cyclin-D1 gene expression during LD showed a trend ($P = .098$) toward and during SD a significant diurnal

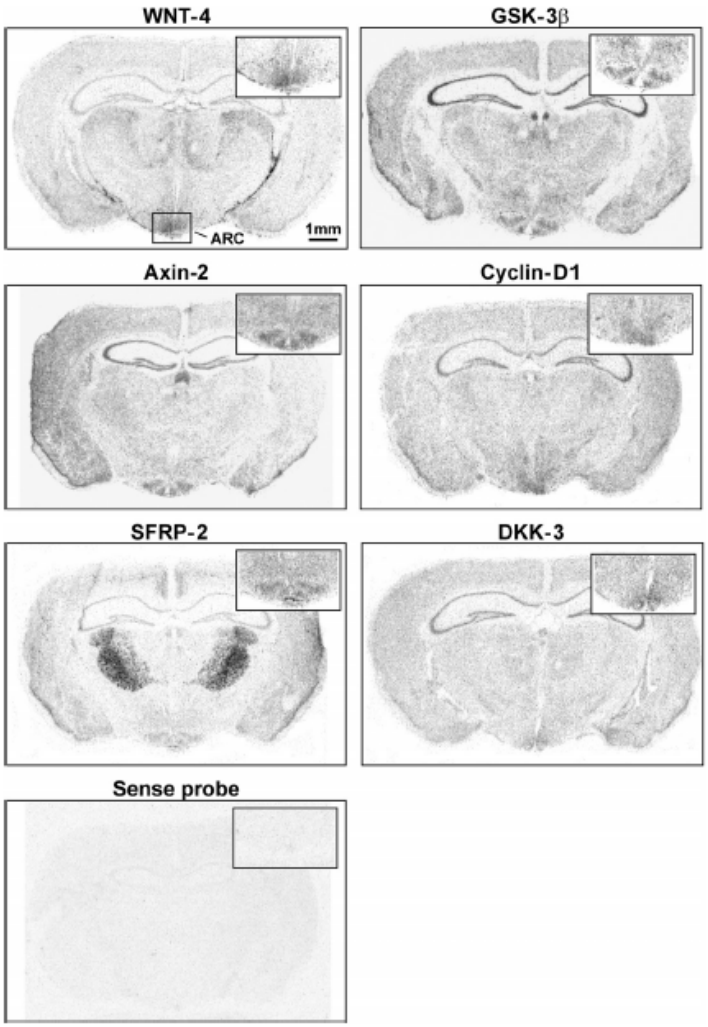

Figure 1. Genes encoding members of the WNT pathway are expressed in the brain of Djungarian hamsters. Genes encoding for the WNT ligand WNT-4, the key enzyme GSK-3β, the WNT target genes *Axin-2* and *Cyclin-D1* and the antagonists SFRP-2 and DKK-3 were detected by in situ hybridization with antisense [^{35}S]-labeled riboprobes. All investigated genes were expressed in the ARC of the hypothalamus. Additionally, some expression occurred in the cortex, hippocampus, and thalamus. Representative for all respective sense riboprobes, an image for *DKK-3* is shown. Inserts depict binding of the riboprobes to the ARC.

rhythmicity ($P = .021$) with decreasing gene expression during the subjective day of the animal and increased gene expression during the subjective night. Consistently, *Cyclin-D1* reached peak values at ZT0 in LD and ZT18 in SD, whereas trough values were achieved at ZT18 in LD and ZT9 in SD.

DKK-3 showed pronounced high-amplitude rhythmicity in LD ($P < .001$) and elevating gene expression throughout the day with peak expression times shortly after the end of the light phase at ZT18 and a trough after the dark phase. Contrarily, in SD, *DKK-3* levels were highest at ZT0 with declining gene expression during the day and elevating gene expression during the night, displaying a generally lower amplitude ($P = .023$).

For *Axin-2*, *Cyclin-D1* and *DKK-3* we found that gene expression was regulated by photoperiod at individual time points. In LD a generally higher expression of *Axin-2* and *Cyclin-D1* was displayed relative to SD, with a trend toward higher *Axin-2* expression at ZT6 ($P = .051$) and significantly elevated *Axin-2* expression at ZT9 and ZT12 (Figure 2A; $P < .01$). *Cyclin-D1* expression in LD was elevated at ZT0, ZT3, ZT6, and ZT9 (Figure 2B; $P < .05$) compared with SD. *DKK-3* showed a seasonally regulated gene expression with a declined expression at ZT3 (Figure 2C; $P = .011$) and, conversely regulated, elevated expression at ZT6 ($P = .011$) in LD relative to SD.

No diurnal rhythmicity was detected for *WNT-4*, *SFRP-2*, and *GSK-3β* (Figure 3, A–C). However, averaged expression throughout the diurnal cycle revealed that the nonrhythmic genes *WNT-4* and *SFRP-2* were down-regulated in the ARC of SD hamsters compared with LD hamsters by about 20% and 35%, respectively (Figure 3, A and B; $P = .012$ and $P = .005$, respectively). In contrast, there was no effect of photoperiod on gene expression of the pathway-inactivating enzyme *GSK-3β* (Figure 3C; $P = .745$).

Effects of photoperiod and leptin on WNT coreceptor activation

After having established that several key components of the WNT pathway are differentially expressed during long and short photoperiod as well as throughout the day, we next tested whether activation of the WNT pathway at the level of the coreceptor might be dependent on photoperiod. Therefore, we performed immunohistochemistry to

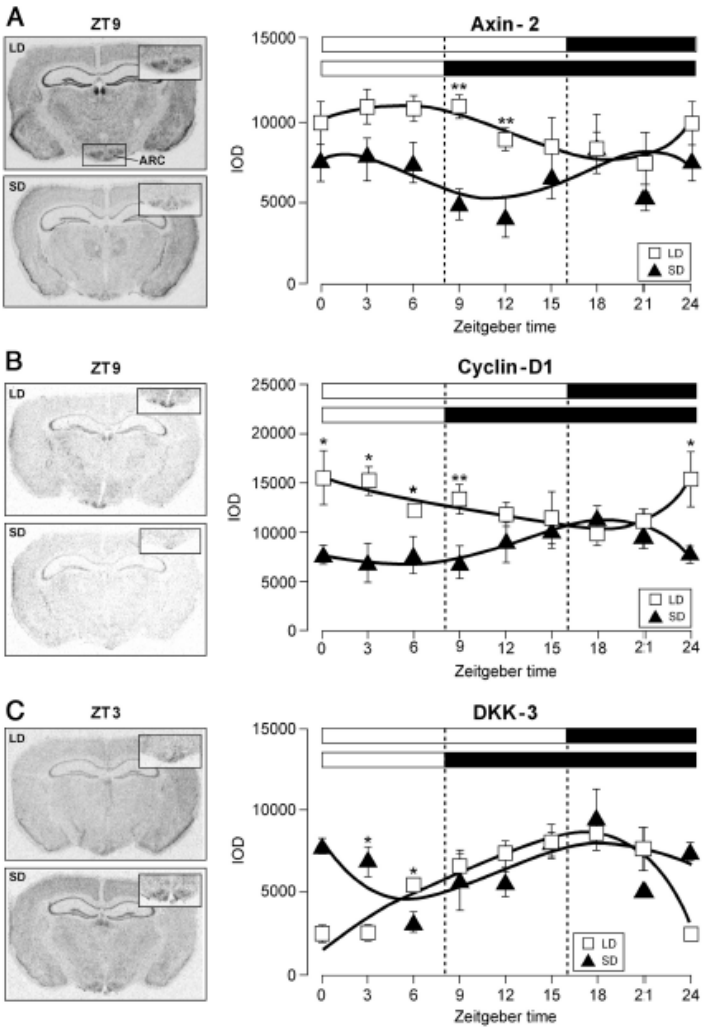

Figure 2. Temporal expression profiles of WNT signaling genes in the ARC of Djungarian hamsters acclimated to either LD (□) or SD (▲) photoperiod. *Axin-2* (A), *Cyclin-D1* (B), and *DKK-3* (C) were rhythmically expressed in both photoperiods. The left panels depict autoradiographs of representative coronal brain sections from time points when temporal gene expression was different between LD and SD; inserts in the left panels show binding of riboprobes to the ARC. The right panels show line charts of quantified signals in the ARC from three to four sections per animal. Open and solid bars at the top of each graph represent light and dark periods, respectively. Data are presented as means ± SEM (n = 2–6 at each time point). *, $P \leq .05$, **, $P \leq .01$ reveal significantly different time points of gene expression between LD and SD. IOD, integrated OD.

detect phospho-LRP-6 (Ser1490)-immunoreactive cells in the ARC of hamsters in LD and SD that were furthermore challenged by ip leptin injections. Two-way ANOVA revealed a statistically significant effect of photoperiod ($P < .001$) as well as leptin treatment ($P = .011$) on WNT coreceptor activation; however, the effect of leptin was independent of which photoperiod was present ($P = .837$; Figure 4). SD hamsters showed a significant decrease in the number of phospho-LRP-6 (Ser1490)-immunoreactive cells of about 40% compared with their littermates in LD. Interestingly, leptin-sensitive SD hamsters as well as LD hamsters, which are known to be leptin resistant (1, 26), revealed an increase in phospho-LRP-6 (Ser1490)-immunoreactive cells of about 45% and 30%, respectively, in response to ip leptin compared with hamsters that received vehicle.

Discussion

The WNT pathway has been well characterized in embryogenesis and tumorigenesis. However, recent data suggested that this pathway has a much broader function in the central nervous system than was initially thought. Accumulating evidence suggests that it is involved in adult neurogenesis (7), the remodeling of the adult hypothalamus (8), and the neuroendocrine control of metabolism (5, 9). In the present study, we investigated the primary effects of the photoperiod on WNT signaling in the seasonal mammal *P sungorus* to unravel its role in long-term seasonal changes in energy metabolism. Furthermore, we characterized whether mRNA expression is regulated in a diurnal manner.

We demonstrated that all investigated genes involved in the WNT pathway are expressed in the hypothalamic ARC, a key region in neuronal control of body weight and food intake. However, it is important to note that the expression of WNT genes also occurred in extrahypothalamic brain regions such as the cortex, thalamus and hippocampus. The change in the mRNA expression of several WNT components (*WNT-4*, *Axin-2*, *Cyclin-D1*, *DKK-3*, and *SFRP-2*) during the differential photoperiods indicates that central WNT signaling may play an important role in the seasonal regulation of body weight and food intake in adult Djungarian hamsters. We have pre-

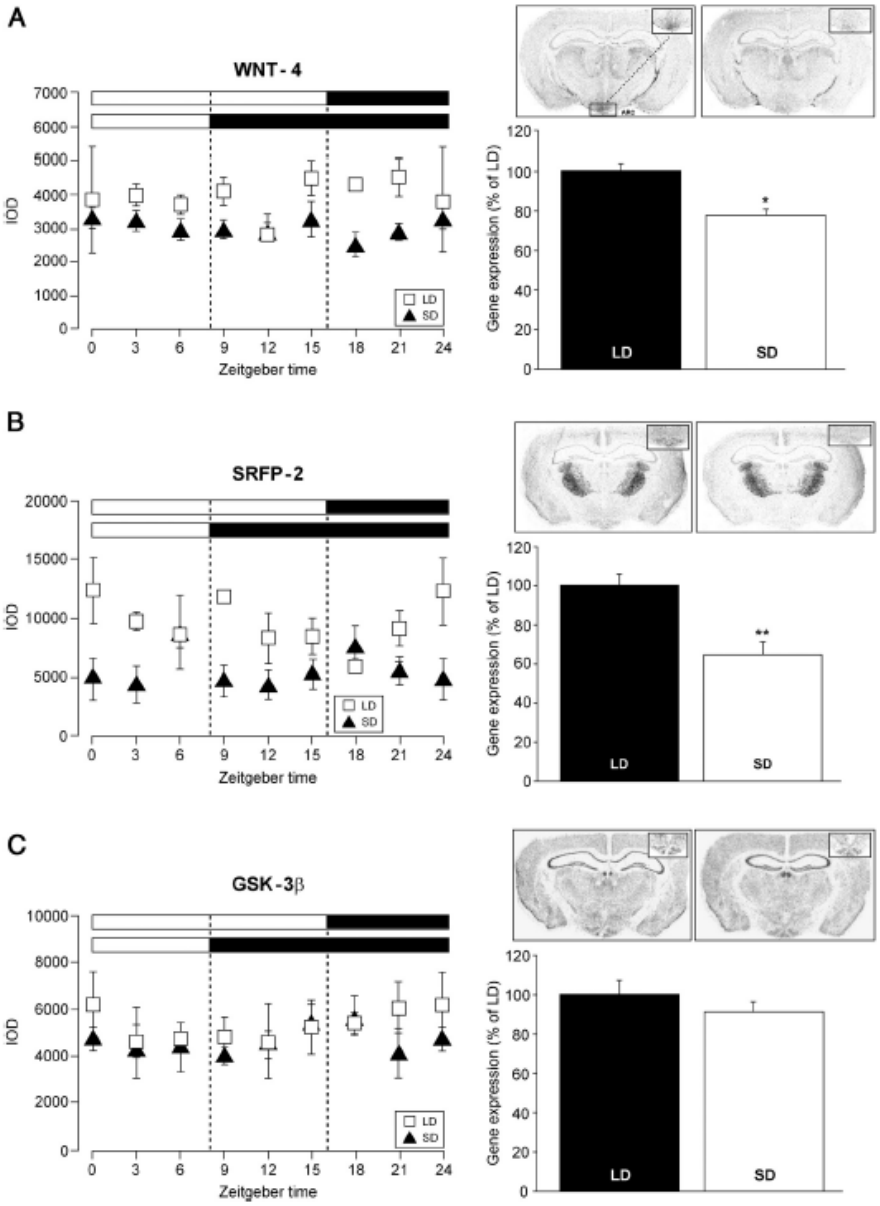

Figure 3. Temporal expression profiles of WNT genes of which no rhythmicity was detected over 24 hours. Averaged expression over 24 hours of *WNT-4* (A) and *SFRP-2* (B) was elevated in LD compared with SD, whereas *GSK-3β* gene expression (C) was not affected by the photoperiod. The left panels show line charts of quantified signals in the ARC from three to four sections per animal. The right panels show bar charts of averaged expression throughout the diurnal cycle with autoradiographs of representative coronal brain sections from LD and SD; inserts depict binding of riboprobes to the ARC. Data are presented as means ± SEM. *, $P \leq .05$, **, $P \leq .01$. IOD, integrated OD.

viously demonstrated that WNT signaling is active in the adult murine brain (5). The expression of key members of the WNT pathway in several brain regions of two rodent species together with the finding that WNT genes are differentially expressed in response to changing photoperiod in *P sungorus* corroborates the importance of this pathway in the neuronal control of metabolism and its prominence in the adult brain.

We focused on WNT-4 and WNT-7a (27) as ligands for the WNT pathway because both have been shown to be

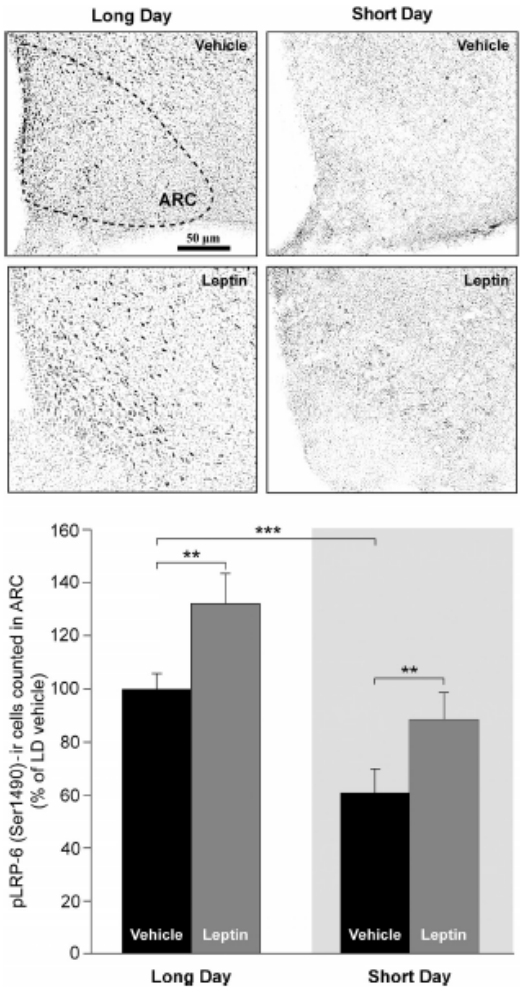

Figure 4. Photoperiod and leptin administration had a significant effect on WNT coreceptor activation. Immunoreactivity of phospho-LRP-6 (Ser1490) was increased in the ARC of LD compared with SD hamsters. Independent of photoperiod, leptin (2 mg/kg) administered ip led to a significant increase of phospho-LRP-6 (Ser1490)-immunoreactive cells in the ARC compared with vehicle. Upper panels depict representative coronal brain sections of each group, and lower panels show bar charts of quantified phospho-LRP-6-immunoreactive cells in the ARC from three sections per animal. Data are presented as the mean percentage values of LD control ± SEM. **, $P \leq .01$, ***, $P \leq .001$.

implicated in neural development, such as anterior-posterior guidance of commissural axon growth (28), maturation of synapses (29), neuronal differentiation (30), and central nervous system vascularization (31). Unfortunately, we could analyze gene expression data only for *WNT-4* because *WNT-7a* expression was below the detection limit of the very sensitive in situ hybridization using radiolabeled probes. Gene expression of the ligand *WNT-4*, which activates the WNT pathway (32), was up-regulated in the ARC of LD relative to SD hamsters. This suggests an improved receptor activation of the WNT pathway in the ARC of LD-acclimated hamsters. Together with our finding that the WNT target genes *Axin-2* (33) and *Cyclin-D1* (34) were increased at certain time points throughout the diurnal rhythm in LD relative to SD, these data imply enhanced activation of the WNT signal transduction pathway in this photoperiod. Cyclin-D1 is a prominent mediator of mammalian cell growth (35, 36), and furthermore, WNT/β-catenin-mediated cyclin-D1 expression directly leads to enhanced cell proliferation (34). Thus, our data indicate increased neural cell proliferation in LD.

A crucial regulatory enzyme of WNT signaling is GSK-3β because ligands binding to WNT receptors lead to the inactivation of GSK-3β and thereby activation of the pathway. We did not find the regulation of GSK-3β by photoperiod on the level of gene expression. However, GSK-3β activity is regulated by posttranslational modification and the formation of an Axin-including degradation complex (37). Therefore, gene expression data of this particular member of the WNT pathway are not very informative, and we attempted to detect phosphorylated GSK-3β, which would allow us to determine the activity of this enzyme. Unfortunately, the readily available commercial antibodies to detect phospho-GSK-3β did not cross-react with hamster brain tissue.

SFRP-2 mRNA was significantly up-regulated in the ARC of LD-acclimated hamsters compared with SD-acclimated hamsters. This is consistent with our previous study that showed that *SFRP-2* gene expression is increased in the hypothalamus of photoperiod-responsive F344 rats under LD relative to SD conditions (8). Some studies have shown that SFRP-2 acts as an antagonist of the WNT pathway via interaction with WNT ligands to prevent them from binding to Fz receptors (38–40), and this appears contradictory to activated WNT signaling in LD. However, the WNT-antagonizing effect of SFRP-2 has not been clearly established because, in contrast, Yoshino et al (41) demonstrated that SFRP-2 inhibits other SFRPs to promote WNT activity. Interestingly, there is evidence that WNT-4 does not only induce SFRP-2 expression in particular tissues, but SFRP-2 also binds WNT-4 and enhances its signal transduction (39, 41). The mutual up-regulation of both genes in the ARC of LD hamsters might thereby have a synergistic effect, which might cause the up-regulation of the targets *Axin-2* and *Cyclin-D1* observed in this study.

In a previous study, we observed a marked photoperiodic response of *DKK-3* with elevated gene expression

during LD in F344 rats (8, 10). In the present study, *DKK-3* gene expression was profoundly coupled to the diurnal rhythm and regulated by photoperiod. Whether *DKK-3* was elevated or reduced in LD relative to SD was dependent on the time of day, suggesting that the diurnal control of this WNT-related gene overrides any photoperiodic regulation. In LD hamsters *DKK-3* gene expression was tightly coupled to the light/dark phase. It continuously increased throughout the light phase followed by a decrease during the dark phase. DKK-3 is a member of the DKK family that inhibits WNT signaling by binding to the LRP-5/6 coreceptors (42). In line with the WNT inhibitory function of DKK-3, expression of the WNT target genes *Axin-2* and *Cyclin-D1* declined during the animals' subjective day and elevated during their subjective night in LD. The diurnal regulation of *DKK-3* on the one hand and reciprocal *Axin-2* and *Cyclin-D1* gene expression on the other hand implies that diurnal regulation of *DKK-3* in LD hamsters might have a yet-unknown physiological function to regulate WNT target genes in a circadian manner that is restricted to this photoperiod. Diurnal *DKK-3* gene expression in SD did not affect *Axin-2* and *Cyclin-D1* mRNA in the same manner as in LD. Surprisingly, the precise function of DKK-3 in WNT signal transduction has not yet been established. Although some studies have shown that DKK-3 has no influence on LRP-5/6 activation or nuclear β-catenin accumulation (43, 44), others revealed effects on cytoplasmic β-catenin levels (45, 46). Moreover, an implication of DKK-3 in noncanonical WNT/c-Jun N-terminal kinase signal transduction is being discussed (47, 48).

The diurnal rhythmicity of several WNT genes in the ARC might be suggestive for an interaction of the WNT pathway and the circadian clock. Although the master circadian clock resides in the suprachiasmatic nucleus, a food-entrainable oscillator has been proposed to be located in the ARC (49). In fact, WNT signal transduction was shown to be modulated by the clock gene brain and muscle Arnt-like 1 (Bmal1), with declined WNT signaling after attenuation of Bmal1 function (50). Because Bmal1 is known to be a prominent regulator of the genes that control metabolism (51), these data support the potential role of WNT signaling in the control of metabolic processes in the Djungarian hamster.

Initiation of the canonical WNT pathway requires activation of both the Fz receptor and the LRP-5/6 coreceptor. LRP-6 is activated by phosphorylation at Ser1490 (12), leading to the recruitment of Axin to the intracellular domain of the coreceptor (52–54) and subsequent inhibition of GSK-3β. The number of phospho-LRP-6 (Ser1490)-immunoreactive cells was enhanced in the ARC of LD hamsters compared with SD hamsters. Peripheral administration of the adipokine leptin induced an increase of phospho-LRP-6 (Ser1490) immunoreactivity in LD as well as in SD hamsters. This is consistent with our previous finding in obese leptin deficient $Lep^{ob/ob}$ mice, which exhibited increased phospho-LRP-6 (Ser1490) immunoreactivity and *Axin-2* and *Cyclin-D1* gene expression after leptin injection (5).

Notably, in the brain regions in which we detected WNT gene expression, the long form of the leptin receptor (Lep^{Rb}) is also widely expressed in the Djungarian hamster and other rodent models (55–58). The coexistence of both leptin and WNT signaling in these brain regions indicates that the two pathways interact. By corroborating our findings from mice (5) in hamsters, we provide the first evidence of a novel, previously unknown central effect of leptin, ie, leptin is capable of activating the WNT coreceptor

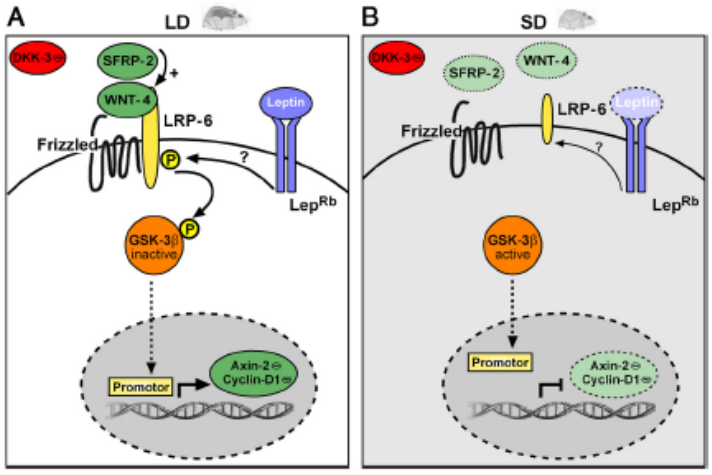

Figure 5. Model proposing the seasonal regulation of the WNT pathway in the hypothalamus of the Djungarian hamster. A, During LD, when leptin levels are elevated, phosphorylation of LRP-6 is increased, which might be mediated via synergistic action of up-regulated WNT-4 and SFRP-2 on the one hand and leptin on the other hand. LRP-6 is known to phosphorylate and thereby inactivate GSK-3β. This overrides the inhibitory effect of GSK-3β on WNT target gene expression and therefore increases *Axin-2* and *Cyclin-D1* mRNA. B, During SD, when leptin levels are low, reduced levels of WNT-4, SFRP-2, and leptin fail to activate LRP-6, leading to the enhanced activity of GSK-3β, which in turn would lead to reduced WNT target gene expression. The putative LRP-5/6 antagonist DKK-3 is differentially regulated at individual time points in LD and SD, yet its role in WNT signaling is still unclear. Furthermore, the gene expression of *DKK-3* as well as the WNT target genes *Axin-2* and *Cyclin-D1* was under diurnal rhythmicity, indicated by ⊖.

LRP-6 across different species, revealing a potentially very important physiological regulation of the WNT pathway by leptin. This activation occurred at the level of the coreceptor LRP-6, which suggests that leptin activates the canonical WNT pathway. Future studies, however, are required to determine whether this hormone also affects noncanonical WNT signaling such as the planar cell polarity and Ca^{2+} pathways (59, 60).

Intriguingly, leptin enhanced LRP-6 activation in hamsters from both photoperiods. During the LD photoperiod, hamsters are resistant to exogenous leptin in terms of its catabolic effect (1) and also in terms of its ability to activate the signal transducer and activator of transcription 3 (STAT3) (61). The transcription factor STAT3 is part of the best-characterized Janus kinase 2-STAT3 leptin signaling pathway. Also, gene expression of the suppressor of cytokine signaling 3, which inhibits leptin signaling, was increased in LD compared with SD conditions (26, 62, 63). It is plausible that leptin activates the WNT pathway at the level of LRP-6 independent of Janus kinase 2-STAT3 signaling. Although leptin levels are elevated in LD compared with SD, in neither photoperiod circadian regulation of mean serum leptin levels was detected over a 24-hour profile in Djungarian hamsters (64, 65). This suggests that the diurnal regulation of WNT target genes and *DKK-3* might be independent of circulating leptin. It has been reported, however, that gene expression of Lep^{Rb} is regulated in a circadian manner in the ARC of hamsters exposed to LD (64). This indicates that Lep^{Rb} might be involved in circadian regulation of WNT signaling components. Circadian changes in Lep^{Rb} expression were confined to LD hamsters (64), suggesting that leptin sensitivity is under the control of the circadian rhythm in LD, which counteracts to the perception that LD hamsters are generally leptin resistant relative to SD hamsters. The necessity to further assess the role of leptin sensitivity in seasonal body weight regulation is further supported by our finding that leptin activated LRP-6 in both photoperiods. Regulation of leptin sensitivity might be fine-tuned at different levels in the leptin receptor signaling cascade.

In LD hamsters, high circulating levels of leptin in combination with the synergistic effect of WNT-4 and SFRP-2 might potentiate the induction of phosphorylation of LRP-6, probably preventing the Axin-GSK-3β complexation and inhibiting GSK-3β. This would facilitate the expression of the WNT target genes such as *Axin-2* and *Cyclin-D1*. During SD, lower leptin levels in combination with reduced WNT-4 and SFRP-2 would explain the lower basal activation of LRP-6 relative to LD. Less activation of WNT signaling would attenuate the inhibition of GSK-3β, which as a negative WNT pathway regulator would lead to the further reduction of WNT signaling and reduced target gene expression (Figure 5).

In conclusion, we provide strong evidence that WNT signaling is involved in the seasonal as well as the diurnal regulation of metabolism in the hypothalamus of the Djungarian hamster. The expression pattern of the investigated genes involved in WNT signaling and the posttranslational modification of the WNT coreceptor strongly indicate that this pathway is functionally impaired in the hypothalamus of Djungarian hamsters during SD and reinstated during the LD photoperiod. Furthermore, these data corroborate our previous observation of leptin's ability to activate the WNT signal transduction in mice and imply a fundamental importance of WNT signaling in metabolic control (5).

Acknowledgments

Address all correspondence and requests for reprints to: Alexander Tups, PhD, Department of Physiology, Otago School of Medical Sciences, University of Otago, PO Box 913, Dunedin, New Zealand. E-mail: alexander.tups@otago.ac.nz.

This work was supported by the German Ministry of Education and Research and by the German Research Foundation (to A.T.).

Disclosure Summary: The authors have nothing to disclose.

References

1. **Klingenspor M, Niggemann H, Heldmaier G.** Modulation of leptin sensitivity by short photoperiod acclimation in the Djungarian hamster, *Phodopus sungorus*. *J Comp Physiol B*. 2000;170:37–43.
2. **Moon RT, Brown JD, Torres M.** WNTs modulate cell fate and behavior during vertebrate development. *Trends Genet*. 1997;13:157–162.
3. **Peifer M, Polakis P.** Wnt signaling in oncogenesis and embryogenesis—a look outside the nucleus. *Science*. 2000;287:1606–1609.
4. **Ohba S, Lanigan TM, Roessler BJ.** Leptin receptor JAK2/STAT3 signaling modulates expression of Frizzled receptors in articular chondrocytes. *Osteoarthritis Cartilage*. 2010;18:1620–1629.
5. **Benzler J, Andrews ZB, Pracht C, et al.** Hypothalamic WNT signalling is impaired during obesity and reinstated by leptin treatment in male mice. *Endocrinology*. 2013;154:4737–4745.
6. **Ross SE, Hemati N, Longo KA, et al.** Inhibition of adipogenesis by Wnt signaling. *Science*. 2000;289:950–953.
7. **Inestrosa NC, Arenas E.** Emerging roles of Wnts in the adult nervous system. *Nat Rev Neurosci*. 2010;11:77–86.
8. **Helfer G, Ross AW, Russell L, et al.** Photoperiod regulates vitamin A and Wnt/β-catenin signaling in F344 rats. *Endocrinology*. 2012;153:815–824.
9. **Benzler J, Ganjam GK, Kruger M, et al.** Hypothalamic glycogen synthase kinase 3β has a central role in the regulation of food intake and glucose metabolism. *Biochem J*. 2012;447:175–184.
10. **Helfer G, Ross AW, Morgan PJ.** Neuromedin U partly mimics thyroid-stimulating hormone and triggers Wnt/β-catenin signalling in the photoperiodic response of F344 rats. *J Neuroendocrinol*. 2013;25:1264–1272.

11. **Ross AW, Helfer G, Russell L, Darras VM, Morgan PJ.** Thyroid hormone signalling genes are regulated by photoperiod in the hypothalamus of F344 rats. *PLoS One*. 2011;6:e21351.
12. **Tamai K, Semenov M, Kato Y, et al.** LDL-receptor-related proteins in Wnt signal transduction. *Nature*. 2000;407:530–535.
13. **MacDonald BT, Tamai K, He X.** Wnt/β-catenin signaling: components, mechanisms, and diseases. *Dev Cell*. 2009;17:9–26.
14. **Reppert SM, Weaver DR.** Coordination of circadian timing in mammals. *Nature*. 2002;418:935–941.
15. **Asher G, Schibler U.** Crosstalk between components of circadian and metabolic cycles in mammals. *Cell Metab*. 2011;13:125–137.
16. **Lamia KA, Sachdeva UM, DiTacchio L, et al.** AMPK regulates the circadian clock by cryptochrome phosphorylation and degradation. *Science*. 2009;326:437–440.
17. **Harada Y, Sakai M, Kurabayashi N, Hirota T, Fukada Y.** Ser-557-phosphorylated mCRY2 is degraded upon synergistic phosphorylation by glycogen synthase kinase-3β. *J Biol Chem*. 2005;280:31714–31721.
18. **Yin L, Wang J, Klein PS, Lazar MA.** Nuclear receptor Rev-erbα is a critical lithium-sensitive component of the circadian clock. *Science*. 2006;311:1002–1005.
19. **Spengler ML, Kuropatwinski KK, Schumer M, Antoch MP.** A serine cluster mediates BMAL1-dependent CLOCK phosphorylation and degradation. *Cell Cycle*. 2009;8:4138–4146.
20. **Sahar S, Zocchi L, Kinoshita C, Borrelli E, Sassone-Corsi P.** Regulation of BMAL1 protein stability and circadian function by GSK3β-mediated phosphorylation. *PLoS One*. 2010;5:e8561.
21. **Ko HW, Kim EY, Chiu J, Vanselow JT, Kramer A, Edery I.** A hierarchical phosphorylation cascade that regulates the timing of PERIOD nuclear entry reveals novel roles for proline-directed kinases and GSK-3β/SGG in circadian clocks. *J Neurosci*. 2010;30:12664–12675.
22. **Fu L, Pelicano H, Liu J, Huang P, Lee C.** The circadian gene Period2 plays an important role in tumor suppression and DNA damage response in vivo. *Cell*. 2002;111:41–50.
23. **Tups A, Anderson GM, Rizwan M, et al.** Both p110α and p110β isoforms of phosphatidylinositol 3-OH-kinase are required for insulin signalling in the hypothalamus. *J Neuroendocrinol*. 2010;22:534–542.
24. **Mercer JG, Lawrence CB, Beck B, Burlet A, Atkinson T, Barrett P.** Hypothalamic NPY and prepro-NPY mRNA in Djungarian hamsters: effects of food deprivation and photoperiod. *Am J Physiol*. 1995;269:R1099–R1106.
25. **Paxinos G, Franklin KBJ, Franklin KBJ.** *The Mouse Brain in Stereotaxic Coordinates*. 2nd ed. San Diego: Academic Press; 2001.
26. **Tups A, Ellis C, Moar KM, et al.** Photoperiodic regulation of leptin sensitivity in the Siberian hamster, *Phodopus sungorus*, is reflected in arcuate nucleus SOCS-3 (suppressor of cytokine signaling) gene expression. *Endocrinology*. 2004;145:1185–1193.
27. **Cerpa W, Godoy JA, Alfaro I, et al.** Wnt-7a modulates the synaptic vesicle cycle and synaptic transmission in hippocampal neurons. *J Biol Chem*. 2008;283:5918–5927.
28. **Lyuksyutova AI, Lu CC, Milanesio N, et al.** Anterior-posterior guidance of commissural axons by Wnt-frizzled signaling. *Science*. 2003;302:1984–1988.
29. **Hall AC, Lucas FR, Salinas PC.** Axonal remodeling and synaptic differentiation in the cerebellum is regulated by WNT-7a signaling. *Cell*. 2000;100:525–535.
30. **Hirabayashi Y, Itoh Y, Tabata H, et al.** The Wnt/β-catenin pathway directs neuronal differentiation of cortical neural precursor cells. *Development*. 2004;131:2791–2801.
31. **Stenman JM, Rajagopal J, Carroll TJ, Ishibashi M, McMahon J, McMahon AP.** Canonical Wnt signaling regulates organ-specific assembly and differentiation of CNS vasculature. *Science*. 2008;322:1247–1250.
32. **Lyons JP, Mueller UW, Ji H, et al.** Wnt-4 activates the canonical β-catenin-mediated Wnt pathway and binds Frizzled-6 CRD: functional implications of Wnt/β-catenin activity in kidney epithelial cells. *Exp Cell Res*. 2004;298:369–387.
33. **Jho EH, Zhang T, Domon C, Joo CK, Freund JN, Costantini F.** Wnt/β-catenin/Tcf signaling induces the transcription of Axin2, a negative regulator of the signaling pathway. *Mol Cell Biol*. 2002;22:1172–1183.
34. **Tetsu O, McCormick F.** β-Catenin regulates expression of cyclin D1 in colon carcinoma cells. *Nature*. 1999;398:422–426.
35. **Quelle DE, Ashmun RA, Shurtleff SA, et al.** Overexpression of mouse D-type cyclins accelerates G1 phase in rodent fibroblasts. *Genes Dev*. 1993;7:1559–1571.
36. **Lahti JM, Li H, Kidd VJ.** Elimination of cyclin D1 in vertebrate cells leads to an altered cell cycle phenotype, which is rescued by overexpression of murine cyclins D1, D2, or D3 but not by a mutant cyclin D1. *J Biol Chem*. 1997;272:10859–10869.
37. **Ding VW, Chen RH, McCormick F.** Differential regulation of glycogen synthase kinase 3β by insulin and Wnt signaling. *J Biol Chem*. 2000;275:32475–32481.
38. **Rattner A, Hsieh JC, Smallwood PM, et al.** A family of secreted proteins contains homology to the cysteine-rich ligand-binding domain of frizzled receptors. *Proc Natl Acad Sci USA*. 1997;94:2859–2863.
39. **Lescher B, Haenig B, Kispert A.** sFRP-2 is a target of the Wnt-4 signaling pathway in the developing metanephric kidney. *Dev Dyn*. 1998;213:440–451.
40. **Ladher RK, Church VL, Allen S, et al.** Cloning and expression of the Wnt antagonists Sfrp-2 and Frzb during chick development. *Dev Biol*. 2000;218:183–198.
41. **Yoshino K, Rubin JS, Higinbotham KG, et al.** Secreted Frizzled-related proteins can regulate metanephric development. *Mech Dev*. 2001;102:45–55.
42. **Krupnik VE, Sharp JD, Jiang C, et al.** Functional and structural diversity of the human Dickkopf gene family. *Gene*. 1999;238:301–313.
43. **Mao B, Wu W, Li Y, et al.** LDL-receptor-related protein 6 is a receptor for Dickkopf proteins. *Nature*. 2001;411:321–325.
44. **Tsuji T, Miyazaki M, Sakaguchi M, Inoue Y, Namba M.** A REIC gene shows down-regulation in human immortalized cells and human tumor-derived cell lines. *Biochem Biophys Res Commun*. 2000;268:20–24.
45. **Caricasole A, Ferraro T, Iacovelli L, et al.** Functional characterization of WNT7A signaling in PC12 cells: interaction with A FZD5 × LRP6 receptor complex and modulation by Dickkopf proteins. *J Biol Chem*. 2003;278:37024–37031.
46. **Hoang BH, Kubo T, Healey JH, et al.** Dickkopf 3 inhibits invasion and motility of Saos-2 osteosarcoma cells by modulating the Wnt-β-catenin pathway. *Cancer Res*. 2004;64:2734–2739.
47. **Abarzua F, Sakaguchi M, Takaishi M, et al.** Adenovirus-mediated overexpression of REIC/Dkk-3 selectively induces apoptosis in human prostate cancer cells through activation of c-Jun-NH2-kinase. *Cancer Res*. 2005;65:9617–9622.
48. **Ueno K, Hirata H, Majid S, et al.** Wnt antagonist DICKKOPF-3 (Dkk-3) induces apoptosis in human renal cell carcinoma. *Mol Carcinog*. 2011;50:449–457.
49. **Tan K, Knight ZA, Friedman JM.** Ablation of AgRP neurons impairs adaption to restricted feeding. *Mol Metab*. 2014;3:694–704.
50. **Guo B, Chatterjee S, Li L, et al.** The clock gene, brain and muscle Arnt-like 1, regulates adipogenesis via Wnt signaling pathway. *FASEB J*. 2012;26:3453–3463.
51. **Hatanaka F, Matsubara C, Myung J, et al.** Genome-wide profiling of the core clock protein BMAL1 targets reveals a strict relationship with metabolism. *Mol Cell Biol*. 2010;30:5636–5648.
52. **Mao J, Wang J, Liu B, et al.** Low-density lipoprotein receptor-related protein-5 binds to Axin and regulates the canonical Wnt signaling pathway. *Mol Cell*. 2001;7:801–809.
53. **Tolwinski NS, Wehrli M, Rives A, Erdeniz N, DiNardo S, Wieschaus E.** Wg/Wnt signal can be transmitted through arrow/

LRP5,6 and Axin independently of Zw3/Gsk3β activity. *Dev Cell*. 2003;4:407–418.
54. **Tamai K, Zeng X, Liu C, et al.** A mechanism for Wnt coreceptor activation. *Mol Cell*. 2004;13:149–156.
55. **Mercer JG, Moar KM, Ross AW, Hoggard N, Morgan PJ.** Photoperiod regulates arcuate nucleus POMC, AGRP, and leptin receptor mRNA in Siberian hamster hypothalamus. *Am J Physiol Regul Integr Comp Physiol*. 2000;278:R271–R281.
56. **Mercer JG, Hoggard N, Williams LM, Lawrence CB, Hannah LT, Trayhurn P.** Localization of leptin receptor mRNA and the long form splice variant (Ob-Rb) in mouse hypothalamus and adjacent brain regions by in situ hybridization. *FEBS Lett*. 1996;387:113–116.
57. **Hakansson ML, Brown H, Ghilardi N, Skoda RC, Meister B.** Leptin receptor immunoreactivity in chemically defined target neurons of the hypothalamus. *J Neurosci*. 1998;18:559–572.
58. **Shioda S, Funahashi H, Nakajo S, Yada T, Maruta O, Nakai Y.** Immunohistochemical localization of leptin receptor in the rat brain. *Neurosci Lett*. 1998;243:41–44.
59. **Boutros M, Paricio N, Strutt DI, Mlodzik M.** Dishevelled activates JNK and discriminates between JNK pathways in planar polarity and wingless signaling. *Cell*. 1998;94:109–118.
60. **Slusarski DC, Corces VG, Moon RT.** Interaction of Wnt and a Frizzled homologue triggers G-protein-linked phosphatidylinositol signalling. *Nature*. 1997;390:410–413.
61. **Tups A, Stohr S, Helwig M, et al.** Seasonal leptin resistance is associated with impaired signalling via JAK2-STAT3 but not ERK, possibly mediated by reduced hypothalamic GRB2 protein. *J Comp Physiol B*. 2012;182:553–567.
62. **Bjorbaek C, Elmquist JK, Frantz JD, Shoelson SE, Flier JS.** Identification of SOCS-3 as a potential mediator of central leptin resistance. *Mol Cell*. 1998;1:619–625.
63. **Tups A, Barrett P, Ross AW, Morgan PJ, Klingenspor M, Mercer JG.** The suppressor of cytokine signalling 3, SOCS3, may be one critical modulator of seasonal body weight changes in the Siberian hamster, *Phodopus sungorus*. *J Neuroendocrinol*. 2006;18:139–145.
64. **Ellis C, Moar KM, Logie TJ, Ross AW, Morgan PJ, Mercer JG.** Diurnal profiles of hypothalamic energy balance gene expression with photoperiod manipulation in the Siberian hamster, *Phodopus sungorus*. *Am J Physiol Regul Integr Comp Physiol*. 2008;294:R1148–R1153.
65. **Horton TH, Buxton OM, Losee-Olson S, Turek FW.** Twenty-four-hour profiles of serum leptin in Siberian and golden hamsters: photoperiodic and diurnal variations. *Horm Behav*. 2000;37:388–398.

4.3. Hypothalamic Leptin Sensitivity and Benefits of Time-Restricted Feeding are Dependent on the Time of Day

Hypothalamic Leptin Sensitivity and Benefits of Time-Restricted Feeding are Dependent on the Time of Day

Alisa Boucsein[1,2,5], Mohammed Z. Rizwan[1,2,3,4] and Alexander Tups[1,2,4,5]

[1]Centre for Neuroendocrinology and Brain Health Research Centre, University of Otago, Dunedin, New Zealand

[2]Department of Physiology and [3]Department of Anatomy, School of Biomedical Sciences, University of Otago, Dunedin, New Zealand

[4]Maurice Wilkins Centre for Molecular Biodiscovery, University of Auckland, Auckland, New Zealand

[5]Department of Animal Physiology, Faculty of Biology, Philipps University of Marburg, Marburg, Germany

Abbreviated Title: Daily rhythms of energy metabolism

Keywords: hypothalamus, daily rhythm, leptin, circadian clock, energy metabolism, time restricted feeding, periodic fasting

Funding: This work was supported by the German Ministry of Education and Research and by the German Research Foundation (to AT), the Royal Society of New Zealand (to AT and MR) and the British Society for Neuroendocrinology (to AB).

Disclosure Summary: The authors have nothing to disclose.

Proofs and correspondence to:

Dr. Alexander Tups

Department of Physiology

University of Otago

PO Box 913

Dunedin, New Zealand

E-mail: alexander.tups@otago.ac.nz

Abstract

Synchronisation between biological temporal clocks and metabolism is crucial for the survival of most species. It is unknown as to whether the circadian timing of time-restricted feeding (TRF), a diet strategy with apparent efficacy in promoting weight loss, is important for maximising its beneficial effects. Here, we examined whether leptin signalling, important for the control of energy metabolism, is regulated by a 24-hour rhythm in the hypothalamus of mice and whether diet-induced obesity (DIO) affects this rhythmicity. Furthermore, we investigated whether the beneficial effects of TRF depend on the timing of the feeding period. Therefore, we examined the ability of leptin to induce leptin signalling in the arcuate nucleus (ARC) of fasted mice throughout the 24-hour rhythm by immunohistochemistry. By measuring activated phospho-STAT3-immunoreactive cells after leptin injection, we found that leptin sensitivity was regulated in a 24-rhythmic manner in control mice. In these mice leptin sensitivity was highest in the early morning around Zeitgeber time (ZT) 0, after lights on, with sensitivity declining throughout the light phase and increasing throughout the dark phase. Surprisingly, leptin resistance in mice fed a high-fat diet (HFD) was only temporary and varied during the 24-hour rhythm, with deteriorated leptin signalling occurring only during the last half of the dark phase and the first half of the light phase compared with control animals. At all other time points, leptin sensitivity was similar to control mice. To investigate the physiological effect of this rhythmicity, we next injected leptin or vehicle in control and HFD mice either at ZT0 or ZT12 and compared their caloric intake. Surprisingly, control mice showed decreased caloric intake only when leptin injections occurred at ZT0, while HFD mice remained resistant to leptin at both ZT0 and ZT12, suggesting that control mice are sensitive to exogenous leptin on a behavioural level exclusively during the first part of the light phase. The daily rhythm of caloric intake between control and HFD mice was identical over the 24-hour rhythm, except for elevated caloric intake in HFD mice between ZT21-3 (3 hours of dark and 3 hours of light period, the period when HFD mice were leptin resistant on a molecular level) independent of locomotor activity. TRF (a limitation of HFD to 6 hours each day continuously for 3 weeks) regardless of circadian timing led to a marked reduction in food intake and body weight, but not in locomotor activity or energy expenditure compared with *ad libitum* fed mice. Specifically when TRF occurred from ZT21-3, it led to a disruption in the daily rhythm of locomotor activity and energy expenditure, as

well as to increased plasma insulin levels compared with other TRF periods. These data provide evidence that the circadian clock plays a crucial role in the control of leptin action and whole body energy homeostasis. Furthermore, TRF may be a promising weight loss strategy and its beneficial effects depend on circadian timing.

Introduction

Synchronisation between daily environmental alterations and biological processes is crucial for the survival of most living organisms. Endogenous circadian clocks adjust these processes to the most beneficial time of day in a broad range of species. In mammals, the master pacemaker resides in the suprachiasmatic nucleus (SCN) of the hypothalamus and is entrained by external cues (*Zeitgebers*), of which light is the primary entrainment signal. This central circadian clock controls local clocks in other brain regions as well as the periphery to orchestrate physiological and behavioural rhythms (1-3).

In recent years, numerous studies have highlighted a close correlation of the circadian clock system and the maintenance of energy metabolism (4-9). In mice, SCN lesions as well as various clock gene mutations result in metabolic disorders, including obesity, hyperlipidemia, hyperglycemia and an impairment in glucose tolerance and insulin sensitivity (8, 10-13). In humans, circadian misalignments such as shift work and social jet lag have been shown to be associated with symptoms of the metabolic syndrome, including an increased BMI, impaired glucose tolerance and insulin sensitivity and an increase in mean arterial blood pressure (14, 15).

The adipocyte-derived hormone leptin plays a crucial role in the control of metabolism by reducing food intake and increasing energy expenditure, ultimately leading to a decrease of body weight (BW) (16-18). Diet-induced obesity (DIO), the leading cause for obesity in humans and many rodent models, is accompanied by hyperleptinemia (19). Despite increased circulating leptin levels in most cases of obesity, leptin however fails to mediate its weight-reducing effects (20). Molecularly, this condition of leptin resistance is characterised by a disturbance in the ability of leptin to phosphorylate and activate the transcription factor signal transducer and activator of transcription 3 (STAT3) in the hypothalamus, specifically the arcuate nucleus (ARC), a brain region where large numbers of leptin receptors are expressed and that is crucial for maintaining energy homeostasis (21-24). Recent findings from our laboratory as well as from others show that chronic circadian disruptions cause impaired hypothalamic leptin sensitivity and elevated BW gain (25)(own unpublished observations), providing a possible explanation for the association between circadian misalignment and obesity as seen in humans (14).

While circadian misalignment led to reduced hypothalamic leptin signal transduction (25)(own unpublished observations), high-fat diet (HFD) feeding was also shown to disrupt behavioural and molecular circadian rhythms, including eating behaviour, locomotor activity and expression of circadian clock genes (26-28). Interestingly, feeding of this diet for only one week already causes a disruption of circadian rhythms in the liver, whereas neither the SCN nor other peripheral clocks were impaired (26), suggesting the presence and involvement of an SCN-independent oscillator in this process. Aside from light, food intake has been identified as another *Zeitgeber* for circadian rhythms and the existence of a food-entrainable oscillator involving AgRP/NPY neurons of the hypothalamus was proposed (29-31).

Kohsaka *et al*. showed that time-restricted feeding (TRF) of HFD during the inactive phase of mice results in increased BW, even though caloric intake is similar to mice that have access to HFD during their active phase (28). In line with this, access to HFD only during the active phase protects mice from metabolic disease compared with mice that have *ad libitum* access to HFD (32).

To our knowledge it is still unknown as to whether hypothalamic leptin sensitivity is regulated by a circadian rhythm and how HFD feeding affects leptin signal transduction throughout the day. In the current study we therefore examined the ability of leptin to induce activation of the transcription factor STAT3 (pSTAT3) at different times throughout the 24 hour day in mice that were either fed HFD or low-fat diet (LFD). After identifying that the response to leptin differs throughout the day and depends on the type of diet, we measured the behavioural response to leptin at times when the ability of leptin to activate pSTAT3 was either maximal or minimal. By restricting the timing of food access to 6 hours per day (time-restricted feeding; TRF) at 4 different intervals throughout the 24 hour day we assessed to what extent the beneficial effects of TRF during HFD feeding on BW gain and metabolic health are dependent on the time of day.

Materials and methods

Animals

Adult male C57BL/6J mice were obtained from the University of Otago Taieri Resource Unit and housed individually under controlled conditions of temperature (22 °C ± 1 °C) and light (12 h:12 h light:dark cycle; lights on at Zeitgeber time (ZT) 0, lights off at ZT12) with *ad libitum* access to water and food, unless stated otherwise. Mice aged 3 – 6 months were fed either LFD, with 10% energy from fat (kcal) or HFD with 60% energy from fat (D12450B and D12492, respectively; Research Diets). All experimental protocols were approved by the University of Otago Animal Ethics Committee.

Experiment 1: Daily rhythm in leptin sensitivity

We investigated whether intracellular leptin signalling is modulated by a 24-hour rhythm in the hypothalamus of lean mice and to what extent the consumption of HFD affects this daily rhythm. Therefore, we examined the phosphorylation of STAT3 (Tyr^{705}), as a marker of leptin pathway activation, every 3 h throughout the 24-h day by immunohistochemistry. Mice were fed either LFD or HFD (n = 64 each) for four weeks and were food deprived for 24 h before transcardial perfusion. Animals were subdivided into weight-matched groups and received a single intraperitoneal (i.p.) injection of either recombinant mouse leptin (1.25 mg/kg in PBS; R&D Systems) or vehicle (PBS) every three hours throughout a day, with animals being treated at either ZT0, ZT3, ZT6, ZT9, ZT12, ZT15, ZT18 or ZT21 (n = 4 per group). Thirty minutes after injections, transcardial perfusion was performed and brains were treated as described elsewhere (33). A second cohort of mice was generated as described above, decapitated and trunk blood was collected from these animals, in order to measure serum levels of the adiposity hormones leptin and insulin as well as fasting glucose levels. Animals killed during the dark phase were handled under dim red light.

Experiment 2: Leptin-mediated anorexigenic effects at ZT0 vs ZT12

To assess whether the ability of leptin to reduce food intake is affected by the circadian rhythm, we administered leptin at different times of the day. Mice were fed either LFD or HFD (n = 20 each) for four weeks and were food deprived for 24 h before the experiment. Half of each group was injected at ZT0, the other half at ZT12. Animals were weight-matched for each time point and received a single i.p. injection of either leptin (5.0 mg/kg in 20 mM TRIS-HCl) or vehicle (20 mM TRIS-HCl). Animals were re-fed with their respective diets directly after the injections and food intake was monitored 4 h and 24 h post-injection. For ethical reasons, the experiment was repeated after a recovery period of 3 days as described above and results are presented as pooled data points from both experiments. Animals treated with leptin or vehicle at ZT0 in the first experiment received the same treatment at ZT12 in the second experiment and *vice versa* (n = 6 – 10 per group).

Experiment 3: Effects of time-restricted feeding on energy metabolism

To investigate whether periodic reductions in caloric intake are able to reverse metabolic derangements induced by HFD, mice were put on a time-restricted feeding (TRF) schedule. Mice were fed either LFD (n = 8) or HFD (n = 40) *ad libitum* for 28 days, followed by time-restricted access to HFD for a further 24 days. To examine whether potential beneficial effects of TRF are dependent on the timing of food intake throughout the 24-hour rhythm, mice were granted access to food at different intervals (n = 8 per group). Two control groups had *ad libitum* access to LFD (LFDal) and HFD (HFDal), respectively, whereas four TRF groups had access to HFD for a 6 h continuous interval each day, followed by 18 h of food deprivation, until the end of the experiment. The TRF groups were granted access to food during the following intervals: from ZT3 – ZT9 (group TRF3–9), ZT9 – ZT15 (TRF9–15), ZT15 – ZT21 (TRF15–21) and ZT21 – ZT3 (TRF21–3), respectively (Supplementary figure 1). BW was monitored throughout the entire experiment. For mice fed LFDal and HFDal, these parameters were measured at ZT3, whereas for all TRF groups, they were measured before and after their respective feeding periods. On day 7 of TRF, mice were transferred to metabolic cages for 3 days, followed by a return to their normal housing conditions, as described above. At the end of the experiment, mice were fasted for 18 h;

each group was subdivided and received a single i.p. injection of either leptin (1.25 mg/kg in PBS) or vehicle (PBS) 30 minutes prior to transcardial perfusion (33). Both control groups were injected at ZT3, whereas TRF groups were injected at the start of their usual feeding periods (i.e. injection of TRF3–9 mice at ZT3, injection of TRF9–15 mice at ZT9 etc.). Blood was collected prior to perfusions from the inferior vena cava into heparinized tubes in order to measure plasma levels of leptin, insulin and fasting glucose levels. Animals killed during the dark phase were handled under dim red light.

Metabolic measurements

As part of experiment 3, we examined whether TRF causes changes in energy metabolism and behaviour. Therefore, mice were monitored in a multichannel respirometry system (3721 mouse cages, Promethion, Sable Systems International) for 3 days. The air flow in the cages was adjusted to 2000 ml/min and monitored constantly. The system allowed synchronised analysis of O_2 consumption (VO_2), CO_2 production (VCO_2), energy expenditure (EE), food intake, BW and locomotor activity. Running wheels were removed from the cages during the experiment. Data collected were analysed with the ExpeData data analysis software (Sable Systems Int.). To compare metabolic parameters specific for the different feeding intervals of the TRF groups, raw data for each day were binned into defined 6-hour intervals (ZT3 – ZT9, ZT9 – ZT15, ZT15 – ZT21, ZT21 – ZT3) using a customized automated analysis script (Sable Systems Int.). The average of each of the four 6-hour intervals over the 3 days of measurement was then calculated and compared between the six groups. Additionally, we compared these metabolic parameters over the 24-hour cycle, by combining the data from the 6-hour intervals.

Immunohistochemistry

Free-floating brain sections were pre-treated with 10% methanol, 1% NaOH and 1% H_2O_2 in H_2O for 20 min, 0.3% glycine for 10 min and 0.03% sodium dodecyl sulphate for 10 min. Next, sections were blocked for 1 h with 1% normal goat serum and 5% bovine serum albumin in Tris-buffered saline (TBS)-Triton X-100 (0.5%), followed by

overnight incubation at 4 °C using a rabbit anti-phospho-STAT3 (Tyr705) antibody (1:1000 in blocking solution; catalogue no. 9131, Cell Signaling Technology, Inc.). On the next day, sections were rinsed and incubated for 1 h with biotinylated goat anti-rabbit antibody (1:1000 in blocking solution), followed by 1 h in avidin-biotin complex solution (Vector Laboratories, Inc.). Then, the signal was developed by diaminobenzidine solution (Vector Laboratories, Inc.), giving a grey precipitate. Pictures were taken and immunoreactive (ir) cells in the ARC were counted in three sections per animal by two investigators who were blinded to the treatments.

Enzyme-linked immunosorbent assays and Glucose assays

To measure circulating levels of leptin, insulin and glucose, blood was collected from mice as described above. After collection, blood was immediately placed on ice and then centrifuged for 20 minutes at 4 °C and 13000 rpm. Serum and plasma were stored at -80 °C until assayed. Enzyme-linked immunosorbent assays and glucose assays (Mouse Leptin ELISA Kit, catalogue no. 90030; Ultra Sensitive Mouse Insulin ELISA Kit, catalogue no. 90080; Mouse Glucose Assay Kit, catalogue no. 81692; Crystal Chem Inc.) were performed in accordance with the kit instructions and all samples were assayed in duplicate. Because circulating leptin levels of mice fed HFD were expected to be above the sensitivity range of the leptin assay, serum and plasma samples of those mice were diluted 1:8 with the kits' own sample diluent to allow the analysis of circulating leptin levels.

Statistical analysis

The 24-hour rhythmicity of leptin sensitivity was analysed by three-way ANOVA with *diet* (LFD or HFD), *treatment* (vehicle or leptin) and *time* (ZT) as variables, followed by a Tukey's range post hoc test using SigmaStat statistical software (Systat Software, Inc.). To illustrate rhythmicity, a fourth order polynomial nonlinear regression curve was fitted with GraphPad Prism software (GraphPad Software, Inc.). Serum insulin levels were analysed by three-way ANOVA, as described above. All other data were analysed by either one- or two-way ANOVA, as appropriate, with *diet* and *time* as variables for serum leptin levels throughout the 24-hour cycle or *time of food access*

(LFDal, HFDal, TRF3–9, TRF9–15, TRF15–21 or TRF21–3) and *period of day* (ZT3 – ZT9, ZT9 – ZT15, ZT15 – ZT21, ZT21 – ZT3) for metabolic measurements or *treatment* for both leptin sensitivity and plasma insulin levels of TRF mice. BW trajectory of TRF mice was analysed by two-way repeated measures ANOVA. Where appropriate, this was followed by a Tukey's range post hoc test using GraphPad Prism software. Results are presented as the mean ± SEM and $P < 0.05$ was considered statistically significant.

Results

Experiment 1:

Daily rhythm in the regulation of hypothalamic leptin sensitivity in mice on LFD and HFD

To investigate how leptin sensitivity is regulated over the course of a day, we evaluated the number of pSTAT3 (Tyr705)-ir cells in the ARC of 24 h fasted mice on LFD or HFD every 3 h throughout the 24-hour cycle. We found a 24-hour rhythm of pSTAT3 activation in both LFD and HFD-fed mice, with significant interactions between diet and time ($P < 0.001$), diet and treatment ($P < 0.001$) and diet, treatment and time ($P = 0.005$; Fig. 1, A and B), but not treatment and time ($P = 0.692$). In both LFD- and HFD-fed mice, leptin compared with vehicle treatment led to an increase of pSTAT3-ir cells in the ARC at all examined time points (LFD, $P < 0.001$; HFD, $P \leq 0.012$).

In vehicle-treated mice on LFD the number of pSTAT3-ir cells differed dependent on the time of day ($P < 0.001$) The highest number was detected at the beginning of the light phase at ZT0 (34 ± 3 cells), followed by declining levels throughout the light and increasing levels throughout the dark phase. Relative to ZT0, the number of pSTAT3-ir cells was reduced by about 65% at ZT3 ($P = 0.016$), 84% at ZT6 ($P < 0.001$), 78% at ZT9 ($P = 0.001$) and 66% at ZT12 ($P = 0.008$). For vehicle-treated mice on HFD an overall rhythmicity in basal pSTAT3-ir levels was detected ($P = 0.027$), however contrary to mice fed LFD, the subsequent Tukey's multiple comparisons test did not reveal significant differences between any of the individual time points (48 ± 10 cells at ZT0).

Leptin-treated mice fed LFD revealed a significant difference in the number of pSTAT3-ir cells over the 24-hour rhythm ($P = 0.023$) with levels peaking at the beginning of the light phase at ZT0 (198 ± 16 cells). Levels declined throughout the light phase and were reduced by about 26% at ZT9 compared with ZT0 ($P = 0.015$). This trough at the end of the light phase was followed by increasing levels of pSTAT3-ir cells throughout the dark phase. Leptin treatment in mice fed HFD revealed a 24-hour rhythm in the activation of STAT3 ($P < 0.001$), but this rhythm was inverted compared to mice fed LFD, revealing lowest levels at ZT0 (110 ± 15 cells). Levels then increased during the light phase, reaching peak values half-way throughout the dark

phase at ZT18 and subsequently decreased during the second half of the dark phase. Activation of STAT3 was elevated by about 46% at ZT9 ($P = 0.049$), 49% at ZT12 ($P = 0.032$), 70% at ZT15 ($P < 0.001$) and 75% at ZT18 ($P = 0.001$).

We found that the number of pSTAT3-ir cells, when compared between mice fed LFD vs HFD (in both vehicle- and leptin-treated groups), was not consistently different throughout the whole 24-hour cycle, but differences were dependent on the time of day. Vehicle-treated mice fed HFD compared with LFD showed an increased number of pSTAT3-ir cells at ZT6 ($P = 0.023$), ZT9 ($P = 0.024$), ZT12 ($P = 0.003$), ZT15 ($P < 0.001$) and ZT18 ($P < 0.001$), whereas at ZT0, ZT3 and ZT21 no differences were revealed. Leptin treatment, by contrast, revealed reduced levels in mice fed HFD compared with LFD during the first half of the light phase at ZT0 ($P < 0.001$), ZT3 ($P < 0.001$) and ZT6 ($P < 0.001$) and towards the end of the dark phase at ZT21($P = 0.018$), whereas levels remained similar between LFD- and HFD-fed mice from ZT9 to ZT18.

Daily rhythm of serum leptin levels in fasted mice on LFD and HFD

We next investigated to what extent endogenous leptin levels vary throughout the 24-hour rhythm in 24 h fasted mice on LFD and HFD. To reflect endogenous leptin levels only measurements of vehicle-injected mice were included whereas analysis of leptin-injected mice was excluded from the study due to excessively high leptin concentrations. We found significant effects of diet and time ($P < 0.001$), as well as an interaction between diet and time on levels of circulating leptin ($P < 0.001$). Mice on LFD revealed no significant changes in serum leptin concentrations over the course of the day, with concentrations ranging between a maximum of 6.08 ± 0.59 ng/mL at ZT9 and a minimum of 3.37 ± 1.48 ng/mL at ZT12 ($P \geq 0.997$; Fig. 2, A). Mice on HFD on the other hand showed a daily rhythm of serum leptin levels with elevated levels during the first half of the light phase, reaching a peak at ZT6 with a concentration of 48.08 ± 2.60 ng/mL, followed by reduced levels during the second half of the light phase and continuously low levels during the dark phase. Leptin levels reached a minimum of 13.68 ± 2.57 ng/mL at ZT18. Leptin levels were elevated at ZT3 compared with ZT0, ZT12, ZT15, ZT18 and ZT21 ($P < 0.05$, each), at ZT6 compared with ZT0, ZT9, ZT12, ZT15, ZT18 and ZT21 ($P < 0.05$, each) and at ZT9 compared with ZT0, ZT12, ZT18

and ZT21 ($P < 0.01$, each). HFD feeding led to an overall increase of serum leptin levels across all examined time points compared with LFD feeding (LFD = 4.80 ± 0.94 ng/mL on average; HFD = 26.65 ± 1.05 ng/mL on average; $P < 0.05$ for each ZT).

Effects of diet, leptin injections and time on serum insulin levels in fasted mice

We measured serum insulin levels over the 24-hour time course in fasted mice on LFD and HFD that were challenged with either vehicle or leptin injections. The 24-hour profile of circulating insulin levels revealed a significant effect of diet ($P < 0.001$; Fig. 2, B), whereas neither leptin treatment nor time of day had a significant effect on insulin concentrations ($P = 0.229$ and $P = 0.541$, respectively). Mice on HFD as compared with LFD showed an overall increase in serum insulin concentrations (LFD = 0.49 ± 0.03 ng/mL on average; HFD = 0.69 ± 0.03 ng/mL on average) that was independent of both the treatment and the time of day.

Effects of diet, leptin injections and time on fasting serum glucose levels in mice

Fasting glucose concentrations were significantly affected by of both diet and time of day ($P = 0.003$ and $P < 0.001$, respectively), whereas leptin injections did not alter serum glucose levels ($P = 0.845$). The effect of different times throughout the day was dependent on which diet was present (ZT x Diet, $P = 0.010$). In LFD-fed animals, no significant changes in glucose levels over the 24-hour course were detected, with concentrations ranging from a minimum of 108.79 ± 16.23 mg/dL at ZT0 to a maximum of 152.18 ± 6.02 mg/dL at ZT21 in vehicle-treated mice and between 143.74 ± 19.20 mg/dL at ZT 3 and 102.25 ± 8.90 mg/dL at ZT6 in leptin-treated mice (Fig. 2, C). HFD-fed mice on the other hand revealed a time-dependent rhythm in glucose levels with continuously low levels during the light phase, with vehicle-treated mice reaching a nadir at ZT9 (concentrations of 103.37 ± 2.58 mg/dL) and leptin-treated mice revealing lowest levels at ZT6 with 108.67 ± 4.78 mg/dL. This was followed by increasing levels during the dark phase, with both vehicle- and leptin-treated mice reaching a peak at ZT21 with concentrations of 166.25 ± 15.59 mg/dL and 192.86 ± 11.77 mg/dL, respectively. Glucose levels in mice on HFD at ZT0, ZT3, ZT6 and ZT9 were reduced compared with ZT21, as well as at ZT6 and ZT9 compared with both ZT15 and ZT18 ($P < 0.05$, for each time comparison). HFD feeding as compared

with LFD caused an increase in glucose concentrations at ZT15, ZT18 and ZT21 ($P = 0.017$, $P = 0.006$ and $P = 0.004$, respectively), whereas at all other times glucose concentrations remained similar between the two diets.

Experiment 2:

Leptin's anorexigenic effects are restricted to the relative leptin sensitive phase in mice fed LFD

After we had established that leptin sensitivity on a molecular level in the ARC is altered depending on the time of day, we next investigated whether leptin responsiveness at a behavioural level is also rhythmically regulated. Therefore, caloric intake was measured following leptin injections at times when DIO mice were leptin resistant (ZT0) and sensitive (ZT12) compared with mice fed LFD. Two-way ANOVA revealed a significant effect of leptin treatment ($P < 0.001$), which was dependent on the time of the injections (interaction, $P = 0.024$). For further analysis, we next compared the accumulated caloric intake over 4 h (Fig. 1, C) and 24 h (Fig. 1, D) after injections between vehicle-treated mice and their respective leptin-treated counterparts. Therefore, we defined the average caloric intake of vehicle-treated mice as baseline and compared it with the deviant caloric intake of leptin-treated mice that were fed the same diet and injected at the same time point. We found that in mice fed LFD, leptin administration at ZT0 led to a decrease in accumulated caloric intake over 4 h (Δ 1.97 ± 0.45 kcal, $P = 0.013$) as well as 24 h (Δ 2.07 ± 0.60 kcal; $P = 0.024$) after injections compared with vehicle-treated mice. In contrast, mice fed HFD and injected with leptin at ZT0 showed no differences in caloric intake after 4 h (Δ 0.77 ± 0.40 kcal) and 24 h (Δ 0.26 ± 0.86 kcal) compared with their vehicle-treated counterparts. Leptin injections at ZT12 did not lead to a decrease in caloric intake in mice fed either LFD (4 h: Δ 0.75 ± 0.22 kcal; 24 h: Δ 0.65 ± 0.55 kcal) or HFD (4 h: Δ 0.71 ± 0.63 kcal; 24 h: Δ 0.45 ± 1.00 kcal).

Experiment 3:

Body weight trajectory of TRF mice

We established that HFD-induced leptin resistance on a molecular level is restricted to the period between ZT21 – ZT6 whereas mice fed HFD revealed an identical absolute increase in the number of pSTAT3-ir cells compared with mice fed LFD, suggesting molecular leptin sensitivity between ZT9 – ZT18. To investigate the potential impact of food restriction to these time periods, we restricted access to HFD to 6-hour intervals with TRF9–15 mice receiving HFD exclusively during their leptin sensitive interval and TRF21–3 mice exclusively during their leptin resistant interval. The BW of mice from experiment 3 was monitored every second day for the first 3 weeks while all mice had *ad libitum* access to their respective diets and then daily with the onset of TRF throughout the remainder of the experiment. By day 9 of exposure to their respective diets, mice fed HFD had a significantly increased BW compared with mice fed LFD (Fig. 3). This BW increase in HFDal mice persisted until the end of the experiment ($P \leq 0.023$). After 28 days of *ad libitum* feeding, mice on HFD were transferred to the TRF regimen. While mice fed HFDal were still on a positive BW trajectory until the end of the experiment, TRF mice decreased their BW shortly after the start of TRF, but retained a higher BW compared with mice fed LFDal until all animals were transferred into the metabolic cages on day 35 of the experiment ($P \leq 0.027$). By day 40, all TRF mice had reduced their BW to levels similar to LFDal mice. TRF3–9, TRF9–15 and TRF21–3 mice had a significantly lower BW after 16 days of restricted food access and TRF15–21 mice after 18 days compared with HFDal mice ($P \leq 0.034$). There was no difference in BW between the four TRF groups throughout the whole experiment. At the end of the experiment, BW was 30.8 ± 0.7 g for mice on LFDal, 38.4 ± 1.3 g for mice on HFDal, 32.5 ± 0.8 g for TRF3–9 mice, 32.9 ± 0.9 g for TRF9–15 mice, 33.6 ± 0.4 g for TRF15–21 mice and 33.4 ± 0.8 g for TRF21–3 mice.

Mice on HFD were susceptible to caloric overconsumption exclusively during their relative leptin insensitive phase from ZT21 – ZT3

Using metabolic cages, we assessed the average caloric intake during the four TRF intervals throughout the 24-hour time course. TRF mice with limited access to food

consumed their food allocations exclusively during their respective food access intervals (Fig. 4, A). Comparing caloric intake for each of the defined intervals throughout the day amongst mice fed LFDal and HFDal, we found a distinct daily rhythm that was present in mice fed LFD, but less pronounced in mice fed HFD (Fig. 4, A). With a caloric intake of 0.92 ± 0.20 kcal, mice fed LFD revealed the lowest caloric intake during the light phase from ZT3 – ZT9, coinciding with their inactive phase. Compared with the preceding interval, their caloric intake increased significantly during ZT9 – ZT15 (3.49 ± 0.33 kcal; $P < 0.001$) and remained high during the dark phase between ZT15 – ZT21 (3.85 ± 0.38 kcal; Vs ZT3 – ZT9, $P < 0.001$). This was followed by a significant reduction in caloric intake during ZT21 – ZT3 (2.24 ± 0.31 kcal; $P = 0.025$, vs ZT15 – ZT21), with a return to levels that were statistically similar to ZT3 – ZT9. Caloric intake in mice fed HFD during ZT3 – ZT9 (1.54 ± 0.35 kcal), ZT9 – ZT15 (3.91 ± 0.48 kcal) and ZT15 – ZT21 (4.69 ± 0.42 kcal) was not significantly different from caloric intake in LFD during their respective intervals. Surprisingly, HFD feeding led to the consumption of more calories compared with LFD exclusively during the relative leptin insensitive interval of mice on HFD from ZT21 – ZT3 (4.04 ± 0.40 kcal; $P = 0.011$). While in mice on LFD food intake dropped distinctly after the dark period, it remained elevated in mice on HFD (ZT15 – ZT21 vs ZT21 – ZT3; LFD, $P = 0.025$; HFD, $P = 0.912$).

Additionally, we evaluated the cumulative caloric intake over 24 hours for each group (Suppl Fig. 2, A). The overall daily caloric intake was 10.50 ± 0.61 kcal for mice that received LFDal, 14.17 ± 0.47 kcal for HFDal, 5.94 ± 0.72 kcal for TRF3–9, 7.09 ± 0.71 kcal for TRF9–15, 7.70 ± 0.76 kcal for TRF15–21 and 8.07 ± 0.69 kcal for TRF21–3. One-way ANOVA revealed that mice on HFDal consumed significantly more calories than any other group (vs. LFDal, $P = 0.003$; vs. all other groups, $P < 0.001$). The daily caloric intake of mice from the TRF3–9 and TRF9–15 groups was significantly lower compared with mice on LFDal ($P < 0.001$ and $P = 0.013$, respectively), whereas it was similar to the TRF15–21 and TRF21–3 groups, which were also not different to mice on LFDal.

TRF21–3 mice lose their daily rhythm of locomotor activity

We next investigated whether the rhythm that we observed in the feeding pattern is associated with alterations in locomotor activity. Two-way ANOVA revealed significant effects of both time of food access and the period of day, as well as a significant interaction between both parameters ($P < 0.001$, each; Fig. 4, B). Locomotor activity during the intervals ZT3 – ZT9, ZT9 – ZT15, ZT15 – ZT21 and ZT21 – ZT3 was 16.65 ± 1.97 m, 45.32 ± 3.50 m, 83.00 ± 8.01 m, 47.91 ± 4.25 m in LFDal mice, 16.54 ± 1.53 m, 34.04 ± 2.76 m, 52.16 ± 3.39 m, 34.59 ± 2.45 m in HFDal mice, 15.83 ± 1.63 m, 56.46 ± 5.30 m, 63.38 ± 4.83 m, 35.98 ± 2.93 m in TRF3–9, 18.05 ± 1.96 m, 51.34 ± 3.65 m, 70.82 ± 5.96 m, 43.28 ± 5.69 m in TRF9–15, 15.43 ± 1.67 m, 47.00 ± 3.51 m, 63.11 ± 5.09 m, 51.30 ± 4.16 m in TRF15–21 and 19.28 ± 1.84 m, 52.80 ± 2.98 m, 48.79 ± 3.14 m, 48.70 ± 3.69 m in TRF21–3 mice, respectively. Mice fed LFDal as well as HFDal demonstrated a circadian rhythm of locomotor activity, with lowest activity levels during their inactive phase from ZT3 – ZT9 and highest activity levels during their active phase from ZT15 – ZT21 (LFDal: $P < 0.001$; HFDal: $P < 0.001$). During ZT9 – ZT15 and ZT21 – ZT3, activity levels were halfway between those extremes in both groups. Locomotion in mice fed HFDal during ZT3 – ZT9, ZT9 – ZT15 and ZT21 – ZT3 was similar compared with mice fed LFDal during their respective periods. Notably, mice fed HFDal showed decreased locomotion relative to LFDal exclusively during ZT15 – ZT21 ($P < 0.001$). TRF9–15 mice, which received HFD only during their relative leptin sensitive phase, showed the same circadian rhythm of locomotor activity compared with both LFDal and HFDal groups, with increased levels of activity solely during ZT9 – ZT15 compared with the respective interval in mice on HFDal ($P < 0.001$). In contrast, TRF21–3 mice, which received HFD exclusively during their relative leptin insensitive phase, showed a loss of the rhythmic pattern in locomotion with similar activity levels during ZT9 – ZT15, ZT15 – ZT21 and ZT21 – ZT3. Both TRF3–9 and TRF15–21 mice still revealed rhythmic variations in locomotion, even though less pronounced compared with LFDal, HFDal and TRF9–15 mice (Fig. 4, B).

Summated over 24 hours, locomotion was 194.94 ± 18.30 m in LFDal, 137.09 ± 4.70 m in HFDal, 176.66 ± 13.86 m in TRF3–9, 179.57 ± 21.02 m in TRF9–15, 177.09 ± 12.17 m in TRF15–21 and 169.58 ± 7.45 m in TRF21–3 mice (Suppl. Figure 2, B). One-way ANOVA revealed no significant differences between any of the groups, although

HFDal caused a trend towards a significant reduction of locomotion compared with LFDal feeding ($P = 0.060$).

TRF21–3 mice lose their daily rhythm of VO_2

Next, we investigated whether the alterations in feeding and locomotor activity patterns are correlated with differences in average metabolic rate (VO_2), defined by ml of oxygen consumption per minute. VO_2 during the intervals ZT3 – ZT9, ZT9 – ZT15, ZT15 – ZT21 and ZT21 – ZT3 was 1.07 ± 0.03 ml O_2/min, 1.30 ± 0.02 ml O_2/min, 1.62 ± 0.04 ml O_2/min, 1.30 ± 0.05 ml O_2/min in LFDal mice, 1.24 ± 0.03 ml O_2/min, 1.42 ± 0.03 ml O_2/min, 1.55 ± 0.03 ml O_2/min, 1.42 ± 0.02 ml O_2/min in HFDal, 1.20 ± 0.02 ml O_2/min, 1.39 ± 0.03 ml O_2/min, 1.37 ± 0.02 ml O_2/min, 1.26 ± 0.02 ml O_2/min in TRF3–9, 1.00 ± 0.02 ml O_2/min, 1.37 ± 0.02 ml O_2/min, 1.41 ± 0.03 ml O_2/min, 1.17 ± 0.03 ml O_2/min in TRF9–15, 1.20 ± 0.02 ml O_2/min, 1.32 ± 0.03 ml O_2/min, 1.56 ± 0.02 ml O_2/min, 1.42 ± 0.03 ml O_2/min in TRF15–21 and 1.17 ± 0.03 ml O_2/min, 1.29 ± 0.03 ml O_2/min, 1.25 ± 0.05 ml O_2/min, 1.41 ± 0.05 ml O_2/min in TRF21–3 mice, respectively. Two-way ANOVA revealed significant effects of both time of food access and the period of day, as well as a significant interaction between both factors ($P < 0.001$, each; Suppl. Fig. 3, A). Mice on LFDal as well as HFDal showed a prominent circadian rhythm of VO_2 with lowest rates during ZT3 – ZT9 and highest rates during ZT15 – ZT21 (LFDal: $P < 0.001$; HFDal: $P < 0.001$), while VO_2 was situated between those extremes during ZT9 – ZT15 and ZT21 – ZT3. Interestingly, VO_2 was increased during ZT3 – ZT9 and ZT9 – ZT15 in HFDal- compared with LFDal-fed mice ($P < 0.001$ and $P < 0.001$), but similar during ZT15 – ZT21 and ZT21 – ZT3. The circadian rhythm of VO_2 found in both *ad libitum* fed groups was altered in all TRF groups. Notably, VO_2 appeared to be elevated during the respective intervals when TRF mice had access to food. Taking this food intake-related increase in VO_2 into account, TRF9–15 mice, which had access to food during their leptin sensitive phase, showed a circadian rhythm that is most similar to the LFDal and HFDal groups with lowest VO_2 during ZT3 – ZT9 and highest rates during ZT15 – ZT21 ($P < 0.001$). In contrast, TRF21–3 mice, which had access to food during their relative leptin insensitive phase, showed no differences in VO_2 between ZT3 – ZT9, ZT9 – ZT15 and

ZT15 – ZT21. Here, VO_2 was highest during ZT21 – ZT3, when they had access to food (Suppl. Fig. 3, A).

We corrected for the influence of BW by calculating VO_2 per g BW. VO_2 during the intervals ZT3 – ZT9, ZT9 – ZT15, ZT15 – ZT21 and ZT21 – ZT3 was 0.036 ± 0.001 ml O_2/g/min, 0.044 ± 0.001 ml O_2/g/min, 0.053 ± 0.001 ml O_2/g/min, 0.043 ± 0.001 ml O_2/g/min in LFDal mice, 0.034 ± 0.001 ml O_2/g/min, 0.039 ± 0.001 ml O_2/g/min, 0.043 ± 0.001 ml O_2/g/min, 0.039 ± 0.001 ml O_2/g/min in HFDal, 0.035 ± 0.001 ml O_2/g/min, 0.040 ± 0.001 ml O_2/g/min, 0.040 ± 0.001 ml O_2/g/min, 0.037 ± 0.001 ml O_2/g/min in TRF3–9, 0.029 ± 0.001 ml O_2/g/min, 0.039 ± 0.001 ml O_2/g/min, 0.040 ± 0.001 ml O_2/g/min, 0.034 ± 0.001 ml O_2/g/min in TRF9–15, 0.035 ± 0.001 ml O_2/g/min, 0.038 ± 0.001 ml O_2/g/min, 0.045 ± 0.001 ml O_2/g/min, 0.041 ± 0.001 ml O_2/g/min in TRF15–21 and 0.034 ± 0.001 ml O_2/g/min, 0.039 ± 0.001 ml O_2/g/min, 0.037 ± 0.001 ml O_2/g/min, 0.042 ± 0.001 ml O_2/g/min in TRF21–3 mice, respectively. Two-way ANOVA revealed significant effects of both time of food access and the period of day, as well as a significant interaction between both factors ($P < 0.001$, each; Fig. 4, C). As described for the non-BW-corrected values, mice on LFDal as well as HFDal showed a prominent circadian rhythm of VO_2 with lowest rates during ZT3 – ZT9 and highest rates during ZT15 – ZT21 (LFDal: $P < 0.001$; HFDal: $P < 0.001$), while VO_2 was situated between those extremes during ZT9 – ZT15 and ZT21 – ZT3. In the *ad libitum*-fed groups, mice fed LFD had increased VO_2 during ZT9 – ZT15 and ZT15 – ZT21 compared with mice fed HFD ($P = 0.007$ and $P < 0.001$, respectively). The here observed rhythm was altered in all TRF groups. TRF9–15 mice, which had access to food during their leptin sensitive phase, as well as TRF15–21 showed a slightly dampened rhythm relative to LFDal and HFDal groups, whereas TRF3–9 as well as TRF21–3 mice, which had access to food during their relative leptin insensitive phase, showed no differences during the three intervals from ZT9–ZT3 (Fig. 4, C).

Averaged over 24 hours, VO_2 was 1.32 ± 0.04 ml O_2/min in LFDal, 1.41 ± 0.04 ml O_2/min in HFDal, 1.31 ± 0.03 ml O_2/min in TRF3–9, 1.24 ± 0.03 ml O_2/min in TRF9–15, 1.37 ± 0.01 ml O_2/min in TRF15–21 and 1.28 ± 0.06 ml O_2/min in TRF21–3 mice (Suppl. Figure 2, C). One-way ANOVA revealed a significantly reduced VO_2 in TRF9–15 compared with HFDal-fed mice ($P = 0.034$), whereas there were no differences amongst the other groups.

However, the BW-corrected VO_2 over the course of 24 hours revealed a reduction in VO_2 in TRF9–15 of about 20% per day and in TRF21–3 of about 14% per day relative to LFDal mice (P = 0.003, P = 0.044, respectively). BW-corrected daily VO_2 was 0.044 ± 0.001 ml O_2/g/min in LFDal mice, 0.039 ± 0.001 ml O_2/g/min in HFDal, 0.038 ± 0.001 ml O_2/g/min in TRF3–9, 0.036 ± 0.002 ml O_2/g/min in TRF9–15, 0.040 ± 0.001 ml O_2/g/min in TRF15–21 and 0.038 ± 0.02 ml O_2/g/min in TRF21–3 (Suppl. Fig. 4, A).

The daily rhythm of energy expenditure is disrupted in TRF21–3 mice

Energy expenditure (EE) during the intervals ZT3 – ZT9, ZT9 – ZT15, ZT15 – ZT21 and ZT21 – ZT3 was 1.93 ± 0.06 kcal, 2.40 ± 0.03 kcal, 3.03 ± 0.07 kcal, 2.39 ± 0.10 kcal in LFDal mice, 2.21 ± 0.05 kcal, 2.53 ± 0.05 kcal, 2.77 ± 0.05 kcal, 2.51 ± 0.04 kcal in HFDal, 2.14 ± 0.03 kcal, 2.47 ± 0.05 kcal, 2.41 ± 0.04 kcal, 2.23 ± 0.04 kcal in TRF3–9, 1.74 ± 0.04 kcal, 2.43 ± 0.03 kcal, 2.49 ± 0.05 kcal, 2.03 ± 0.06 kcal in TRF9–15, 2.11 ± 0.03 kcal, 2.33 ± 0.05 kcal, 2.78 ± 0.04 kcal, 2.52 ± 0.05 kcal in TRF15–21 and 2.05 ± 0.07 kcal, 2.28 ± 0.05 kcal, 2.18 ± 0.09 kcal, 2.50 ± 0.09 kcal in TRF21–3 mice, respectively. Two-way ANOVA revealed significant effects of both time of food access and the period of day, as well as a significant interaction between both factors (P < 0.001, each; Suppl. Fig. 3, B). Similar to VO_2 as described above, EE was of a rhythmic pattern in mice on LFDal as well as HFDal with lowest EE during their inactive phase from ZT3 – ZT9 and highest EE during their active phase during ZT15 – ZT21, while EE was situated between those extremes during ZT9 – ZT15 and ZT21 – ZT3. In mice on HFDal EE was increased during ZT3 – ZT9 compared with mice on LFDal (P = 0.004), whereas it was similar between both groups during the other intervals. In all TRF groups, the rhythmic pattern of EE was identical to the one described for VO_2, with TRF9–15 showing a rhythm that was most similar to that observed in both *ad libitum* fed groups and TRF21–3 mice showing the least pronounced rhythm once the food intake-related increase of EE was taken into account (Suppl. Fig. 3, B).

BW-corrected EE during the intervals ZT3 – ZT9, ZT9 – ZT15, ZT15 – ZT21 and ZT21 – ZT3 was 0.065 ± 0.002 kcal/g, 0.080 ± 0.002 kcal/g, 0.103 ± 0.003 kcal/g, 0.080 ± 0.002 kcal/g in LFDal mice, 0.061 ± 0.001 kcal/g, 0.070 ± 0.001 kcal/g, 0.080

± 0.003 kcal/g, 0.070 ± 0.001 kcal/g in HFDal, 0.063 ± 0.001 kcal/g, 0.071 ± 0.001 kcal/g, 0.072 ± 0.002 kcal/g, 0.066 ± 0.002 kcal/g in TRF3–9, 0.050 ± 0.001 kcal/g, 0.070 ± 0.002 kcal/g, 0.074 ± 0.003 kcal/g, 0.059 ± 0.002 kcal/g in TRF9–15, 0.061 ± 0.001 kcal/g, 0.067 ± 0.001 kcal/g, 0.081 ± 0.002 kcal/g, 0.072 ± 0.003 kcal/g in TRF15–21 and 0.060 ± 0.002 kcal/g, 0.068 ± 0.002 kcal/g, 0.072 ± 0.004 kcal/g, 0.074 ± 0.003 kcal/g in TRF21–3 mice, respectively. Two-way ANOVA revealed significant effects of both time of food access and the period of day, as well as a significant interaction between both factors ($P < 0.001$, each; Fig. 4, D). In the *ad libitum*-fed groups, mice fed LFD had increased BW-corrected EE during ZT9 – ZT15 ($P < 0.001$), ZT15 – ZT21 ($P < 0.001$) and ZT21 – ZT3 ($P = 0.037$) compared with HFDal. As described for the non-BW-corrected values, mice on LFDal as well as HFDal showed a rhythm in EE with lowest rates during ZT3 – ZT9 and highest rates during ZT15 – ZT21 (LFDal: $P < 0.001$; HFDal: $P < 0.001$). This rhythm was altered in all TRF groups. TRF9–15 mice, which had access to food during their leptin sensitive phase, as well as TRF15–21 showed a slight dampening in their 24-hour rhythm relative to LFDal and HFDal groups, whereas TRF21–3 mice, which had access to food during their relative leptin insensitive phase, showed no differences during the three intervals from ZT9–ZT3 (Fig. 4, C).

Summed over 24 hours, total energy expenditure was 9.72 ± 0.31 kcal in LFDal, 10.07 ± 0.26 kcal in HFDal, 9.31 ± 0.23 kcal in TRF3–9, 8.71 ± 0.23 kcal in TRF9–15, 9.72 ± 0.11 kcal in TRF15–21 and 9.03 ± 0.44 kcal in TRF21–3 mice (Suppl. Fig. 2, D). As shown with VO_2, there was a statistically significant reduction of EE in TRF9–15 compared with mice on HFDal ($P = 0.035$), but none of the other groups revealed significant differences between each other.

The BW-corrected energy expenditure summed over 24 hours was 0.33 ± 0.01 kcal/g in LFDal, 0.28 ± 0.01 kcal/g in HFDal, 0.27 ± 0.01 kcal/g in TRF3–9, 0.25 ± 0.01 kcal/g in TRF9–15, 0.28 ± 0.01 kcal/g in TRF15–21 and 0.28 ± 0.01 kcal/g in TRF21–3 mice (Suppl. Fig. 4, B). Thus, LFDal mice had the highest energy expenditure per day compared with all other groups ($P < 0.019$ for all groups), but there were no significant differences amongst the other groups.

TRF decreases plasma leptin levels in mice fed HFD

We next investigated whether time-restricted access to HFD alters circulating levels of leptin in the blood plasma of fasted mice that were treated with vehicle. As explained above, samples from animals that were injected with leptin were not included in this experiment due to the extensively high levels of circulating leptin. One-way ANOVA revealed a decrease of plasma leptin concentrations in all TRF groups compared with HFDal feeding, approximating levels found in mice fed LFDal (HFDal vs. LFDal, TRF3–9, TRF9–15, TRF15–21 and TRF21–3; $P < 0.001$, $P = 0.005$, $P = 0.019$, $P = 0.032$ and $P = 0.003$, respectively; Fig. 5, A). Mice fed HFDal showed the highest leptin levels of 49.87 ± 9.18 ng/mL, whereas mice fed LFDal revealed the lowest levels of 4.24 ± 0.19 ng/mL. TRF mice showed concentrations of 13.24 ± 1.31 ng/mL for TRF3–9, 21.43 ± 5.52 ng/mL for TRF9–15, 23.44 ± 6.09 ng/mL for TRF15–21 and 13.68 ± 1.84 ng/mL for TRF21–3 mice.

Access to HFD from ZT21 – ZT3 increases plasma insulin levels

We examined plasma insulin levels in fasted mice from experiment 3 that were challenged with either vehicle or leptin injections. Two-way ANOVA revealed a significant effect of time of food access ($P = 0.036$), but neither an effect of treatment nor an interaction between the two factors. On average, mice on LFDal had plasma insulin levels of 0.21 ± 0.01 ng/mL, mice on HFDal of 0.41 ± 0.09 ng/mL, TRF3–9 of 0.28 ± 0.05 ng/mL, TRF9–15 of 0.41 ± 0.07 ng/mL, TRF15–21 of 0.32 ± 0.04 ng/mL and TRF21–3 of 0.63 ± 0.14 ng/mL (Fig. 5, B). Plasma insulin concentrations of TRF21–3 mice were significantly increased compared with concentrations of mice fed LFDal ($P = 0.021$), whereas none of the other TRF groups revealed a difference in insulin concentrations compared with LFDal and HFDal groups.

Discussion

We discovered a 24-h rhythm in the number of basal pSTAT3-ir cells in the ARC of vehicle-treated mice on LFD that were fasted for 24 hours, indicating rhythmic regulation of leptin sensitivity. With 34 ± 3 pSTAT3-ir cells the level of basal pathway activity was highest at the beginning of the light phase at ZT0 and lowest at ZT6 with as little as 5 ± 1 pSTAT3-ir cells. The very low number of pSTAT3-ir cells around the middle of the light phase suggests a limited physiological role of leptin signalling during this time, whereas leptin pathway activation was significantly higher during the dark phase. In mice on HFD, on the other hand, this 24-h rhythm was absent, with consistent numbers of basal pSTAT3-ir cells throughout the 24-h cycle. Interestingly, HFD vs LFD feeding led to an increase in the number of pSTAT3-ir cells from ZT6 – ZT18, whereas there was no difference from ZT21 – ZT3. To our knowledge this is the first description of HFD-induced activation of pSTAT3 during certain times of the day as well as the first description of rhythmic variations in basal pSTAT3 in wild-type mice fed LFD that suggest 24-h-rhythmic alterations in leptin signal transduction. Other studies so far reported similar numbers of pSTAT3-ir cells in the ARC between wild-type mice fed LFD and HFD (23, 34). This discrepancy might be explained by the time of sampling which is typically performed in the early morning and this was indeed described for at least one of these studies (34).

Leptin-treated mice on both LFD and HFD revealed a 24-h rhythm of leptin-induced pSTAT3 activation in the ARC; however, this rhythm was inversely regulated dependent on the diet. At ZT0 compared with all other times, the number of pSTAT3-ir cells was maximal in mice on LFD, but minimal in mice on HFD. Leptin-treated mice on HFD showed a decreased response to exogenous leptin exemplified by the number of pSTAT3-ir cells compared with mice on LFD only in the first half of the light and the second half of the dark phase. This suggests that HFD-induced leptin resistance is a temporary phenomenon; it is restricted to these specific times of the day. To investigate the behavioural response to exogenous leptin, we injected mice on LFD as well as HFD with leptin at either ZT0 or ZT12 and compared their subsequent caloric intake with vehicle-treated mice. In this experiment, mice fed LFD reduced their caloric intake only when injected at ZT0, the time when relative leptin sensitivity was maximal, whereas in mice fed HFD leptin failed to reduce food intake at both ZT0 and ZT12. This suggests

that in mice fed LFD the behavioural response to the hormone reflects the pattern of molecular leptin sensitivity with leptin eliciting its anorexigenic effects at the beginning of the light phase, when leptin sensitivity at a molecular level was at a maximum. HFD feeding, however, leads to complete resistance to exogenous leptin on a behavioural level.

We discovered that in mice fed LFD a 24-h rhythm in serum leptin concentrations was absent, which can be mostly attributed to the 24-h fasting period preceding blood sampling. Intriguingly, mice fed HFD showed a profound rhythmic regulation of endogenous leptin concentrations with maximal concentrations during the light phase compared with lower levels during the dark phase. Notably, this rhythm occurred despite a 24-h fasting period prior to sampling and is therefore independent of food intake. Intriguingly, the increase in serum leptin levels coincides with the time when leptin sensitivity in the ARC of mice fed HFD was minimal and the nadir in circulating leptin levels coincides with maximal stimulation of STAT3. This finding suggests an inhibitory effect of leptin on pSTAT3 activation in states of DIO and reinforces the notion that hyperleptinemia is a crucial factor in the development of hypothalamic leptin resistance and obesity (35). Neither mice on LFD nor HFD showed rhythmic regulation of serum insulin levels, but HFD feeding led to an overall increase of insulin levels relative to LFD feeding. This is in accordance with other studies, showing that insulin secretion is upregulated to counteract elevated blood glucose levels, representing an ultradian regulatory rhythm reflecting food intake. Chronic HFD feeding is associated with an overall increase of insulin secretion, reflecting the role of the hormone as an adipostat (36). These elevated insulin levels eventually give rise to the manifestation of type 2 diabetes during DIO. Unlike insulin, we found higher serum glucose concentrations in mice on HFD compared with LFD during the dark phase. At this time, serum leptin levels were minimal in mice fed HFD suggesting that increases in leptin levels during the light phase may contribute to glucose uptake. This could be mediated by leptin facilitating insulin action. Indeed, we and others have shown that leptin is required for the activation of the insulin pathway (33, 37-39).

The above-mentioned peak in leptin signal transduction at the beginning of the light phase observed in both vehicle- and leptin-treated mice fed LFD and the behavioural response to leptin at ZT0 indicates a greater anorexigenic effect of leptin with the beginning of the light phase. Since mice are nocturnal this may prepare the animal for

the inhibition of the drive to eat during the inactive (light) phase. Mice fed HFD, on the other hand, show a disruption of the normal 24-h rhythm of leptin signal transduction, which offers an explanation for the development of arrhythmic feeding as well as disrupted expression patterns of leptin-induced hypothalamic genes, typically associated with DIO (26-28). Based on these findings, we conducted a study to examine whether restricting the access to HFD to these intervals of varying leptin sensitivity affects energy metabolism and behaviour.

We exposed mice to HFD for an interval of six hours each day, in which they had access to food either during their relative leptin sensitive phase (ZT9 – ZT15), their relative leptin insensitive phase (ZT21 – ZT3) or during one of the remaining six hours in-between those intervals (ZT3 – ZT9 and ZT15 – ZT21). Intriguingly, we found that *ad libitum*-fed mice on HFD showed increased caloric intake compared with *ad libitum*-fed mice on LFD exclusively during the interval from ZT21 – ZT3, when mice on HFD have lower numbers of leptin-induced pSTAT3-ir cells compared with mice on LFD. The caloric overconsumption observed in mice on HFD during this interval was sufficient to lead to a significant increase in overall caloric intake displayed over the 24-hour cycle. Similar behavioural results were reported by Kohsaka *et al*., showing that even though mice on HFD consume more food during the dark (active) compared with the light (inactive) phase, the relative caloric intake was increased by approximately 20% during the light phase (28). In accordance with other studies, all TRF groups consumed fewer calories over 24 hours and had reduced BW compared to *ad libitum* fed mice on HFD (40). Additionally, TRF of HFD led to a reduction of plasma leptin levels in all TRF groups. Since circulating leptin levels are proportional to adipose tissue mass (41), this suggests that the reduction of BW may be due to a reduction of adipose tissue mass. Indeed, a reduction of body weight due to loss of fat mass has been shown for mice on a TRF protocol (40). Despite the similar reduction of BW, we saw differences in other metabolic parameters between the different TRF groups. The *ad libitum* fed mice on LFD and HFD showed a clear rhythm of locomotor activity, average metabolic rate and energy expenditure, with lowest levels during their inactive phase and highest levels during their active phase. However, HFD feeding caused a dampening of these daily rhythms. For instance, locomotor activity in mice fed HFD was lower during their active phase relative to mice fed LFD. This effect has been demonstrated previously for mice fed HFD compared with control chow diet.

There, a non-significant but consistent increase in locomotion during the light phase relative to the dark phase has been reported for mice fed HFD (28). Interestingly, all metabolic parameters analysed in the current study were reduced by HFD compared with LFD feeding only when access to HFD was limited to specific intervals. For example, mice with access to HFD exclusively during their leptin sensitive interval from ZT9 – ZT15 maintained their rhythm of locomotor activity and showed the most robust rhythm of average metabolic rate and energy expenditure amongst all TRF groups when compared with *ad libitum* fed mice on LFD and HFD. Mice with access to HFD exclusively during their leptin resistant interval from ZT21 – ZT3 on the other hand experienced a disruption of the 24-h rhythms of locomotor activity as well as both average metabolic rate and energy expenditure. Furthermore, those mice had higher plasma insulin concentration compared with mice on LFD, indicating an impairment of insulin signalling that may result in the development of type 2 diabetes. Although all TRF groups had the same duration of food access and similar caloric intake, mice that received HFD during their relative leptin sensitive interval showed ameliorated parameters of metabolic health compared with mice that received HFD during their leptin insensitive interval, which showed evidence for impaired metabolic health.

In conclusion, these data show that leptin sensitivity is controlled by a 24-h rhythm in wild-type mice and that DIO disrupts this rhythm, causing impaired regulation of energy metabolism. Furthermore, we provide strong evidence that HFD-induced leptin resistance is a temporary phenomenon and occurs only at specific intervals during the 24-h cycle. These intervals seem to be decisive for the detrimental effects of HFD on metabolic health.

Figures

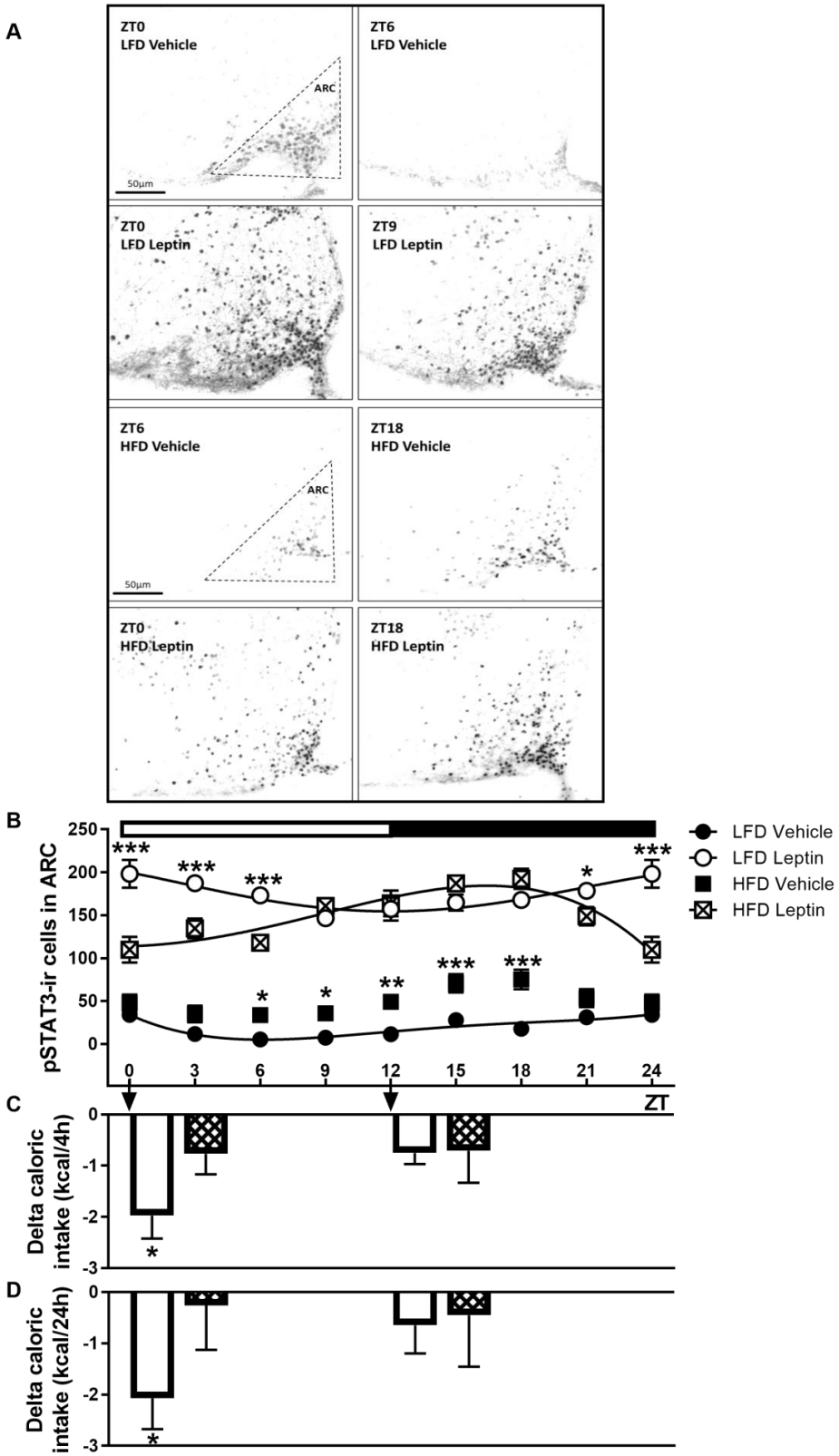

Figure 1

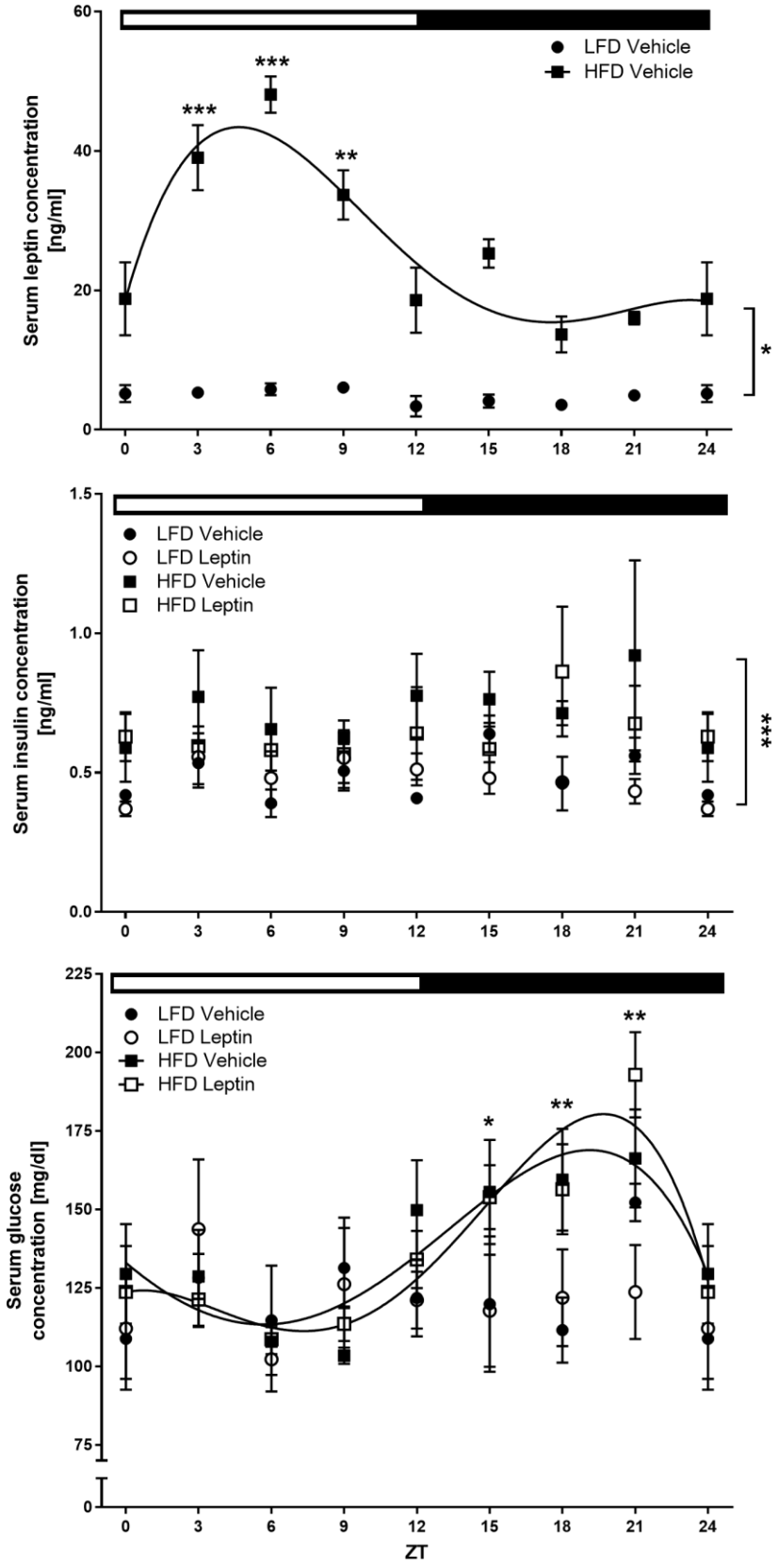
Serum leptin concentration [ng/ml]
LFD Vehicle
HFD Vehicle
***
***
**
*
Serum insulin concentration [ng/ml]
LFD Vehicle
LFD Leptin
HFD Vehicle
HFD Leptin
***
Serum glucose concentration [mg/dl]
LFD Vehicle
LFD Leptin
HFD Vehicle
HFD Leptin
*
**
**
ZT

Figure 2

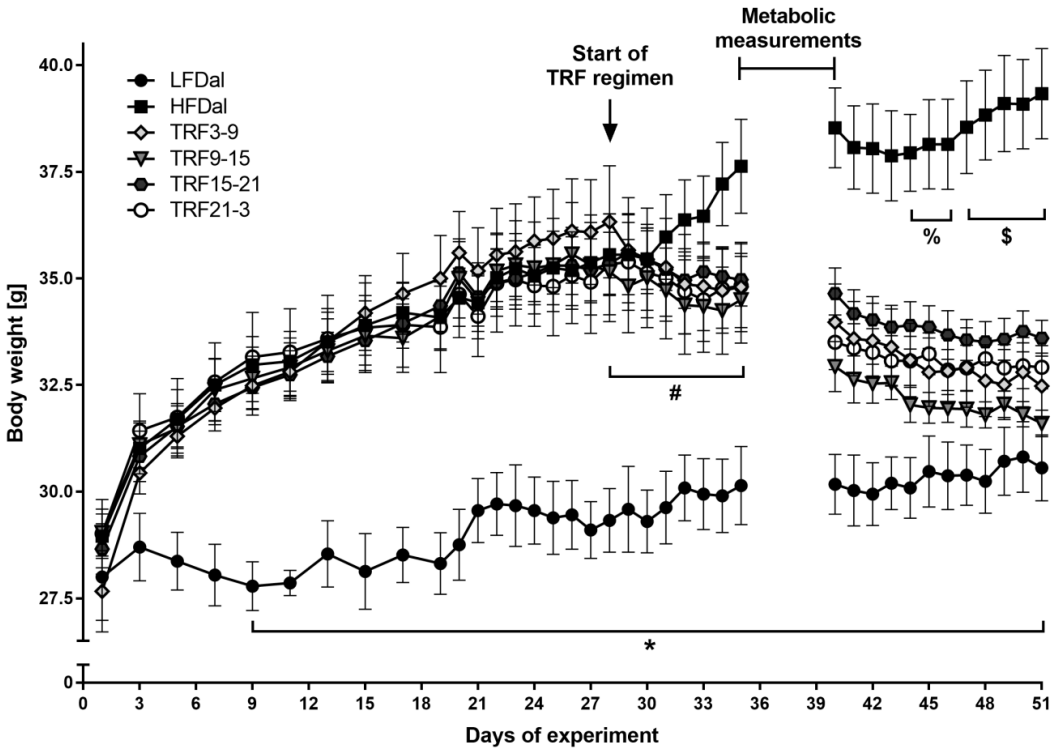
Metabolic measurements
Start of TRF regimen
LFDal
HFDal
TRF3-9
TRF9-15
TRF15-21
TRF21-3
Body weight [g]
Days of experiment
%
$
#
*

Figure 3

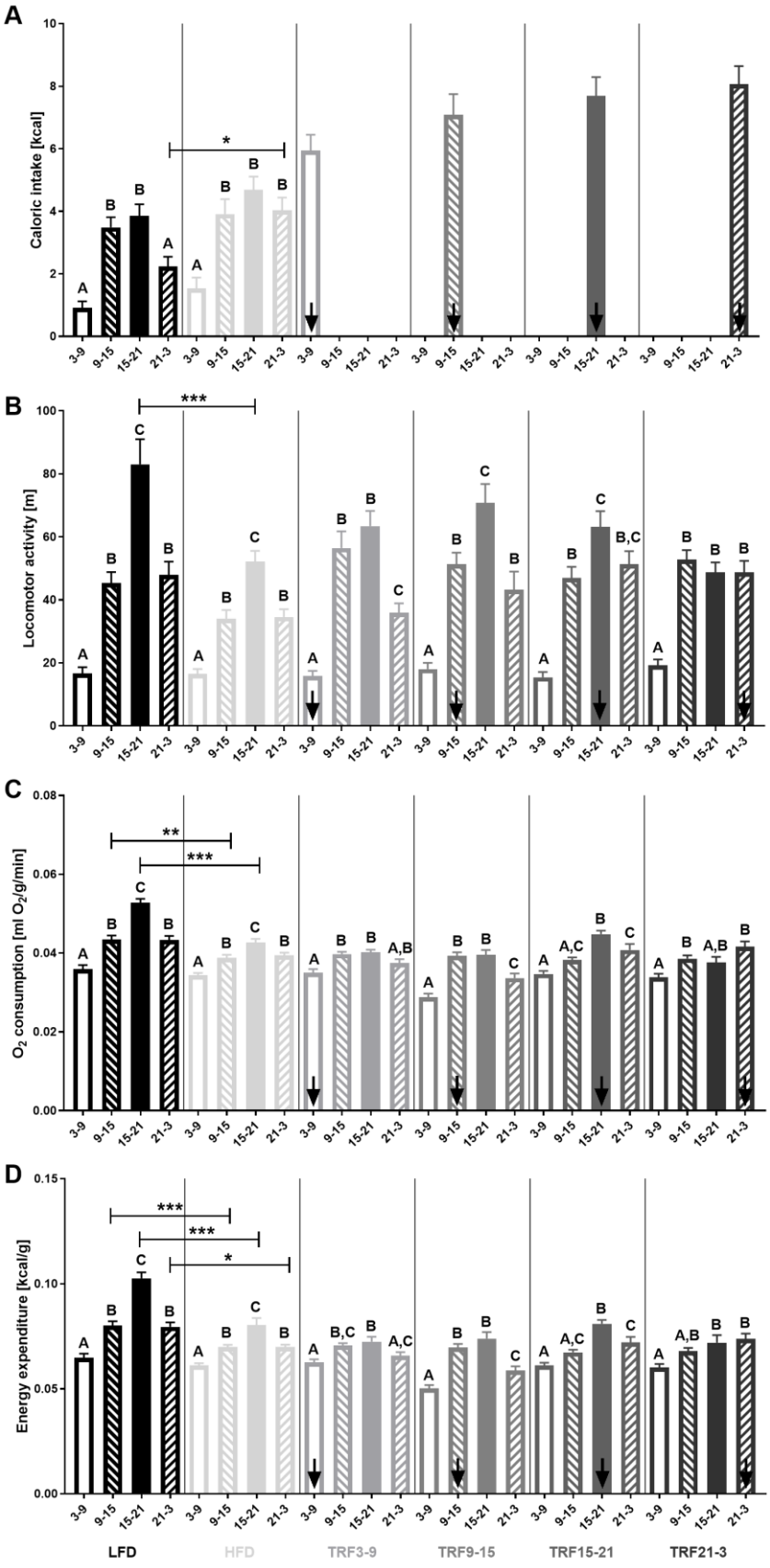
A
Caloric intake [kcal]
B
Locomotor activity [m]
C
O2 consumption [ml O2/g/min]
D
Energy expenditure [kcal/g]
3-9
9-15
15-21
21-3
LFD
HFD
TRF3-9
TRF9-15
TRF15-21
TRF21-3

Figure 4

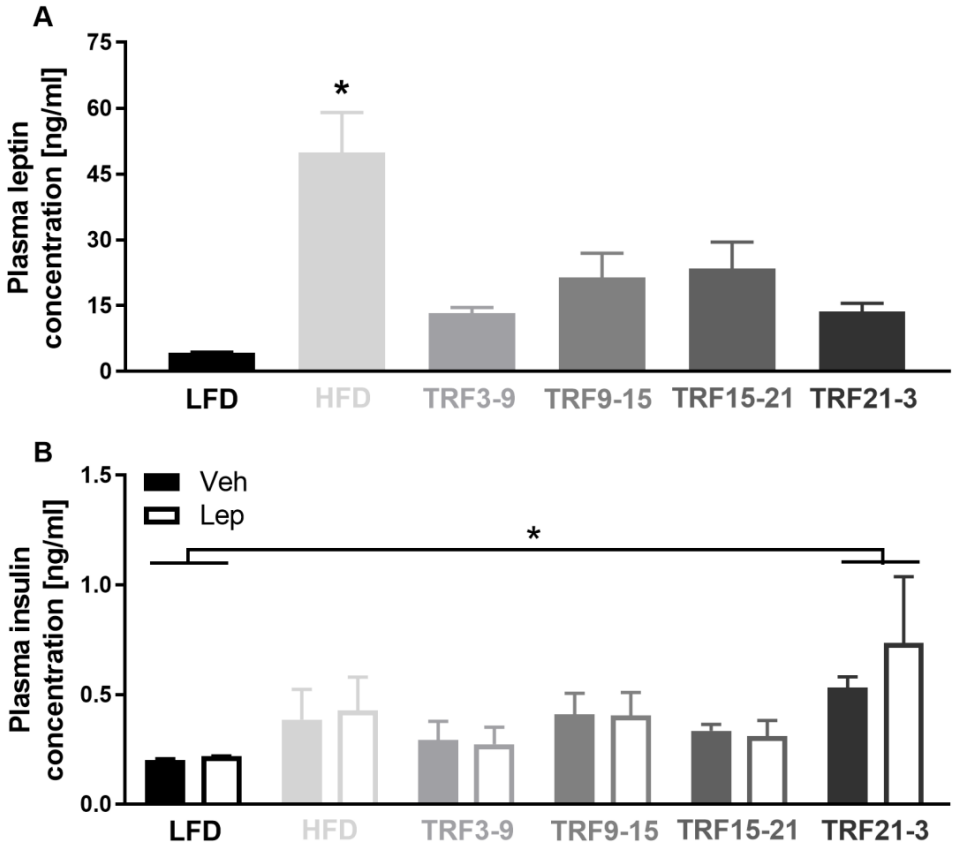
A
Plasma leptin concentration [ng/ml]
75
60
45
30
15
0
*
LFD
HFD
TRF3-9
TRF9-15
TRF15-21
TRF21-3
B
Plasma insulin concentration [ng/ml]
1.5
1.0
0.5
0.0
Veh
Lep
*
LFD
HFD
TRF3-9
TRF9-15
TRF15-21
TRF21-3

Figure 5

Figure legends

Figure 1: Experiments 1 and 2. **A)** Representative coronal brain sections with highest and lowest pSTAT3-ir cell numbers for mice fed LFD or HFD and treated with i.p. vehicle or leptin and **B)** quantified pSTAT3-immunoreactive cells in the ARC of mice at the respective time points, representing the circadian rhythm of hypothalamic leptin sensitivity. Rhythmicity is represented by a fourth order polynomial nonlinear regression curve. **C)** Leptin-induced reduction in caloric intake after injections at ZT0 and ZT12 after 4 hours and **D)** after 24 hours relative to vehicle-treated mice with the same dietary background (= baseline). *, $P \leq .05$; **, $P \leq .01$; ***, $P \leq .001$ reveal significance between vehicle- and leptin-treated mice with the same dietary background.

Figure 2: Experiment 1. 24-hour rhythms of circulating metabolic markers in mice fed LFD or HFD and treated with i.p. vehicle or leptin. **A)** serum leptin concentrations, **B)** serum insulin concentrations and **C)** serum glucose concentrations. Rhythmicity is represented by a fourth order polynomial nonlinear regression curve. *, $P \leq .05$; **, $P \leq .01$; ***, $P \leq .001$ reveal significance between mice fed LFD and mice fed HFD,] indicates significance at all time points.

Figure 3: Experiment 3. Body weight trajectory of mice fed LFD and HFD *ad libitum* and TRF mice throughout the experiment. *, $P \leq .05$ reveals significance between mice fed LFD *ad libitum* and HFD *ad libitum*; #, $P \leq .05$ between LFD *ad libitum* and all TRF groups; %, $P \leq .05$ between HFD *ad libitum* and TRF3–9, TRF15–21 and TRF21–3; $, $P \leq .05$ between HFD *ad libitum* and all TRF groups.

Figure 4: Experiment 3. Metabolic measurements in mice fed LFD and HFD *ad libitum* and TRF mice binned into 6-hour intervals. **A)** Caloric intake, **B)** locomotor activity, **C)** oxygen consumption per g body weight and **D)** energy expenditure per g body weight. Statistical information shown with A, B, C, D depicts comparisons within each TRF group only, while comparisons between mice fed LFD *ad libitum* and HFD *ad libitum* are depicted by asterisk (*).*, $P \leq .05$; **, $P \leq .01$; ***, $P \leq .001$.

Figure 5: Experiment 3. Circulating metabolic markers in mice fed LFD and HFD *ad libitum* and TRF mice. **A.** Plasma leptin concentrations and **B.** plasma insulin concentrations**.** *, $P \leq .05$.

Supplementary Figures

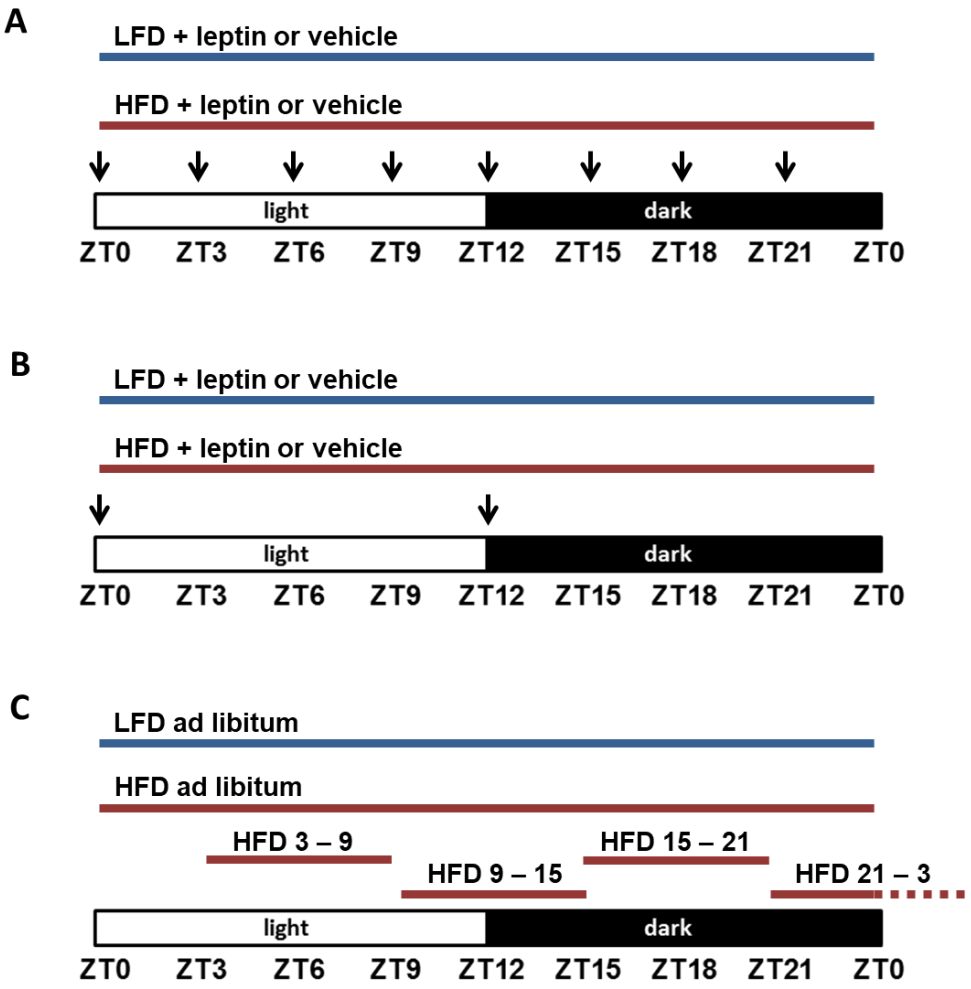

Suppl. Figure 1

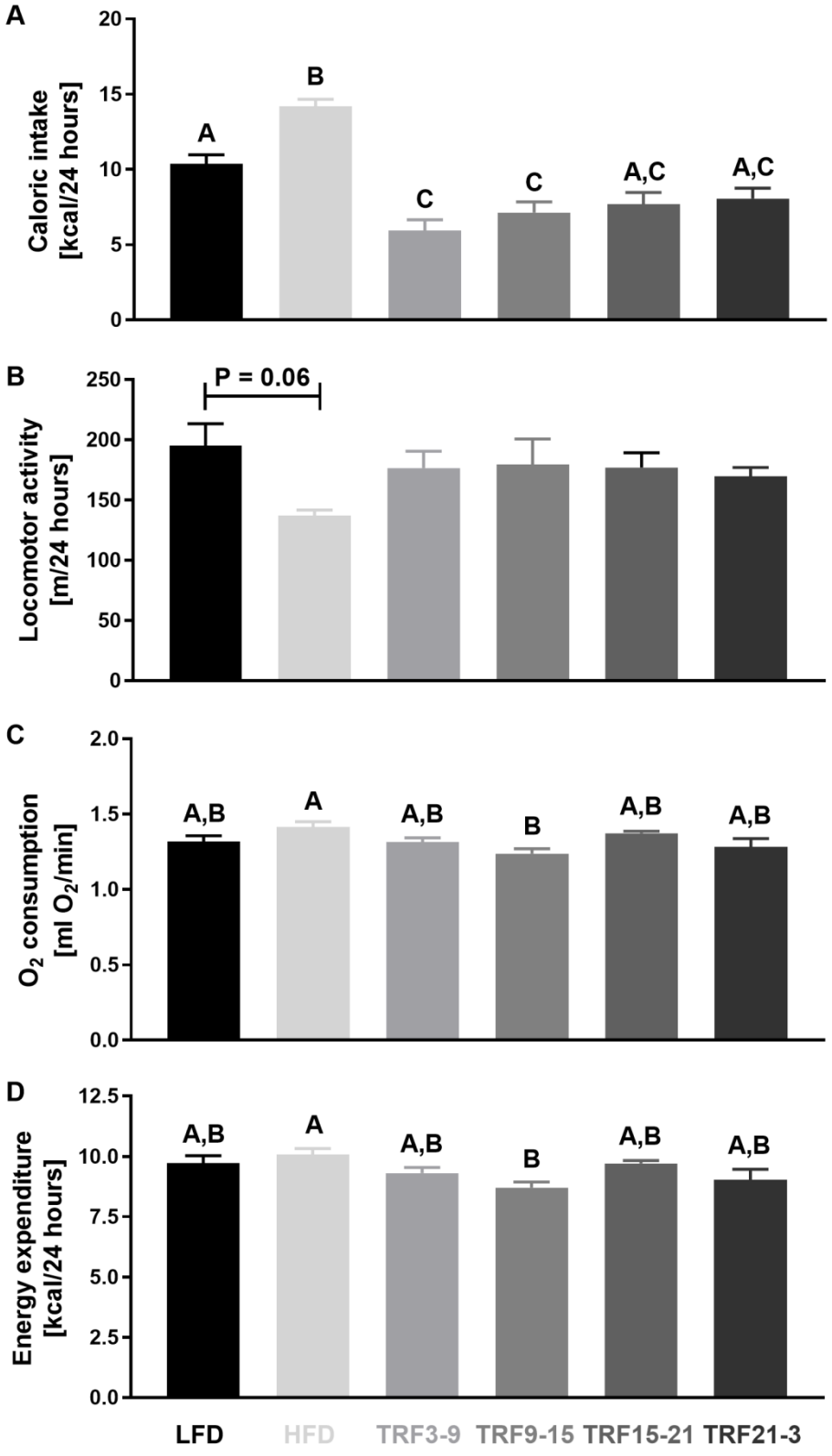

Suppl. Figure 2

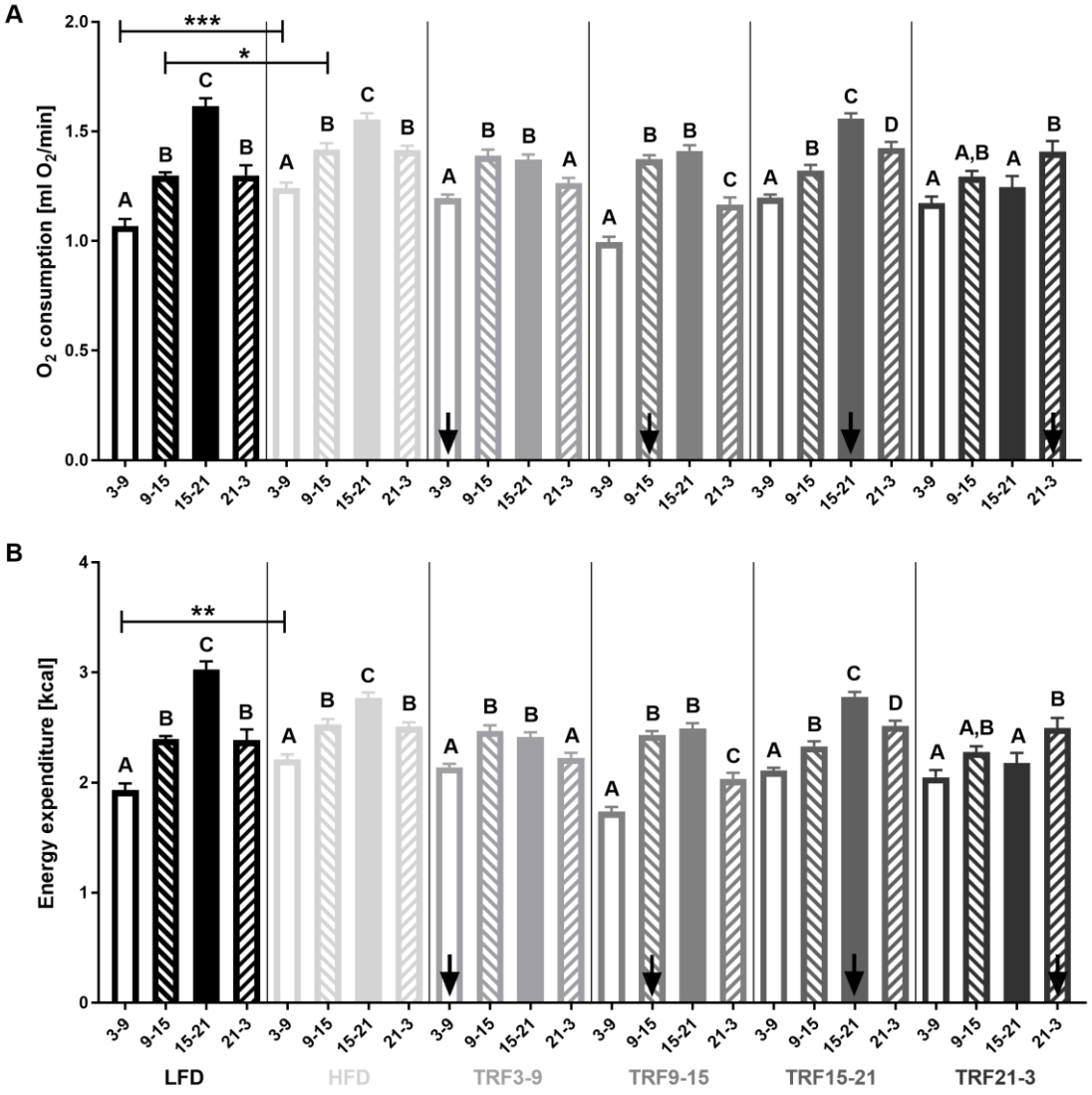

Suppl. Figure 3

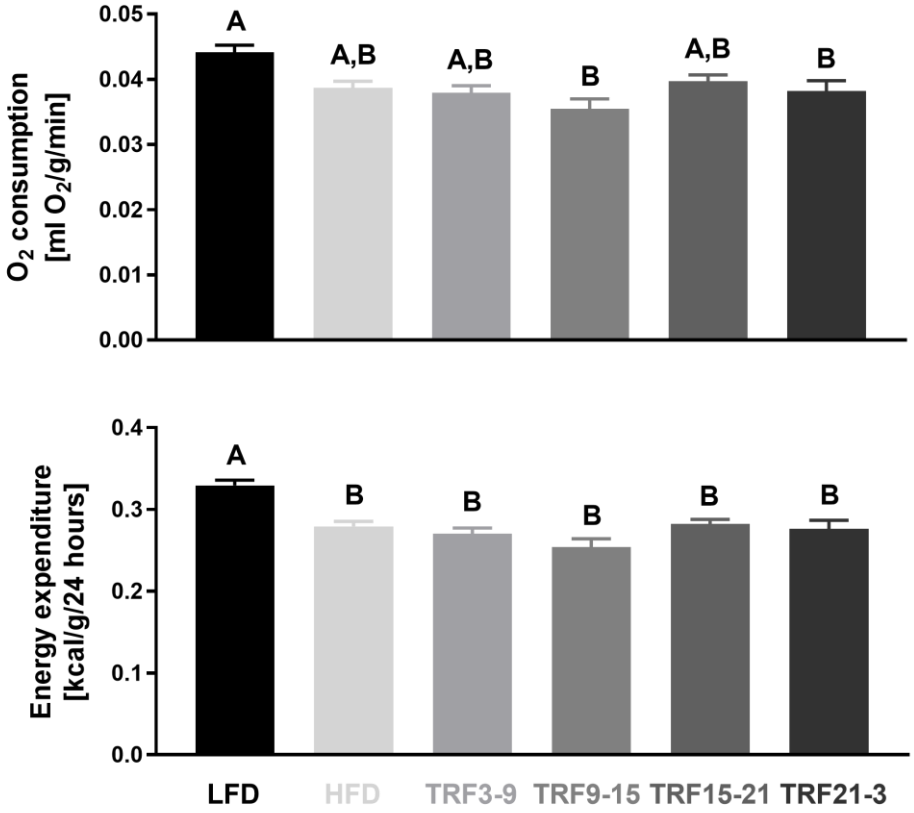

Suppl. Figure 4

Supplementary figure legends

Suppl. Figure 1: Experimental designs of this study. **A.** Experiment 1. Mice received low fat-diet (LFD) or high fat-diet (HFD) for four weeks. They were then fasted for 24 hours before being injected with either leptin or vehicle prior to perfusions. Mice were perfused at ZT0, ZT3, ZT6, ZT9, ZT12, ZT15, ZT18 or ZT21 (n = 4). Blood was collected to analyse circulating metabolic markers and immunohistochemistry was performed to assess the number of pSTAT3 (Tyr705)-ir cells at each time point. **B.** Experiment 2. Mice fed LFD and HFD were fasted for 24 hours and received a single ip injection of either leptin or vehicle at either ZT0 or ZT12. Mice were re-fed after injections and food intake as well as body weight change were monitored for 24 hours (n = 6–10). **C.** Experiment 3. Two groups of mice had *ad libitum* access to either LFD or HFD throughout the entire experiment, whereas four other groups had time-restricted access to HFD for six hours each day, either from ZT3 – ZT9, ZT9 – ZT15, ZT15 – ZT21 or ZT21 – ZT3. Metabolic parameters were recorded using metabolic cages (n = 8). At the end of the experiment mice were fasted for 18 hours followed by i.p. injections of either leptin or vehicle prior to perfusions. Blood was collected to analyse circulating metabolic markers (n = 4).

Suppl. Figure 2: Experiment 3. Metabolic measurements in mice fed LFD and HFD *ad libitum* and TRF mice summed over 24 hours. **A)** Caloric intake, **B)** locomotor activity, **C)** oxygen consumption and **D)** energy expenditure.

Suppl. Figure 3: Experiment 3. Metabolic measurements in mice fed LFD and HFD *ad libitum* and TRF mice binned into 6-hour intervals. **A)** Oxygen consumption and **B)** energy expenditure. Statistical information shown with A, B, C, D depicts comparisons within each TRF group only, while comparisons between mice fed LFD *ad libitum* and HFD *ad libitum* are depicted by asterisk (*). *, $P \leq .05$; **, $P \leq .01$; ***, $P \leq .001$.

Suppl. Figure 4: Experiment 3. Body weight-corrected metabolic measurements in mice fed LFD and HFD *ad libitum* and TRF mice summed over 24 hours. **A)** Oxygen consumption per g body weight and **B)** energy expenditure per g body weight.

References

1. Yamazaki S, Yoshikawa T, Biscoe EW, Numano R, Gallaspy LM, Soulsby S, et al. Ontogeny of circadian organization in the rat. J Biol Rhythms. 2009;24(1):55-63.

2. Yoo SH, Yamazaki S, Lowrey PL, Shimomura K, Ko CH, Buhr ED, et al. PERIOD2::LUCIFERASE real-time reporting of circadian dynamics reveals persistent circadian oscillations in mouse peripheral tissues. Proceedings of the National Academy of Sciences of the United States of America. 2004;101(15):5339-46.

3. Takahashi JS, Hong HK, Ko CH, McDearmon EL. The genetics of mammalian circadian order and disorder: implications for physiology and disease. Nat Rev Genet. 2008;9(10):764-75.

4. Gerhart-Hines Z, Lazar MA. Circadian metabolism in the light of evolution. Endocr Rev. 2015;36(3):289-304.

5. Asher G, Schibler U. Crosstalk between components of circadian and metabolic cycles in mammals. Cell metabolism. 2011;13(2):125-37.

6. Bass J, Takahashi JS. Circadian integration of metabolism and energetics. Science. 2010;330(6009):1349-54.

7. Lamia KA, Sachdeva UM, DiTacchio L, Williams EC, Alvarez JG, Egan DF, et al. AMPK regulates the circadian clock by cryptochrome phosphorylation and degradation. Science. 2009;326(5951):437-40.

8. Green CB, Takahashi JS, Bass J. The meter of metabolism. Cell. 2008;134(5):728-42.

9. Rutter J, Reick M, McKnight SL. Metabolism and the control of circadian rhythms. Annu Rev Biochem. 2002;71:307-31.

10. Coomans CP, van den Berg SA, Lucassen EA, Houben T, Pronk AC, van der Spek RD, et al. The suprachiasmatic nucleus controls circadian energy metabolism and hepatic insulin sensitivity. Diabetes. 2013;62(4):1102-8.

11. Shi SQ, Ansari TS, McGuinness OP, Wasserman DH, Johnson CH. Circadian disruption leads to insulin resistance and obesity. Curr Biol. 2013;23(5):372-81.

12. Marcheva B, Ramsey KM, Buhr ED, Kobayashi Y, Su H, Ko CH, et al. Disruption of the clock components CLOCK and BMAL1 leads to hypoinsulinaemia and diabetes. Nature. 2010;466(7306):627-31.

13. Turek FW, Joshu C, Kohsaka A, Lin E, Ivanova G, McDearmon E, et al. Obesity and metabolic syndrome in circadian Clock mutant mice. Science. 2005;308(5724):1043-5.

14. Roenneberg T, Allebrandt KV, Merrow M, Vetter C. Social jetlag and obesity. Curr Biol. 2012;22(10):939-43.

15. Scheer FA, Hilton MF, Mantzoros CS, Shea SA. Adverse metabolic and cardiovascular consequences of circadian misalignment. Proceedings of the National Academy of Sciences of the United States of America. 2009;106(11):4453-8.

16. Friedman JM, Halaas JL. Leptin and the regulation of body weight in mammals. Nature. 1998;395(6704):763-70.

17. Farooqi IS, Jebb SA, Langmack G, Lawrence E, Cheetham CH, Prentice AM, et al. Effects of recombinant leptin therapy in a child with congenital leptin deficiency. N Engl J Med. 1999;341(12):879-84.

18. Montague CT, Farooqi IS, Whitehead JP, Soos MA, Rau H, Wareham NJ, et al. Congenital leptin deficiency is associated with severe early-onset obesity in humans. Nature. 1997;387(6636):903-8.

19. Prolo P, Wong ML, Licinio J. Leptin. Int J Biochem Cell Biol. 1998;30(12):1285-90.

20. Campfield LA, Smith FJ, Guisez Y, Devos R, Burn P. Recombinant mouse OB protein: evidence for a peripheral signal linking adiposity and central neural networks. Science. 1995;269(5223):546-9.

21. Koch CE, Lowe C, Pretz D, Steger J, Williams LM, Tups A. High-fat diet induces leptin resistance in leptin-deficient mice. Journal of neuroendocrinology. 2014;26(2):58-67.

22. Tups A, Stohr S, Helwig M, Barrett P, Krol E, Schachtner J, et al. Seasonal leptin resistance is associated with impaired signalling via JAK2-STAT3 but not ERK,

possibly mediated by reduced hypothalamic GRB2 protein. Journal of comparative physiology B, Biochemical, systemic, and environmental physiology. 2012;182(4):553-67.

23. Munzberg H, Flier JS, Bjorbaek C. Region-specific leptin resistance within the hypothalamus of diet-induced obese mice. Endocrinology. 2004;145(11):4880-9.

24. Mercer JG, Hoggard N, Williams LM, Lawrence CB, Hannah LT, Trayhurn P. Localization of leptin receptor mRNA and the long form splice variant (Ob-Rb) in mouse hypothalamus and adjacent brain regions by in situ hybridization. FEBS letters. 1996;387(2-3):113-6.

25. Kettner NM, Mayo SA, Hua J, Lee C, Moore DD, Fu L. Circadian Dysfunction Induces Leptin Resistance in Mice. Cell metabolism. 2015;22(3):448-59.

26. Pendergast JS, Branecky KL, Yang W, Ellacott KL, Niswender KD, Yamazaki S. High-fat diet acutely affects circadian organisation and eating behavior. Eur J Neurosci. 2013;37(8):1350-6.

27. Branecky KL, Niswender KD, Pendergast JS. Disruption of Daily Rhythms by High-Fat Diet Is Reversible. PloS one. 2015;10(9):e0137970.

28. Kohsaka A, Laposky AD, Ramsey KM, Estrada C, Joshu C, Kobayashi Y, et al. High-fat diet disrupts behavioral and molecular circadian rhythms in mice. Cell metabolism. 2007;6(5):414-21.

29. Stephan FK, Swann JM, Sisk CL. Entrainment of circadian rhythms by feeding schedules in rats with suprachiasmatic lesions. Behav Neural Biol. 1979;25(4):545-54.

30. Krieger DT, Hauser H, Krey LC. Suprachiasmatic nuclear lesions do not abolish food-shifted circadian adrenal and temperature rhythmicity. Science. 1977;197(4301):398-9.

31. Tan K, Knight ZA, Friedman JM. Ablation of AgRP neurons impairs adaption to restricted feeding. Molecular metabolism. 2014;3(7):694-704.

32. Hatori M, Vollmers C, Zarrinpar A, DiTacchio L, Bushong EA, Gill S, et al. Time-restricted feeding without reducing caloric intake prevents metabolic diseases in mice fed a high-fat diet. Cell metabolism. 2012;15(6):848-60.

33. Koch C, Augustine RA, Steger J, Ganjam GK, Benzler J, Pracht C, et al. Leptin rapidly improves glucose homeostasis in obese mice by increasing hypothalamic insulin sensitivity. The Journal of neuroscience : the official journal of the Society for Neuroscience. 2010;30(48):16180-7.

34. Rizwan MZ, Mehlitz S, Grattan DR, Tups A. Temporal and regional onset of leptin resistance in diet-induced obese mice. Journal of neuroendocrinology. 2017;29(10).

35. Knight ZA, Hannan KS, Greenberg ML, Friedman JM. Hyperleptinemia is required for the development of leptin resistance. PloS one. 2010;5(6):e11376.

36. Schwartz MW, Woods SC, Porte D, Jr., Seeley RJ, Baskin DG. Central nervous system control of food intake. Nature. 2000;404(6778):661-71.

37. Benzler J, Ganjam GK, Kruger M, Pinkenburg O, Kutschke M, Stohr S, et al. Hypothalamic glycogen synthase kinase 3beta has a central role in the regulation of food intake and glucose metabolism. The Biochemical journal. 2012;447(1):175-84.

38. Benzler J, Andrews ZB, Pracht C, Stohr S, Shepherd PR, Grattan DR, et al. Hypothalamic WNT signalling is impaired during obesity and reinstated by leptin treatment in male mice. Endocrinology. 2013;154(12):4737-45.

39. Morton GJ, Gelling RW, Niswender KD, Morrison CD, Rhodes CJ, Schwartz MW. Leptin regulates insulin sensitivity via phosphatidylinositol-3-OH kinase signaling in mediobasal hypothalamic neurons. Cell metabolism. 2005;2(6):411-20.

40. Delahaye LB, Bloomer RJ, Butawan MB, Wyman JM, Hill JL, Lee HW, et al. Time-restricted feeding of a high fat diet in C57BL/6 male mice reduces adiposity, but does not protect against increased systemic inflammation. Appl Physiol Nutr Metab. 2018.

41. Frederich RC, Hamann A, Anderson S, Lollmann B, Lowell BB, Flier JS. Leptin levels reflect body lipid content in mice: evidence for diet-induced resistance to leptin action. Nat Med. 1995;1(12):1311-4.

4.4. All in the Timing: Regulation of Body Weight, Glucose Homeostasis and Memory Coordination by the Circadian Clock

All in the Timing: Regulation of Body Weight, Glucose Homeostasis and Memory Coordination by the Circadian Clock

Alisa Boucsein[1,2], Aline Löhfelm[1], Dominik Pretz[1,2] and Alexander Tups[1,2]

[1]Centre for Neuroendocrinology and Brain Health Research Centre, Department of Physiology, School of Biomedical Sciences, University of Otago, Dunedin, New Zealand

[2]Department of Animal Physiology, Faculty of Biology, Philipps University of Marburg, Marburg, Germany

Correspondence to:
Dr. Alexander Tups
Department of Physiology
University of Otago
PO Box 913
Dunedin, New Zealand
E-mail: alexander.tups@otago.ac.nz

Abstract

Metabolic syndrome and Alzheimer´s disease are two major health issues of our modern society causing an extraordinary financial burden for the world´s healthcare systems. In past decades a tight link between the pathologies of obesity and type 2 diabetes and more recently between type 2 diabetes and Alzheimer's disease was discovered. This review focuses on central insulin resistance, altered glycogen synthase kinase 3β signalling and central inflammation as common features of the three metabolic disorders and how pathological changes in one disease can contribute to the development of another. Furthermore, we discuss the role of circadian disruptions in the development and progress of metabolic derangements and vice versa. Based on the shared features, combined therapeutic interventions will be discussed briefly.

Metabolic Disorders and the Circadian Clock

Since 1975, the worldwide prevalence of obesity has nearly trebled, accompanied by a dramatic increase of type 2 diabetes (T2D), which is predicted to affect 629 million people by 2045 [1, 2]. A large body of evidence links diet-induced obesity (DIO) to the development of other metabolic diseases such as T2D and Alzheimer's disease (AD). Over the last decades, these disorders became more prevalent, causing a high financial burden for health systems and impacting quality of life. More recently, the essential role of the brain in the pathogenesis of these metabolic diseases has been highlighted. Common hallmarks of DIO, T2D and AD are central insulin resistance, altered **glycogen synthase kinase 3β (GSK3β)** (see Glossary) signalling as well as central inflammation. In this review, we discuss the shared molecular derangements that underlie these pathologies and focus on the connection between energy metabolism and **circadian rhythms**. In our modern society, these internal timekeeping systems become disrupted due to lifestyle changes and technological advances, including social jetlag, transmeridian travel, night shift work and constant exposure to bright artificial light sources. Here, we describe how circadian disruptions are associated with the development of metabolic derangements in both rodents and humans, as well as the efficacy of fasting regimens, such as **time-restricted feeding (TRF)**, as a therapeutic intervention to reinstate metabolic health. Finally, we highlight future challenges and open questions in this field of research.

Obesity, Type 2 Diabetes and Alzheimer's Disease: Three Distinct Diseases With Similar Aetiology?

a) Neuroendocrine Pathways in the Regulation of Energy Homeostasis

In both rodents and humans, DIO is characterised by a marked increase in circulating leptin levels, which are proportional to the amount of white adipose tissue. Although there is some evidence for ongoing leptin activity in obesity, in that a leptin antagonist can increase food intake and body weight in DIO mice [3], in common forms of obesity in humans and mice hyperleptinemia as well as administration of exogenous leptin are ineffective to properly mediate the hormone's catabolic and anorexigenic effects in the hypothalamic arcuate nucleus (ARC), a key brain region for the regulation of energy homeostasis. This phenomenon was termed central leptin resistance.

Furthermore, low grade systemic and central inflammation are associated with obesity [4] and increased activity of pro-inflammatory pathways in the hypothalamus has been linked to the development of DIO [5, 6]. By central inhibition of the inhibitor of nuclear factor-κB kinase β (IKKβ)/nuclear factor-κ-light-chain-enhancer of B-cells (NF-κB) pathway, the involvement of this pro-inflammatory pathway in the development of hypothalamic leptin resistance during DIO was demonstrated in mice [5]. A possible link between both pathways is the suppressor of cytokine signalling 3 (SOCS3), which is a potent inhibitor of leptin signalling as well as a prominent target of the NF-κB signalling cascade [7]. In line with this, we showed that gene-therapeutic inhibition of IKKβ/NF-κB signalling in the ARC led to reduced *socs3* gene expression [5]. Although this finding suggests that central inflammation might be a causative factor in the development of leptin resistance further research is required to identify the origin of leptin resistance.

The occurrence of T2D correlates strongly with obesity [8]. Leptin resistance during DIO, a lack leptin secretion in leptin deficient patients or mice ($Lep^{ob/ob}$ mouse) or mutations in the receptor ($Lep^{db/db}$ mouse) is accompanied by hyperglycaemia and hyperinsulinemia. In certain cases leptin can be used as a replacement therapy for insulin and leptin is more potent at regulating glucose homeostasis than at regulating body weight [9]. In a leptin deficient patient it could be demonstrated that leptin replacement re-established insulin function in the hypothalamus [10]. Collectively,

these findings provide evidence that functional leptin action is crucial for functional insulin signalling.

Molecularly, leptin administration leads to elevated activation of insulin receptor substrate 1 (IRS1) and we could show that it alters phosphorylation of IRS1 at Ser^{612} and Ser^{307} [11], resulting in activation of the phosphoinositide 3-kinases (PI3K) - protein kinase B (AKT) pathway. Interestingly, pharmacological inhibition of hypothalamic GSK3β was shown to have similar effects on the activation of intracellular PI3K-AKT signalling [12]. GSK3β is a key enzyme of the WNT pathway, which was recently shown to play an important role in the neuroendocrine control of energy metabolism [13-15]. Canonical WNT signal transduction leads to the inactivation of GSK3β [16]. Leptin injections in rodents were indeed shown to activate the WNT pathway and inhibit GSK3β in leptin-deficient obese mice [14, 17]. GSK3β is a potent inhibitor of insulin signal transduction. Therefore, the inhibition of GSK3β by leptin possibly via the WNT pathway might be the explanation for leptin-induced sensitisation of insulin signalling. The disruption of insulin signalling in the brain, which is essential for the regulation of glucose homeostasis, leads to central insulin resistance and ultimately results in the development of T2D [18]. T2D is characterized by chronically elevated blood glucose concentrations, attenuated insulin sensitivity and hyperinsulinemia in the early stages, leading to the death of pancreatic β-cells during the manifestation of the disease [19]. Common complications in many patients suffering from T2D involve neuropathy due to pathologically elevated blood glucose as well as neurodegeneration. In this regard, midlife obesity as well as pathological changes in the brain, such as central insulin resistance and central inflammation, moved into the focus of AD research as risk factors for the development of sporadic AD (90% or more cases of AD).

b) Neuroendocrine Disruptions in the Development of Alzheimer's Disease

AD is the most common cause of dementia. Underlying the pathology of AD are the progressive loss of synapses and neuronal death, resulting in cognitive decline and memory loss. Extracellular amyloid plaques (Aβ), caused by alternative severing of the amyloid precursor protein (APP) by the enzymes β-secretase 1 (BACE1) and γ-secretase, as well as intraneuronal neurofibrillary tangles (NFTs) consisting of hyper-

phosphorylated and aggregated tau protein, are the two traditional hallmarks of this disease [20].

Leptin was shown to exhibit neuroprotective and neurotrophic properties in different AD mouse models. In primary neuronal cultures as well as in APP/PS1 mice leptin was able to reduce tau phosphorylation and improve Aβ related pathologies [21, 22]. Additionally, subcutaneous leptin supplementation for 8 weeks reduced total brain Aβ in a transgenic mouse model of AD [23]. In line with deteriorated leptin signal transduction in DIO, impaired learning and memory performances and compromised working memory was demonstrated in DIO rodent models shortly after their diet was switched to a high-fat diet with 60% kcal from fat (HFD) [24]. High levels of cholesterol, present in obesity, further stimulate the alternative processing of APP and thus promote Aβ production and aggregation *in vivo* and *in vitro* [25].

Another common feature of both DIO and AD is central inflammation, contributing to both pathologies in manifold ways [26]. In this regard, TLR-4-mediated PTEN/PI3K/AKT/NF-κB signalling was proposed as a link between DIO, T2D and AD [27, 28]. Basal NF-κB signalling can promote neuronal survival and regeneration, whereas sustained inflammation is associated with increased Aβ deposition and pathological tissue damage [27, 28].

Highlighting the profound role of impaired insulin signalling in the development and progression of AD, the term type 3 diabetes was proposed by Steen and colleagues in 2005 [29]. Insulin receptors (IR) are expressed in many brain areas by neurons and glial cells with high abundance in the hypothalamus and hippocampus, where they regulate neuronal survival and differentiation, cytoskeletal rearrangements, neuronal plasticity, neurotransmitter release, gene expression, protein synthesis as well as central and whole-body energy homeostasis [30]. *Ex vivo* studies in post-mortem brains from non-diabetic elderly with and without AD provided strong evidence for central insulin resistance as a prominent feature of the neurodegenerative disease. Talbot and colleagues stimulated post-mortem hippocampal tissue samples with physiological doses of insulin and revealed a reduced phosphorylation of IR, IRS1, AKT and GSK3β in AD patients in comparison to age-matched healthy controls, indicating a decreased action of the hormone [31]. Furthermore, these aberrations were correlated positively with Aβ load and the extent of tau phosphorylation as well as negatively with cognition

and memory scores of patients [31]. Additionally, decreases in gene expression and protein levels of insulin pathway molecules such as insulin, IR and IRS1 were observed [29]. Furthermore, insulin signal transduction was shown to be negatively correlated with aging and the pathogenesis of AD due to declining hormone levels in the CSF and decreased binding capacity of insulin to its receptor [32]. In line with those results, insulin-mediated gene expression declines with AD progression.

Since glucose is the main energy source of the brain, the disturbances in glucose homeostasis caused by deteriorated central insulin signalling lead to a "starvation state" of the brain and thus to oxidative stress and cell death. Even though the uptake of glucose into the brain and into neurons is mediated by insulin-independent GLUT-3 and GLUT-1 glucose transporters, respectively, a direct association between insulin resistance and a reduction in brain glucose metabolism was demonstrated by fluorodeoxyglucose (FDG) positron emission tomography (PET) in AD patients [33]. Accordingly, reduced glucose uptake in the brain measured by PET is an early and accurate indicator of neurodegeneration in humans and goes along with the severity of cognitive decline and memory impairments. Age-dependent impairments in central glucose homeostasis can also be observed in mouse models of AD [34]. Here, decreased brain glucose levels are associated with accelerated disease progression and GLUT-1 deficiency in endothelial cells was shown to enhance neuronal atrophy, Aβ plaque formation and cognitive impairments. In turn, overexpression of GLUT-1 improved neurodegeneration and behavioural alterations in a fruit fly model of AD [35].

However, the negative effects of diminished insulin pathway activation are not only due to direct effects on energy metabolism, but also to changes in the regulation of important downstream pathways and molecules. A direct link between central insulin action and cognitive function was demonstrated by studies that depleted insulin receptors in the brain or inhibited central insulin signalling in rodents, causing profound cognitive impairments and AD-like molecular and biochemical changes [36, 37]. Insulin exhibits anti-apoptotic and anti-inflammatory properties via inhibition of Forkhead box O (FOXO), Bcl-2-associated death promoter (BAD), GSK3β and NF-κB pathways. In the case of insulin deficiency, these detrimental pathways remain activated, causing central inflammation and apoptosis. Moreover, the formation of cytotoxic Aβ plaques and of hyperphosphorylated tau aggregates is promoted on

different levels. On a transcriptional level, insulin is involved in the regulation of tau and APP expression, causing elevated levels of APP and decreased levels of *tau* mRNA in post-mortem AD brains [29]. Since functional insulin signalling is also essential for the trafficking of Aβ peptides from their production site in the trans-Golgi network to the plasma membrane, for secretion and degradation via insulin-degrading enzymes (IDE), disturbed insulin signalling leads to reduced Aβ clearance [38]. IDE expression and membrane localisation are induced by insulin stimulation in cultured astrocytes, where insulin facilitates the degradation of exogenous Aβ [39]. In turn, Aβ oligomers inhibit IRS1 through activation of the JNK pathway, decrease the binding affinity of insulin, reduce IR surface expression and interfere with PI3K-mediated activation of AKT, thereby exacerbating insulin signal transduction [40].

Furthermore, GSK3β, which is inhibited by the insulin pathway, can phosphorylate tau at multiple sites, promoting the aggregation of hyper-phosphorylated tau and causing the formation of NFTs [41]. Eventually, this leads to a disruption of intraneuronal transport mechanisms, the collapse of the cytoskeletal structures, neurite retraction and the loss of synaptic connections.

c) Antidiabetic Drugs in the Treatment of Alzheimer's Disease

Based on the shared features between T2D and AD, it is not surprising that antidiabetic drugs not only improve symptoms of T2D but also exhibit positive effects in AD patients. Recent studies showed promising results in rodent models and several drugs have been tested in clinical trials in AD patients. The most prominent treatment linking T2D to AD is intranasally administered insulin. In patients with mild cognitive impairment and AD, both acute and chronic treatment improved memory and plasma Aβ 40/42 ratio [42, 43]. Various other diabetes medications were tested in animal models of AD. Promising results were demonstrated for glucagon-like peptide-1 receptor agonists (GLP-1RA), dipeptidyl peptidase-4 inhibitors, metformin and thiazolidinediones. Systemic GLP-1RA administration in rodents and non-human primates, for instance, greatly improved numerous markers of memory function, neuronal survival, insulin signalling and inflammation. Additionally, hippocampal Aβ load and tau pathology were reduced [44-46]. So far, only a limited number of controlled studies with yet inconclusive outcomes were conducted in humans.

The Circadian Clock in Health and Disease

a) Reciprocal Regulation of the Circadian Clock and Energy Metabolism

The importance of the circadian clock in the control of whole body energy metabolism has been demonstrated in numerous studies over the last decade [47]. Considerable progress in this field has derived from lesions of the **suprachiasmatic nucleus (SCN)** and studies conducted in transgenic rodent models. For example, SCN-lesioning in mice leads to the absence of a circadian rhythmicity in oxygen consumption, food intake and activity, together with an increase in body weight and fat mass, as well as hepatic insulin resistance [48]. Furthermore, a missense mutation in the murine *clock* gene evokes loss of rhythmic expression of key metabolic genes in liver, skeletal muscle and pancreas, resulting in disruption of glucose and lipid homeostasis and an obese phenotype [49, 50]. Deletion of the *bmal1* gene in pancreatic β-cells results in a diabetic phenotype with insulin deficiency, impaired glucose tolerance and hyperglycemia [49].

In humans, chronic circadian misalignment has been shown to evoke symptoms of metabolic syndrome. Continuous shift-work and social jet lag lead to decreased insulin sensitivity and impaired glucose tolerance, both indicators of type 2 diabetes, as well as increased body mass index and symptoms of cardiovascular disease [51-53]. Mice exposed to chronic circadian disruptions in the form of repeated jet lags display reduced hypothalamic leptin sensitivity and increased body weight [54], illustrating a potential explanation for the eminent correlation between circadian misalignment and the development of obesity as described in humans and rodents.

Circadian rhythms and clock gene expression are altered simultaneously in states of metabolic derailment. DIO leads to arrhythmic patterns of locomotor activity, food intake and clock gene expression [55, 56]. One possible explanation for the correlation of circadian misalignments and obesity derives from the close interplay between circadian and inflammatory processes. For instance cytokines and other immune mediators are under direct control of circadian rhythms in a broad variety of tissues [57, 58]. CRY ablation leads to constitutive activation of the pro-inflammatory transcription factor NF-κB [59], whereas the heterodimerisation of CLOCK and BMAL-1 results in rhythmic repression of pro-inflammatory gene expression [60]. Thus, altered

inflammatory activity as a consequence of disrupted circadian clock rhythms might be a crucial factor for obesity and related co-morbidities.

A unique involvement of the ARC in the generation of feeding rhythms has been demonstrated by ARC-targeted ablation of leptin sensitive neurons in rats, resulting in an obese phenotype as well as impaired feeding rhythms, whereas this was not the case in other hypothalamic areas [61]. Recently, hypothalamic AgRP/NPY neurons were identified to be a crucial component of an SCN-independent, food-entrained oscillator [62].

The interaction between circadian rhythmicity and energy metabolism is further highlighted by the finding that rhythmic genomic binding and thus transcriptional activity of the CLOCK/BMAL1 complex is directly regulated by the cellular energy status. The reduced forms of the nicotinamide adenine dinucleotide (NAD) redox cofactors, NAD(H) and NADP(H), enhance the DNA binding of the heterodimeric complex, whereas the oxidised forms, NAD(+) and NADP(+), inhibit its binding [63]. Furthermore, rhythmic levels of NAD(+) activate the NAD(+)-dependent protein deacetylase sirtuin 1 (SIRT1), which oscillates and binds CLOCK/BMAL1 heterodimers in a circadian manner, thereby facilitating the degradation of PER2 and directly regulating circadian output [64]. These results demonstrate how cellular energy metabolism directly regulates the circadian clockwork machinery.

b) Circadian Disruptions in Alzheimer's Disease

Beside metabolic derangements, disruptions in circadian rhythms are associated with a number of different diseases such as cancer, mood disorders and also AD. In fruit fly and rodent models, mutations or knock-outs of the clock genes *bmal1* and *period* cause an accelerated aging phenotype characterised by an earlier decline in cognitive functions, a high rate of oxidative tissue damage and an overall shorter life-span [65, 66].

The influence of the pathology of AD on circadian rhythms was already observed decades ago. More recently it became clear that circadian disturbances are one of the earliest symptoms of AD and often they precede the onset of cognitive and motor

symptoms by years [67]. AD patients exhibit abnormal behavioural rhythms such as disturbed sleep/wake cycles and emotional imbalances. While nocturnal sleep becomes more and more fragmented, night-time activity and daytime sleepiness intensify in these patients [68, 69]. This is accompanied by the 'sundown syndrome' that describes a state of increased distress, emotional volatility and aggression in the evening. Physiological and biochemical processes such as hormone release patterns or anti-oxidative defence rhythms are also changed [70]. The hormone melatonin, which is produced by the pineal gland, is involved in the entrainment of circadian rhythms in the SCN and acts as an effective free radical scavenger. In healthy individuals its release peaks during night-time and is suppressed by daylight. However, in AD patients and individuals with pre-clinical cognitive symptoms of dementia melatonin levels are reduced and its rhythmic oscillation is flattened [70, 71]. Further circadian abnormalities were detected in the core body temperature rhythm, which is delayed and its amplitude decreased [72]. In line with these results, post-mortem AD brains display a severe loss of hypothalamic tissue, including SCN cells and lowered melatonin receptor (MT1) levels [73].

Recent studies in animal models of AD indicate changes in the rhythmic expression patterns of the clock genes *bmal1*, *per1* and *cry1* in the brain. Although *bmal1* expression remains rhythmic in several brain regions and peripheral tissues, the temporal phase relationship between different areas seems to vary in comparison to healthy controls [69]. Additionally, the *bmal1*, *per1* and *cry1* mRNA rhythmicity is lost in cells of the pineal gland [74]. Regarding the pathology of AD, *presilin-2* expression is regulated by CLOCK/BMAL1 heterodimers on a transcriptional and post-transcriptional level in peripheral tissue [75]. Mutations in *presilin-2* are associated with the development and Aβ pathology of familial, early-onset AD.

A direct link between desynchronised body clocks and the Aβ pathology was recently shown in different cell culture and mouse models. The treatment of human skin fibroblast, human A172 glioma cells as well as primary cortical and hippocampal mouse neurons with physiological concentrations of $A\beta_{1–42}$ peptides caused a dampening in metabolic ATP level oscillations and mitochondrial respiration rhythms leading to increased oxidative stress in those cells [76]. In turn, the disruption of circadian rhythmicity either globally or locally in the brain, achieved by the deletion of the clock gene *bmal1* in a β-amyloidosis mouse model, exposed a direct effect of

central circadian disruptions on daily Aβ fluctuations in the hippocampal interstitial fluid, promoting Aβ plaques deposition [77]. Furthermore, a global *bmal1* deletion resulted in elevated *apoe* expression in the brain parenchyma and the formation of fibrillary plaques [77].

The number of circadian abnormalities in AD and metabolic syndrome leads inevitably to the question whether circadian disruptions are the cause or consequence of the pathogenesis of AD and other neurodegenerative diseases. So far, this question cannot be answered easily even though there is some evidence that changes in the master clock deteriorate rather than initiate pathological processes in AD [78].

c) Time-Restricted Feeding as a Therapeutic Intervention to Combat Circadian Disruptions and Metabolic Diseases

Considering the close relationship between circadian clocks and energy homeostasis, behavioural interventions, such as fasting regimens, to combat the consequences of disrupted rhythms and metabolism appear as a favourable tool. Intriguingly, fasting and caloric restriction (CR) protocols increase SIRT1 activity in the hypothalamus as well as the periphery [79]. SIRT1 possesses potent anti-inflammatory capacities and was shown to improve metabolic health by its ability to interact with a variety of transcription factors that control energy homeostasis [79]. These findings offer an explanation for the beneficial effects of intermittent fasting (IF) and time-restricted feeding (TRF) on the detrimental consequences of DIO and related metabolic disorders. TRF is a form of IF wherein food intake is restricted to specified hours each day. In a broad variety of species from fruit flies to mice and humans, CR and TRF lead to an extension of lifespan, promote weight loss, prevent the development of metabolic diseases and/or reduce levels of pro-inflammatory cytokines [80-82]. Recent studies suggest that the beneficial effects of TRF strongly depend on the timing of food intake. Time-restricted access to HFD during the active (dark) phase of mice prevents body weight gain, hyperinsulinemia, glucose intolerance and systemic inflammation, whereas mice with access to HFD both *ad libitum* and exclusively during their inactive (light) phase develop metabolic disorders, even when caloric intake is identical [56, 81]. Timing of food intake is such a strong circadian entrainment cue that TRF of HFD can restore the expression phase of the hepatic clock genes *Clock* and *Cry1* and phase-

advance the expression of *Bmal1, Per1/2*, *Cry2*, amongst others, compared with mice fed HFD *ad libitum* [83]. These findings suggest that TRF can be employed as a behavioural intervention strategy to counteract the detrimental effects of obesity and/or circadian disruptions.

In line with this, circadian-focussed therapies were suggested to improve the symptoms of AD. These interventions, including bright light therapy and timed administration of melatonin resulted in inconsistent outcomes, thus their benefit is still controversial [84-87]. Studies to determine the therapeutic effects of food as a time cue to resynchronise peripheral clocks are underway. Restricting meal times to certain hours of the day may be a promising long-term strategy to combat metabolic disease.

Conclusion

The brain plays a crucial role in the development of obesity, T2D and AD and disruptions of neuroendocrine signalling cascades deteriorate metabolic health. Central insulin resistance, altered GSK3β signalling and an increase in inflammatory processes are shared hallmarks of these metabolic diseases. The development of one of these disorders can therefore facilitate further metabolic derangement. Furthermore, the close regulatory relationship between energy metabolism as well as cognitive health and the circadian clock identifies circadian disruptions as a major risk factor in the development of obesity, T2D and AD. Accordingly, TRF regimens are an efficient therapeutic intervention to re-entrain disrupted circadian rhythms as well as metabolic health.

Appendix

The pathogenesis of Alzheimer´s disease

Clinically, Alzheimer´s disease (AD) is characterised by an initially mild impairment in memory, especially concerning word- and recent event recollection. With the progression of AD symptoms worsen gradually and individuals undergo a severe decline in cognitive abilities accompanied by neurological symptoms and behavioural changes. These range from difficulties to complete familiar tasks to pronounced disorientation and confusion about time, location and events and difficulties to speak, swallow or walk [88].

The brains of AD patients are characterised by manifold histopathological changes. The most prominent and most studied features are amyloid β plaques and neurofibrillary tangles, which have been the gold standard for diagnosis for decades [20]. Aβ peptides originate from the alternative processing of the amyloid precursor protein (APP) by β- and γ-secretases, yielding in 38-43 amino acid long, hydrophobic peptides, which are prone to aggregation into soluble Aβ oligomers or extracellular amyloid plaques [20]. The isoforms Aβ40 and Aβ42 are most common in AD, whereas Aβ42 is considered to have the highest hydrophobicity and toxicity. Since Aβ42 production is enhanced on the expenses of Aβ40 synthesis, the plasma Aβ42/Aβ40 ratio serves as a reliable biomarker to predict brain depositions [89]. The brain Aβ load is further increased in AD by a reduction in Aβ degrading enzymes, a decrease in the brain clearing rate and an increase in the brain uptake of soluble Aβ oligomers via multi-ligand advanced glycation end products receptors (RAGE). Additionally, interaction of RAGE with Aβ causes activation of pro-inflammatory signalling in endothelial cells of the blood-brain-barrier, which in turn leads to endothelial apoptosis and a decrease in cerebral blood flow rate [90]. This effect of Aβ might contribute to the neurovascular changes overserved in AD. The second prominent pathological feature of the brain in AD are intracellular neurofibrillary tangles, consisting of abnormal phosphorylated tau protein. Tau phosphorylation in different sites is thereby mediated by a variety of kinases involved in manifold pathways such as GSK3β [20]. Hyper-phosphorylation of tau causes its translocation into the somatodendritic area and its aggregation, thus, causing the break-down of cytoskeletal structures and a disruption of intracellular transport and signal transduction in neurons [20]. Further pathological brain features are oxidative

stress due to excessive reactive oxygen species (ROS) production, a disturbed calcium homeostasis and alterations in neurotransmitter signalling caused by changes in neurotransmitter release, its clearing from the synaptic cleft and receptor expression. All these molecular alterations lead to a loss of synapses and finally to neuronal death [91].

Interestingly, histopathological changes in the brain precede cognitive symptoms by decades, emphasizing the importance for new screening methods to detect early molecular changes. Currently, diagnoses are made by clinical and neuropsychological tests. Neuroimaging in form of computer tomography (CT) and magnetic resonance imaging (MRI) is not sufficient to diagnose AD and can only be used to exclude other brain diseases such as strokes or tumours. Therefore, there is a need for new imaging techniques to diagnose AD. Amyloid-β positron-emission tomography (PET) imaging and the measurement of amyloid-β in cerebrospinal fluid can estimate the Aβ burden of a patient, however these techniques are very expensive and laborious [92]. Recently structural and functional MRI and PET studies measuring cerebral metabolism provided promising results even in pre-symptomatic stages of AD [33]. A new blood test developed by Nakamura and colleagues, measuring the APP/Aβ42 and the Aβ40/Aβ42 ratios in blood, still in preliminary stages, may provide a feasible and less expensive alternative to neuroimaging [93].

Type 3 diabetes

Central insulin resistance can have a high impact on the histopathological changes seen in AD brains due to impaired glucose uptake and utilisation and altered signal transduction as described in the main text. Accordingly, patients suffering from T2D have a 50-65% higher risk to develop AD and other forms of dementia [94]. Emphasising the similarities between both diseases, the term type 3 diabetes was coined for patients suffering from both medical conditions, T2D and AD/dementia. Common molecular features of both diseases, beside central insulin resistance, are the occurrence of amyloidogenic protein aggregates in the brain and/or pancreas, increased pro-inflammatory signalling, severe oxidative stress, neurodegeneration, microvascular changes and an advanced production of glycation end-products.

Glossary

- **Circadian rhythms:** endogenously generated rhythms with a free-running period of approximately 24 hours, meaning they persist under constant conditions. Circadian rhythms are entrainable by external cues ("Zeitgebers"). In mammals, light is the primary Zeitgeber, resulting in a 24-hour oscillation of physiological and behavioural rhythms. Time of food intake is another prominent Zeitgeber.
- **Glycogen synthase kinase 3β (GSK3β):** GSK3β is a proline-directed serine/threonine protein kinase that is ubiquitously expressed and constitutively active. GSK3β activity is controlled by phosphorylation at different sites. The major inhibitory phosphorylation site is Ser^{9}. This inhibitory phosphorylation is mediated by different kinases and pathways amongst which the insulin pathway-related kinase AKT is most prominent. GSK3β is also involved in the regulation of oxidative stress, apoptosis and gene transcription. The latter is mediated by the GSK3β regulation of diverse co-/transcription factors such as NF-κB, STAT3 or β-catenin. An over-activation of GSK3β is implicated in several diseases, including T2D, AD and other neurodegenerative disorders, inflammation, cancer and cardiovascular diseases.
- **Suprachiasmatic nucleus:** Located in the anterior hypothalamus, the SCN is the central master pacemaker of mammalian circadian rhythms. The main role of the SCN is the synchronisation of peripheral circadian clocks, which are present in virtually all tissues, to ensure a tranquil coordination between physiological and behavioural processes.
- **Time-restricted feeding:** A feeding regimen in which food intake is restricted to a specified period each day, followed by an extended period of food deprivation. TRF does not necessarily imply a reduction in caloric intake, but beneficial outcomes on metabolic health are dependent on the circadian timing of caloric intake.

Trends

- On the molecular level obesity, T2D and AD share common features such as central insulin resistance, chronic low-grade inflammation and altered GSK3 signalling.
- Several antidiabetic drugs showed positive effects in AD patients underpinning the molecular similarities of both diseases.
- Recent studies emphasize the circadian clock as an important player in whole body energy metabolism. Circadian rhythms and clock gene expression are altered in states of metabolic derailment and disruptions in circadian rhythms are associated with a number of different diseases including T2D and AD
- Considering the close relationship between circadian clocks and energy homeostasis, behavioural interventions, such as fasting regimens, to combat the consequences of disrupted rhythms and metabolism appear as a favourable tool

Outstanding Questions

- How important is the timing of meals for the synchronization of the master clock and do abnormal eating patterns lead to a disruption of circadian rhythms?
- Are neuroendocrine pathways, which control energy metabolism, regulated in a circadian manner in the brain?
- Are central insulin resistance, altered GSK3 signalling and chronic low-grade inflammation accompanying symptoms of a disrupted clock?
- Are circadian disruptions the cause or consequence of the pathogenesis of AD and other neurodegenerative diseases? Recent evidence suggests that circadian disruptions deteriorate rather than initiate pathological processes in AD but little is known about the underlying mechanisms.
- Can IF/TRF restore a misalignment of the circadian clock and thereby alleviate/reverse metabolic derangements and what are the molecular mechanisms?

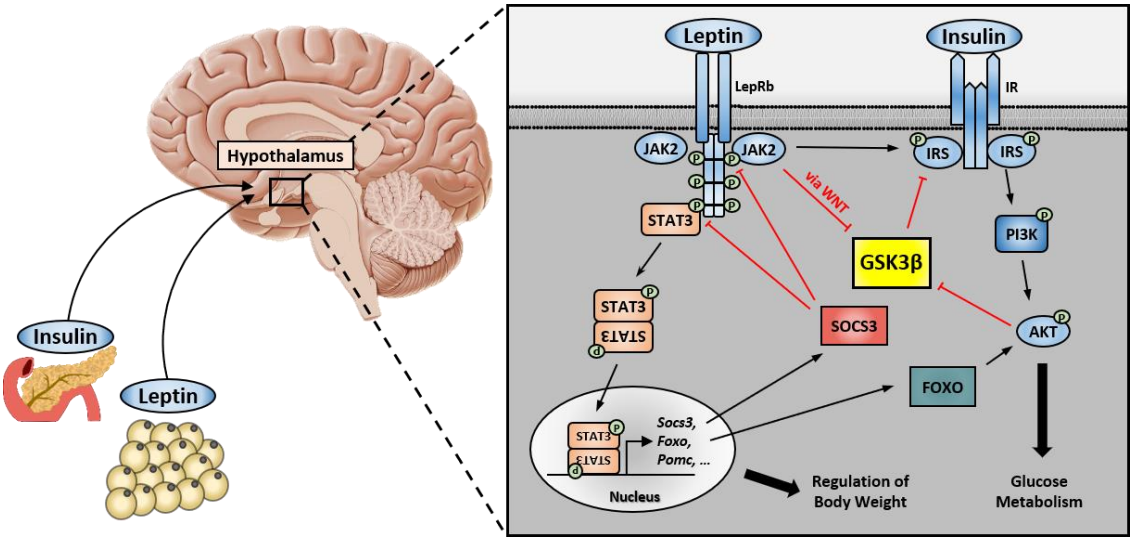

Figure 1. Insulin and leptin signalling in the brain. Insulin, secreted by pancreatic β-cells, crosses the blood brain barrier and binds to IR expressed by neurons. Upon binding of insulin to IR its intrinsic tyrosine kinase domain phosphorylates IRS1. Activated IRS1 phosphorylates PI3K leading to downstream activation of AKT. Activated AKT exhibits pleiotropic effects, most importantly controlling FOXO and GSK3β thereby regulating key processes such as cell survival, proliferation and metabolic adaptions. The adipokine leptin controls energy homeostasis and body weight primarily by targeting orexigenic as well as anorexigenic neurons in the hypothalamus. Binding of leptin to LepRb leads to an activation of JAK2 resulting in a phosphorylation of the three intracellular receptor tyrosine residues Tyr^{985}, Tyr^{1077} and Tyr^{1138}. The phosphorylation of Tyr^{1138} causes the recruitment of STAT3. STAT3 is subsequently phosphorylated by JAK2 at the phosphorylation site Tyr^{705}, which leads to homodimerization and nuclear translocation of STAT3. In the nucleus, STAT3 acts as a transcription factor and induces target gene expression, including SOCS3. SOCS3 initiates a negative feedback loop inhibiting JAK2 activation thereby decreasing leptin action. In addition to its fundamental effects on body weight via the JAK2/STAT3 pathway, leptin also inactivates GSK3β, linking leptin signalling to various metabolic processes. Glycogen synthase kinase 3β (GSK3β), insulin receptor (IR), insulin receptor substrate 1 (IRS1), Janus kinase 2 (JAK2), phosphoinositide 3-kinases (PI3K), protein kinase B (AKT), signal transducer and activator of transcription 3 (STAT3), suppressor of cytokine signalling 3 (SOCS3).

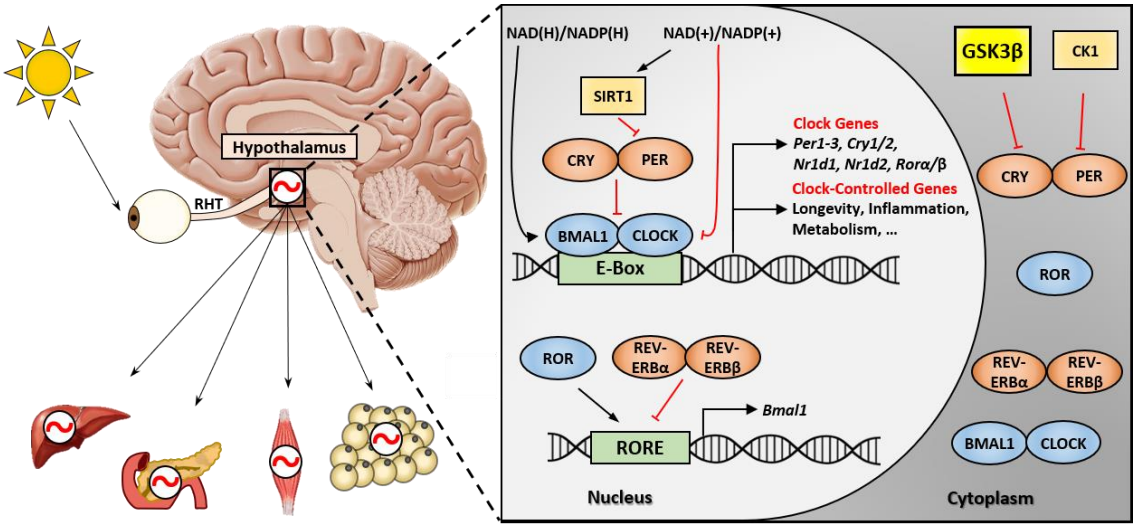

Figure 2. Regulation of cell autonomous circadian rhythms. The master pacemaker of circadian rhythm is the central circadian clock that resides in the SCN of the hypothalamus and synchronizes peripheral clocks in the body. On the molecular level, circadian rhythms are driven by a cell autonomous transcriptional translational feedback loop that occurs in virtually all cells. The positive arm of the mammalian circadian clock consists of the clock proteins CLOCK and BMAL1, which heterodimerize and bind to E-box regions in promotors of the clock genes *cry 1/2* and *per 1-3* initiating their transcription. Additionally, CLOCK/BMAL1 induces *rev-erbα* and *rorα/β* gene expression. The negative arm is represented by CRY, PER and REV-ERBα. CRY/PER heterodimers, translocate into the nucleus and repress the binding of the CLOCK/BMAL1 complex to target promotor regions thereby inhibiting their own transcription. Furthermore, REV-ERBα negatively regulates *bmal1* expression, while RORα/β induces its expression. CLOCK/BMAL1 is directly regulated by NAD(H) and NADP(H), which enhance the transcriptional activity of the complex. Their oxidised forms, NAD(+) and NADP(+), inhibit CLOCK/BMAL1 binding to the DNA. Furthermore, SIRT1 oscillates and binds CLOCK/BMAL1 heterodimers in a circadian manner, facilitating the degradation of PER2 and directly regulating circadian rhythms. Another regulatory mechanism for this rhythmic machinery is represented by the cytosolic enzymes CK1 and GSK3β, which label CRY and PER for degradation. This transcriptional translational feedback loop is repeated approximately once every 24 hours. Brain and muscle ARNT-like protein 1 (BMAL1), casein kinases (CK1), circadian locomotor output cycles kaput (CLOCK), cryptochrome (CRY), glycogen synthase kinase 3β (GSK3β), nicotinamide adenine dinucleotide redox cofactors

(NAD/NADP), period (PER), reverse erythoblastoma (REV-ERB), retinoid orphan receptor (ROR), suprachiasmatic nucleus (SCN), sirtuin 1 (SIRT1).

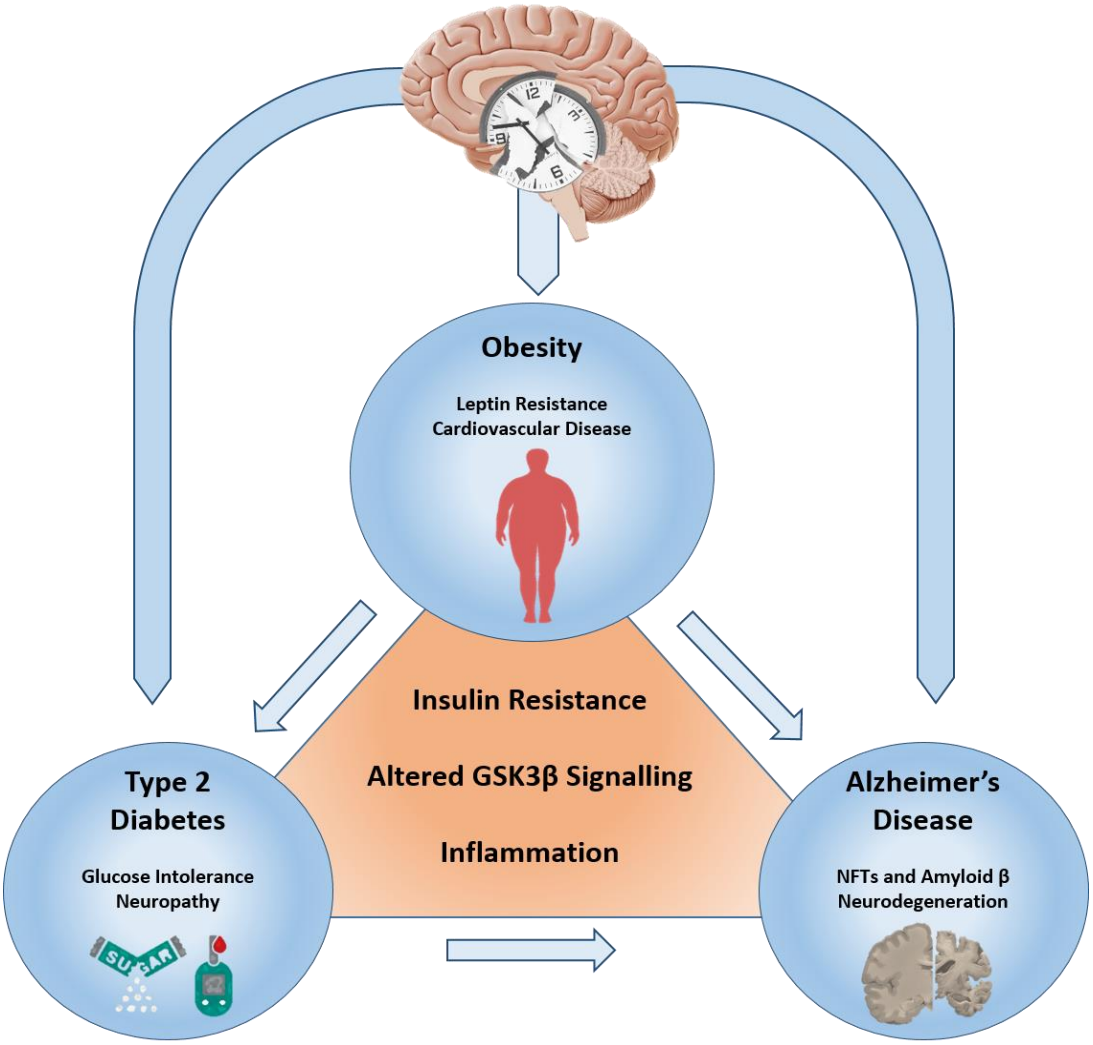

Figure 3 (Key Figure). Obesity, type 2 diabetes and Alzheimer´s disease are tightly linked disorders with obesity being a major risk factor for the development of T2D and AD. Impaired glucose homeostasis in T2D also increases the risk for the development of sporadic AD. Pathological changes such as insulin resistance, altered GSK3β signalling and central inflammation are common features of all three diseases. Recent research could also provide evidence, that a disruption of the circadian clock can further promote the progression of all three disorders. Alzheimer´s disease (AD), glycogen synthase kinase 3β (GSK3β), type 2 diabetes (T2D).

References

1. *International Diabetes Federation*. Available from: https://www.idf.org/aboutdiabetes/what-is-diabetes/facts-figures.html.

2. *World Health Organization*. Available from: http://www.who.int/news-room/fact-sheets/detail/obesity-and-overweight.

3. Ottaway, N., et al., *Diet-induced obese mice retain endogenous leptin action.* Cell Metab, 2015. **21**(6): p. 877-82.

4. Hotamisligil, G.S., *Inflammation and metabolic disorders.* Nature, 2006. **444**(7121): p. 860-7.

5. Benzler, J., et al., *Central inhibition of IKKbeta/NF-kappaB signaling attenuates high-fat diet-induced obesity and glucose intolerance.* Diabetes, 2015. **64**(6): p. 2015-27.

6. Purkayastha, S. and D. Cai, *Neuroinflammatory basis of metabolic syndrome.* Mol Metab, 2013. **2**(4): p. 356-63.

7. Zhang, X., et al., *Hypothalamic IKKbeta/NF-kappaB and ER stress link overnutrition to energy imbalance and obesity.* Cell, 2008. **135**(1): p. 61-73.

8. Feve, B., J.P. Bastard, and H. Vidal, *[Relationship between obesity, inflammation and insulin resistance: new concepts]*. C R Biol, 2006. **329**(8): p. 587-97; discussion 653-5.

9. Knight, Z.A., et al., *Hyperleptinemia is required for the development of leptin resistance.* PLoS One, 2010. **5**(6): p. e11376.

10. Frank-Podlech, S., et al., *Leptin Replacement Reestablishes Brain Insulin Action in the Hypothalamus in Congenital Leptin Deficiency.* Diabetes Care, 2018. **41**(4): p. 907-910.

11. Koch, C., et al., *Leptin rapidly improves glucose homeostasis in obese mice by increasing hypothalamic insulin sensitivity.* J Neurosci, 2010. **30**(48): p. 16180-7.

12. Benzler, J., et al., *Hypothalamic glycogen synthase kinase 3beta has a central role in the regulation of food intake and glucose metabolism.* Biochem J, 2012. **447**(1): p. 175-84.

13. Inestrosa, N.C. and E. Arenas, *Emerging roles of Wnts in the adult nervous system.* Nat Rev Neurosci, 2010. **11**(2): p. 77-86.

14. Benzler, J., et al., *Hypothalamic WNT signalling is impaired during obesity and reinstated by leptin treatment in male mice.* Endocrinology, 2013. **154**(12): p. 4737-45.

15. McEwen, H.J.L., et al., *Feeding and GLP-1 receptor activation stabilize beta-catenin in specific hypothalamic nuclei in male rats.* J Neuroendocrinol, 2018: p. e12607.

16. MacDonald, B.T., K. Tamai, and X. He, *Wnt/beta-catenin signaling: components, mechanisms, and diseases.* Dev Cell, 2009. **17**(1): p. 9-26.

17. Boucsein, A., et al., *Photoperiodic and Diurnal Regulation of WNT Signaling in the Arcuate Nucleus of the Female Djungarian Hamster, Phodopus sungorus.* Endocrinology, 2016. **157**(2): p. 799-809.

18. Abraham, M.A., et al., *Insulin action in the hypothalamus and dorsal vagal complex.* Exp Physiol, 2014. **99**(9): p. 1104-9.

19. Kahn, S.E., et al., *Quantification of the relationship between insulin sensitivity and beta-cell function in human subjects. Evidence for a hyperbolic function.* Diabetes, 1993. **42**(11): p. 1663-72.

20. Kametani, F. and M. Hasegawa, *Reconsideration of Amyloid Hypothesis and Tau Hypothesis in Alzheimer's Disease.* Front Neurosci, 2018. **12**: p. 25.

21. Perez-Gonzalez, R., et al., *Leptin gene therapy attenuates neuronal damages evoked by amyloid-beta and rescues memory deficits in APP/PS1 mice.* Gene Ther, 2014. **21**(3): p. 298-308.

22. Greco, S.J., et al., *Leptin inhibits glycogen synthase kinase-3beta to prevent tau phosphorylation in neuronal cells.* Neurosci Lett, 2009. **455**(3): p. 191-4.

23. Greco, S.J., et al., *Leptin reduces pathology and improves memory in a transgenic mouse model of Alzheimer's disease.* J Alzheimers Dis, 2010. **19**(4): p. 1155-67.

24. Cordner, Z.A. and K.L. Tamashiro, *Effects of high-fat diet exposure on learning & memory.* Physiol Behav, 2015. **152**(Pt B): p. 363-71.

25. Habchi, J., et al., *Cholesterol catalyses Abeta42 aggregation through a heterogeneous nucleation pathway in the presence of lipid membranes.* Nat Chem, 2018. **10**(6): p. 673-683.

26. Heppner, F.L., R.M. Ransohoff, and B. Becher, *Immune attack: the role of inflammation in Alzheimer disease.* Nat Rev Neurosci, 2015. **16**(6): p. 358-72.

27. Huang, N.Q., et al., *TLR4 is a link between diabetes and Alzheimer's disease.* Behav Brain Res, 2017. **316**: p. 234-244.

28. Zhao, M., et al., *The role of TLR4-mediated PTEN/PI3K/AKT/NF-kappaB signaling pathway in neuroinflammation in hippocampal neurons.* Neuroscience, 2014. **269**: p. 93-101.

29. Steen, E., et al., *Impaired insulin and insulin-like growth factor expression and signaling mechanisms in Alzheimer's disease--is this type 3 diabetes?* J Alzheimers Dis, 2005. **7**(1): p. 63-80.

30. Gray, S.M., R.I. Meijer, and E.J. Barrett, *Insulin regulates brain function, but how does it get there?* Diabetes, 2014. **63**(12): p. 3992-7.

31. Talbot, K., et al., *Demonstrated brain insulin resistance in Alzheimer's disease patients is associated with IGF-1 resistance, IRS-1 dysregulation, and cognitive decline.* J Clin Invest, 2012. **122**(4): p. 1316-38.

32. Rivera, E.J., et al., *Insulin and insulin-like growth factor expression and function deteriorate with progression of Alzheimer's disease: link to brain reductions in acetylcholine.* J Alzheimers Dis, 2005. **8**(3): p. 247-68.

33. Willette, A.A., et al., *Association of Insulin Resistance With Cerebral Glucose Uptake in Late Middle-Aged Adults at Risk for Alzheimer Disease.* JAMA Neurol, 2015. **72**(9): p. 1013-20.

34. Vandal, M., et al., *Age-dependent impairment of glucose tolerance in the 3xTg-AD mouse model of Alzheimer's disease.* FASEB J, 2015. **29**(10): p. 4273-84.

35. Niccoli, T., et al., *Increased Glucose Transport into Neurons Rescues Abeta Toxicity in Drosophila.* Curr Biol, 2016. **26**(18): p. 2550.

36. de la Monte, S.M., et al., *si-RNA inhibition of brain insulin or insulin-like growth factor receptors causes developmental cerebellar abnormalities: relevance to fetal alcohol spectrum disorder.* Mol Brain, 2011. **4**: p. 13.

37. Grunblatt, E., et al., *Brain insulin system dysfunction in streptozotocin intracerebroventricularly treated rats generates hyperphosphorylated tau protein.* J Neurochem, 2007. **101**(3): p. 757-70.

38. Watson, G.S., et al., *Insulin increases CSF Abeta42 levels in normal older adults.* Neurology, 2003. **60**(12): p. 1899-903.

39. Yamamoto, N., et al., *Insulin-signaling Pathway Regulates the Degradation of Amyloid beta-protein via Astrocytes.* Neuroscience, 2018. **385**: p. 227-236.

40. Ma, Q.L., et al., *Beta-amyloid oligomers induce phosphorylation of tau and inactivation of insulin receptor substrate via c-Jun N-terminal kinase signaling: suppression by omega-3 fatty acids and curcumin.* J Neurosci, 2009. **29**(28): p. 9078-89.

41. Hanger, D.P., et al., *Glycogen synthase kinase-3 induces Alzheimer's disease-like phosphorylation of tau: generation of paired helical filament epitopes and neuronal localisation of the kinase.* Neurosci Lett, 1992. **147**(1): p. 58-62.

42. Reger, M.A., et al., *Effects of intranasal insulin on cognition in memory-impaired older adults: modulation by APOE genotype.* Neurobiol Aging, 2006. **27**(3): p. 451-8.

43. Reger, M.A., et al., *Intranasal insulin improves cognition and modulates beta-amyloid in early AD.* Neurology, 2008. **70**(6): p. 440-8.

44. Cao, Y., et al., *DA5-CH, a novel GLP-1/GIP dual agonist, effectively ameliorates the cognitive impairments and pathology in the APP/PS1 mouse model of Alzheimer's disease.* Eur J Pharmacol, 2018. **827**: p. 215-226.

45. Batista, A.F., et al., *The diabetes drug liraglutide reverses cognitive impairment in mice and attenuates insulin receptor and synaptic pathology in a non-human primate model of Alzheimer's disease.* J Pathol, 2018. **245**(1): p. 85-100.

46. McClean, P.L., et al., *The diabetes drug liraglutide prevents degenerative processes in a mouse model of Alzheimer's disease.* J Neurosci, 2011. **31**(17): p. 6587-94.

47. Ramsey, K.M., et al., *The clockwork of metabolism.* Annu Rev Nutr, 2007. **27**: p. 219-40.

48. Coomans, C.P., et al., *The suprachiasmatic nucleus controls circadian energy metabolism and hepatic insulin sensitivity.* Diabetes, 2013. **62**(4): p. 1102-8.

49. Marcheva, B., et al., *Disruption of the clock components CLOCK and BMAL1 leads to hypoinsulinaemia and diabetes.* Nature, 2010. **466**(7306): p. 627-31.

50. Turek, F.W., et al., *Obesity and metabolic syndrome in circadian Clock mutant mice.* Science, 2005. **308**(5724): p. 1043-5.

51. Roenneberg, T., et al., *Social jetlag and obesity.* Curr Biol, 2012. **22**(10): p. 939-43.

52. Scheer, F.A., et al., *Adverse metabolic and cardiovascular consequences of circadian misalignment.* Proc Natl Acad Sci U S A, 2009. **106**(11): p. 4453-8.

53. Leproult, R., U. Holmback, and E. Van Cauter, *Circadian misalignment augments markers of insulin resistance and inflammation, independently of sleep loss.* Diabetes, 2014. **63**(6): p. 1860-9.

54. Kettner, N.M., et al., *Circadian Dysfunction Induces Leptin Resistance in Mice.* Cell Metab, 2015. **22**(3): p. 448-59.

55. Pendergast, J.S., et al., *High-fat diet acutely affects circadian organisation and eating behavior.* Eur J Neurosci, 2013. **37**(8): p. 1350-6.

56. Kohsaka, A., et al., *High-fat diet disrupts behavioral and molecular circadian rhythms in mice.* Cell Metab, 2007. **6**(5): p. 414-21.

57. Scheiermann, C., Y. Kunisaki, and P.S. Frenette, *Circadian control of the immune system.* Nat Rev Immunol, 2013. **13**(3): p. 190-8.

58. Gibbs, J.E., et al., *The nuclear receptor REV-ERBalpha mediates circadian regulation of innate immunity through selective regulation of inflammatory cytokines.* Proc Natl Acad Sci U S A, 2012. **109**(2): p. 582-7.

59. Narasimamurthy, R., et al., *Circadian clock protein cryptochrome regulates the expression of proinflammatory cytokines.* Proc Natl Acad Sci U S A, 2012. **109**(31): p. 12662-7.

60. Spengler, M.L., et al., *Core circadian protein CLOCK is a positive regulator of NF-kappaB-mediated transcription.* Proc Natl Acad Sci U S A, 2012. **109**(37): p. E2457-65.

61. Li, A.J., et al., *Leptin-sensitive neurons in the arcuate nuclei contribute to endogenous feeding rhythms.* Am J Physiol Regul Integr Comp Physiol, 2012. **302**(11): p. R1313-26.

62. Tan, K., Z.A. Knight, and J.M. Friedman, *Ablation of AgRP neurons impairs adaption to restricted feeding.* Mol Metab, 2014. **3**(7): p. 694-704.

63. Rutter, J., et al., *Regulation of clock and NPAS2 DNA binding by the redox state of NAD cofactors.* Science, 2001. **293**(5529): p. 510-4.

64. Asher, G., et al., *SIRT1 regulates circadian clock gene expression through PER2 deacetylation.* Cell, 2008. **134**(2): p. 317-28.

65. Kondratov, R.V., et al., *Early aging and age-related pathologies in mice deficient in BMAL1, the core componentof the circadian clock.* Genes Dev, 2006. **20**(14): p. 1868-73.

66. Krishnan, N., et al., *The circadian clock gene period extends healthspan in aging Drosophila melanogaster.* Aging (Albany NY), 2009. **1**(11): p. 937-48.

67. Mattis, J. and A. Sehgal, *Circadian Rhythms, Sleep, and Disorders of Aging.* Trends Endocrinol Metab, 2016. **27**(4): p. 192-203.

68. Merlino, G., et al., *Daytime sleepiness is associated with dementia and cognitive decline in older Italian adults: a population-based study.* Sleep Med, 2010. **11**(4): p. 372-7.

69. Weissova, K., et al., *Moderate Changes in the Circadian System of Alzheimer's Disease Patients Detected in Their Home Environment.* PLoS One, 2016. **11**(1): p. e0146200.

70. Waller, K.L., et al., *Melatonin and cortisol profiles in late midlife and their association with age-related changes in cognition.* Nat Sci Sleep, 2016. **8**: p. 47-53.

71. Wu, Y.H., et al., *Molecular changes underlying reduced pineal melatonin levels in Alzheimer disease: alterations in preclinical and clinical stages.* J Clin Endocrinol Metab, 2003. **88**(12): p. 5898-906.

72. Satlin, A., et al., *Circadian locomotor activity and core-body temperature rhythms in Alzheimer's disease.* Neurobiol Aging, 1995. **16**(5): p. 765-71.

73. Wu, Y.H., et al., *Decreased MT1 melatonin receptor expression in the suprachiasmatic nucleus in aging and Alzheimer's disease.* Neurobiol Aging, 2007. **28**(8): p. 1239-47.

74. Wu, Y.H., et al., *Pineal clock gene oscillation is disturbed in Alzheimer's disease, due to functional disconnection from the "master clock".* FASEB J, 2006. **20**(11): p. 1874-6.

75. Belanger, V., N. Picard, and N. Cermakian, *The circadian regulation of Presenilin-2 gene expression.* Chronobiol Int, 2006. **23**(4): p. 747-66.

76. Schmitt, K., A. Grimm, and A. Eckert, *Amyloid-beta-Induced Changes in Molecular Clock Properties and Cellular Bioenergetics.* Front Neurosci, 2017. **11**: p. 124.

77. Kress, G.J., et al., *Regulation of amyloid-beta dynamics and pathology by the circadian clock.* J Exp Med, 2018. **215**(4): p. 1059-1068.

78. Hood, S. and S. Amir, *Neurodegeneration and the Circadian Clock.* Front Aging Neurosci, 2017. **9**: p. 170.

79. Schug, T.T. and X. Li, *Sirtuin 1 in lipid metabolism and obesity.* Ann Med, 2011. **43**(3): p. 198-211.

80. Chaix, A., et al., *Time-restricted feeding is a preventative and therapeutic intervention against diverse nutritional challenges.* Cell Metab, 2014. **20**(6): p. 991-1005.

81. Hatori, M., et al., *Time-restricted feeding without reducing caloric intake prevents metabolic diseases in mice fed a high-fat diet.* Cell Metab, 2012. **15**(6): p. 848-60.

82. Longo, V.D. and M.P. Mattson, *Fasting: molecular mechanisms and clinical applications.* Cell Metab, 2014. **19**(2): p. 181-92.

83. Sherman, H., et al., *Timed high-fat diet resets circadian metabolism and prevents obesity.* FASEB J, 2012. **26**(8): p. 3493-502.

84. Forbes, D., et al., *Light therapy for improving cognition, activities of daily living, sleep, challenging behaviour, and psychiatric disturbances in dementia.* Cochrane Database Syst Rev, 2014(2): p. CD003946.

85. McCurry, S.M., et al., *Increasing walking and bright light exposure to improve sleep in community-dwelling persons with Alzheimer's disease: results of a randomized, controlled trial.* J Am Geriatr Soc, 2011. **59**(8): p. 1393-402.

86. Gehrman, P.R., et al., *Melatonin fails to improve sleep or agitation in double-blind randomized placebo-controlled trial of institutionalized patients with Alzheimer disease.* Am J Geriatr Psychiatry, 2009. **17**(2): p. 166-9.

87. Riemersma-van der Lek, R.F., et al., *Effect of bright light and melatonin on cognitive and noncognitive function in elderly residents of group care facilities: a randomized controlled trial.* JAMA, 2008. **299**(22): p. 2642-55.

88. Lopez, O.L. and S.T. Dekosky, *Clinical symptoms in Alzheimer's disease.* Handb Clin Neurol, 2008. **89**: p. 207-16.

89. Fandos, N., et al., *Plasma amyloid beta 42/40 ratios as biomarkers for amyloid beta cerebral deposition in cognitively normal individuals.* Alzheimers Dement (Amst), 2017. **8**: p. 179-187.

90. Chen, X., et al., *RAGE: a potential target for Abeta-mediated cellular perturbation in Alzheimer's disease.* Curr Mol Med, 2007. **7**(8): p. 735-42.

91. Tonnies, E. and E. Trushina, *Oxidative Stress, Synaptic Dysfunction, and Alzheimer's Disease.* J Alzheimers Dis, 2017. **57**(4): p. 1105-1121.

92. Hornberger, J., et al., *Clinical and cost implications of amyloid beta detection with amyloid beta positron emission tomography imaging in early Alzheimer's disease - the case of florbetapir.* Curr Med Res Opin, 2017. **33**(4): p. 675-685.

93. Nakamura, A., et al., *High performance plasma amyloid-beta biomarkers for Alzheimer's disease.* Nature, 2018. **554**(7691): p. 249-254.

94. Ott, A., et al., *Diabetes mellitus and the risk of dementia: The Rotterdam Study.* Neurology, 1999. **53**(9): p. 1937-42.

5. Curriculum Vitae

[Personal data not included here]

[Personal data not included here]

[Personal data not included here]

6. Acknowledgments

[Personal data not included here]

[Personal data not included here]